

Hyperpositive non-linear effects: enantiodivergence and modelling

Yannick Geiger, Thierry Achard, Aline Maise-François and Stéphane Bellemin-Laponnaz.

Supplementary Information

Summary

I: Supplementary Methods.....	3
I.1 Experimental procedures	3
I.1.1 Additional details to the general procedure of (-)-NME-catalysed addition of dialkylzincs to benzaldehyde.....	3
I.1.2 GC analysis.....	4
I.1.3 Kinetic measurements.....	4
I.2 Mathematical treatment.....	5
I.2.1 Model I: ee_P vs $[Cat_{tot}]$	5
I.2.2 Model I: kinetic rate law.....	7
I.2.3 Model II: ee_P vs ee_L	9
I.2.4 Model II: kinetic rate law.....	15
II: Supplementary Figures.....	17
III: Supplementary Chromatograms	21
III.1 Figure 2a (NME).....	21
III.2 Figure 2a (NBE).....	28
III.3 Figure 2b (NME).....	39
III.4 Figure 2b (NBE).....	44
III.5 Figure 3a	48
III.6 Figure 3b ((-)-NME).....	53
III.7 Figure 3b ((+)-NME).....	63
III.8 Sup. Figure 6	74
III.9 Benzaldehyde/1-phenyl-1-ethanol calibration curve	80
IV: References.....	82

I: Supplementary Methods

I.1 Experimental procedures

All reagents and dry solvents were purchased from commercial chemical suppliers (Acros, Alfa Aesar, Sigma-Aldrich and TCI Europe) and used without further purification, except for benzaldehyde which was dried, distilled and stored under argon over 4 Å molecular sieves prior to use. 1.2 M ZnMe₂ solutions in toluene were prepared from pure ZnMe₂ (purchased from Strem chemicals) and dry toluene in a N₂-filled glovebox in a 10-20 mL-scale and stored outside the glovebox, at 4 °C and protected from light, in a Young's tap-equipped Schlenk tube; the solutions were consumed within 3 weeks. (1*R*,2*S*)-(-)- and (1*S*,2*R*)-(+)-*N*-methylephedrine ((-)-NME and (+)-NME) were prepared from the respective ephedrine enantiomer according to a literature procedure; spectral data were identical to those reported.¹ Enantiomeric excesses were determined on a Varian 3900 gas chromatograph equipped with a CP-8400 autosampler and a Chiraldex G-TA capillary column (25 m long, 250 µm in diameter) with helium as carrier gas.

I.1.1 General procedure for (-)-NME-catalysed addition of dialkylzincs to benzaldehyde

In a N₂-filled glovebox, (1*R*,2*S*)-*N*-methylephedrine¹ (17.9 mg, 20 mol%, 100 µmol) and a magnetic stirring bar were placed in an oven-dried vial, which was then closed with a septum-containing screwcap. The vial was put out of the glovebox and dry toluene (0.4 mL) followed by a 1.2 M ZnMe₂ solution in toluene (0.5 mL, 1.2 equiv, 600 µmol) were added via syringe; gas evolution occurred upon ZnMe₂ addition. The mixture stirred for 10 min, then benzaldehyde (51 µL, 1 equiv, 500 µmol) was added via syringe. The solution stirred at room temperature for 48h, then was quenched carefully with 3 M aqueous HCl under vigorous stirring. The organic phase was then analysed by chiral stationary phase GC.

To obtain the experimental NLE curves the ligand ee was adjusted by preparing appropriate mixtures of the (1*R*,2*S*)-(-)- and (1*S*,2*R*)-(+)-enantiomers of NME. For the catalysts loading screening at 0 °C the amount of NME was reduced to the indicated catalyst loading shown in Figure 5a and the amount of dry toluene increased to keep the benzaldehyde concentration at 0.56 M; below 10 mol%, the reactions were scaled up (1.0-1.5 mL ZnMe₂ solution) to allow sufficiently precise weighing of NME. For temperature screenings, the reaction temperature was adapted as indicated in Figure 6a; reactions at room temperature fluctuated between 20 and 25 °C (always starting at 25 °C). The reaction time was increased to 4 days (7 days if the catalyst loading was lower than 20 mol%) for reaction conducted at 0 °C. The product ee and conversions were determined by GC. Full details of the starting material quantities, reaction conditions and results, including for the previously published NBE runs, are found in the SI_Experimental_Data.xlsx file.

Note: the reference concentration for the NME-catalysed runs (0.56 M benzaldehyde) is slightly lower than the one used previously for NBE (0.83 M). At 0.83 M, the runs with NME exhibited the formation of a white precipitate upon addition of ZnMe₂ at high ee_L and high catalyst loading, which most likely is a homochiral aggregate (cf. Supplementary Figure 6 for an exemplary ee_P vs [Cat_{tot}]-plot). Thus, the

catalytic runs were diluted to 0.56 M to allow full solubilisation of the catalyst. Previous investigations with NBE showed that comparable dilution of the reaction medium alters only slightly ee_P .²

I.1.2 GC analysis

Supplementary Table 1 | GC retention times of the catalysis products issued from the enantioselective addition of $ZnEt_2$ and $ZnMe_2$ to benzaldehyde.

Reagent	Product	t_{major} [min]	t_{minor} [min]
$ZnMe_2$	(R)-1-phenyl-1-ethanol	23.4	24.7

Oven temperature: 110°C; Helium pressure: 16 psi; split: 1/20. The separation conditions were determined by injecting racemic versions of the corresponding product. The product's absolute configuration was deduced from earlier reports using the same catalyst.³ The chromatograms are listed in section III: Supplementary Chromatograms. The product/benzaldehyde response ratio, used to determine the reaction's conversions, was determined from a calibration curve which was obtained by injecting mixtures of benzaldehyde and racemic 1-phenyl-1-ethanol in toluene of known concentration. The data can be found in the Calibration Curve-sheet of the SI_Experimental_Data.xlsx file.

Note: benzyl alcohol is formed as a side-product in dialkylzinc additions, which is occasionally seen as a trace peak in the GC chromatograms (retention time slightly lower than of the R-enantiomer of the 1-phenyl-1-ethanol product).

I.1.3 Kinetic measurements

The kinetic runs were performed in the same conditions as those with NBE,² with the same reactant quantities and concentrations as in Supplementary Figure 6 (0.83 M benzaldehyde), at 30 °C and on a 1.5-2.0 mL $ZnMe_2$ -scale. The ligand was placed in an oven-dried and argon-filled Schlenk tube, then $ZnMe_2$ was added via syringe, followed by toluene. The mixture stirred for 10 min at 30 °C, then benzaldehyde was added via syringe. A DS AgX Comp probe connected to a ReactIR 15 was mounted onto the Schlenk tube and IR recording was started precisely 30 s after benzaldehyde injection. Acquisition parameters: 2000 to 650 cm^{-1} , 4 cm^{-1} resolution; one acquisition every 5 min; 128 scans per acquisition (82 s acquisition time), 20-40 h reaction time (cf. corresponding rate profiles in the SI_Experimental_Data.xlsx file). The background was recorded each time in the empty (but argon-filled) Schlenk tube before addition of the ligand.

The kinetic profiles (Supplementary Fig. 5) were obtained by integrating the 1739 to 1675 cm^{-1} region of the IR spectra (benzaldehyde $\nu(C=O)$ at 1706 cm^{-1}) from a single point baseline at 1739 cm^{-1} ; the solvent was subtracted from the spectra using a previously recorded spectrum of pure toluene at 30 °C. The first acquisition of each run was approximated to correspond to the initial benzaldehyde

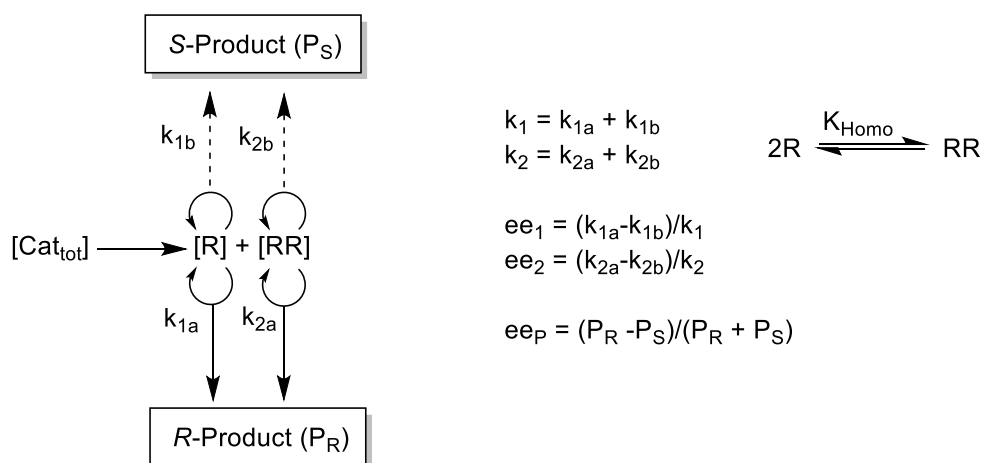
concentration and all following points of the corresponding run were normalised to that value. The complete rate profile data (including the previously published runs with NBE²) can be found in the Sup. Figure 5a and 5b-sheets of the SI_Experimental_Data.xlsx file.

Note: no precipitate appeared at this concentration (0.83 M benzaldehyde) at 30 °C, cf. Supplementary Figure 6.

I.2 Mathematical treatment

Note: full data of the mathematical simulations (ee_P vs $[Cat_{tot}]$, ee_P vs ee_L , $k_{obs}/[Cat_{tot}]$ vs $[Cat_{tot}]$, k_{obs} vs ee_L and c vs catalyst loading-plots) can be found in the

I.2.1 Model I: ee_P vs $[Cat_{tot}]$



$$[Cat_{tot}] = [R] + 2[RR] \quad (I)$$

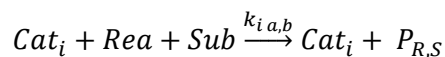
$$K_{Homo} = \frac{[RR]}{[R]^2} \quad (II)$$

Replacement of $[RR]$ in equation (II) through (I) gives a 2nd-order equation in $[R]$ whose only positive root is described by equation (III):

$$[R] = \frac{\sqrt{1 + 8K_{Homo}[Cat_{tot}]} - 1}{4K_{Homo}} \quad (III)$$

The only catalytically active species are the monomeric (R) and the dimeric (RR) complexes. Their enantioselectivities for the synthesis of the R-product are described by ee_1 and ee_2 , respectively.

The chiral products P_R and P_S are synthesised according to the following reaction equation:



With Cat_i referring to R and RR as catalysts, which give P_R and P_S from the substrate (Sub) and the reactant (Rea) with the respective kinetic constant $k_{i,a,b}$.

If we define the catalytic reaction giving the chiral product as the rate-limiting step, with only one catalyst, reactant and substrate molecule involved, the reaction's kinetics are expressed by:

$$\frac{d[P_{R,S}]}{dt} = k_{i,a,b}[Cat_i][Rea][Sub]$$

If the different $[Cat_i]$ are constant over time, we can insert the integrated forms of the kinetic equations into the term for ee_P , simplify and rearrange to make ee_1 and ee_2 appear:

$$ee_P = \frac{\sum_i k_{ia}[Cat_i][Rea][Sub]t - \sum_i k_{ib}[Cat_i][Rea][Sub]t}{\sum_i k_{ia}[Cat_i][Rea][Sub]t + \sum_i k_{ib}[Cat_i][Rea][Sub]t}$$

$$\Leftrightarrow ee_P = \frac{[R]k_{1a} + [RR]k_{2a} - ([R]k_{1b} + [RR]k_{2b})}{[R]k_{1a} + [RR]k_{2a} + ([R]k_{1b} + [RR]k_{2b})}$$

$$\Leftrightarrow ee_P = \frac{[R](k_{1a} - k_{1b}) + [RR](k_{2a} - k_{2b})}{[R](k_{1a} + k_{1b}) + [RR](k_{2a} + k_{2b})}$$

$$\Leftrightarrow ee_P = \frac{[R]k_1 ee_1 + [RR]k_2 ee_2}{[R]k_1 + [RR]k_2}$$

Elimination of $[RR]$ using equation (II) gives:

$$\Leftrightarrow ee_P = \frac{[R]k_1 ee_1 + [R]^2 K_{Homo} k_2 ee_2}{[R]k_1 + [R]^2 K_{Homo} k_2}$$

$$\Leftrightarrow ee_P = \frac{k_1 ee_1 + [R] K_{Homo} k_2 ee_2}{k_1 + [R] K_{Homo} k_2}$$

Elimination of $[R]$ with equation (III) and introduction of the factor γ gives:

$$\Leftrightarrow ee_p = \frac{k_1 ee_1 + \left(\frac{\sqrt{1 + 8K_{Homo}[Cat_{tot}]} - 1}{4K_{Homo}} \right) K_{Homo} k_2 ee_2}{k_1 + \left(\frac{\sqrt{1 + 8K_{Homo}[Cat_{tot}]} - 1}{4K_{Homo}} \right) K_{Homo} k_2}$$

$$\Leftrightarrow ee_p = \frac{ee_1 + \gamma \frac{k_2}{k_1} ee_2}{1 + \gamma \frac{k_2}{k_1}} \quad (1)$$

$$\gamma = \frac{\sqrt{1 + 8K_{Homo}[Cat_{tot}]} - 1}{4} \quad (2)$$

The “Model I ee_p vs $[Cat_{tot}]$ ”-sheet in the SI_Simulated_NLE_xlsx-file allows the computation of ee_p vs $[Cat_{tot}]$ -plots with free choice of the parameters K_{Homo} , k_2/k_1 , ee_1 and ee_2 .

1.2.2 Model I: kinetic rate law

First, the general kinetic equation is established:

$$-\frac{d[Sub]}{dt} = k_1[R][Rea][Sub] + k_2[RR][Rea][Sub]$$

$$\Leftrightarrow -\frac{d[Sub]}{dt} = (k_1[R] + k_2[R]^2 K_{Homo})[Rea][Sub]$$

$[R]$ can be substituted using equation (III):

$$\Leftrightarrow -\frac{d[Sub]}{dt} = \left(k_1 \frac{\sqrt{1 + 8K_{Homo}[Cat_{tot}]} - 1}{4K_{Homo}} + k_2 \left(\frac{\sqrt{1 + 8K_{Homo}[Cat_{tot}]} - 1}{4K_{Homo}} \right)^2 K_{Homo} \right) [Rea][Sub]$$

$$\Leftrightarrow -\frac{d[Sub]}{dt} = \left(k_1 \frac{\sqrt{1 + 8K_{Homo}[Cat_{tot}]} - 1}{4K_{Homo}} + k_2 \frac{(\sqrt{1 + 8K_{Homo}[Cat_{tot}]} - 1)^2}{16K_{Homo}} \right) [Rea][Sub]$$

If $[Rea] = [Sub]$, the equation simplifies to:

$$\Leftrightarrow -\frac{d[Sub]}{dt} = \left(k_1 \frac{\sqrt{1 + 8K_{Homo}[Cat_{tot}]} - 1}{4K_{Homo}} + k_2 \frac{(\sqrt{1 + 8K_{Homo}[Cat_{tot}]} - 1)^2}{16K_{Homo}} \right) [Sub]^2$$

➔ This corresponds to a standard 2nd-order rate law of type:

$$-\frac{d[Sub]}{dt} = k_{obs}[Sub]^2 \quad (6)$$

$$with k_{obs} = k_1 \frac{\sqrt{1 + 8K_{Homo}[Cat_{tot}]} - 1}{4K_{Homo}} + k_2 \frac{(\sqrt{1 + 8K_{Homo}[Cat_{tot}]} - 1)^2}{16K_{Homo}} \quad (9)$$

Integration over [Sub] and t give the integrated form of the 2nd-order rate law:

$$\Leftrightarrow -\int_{[Sub]_0}^{[Sub]_t} \frac{d[Sub]}{[Sub]^2} = k_{obs} \int_0^t dt$$

$$\Leftrightarrow [Sub]_t^{-1} - [Sub]_0^{-1} = k_{obs}t$$

$$\Leftrightarrow [Sub]_t^{-1} = [Sub]_0^{-1} + k_{obs}t \text{ (linearised form of equation (7))}$$

$$[Sub]_t = \left(\frac{1}{[Sub]_0} + k_{obs}t \right)^{-1} \quad (7)$$

$$with k_{obs} = k_1 \frac{\sqrt{1 + 8K_{Homo}[Cat_{tot}]} - 1}{4K_{Homo}} + k_2 \frac{(\sqrt{1 + 8K_{Homo}[Cat_{tot}]} - 1)^2}{16K_{Homo}} \quad (9)$$

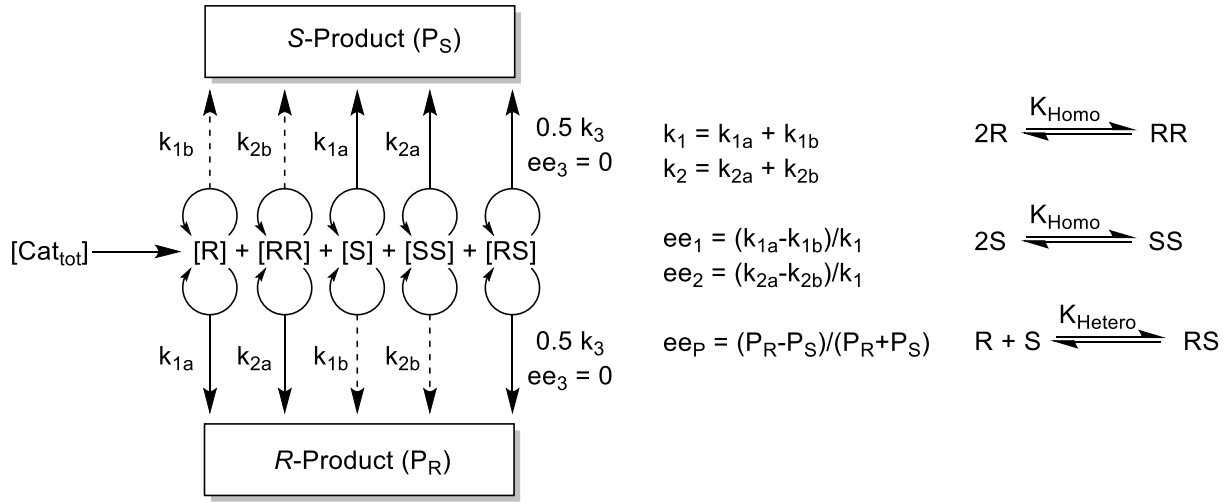
If [Rea]≠[Sub], then the general form of the integrated 2nd-order rate law applies:

$$\ln \frac{[Rea]_t [Sub]_0}{[Sub]_t [Rea]_0} = k_{obs}([Rea]_0 - [Sub]_0)t$$

1.2.2.1 Variable Time-normalised analysis (VTNA) of simulated rate profiles (Figure 9)

Rate profiles were obtained from equations (7) and (9) using different parameter sets (K_{Homo} , k_1 and k_2); for each parameter set, several rate profiles with different $[Cat_{tot}]$ were generated. Then, the rate profiles were normalised to their respective catalyst concentration using the excel spreadsheet provided by Nielsen and Burés.⁴ The catalyst order c of two normalised rate profiles from an identical parameter set, but different $[Cat_{tot}]$, was determined visually. c was then plotted against the mean $[Cat_{tot}]$ of the two respective rate profiles used in order to obtain c vs $[Cat_{tot}]$ -plots. The “Fig. 9”-sheet in the XXX file provides the c vs $[Cat_{tot}]$ datasets, simulated rate profiles and derived time-normalised rate profiles, which allow the independent verification of c for the given dataset.

I.2.3 Model II: ee_P vs ee_L



$$K_{Homo} = \frac{[RR]}{[R]^2} = \frac{[SS]}{[S]^2} \quad (II)$$

$$K_{Hetero} = \frac{[RS]}{[R][S]} \quad (IV)$$

$$[Cat_{tot}] = [R] + 2[RR] + [S] + 2[SS] + 2[RS] \quad (V)$$

As will be shown in the following, obtaining an equation of type $ee_P = f(ee_L)$ is difficult in this case. We will first develop an equation of type $ee_P = f(\alpha)$, then $ee_L = f(\alpha)$ and define the limits of α .

I.2.3.1 Expression for $ee_P = f(\alpha)$

The rate-limiting reaction step and its general kinetic rate law are the same as in Model I. The general expression for ee_P becomes:

$$ee_P = \frac{\sum_{i,a,b \rightarrow P_R} k_{i,a,b} [Cat_i] [Rea] [Sub] t - \sum_{i,a,b \rightarrow P_S} k_{i,a,b} [Cat_i] [Rea] [Sub] t}{\sum_{i,a,b \rightarrow P_R} k_{i,a,b} [Cat_i] [Rea] [Sub] t + \sum_{i,a,b \rightarrow P_S} k_{i,a,b} [Cat_i] [Rea] [Sub] t}$$

$$\Leftrightarrow ee_P = \frac{[R]k_{1a} + [RR]k_{2a} + [S]k_{1b} + [SS]k_{2b} + 0.5[RS]k_3 - ([S]k_{1a} + [R]k_{1b} + [SS]k_{2a} + [RR]k_{2b} + 0.5[RS]k_3)}{([R]k_{1a} + [RR]k_{2a} + [S]k_{1b} + [SS]k_{2b} + 0.5[RS]k_3) + ([R]k_{1b} + [RR]k_{2b} + [S]k_{1a} + [SS]k_{2a} + 0.5[RS]k_3)}$$

$$\Leftrightarrow ee_P = \frac{[R](k_{1a} - k_{1b}) + [RR](k_{2a} - k_{2b}) - ([S](k_{1a} - k_{1b}) + [SS](k_{2a} - k_{2b}))}{[R](k_{1a} + k_{1b}) + [RR](k_{2a} + k_{2b}) + [S](k_{1a} + k_{1b}) + [SS](k_{2a} + k_{2b}) + [RS]k_3}$$

$$\Leftrightarrow ee_P = \frac{([R] - [S])k_1ee_1 + ([RR] - [SS])k_2ee_2}{([R] + [S])k_1 + ([RR] + [SS])k_2 + [RS]k_3}$$

The dimeric complexes [RR], [SS] and [RS] are eliminated using equations (II) and (IV):

$$\Leftrightarrow ee_P = \frac{([R] - [S])k_1ee_1 + ([R]^2 - [S]^2)K_{Homo}k_2ee_2}{([R] + [S])k_1 + ([R]^2 + [S]^2)K_{Homo}k_2 + [R][S]K_{Hetero}k_3}$$

Since [R] and [S] appear simultaneously in sums and products, it is difficult to isolate one of both without ending up with complicated terms. Thus, we will apply a technique used by Noyori⁵ in his model for DAIB: the introduction of parameters α and β through equations (VI) and (VII):

$$\alpha = [R] + [S] \quad (VI)$$

$$\beta = [R][S] \quad (VII)$$

The combination (VI) and (VII), while supposing [R] is the major catalyst enantiomer (i. e. ee_L is defined as (R-S)/(R+S)), gives (VIII) and (IX):

$$[R] = \frac{\alpha + \sqrt{\alpha^2 - 4\beta}}{2} \quad (VIII)$$

$$[S] = \frac{\alpha - \sqrt{\alpha^2 - 4\beta}}{2} \quad (IX)$$

Equations (VI), (VII), (VIII) and (IX) now allow us to eliminate [R] and [S] :

$$\begin{aligned} &\Leftrightarrow ee_P \\ &= \frac{\left(\left(\frac{\alpha + \sqrt{\alpha^2 - 4\beta}}{2} \right) - \left(\frac{\alpha - \sqrt{\alpha^2 - 4\beta}}{2} \right) \right) k_1ee_1 + \left(\left(\frac{\alpha + \sqrt{\alpha^2 - 4\beta}}{2} \right)^2 - \left(\frac{\alpha - \sqrt{\alpha^2 - 4\beta}}{2} \right)^2 \right) K_{Homo}k_2ee_2}{\alpha k_1 + \left(\left(\frac{\alpha + \sqrt{\alpha^2 - 4\beta}}{2} \right)^2 + \left(\frac{\alpha - \sqrt{\alpha^2 - 4\beta}}{2} \right)^2 \right) K_{Homo}k_2 + \beta K_{Hetero}k_3} \end{aligned}$$

$$\begin{aligned} &\Leftrightarrow ee_P \\ &= \frac{\sqrt{\alpha^2 - 4\beta}k_1ee_1 + \left(\frac{\alpha^2 + 2\alpha\sqrt{\alpha^2 - 4\beta} + (\alpha^2 - 4\beta)}{4} - \frac{\alpha^2 - 2\alpha\sqrt{\alpha^2 - 4\beta} + (\alpha^2 - 4\beta)}{4} \right) K_{Homo}k_2ee_2}{\alpha k_1 + \left(\frac{\alpha^2 + 2\alpha\sqrt{\alpha^2 - 4\beta} + (\alpha^2 - 4\beta)}{4} + \frac{\alpha^2 - 2\alpha\sqrt{\alpha^2 - 4\beta} + (\alpha^2 - 4\beta)}{4} \right) K_{Homo}k_2 + \beta K_{Hetero}k_3} \end{aligned}$$

$$\Leftrightarrow ee_P = \frac{\sqrt{\alpha^2 - 4\beta}k_1ee_1 + \alpha\sqrt{\alpha^2 - 4\beta}K_{Homo}k_2ee_2}{\alpha k_1 + (\alpha^2 - 2\beta)K_{Homo}k_2 + \beta K_{Hetero}k_3}$$

$$\Leftrightarrow ee_P = \frac{\sqrt{\alpha^2 - 4\beta} \left(ee_1 + \alpha K_{Homo} \frac{k_2}{k_1} ee_2 \right)}{\alpha + (\alpha^2 - 2\beta)K_{Homo} \frac{k_2}{k_1} + \beta K_{Hetero} \frac{k_2'}{k_1}} \quad (3)$$

The same principle will be applied to ee_L . Both ee_P and ee_L then are described as functions of α (we will later develop the expression for β , which is itself a function of α). NLE curves can then be drawn by choosing appropriate α -values which will give paired ee_P/ee_L datapoints.

1.2.3.2 Expression for $ee_L = f(\alpha)$

$$ee_L = \frac{\sum Cat_{iR} - \sum Cat_{iS}}{[Cat_{tot}]}$$

$$\Leftrightarrow ee_L = \frac{[R] + 2[RR] + [RS] - ([S] + 2[SS] + [RS])}{[Cat_{tot}]}$$

$$\Leftrightarrow ee_L = \frac{([R] - [S]) + 2([RR] - [SS])}{[Cat_{tot}]}$$

Substitution by equations (II), (IV) and (V) gives :

$$\Leftrightarrow ee_L = \frac{([R] - [S]) + 2K_{Homo}([R]^2 - [S]^2)}{[Cat_{tot}]}$$

Replacement of $[R]$ and $[S]$ through equations (VIII) and (IX) gives :

$$\Leftrightarrow ee_L = \frac{\sqrt{\alpha^2 - 4\beta} + 2K_{Homo}\alpha\sqrt{\alpha^2 - 4\beta}}{[Cat_{tot}]}$$

$$\Leftrightarrow ee_L = \frac{\sqrt{\alpha^2 - 4\beta}(1 + 2\alpha K_{Homo})}{[Cat_{tot}]} \quad (4)$$

1.2.3.3 Expression for $\beta = f(\alpha)$

To express β as a function of α , we start from equation (V) into which we integrate equations (II) and (IV):

$$\begin{aligned} [Cat_{tot}] &= [R] + 2[RR] + [S] + 2[SS] + 2[RS] \\ \Leftrightarrow [Cat_{tot}] &= [R] + 2K_{Homo}[R]^2 + [S] + 2K_{Homo}[S]^2 + 2K_{Hetero}[R][S] \\ \Leftrightarrow [Cat_{tot}] &= [R] + [S] + 2K_{Homo}([R]^2 + [S]^2) + 2K_{Hetero}\beta \end{aligned}$$

We then eliminate $[R]$ and $[S]$ using equations (VI), (VII), (VIII) and (IX) and rearrange for β :

$$\begin{aligned} \Leftrightarrow [Cat_{tot}] &= \alpha + 2K_{Homo}(\alpha^2 - 2\beta) + 2K_{Hetero}\beta \\ \Leftrightarrow [Cat_{tot}] &= \alpha + 2K_{Homo}\alpha^2 - 4K_{Homo}\beta + 2K_{Hetero}\beta \\ \Leftrightarrow 4K_{Homo}\beta - 2K_{Hetero}\beta &= \alpha + 2K_{Homo}\alpha^2 - [Cat_{tot}] \\ \Leftrightarrow \beta &= \frac{(\alpha + 2K_{Homo}\alpha^2 - [Cat_{tot}])}{4K_{Homo} - 2K_{Hetero}} \end{aligned} \quad (5)$$

The division precludes that $K_{Hetero} \neq 2K_{Homo}$. This is the point which separates a (+)-NLE ($K_{Hetero} > 2K_{Homo}$) from a (-)-NLE ($K_{Hetero} < 2K_{Homo}$).

In summary:

$$\begin{aligned} \text{NLE (Model II): } \left\{ \begin{array}{l} ee_L = \frac{\sqrt{\alpha^2 - 4\beta}(1 + 2\alpha K_{Homo})}{[Cat_{tot}]} \\ ee_P = \frac{\sqrt{\alpha^2 - 4\beta}(ee_1 + \alpha K_{Homo} \frac{k_2}{k_1} ee_2)}{\alpha + (\alpha^2 - 2\beta)K_{Homo} \frac{k_2}{k_1} + \beta K_{Hetero} \frac{k_2}{k_1}} \end{array} \right. \\ \text{with } \beta = \frac{(\alpha + 2K_{Homo}\alpha^2 - [Cat_{tot}])}{4K_{Homo} - 2K_{Hetero}} \end{aligned}$$

1.2.3.4 Limiting values for α

To build an NLE curve from $ee_P = f(\alpha)$ and $ee_L = f(\alpha)$, we need to define the range of α we may use. In the following we will define the minimum (α_{min}) and maximum (α_{max}) α -values. Both are defined through the minimum (0) and maximum (1) values ee_L can take.

(a) $\alpha_{\min}: 0 \leq ee_L$

$$0 \leq \frac{\sqrt{\alpha^2 - 4\beta}(1 + 2\alpha K_{Homo})}{[Cat_{tot}]}$$

$$\Rightarrow 0 \leq \sqrt{\alpha^2 - 4\beta} \text{ or } 0 \leq (1 + 2\alpha K_{Homo})$$

$$\Rightarrow 0 \leq \alpha^2 - 4\beta$$

Development of β using equation (5) gives a 2nd-order inequality:

$$\Leftrightarrow 0 \leq \alpha^2 - 4 \frac{(\alpha + 2K_{Homo}\alpha^2 - [Cat_{tot}])}{4K_{Homo} - 2K_{Hetero}}$$

$$\Leftrightarrow 0 \leq \frac{(4K_{Homo} - 2K_{Hetero})\alpha^2}{4K_{Homo} - 2K_{Hetero}} + \frac{-4\alpha - 8K_{Homo}\alpha^2 + 4[Cat_{tot}]}{4K_{Homo} - 2K_{Hetero}}$$

$$\Leftrightarrow 0 \leq \frac{-4\alpha + (-4K_{Homo} - 2K_{Hetero})\alpha^2 + 4[Cat_{tot}]}{4K_{Homo} - 2K_{Hetero}}$$

$$\Leftrightarrow 0 \leq \frac{4\alpha + (4K_{Homo} + 2K_{Hetero})\alpha^2 - 4[Cat_{tot}]}{2K_{Hetero} - 4K_{Homo}}$$

$$\Rightarrow 0 \leq (2K_{Homo} + K_{Hetero})\alpha^2 + 2\alpha - 2[Cat_{tot}]$$

The last step is valid only if $K_{Hetero} > 2K_{Homo}$ (positive non-linear effect); if $K_{Hetero} < 2K_{Homo}$ it results in multiplication with a negative value which switches the sign of the inequality. Solution of the 2nd-order inequality gives:

$$\Leftrightarrow \alpha_{\pm} \geq \frac{-2 \pm \sqrt{4 - 4(-2[Cat_{tot}])(2K_{Homo} + K_{Hetero})}}{4K_{Homo} + 2K_{Hetero}}$$

$$\Leftrightarrow \alpha_{\pm} \geq \frac{-1 \pm \sqrt{1 + 2[Cat_{tot}](2K_{Homo} + K_{Hetero})}}{2K_{Homo} + K_{Hetero}}$$

Since $\alpha = [R]+[S]$ must be a positive number, α_+ is the only significant root:

$$\Rightarrow \alpha_{min} \geq \frac{\sqrt{1 + 2[Cat_{tot}](2K_{Homo} + K_{Hetero})} - 1}{2K_{Homo} + K_{Hetero}} \quad (X)$$

α_{\min} defines 0 as the lower limit of ee_L but also of ee_P (cf. the corresponding equation) in case of a (+)-NLE. For a (-)-NLE the inequality is switched, α_{\min} then becomes the *maximal* value α can reach.

2nd factor = 0 :

$$0 = (1 + 2\alpha K_{Homo})$$

$$-1 = 2\alpha K_{Homo}$$

$$-\frac{1}{2K_{Homo}} = \alpha$$

➔ Without significance, since α must be positive.

(b) $\alpha_{\max}: 1 \geq ee_L$

$$1 \geq \frac{\sqrt{\alpha^2 - 4\beta}(1 + 2\alpha K_{Homo})}{[Cat_{tot}]}$$

$$\Leftrightarrow [Cat_{tot}] \geq \sqrt{\alpha^2 - 4\beta}(1 + 2\alpha K_{Homo})$$

Since both sides of the inequality have to be positive values, we can quadrate the inequality to eliminate the square root, leading to a quartic equation:

$$\Leftrightarrow [Cat_{tot}]^2 \geq (\alpha^2 - 4\beta)(1 + 2\alpha K_{Homo})^2$$

$$\Leftrightarrow [Cat_{tot}]^2 \geq \left(\alpha^2 - 4 \left(\frac{(\alpha + 2K_{Homo}\alpha^2 - [Cat_{tot}])}{4K_{Homo} - 2K_{Hetero}} \right) \right) (1 + 2\alpha K_{Homo})^2$$

$$\Leftrightarrow [Cat_{tot}]^2 \geq \left(\frac{(4K_{Homo} - 2K_{Hetero})\alpha^2}{4K_{Homo} - 2K_{Hetero}} + \frac{(-4\alpha - 8K_{Homo}\alpha^2 + 4[Cat_{tot}])}{4K_{Homo} - 2K_{Hetero}} \right) (1 + 2\alpha K_{Homo})^2$$

$$\Leftrightarrow [Cat_{tot}]^2 \geq \left(\frac{(-4\alpha - (4K_{Homo} + 2K_{Hetero})\alpha^2 + 4[Cat_{tot}])}{4K_{Homo} - 2K_{Hetero}} \right) (1 + 4\alpha K_{Homo} + 4\alpha^2 K_{Homo}^2)$$

$$\begin{aligned} \Leftrightarrow [Cat_{tot}]^2 \geq & \left(\frac{(2\alpha + (2K_{Homo} + K_{Hetero})\alpha^2 - 2[Cat_{tot}])}{K_{Hetero} - 2K_{Homo}} \right) \\ & + \left(\frac{(8\alpha^2 K_{Homo} + 4K_{Homo}(2K_{Homo} + K_{Hetero})\alpha^3 - 8\alpha K_{Homo}[Cat_{tot}])}{K_{Hetero} - 2K_{Homo}} \right) \\ & + \left(\frac{(8\alpha^3 K_{Homo}^2 + 4K_{Homo}^2(2K_{Homo} + K_{Hetero})\alpha^4 - 8\alpha^2 K_{Homo}^2[Cat_{tot}])}{K_{Hetero} - 2K_{Homo}} \right) \end{aligned}$$

The next step is valid only if $K_{Hetero} > 2K_{Homo}$, otherwise the sign of the inequality changes:

$$\begin{aligned} \Leftrightarrow [Cat_{tot}]^2 (K_{hetero} - 2K_{Homo}) & \\ \geq (2 - 8K_{Homo}[Cat_{tot}])\alpha + (2K_{Homo} + K_{Hetero} + 8K_{Homo} - 8K_{Homo}^2[Cat_{tot}])\alpha^2 & \\ + (2K_{Homo} + K_{Hetero} + 8K_{Homo}^2)\alpha^3 + 4K_{Homo}^2(2K_{Homo} + K_{Hetero})\alpha^4 - 2[Cat_{tot}] & \end{aligned}$$

$$\Leftrightarrow 0 \geq (2 - 8K_{Homo}[Cat_{tot}])\alpha + (10K_{Homo} + K_{Hetero} - 8K_{Homo}^2[Cat_{tot}])\alpha^2 + (2K_{Homo} + K_{Hetero} + 8K_{Homo}^2)\alpha^3 + 4K_{Homo}^2(2K_{Homo} + K_{Hetero})\alpha^4 - (2[Cat_{tot}] + [Cat_{tot}]^2(K_{hetero} - 2K_{Homo}))$$

$$\Leftrightarrow 0 \geq 4K_{Homo}^2(2K_{Homo} + K_{Hetero})\alpha^4 + (2K_{Homo} + K_{Hetero} + 8K_{Homo}^2)\alpha^3 + (10K_{Homo} + K_{Hetero} - 8K_{Homo}^2[Cat_{tot}])\alpha^2 + (2 - 8K_{Homo}[Cat_{tot}])\alpha - (2[Cat_{tot}] + [Cat_{tot}]^2(K_{Hetero} - 2K_{Homo})) \quad (XI)$$

Equation (XI) can then be solved numerically to obtain the upper limit of α , which is α_{\max} (however, it may give spurious results depending on the software used). If $K_{Hetero} > 2K_{Homo}$ then α_{\max} becomes the *lower* limit of α .

The “Model II ee_p vs ee_L”-sheet in the SI_Simulated_NLE_xlsx-file allows the computation of ee_p vs ee_L-plots with free choice of the parameters [Cat_{tot}], K_{Homo}, K_{Hetero}, k₁, k₂, k₂', ee₁ and ee₂. For this, the user has to set up manually a range of α -values that serve as a base to obtain ee_p vs ee_L-datasets. The first α -value, α_{\min} , is automatically calculated from the inserted parameters (cf. equation (X), it can be either the minimum or maximum α if $K_{Hetero} >$ or $< 2K_{Homo}$, respectively). Upon change of K_{Homo}, K_{Hetero} or [Cat_{tot}] the α -values may have to be readjusted to obtain enough datapoints that span from 0 to 100% ee_L.

1.2.4 Model II: kinetic rate law

First, the general kinetic equation is established and rearranged:

$$-\frac{d[Sub]}{dt} = k_1[R][Rea][Sub] + k_1[S][Rea][Sub] + k_2[RR][Rea][Sub] + k_2[SS][Rea][Sub] + k_2'[RS][Rea][Sub]$$

$$\Leftrightarrow -\frac{d[Sub]}{dt} = (k_1([R] + [S]) + k_2([RR] + [SS]) + k_2'[RS])[Rea][Sub]$$

$$\Leftrightarrow -\frac{d[Sub]}{dt} = (k_1([R] + [S]) + k_2K_{Homo}([R]^2 + [S]^2) + k_2'K_{Hetero}[R][S])[Rea][Sub]$$

[R] and [S] are then replaced by α and β using equations (VI)-(IX) and it is assumed that [Rea]=[Sub]:

$$\Leftrightarrow -\frac{d[Sub]}{dt} = (k_1\alpha + k_2K_{Homo}(\alpha^2 - 2\beta) + k_2'K_{Hetero}\beta)[Rea][Sub]$$

$$\Leftrightarrow -\frac{d[Sub]}{dt} = (k_1\alpha + k_2K_{Homo}(\alpha^2 - 2\beta) + k_2'K_{Hetero}\beta)[Sub]^2$$

➔ This corresponds to a standard 2nd-order rate law of type:

$$-\frac{d[Sub]}{dt} = k_{obs}[Sub]^2 \quad (6)$$

$$[Sub]_t = \left(\frac{1}{[Sub]_0} + k_{obs}t \right)^{-1} \quad (7)$$

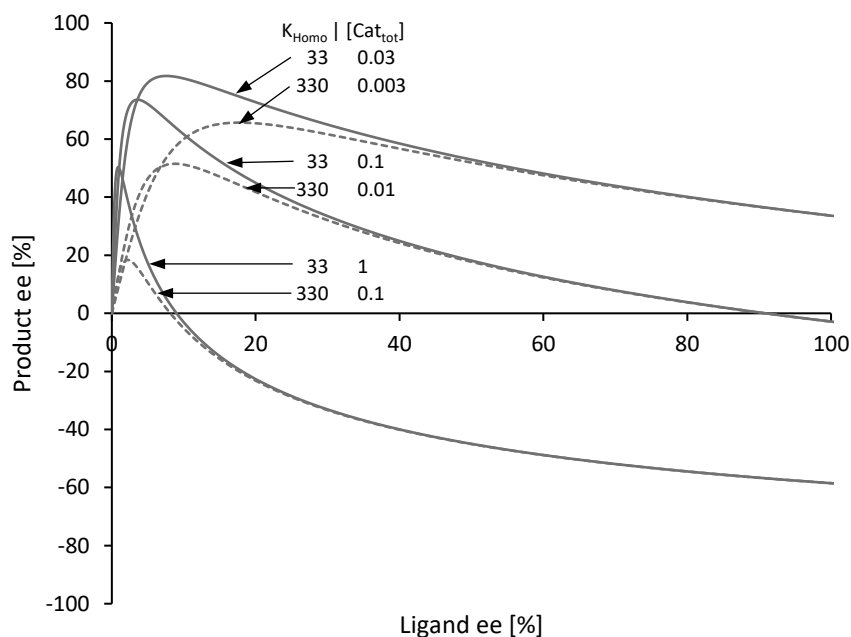
$$\text{with } k_{obs} = k_1\alpha + k_2K_{Homo}(\alpha^2 - 2\beta) + k_2'K_{Hetero}\beta \quad (10)$$

$$ee_L = \frac{\sqrt{\alpha^2 - 4\beta}(1 + 2\alpha K_{Homo})}{[Cat_{tot}]} \text{ and } \beta = \frac{(\alpha + 2K_{Homo}\alpha^2 - [Cat_{tot}])}{4K_{Homo} - 2K_{Hetero}} \quad (4) \text{ \& } (5)$$

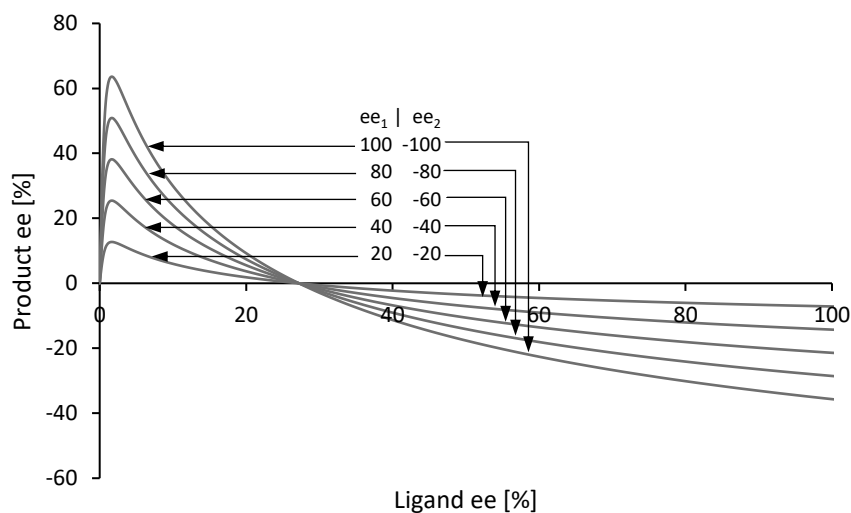
The expressions for ee_L and β (equations (4) and (5)) as well as the maximum and minimum values for α have been established in section I.2.3. As for the ee_P vs ee_L -plots, k_{obs} vs ee_L -plots can be established by choosing appropriate values of α , which give paired k_{obs} and ee_L datapoints. The integrated form of the kinetic rate law is, as for Model I, given by equation (7) (cf. section I.2.2). If $[Rea] \neq [Sub]$, the integrated form of the 2nd-order rate law is given by:

$$\ln \frac{[Rea]_t[Sub]_0}{[Sub]_t[Rea]_0} = k_{obs}([Rea]_0 - [Sub]_0)t$$

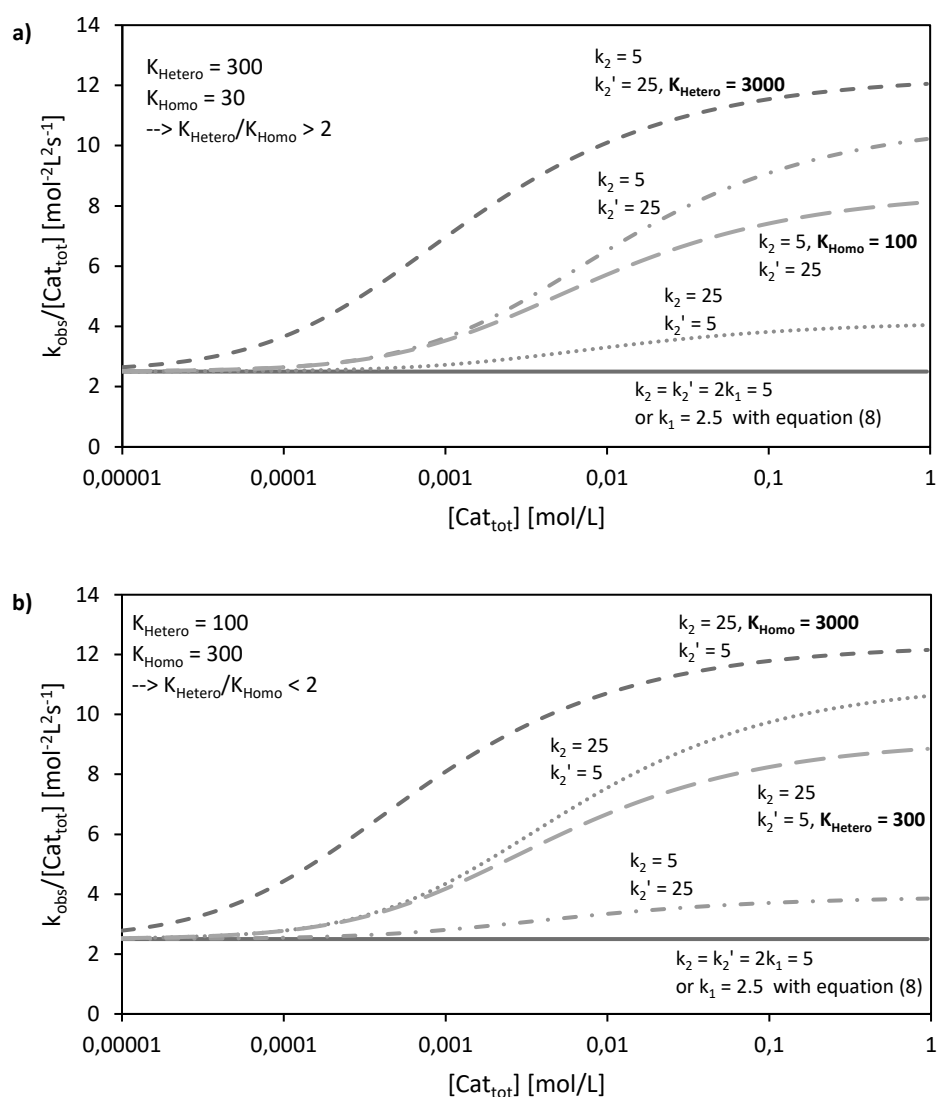
II: Supplementary Figures



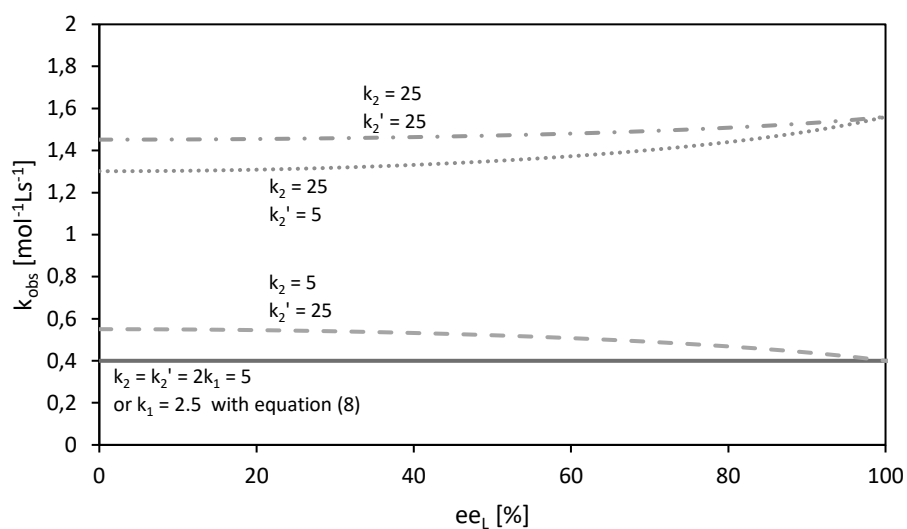
Supplementary Figure 1: Comparison of $[Cat_{tot}]$ - and K_{Homo} -variations in NLE-simulations using Model II, with $k_1/k_2 = 1$, $k_3 = 0$, $K_{Hetero} = 10000$, $ee_1 = 100$ and $ee_2 = -100$. For a given curve (blue full line), simultaneous multiplication of K_{Homo} and division of $[Cat_{tot}]$ by the same number leads to a new curve (grey dashed line). Both have the same ee_P^{100} -value and are essentially identical for ee_L higher than 50; at lower ee_L , the new curve deviates to lower ee_P values.



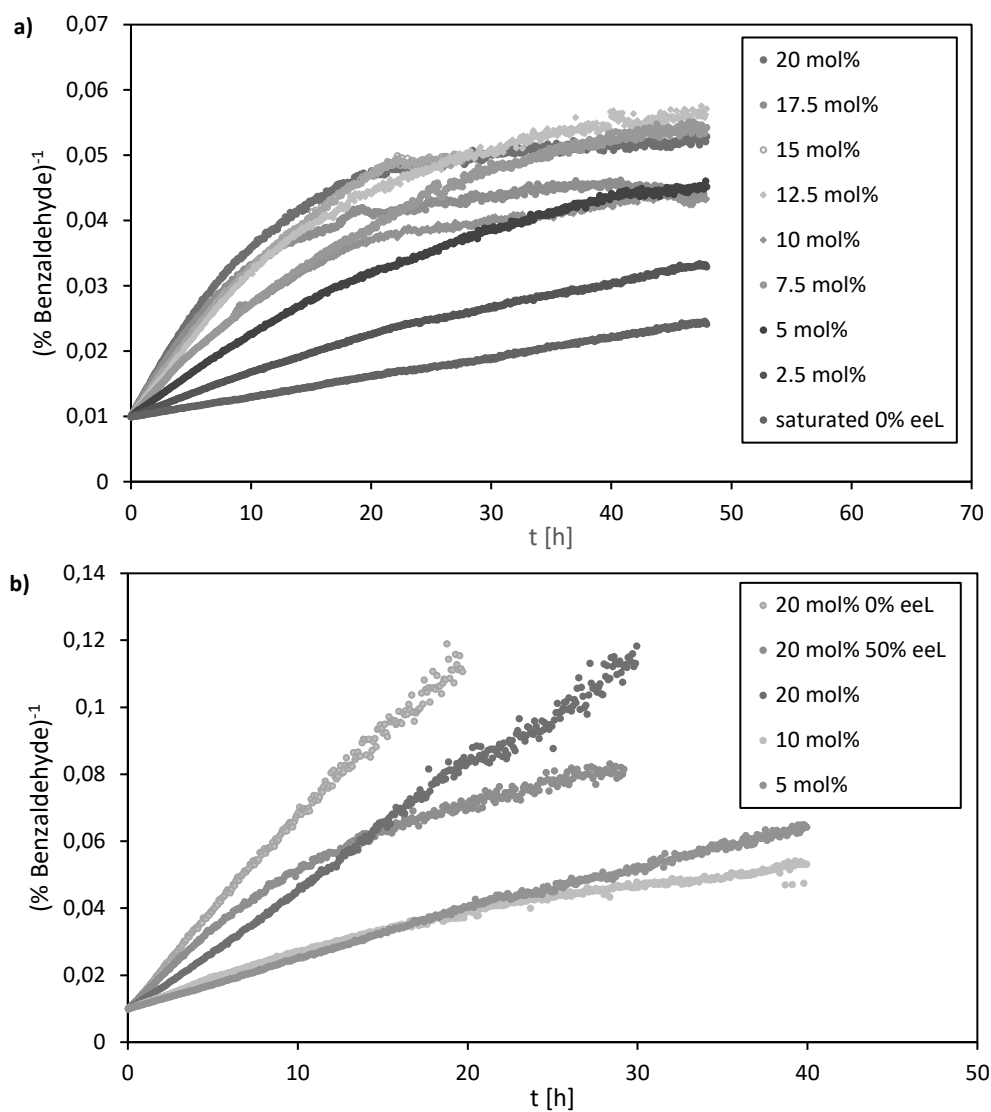
Supplementary Figure 2: Simultaneous decrease of the absolute values of ee_1 and ee_2 (with a constant ee_1/ee_2 -ratio of -1) in NLE-simulations using Model II, with $k_1/k_2 = 1$, $k_3 = 0$, $K_{Homo} = 100$, $K_{Hetero} = 330000$ and $[Cat_{tot}] = 0.11$. The decrease leads to a compression of the curve: ee_P^{100} increases and ee_P^{max} decreases. On the other hand, ee_L^0 and ee_L^{max} stay constant.



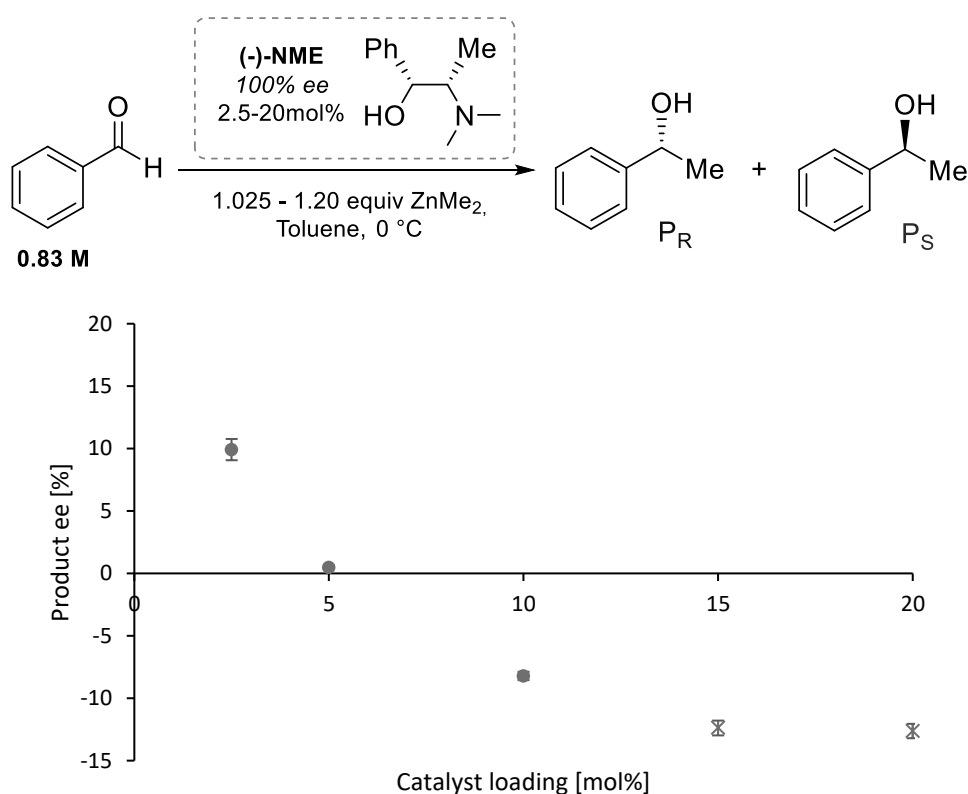
Supplementary Figure 3: Simulated $k_{\text{obs}}/[\text{Cat}_{\text{tot}}]$ vs $[\text{Cat}_{\text{tot}}]$ -plots computed from equation (10) at $ee_L = 0$ (cf. section 1.2.3.4(a)) with a) $K_{\text{Hetero}} = 300$, $K_{\text{Homo}} = 30$ and b) $K_{\text{Hetero}} = 100$, $K_{\text{Homo}} = 300$, unless noted otherwise. In all plots $k_1 = 2.5$, k_2 and k_2' as indicated. In contrast to the case with enantiopure ligand (Figure 7a in the main text) the shape of plots the plots is not only determined by k_2/k_1 but also by k_2'/k_1 . If $k_2 = k_2' = 2k_1$ the plot is flat, regardless of K_{Homo} and K_{Hetero} (blue full line in a) and b)). Increasing k_2 (orange dotted line) and k_2' (green dashed/dotted line) both enhance $k_{\text{obs}}/[\text{Cat}_{\text{tot}}]$ with increasing $[\text{Cat}_{\text{tot}}]$, the effect being more pronounced with k_2' in a) ($K_{\text{Hetero}}/K_{\text{Homo}} > 2$) or with k_2 in b) ($K_{\text{Hetero}}/K_{\text{Homo}} < 2$). When $k_2 \neq k_2'$, increasing the dimerization constant associated to the higher rate constant amplifies the curve (blue dashed lines). On the other hand, increasing the K associated to the lower k depletes the curve (grey long-dashed lines).



Supplementary Figure 4: Simulated k_{obs} vs ee_L -plots computed from equations (10), (4) and (5) ($K_{Homo} = 30$, $K_{Hetero} = 10$, $[Cat_{tot}] = 0.16$, $k_1 = 2.5$, k_2 and k_2' as indicated). Since in this example $K_{Hetero}/K_{Homo} < 2$, the plot's slope is positive when increasing both k_2 and k_2' to 25 (green dashed/dotted line), which stands in contrast to what is seen Figure 7b in the main text. Here, the homochiral dimers are prevalent over the heterochiral ones, which leads to an overall k_{obs} increase at any ee_L (not only at high ee_L as in Figure 7b) when increasing k_2 (orange dotted line). On the other hand, an increase of k_2' has only little effect (grey dashed line). As discussed in the main text, $k_2 = k_2' = 2k_1 = 5$ results in a constant k_{obs} over varying ee_L (blue full line).



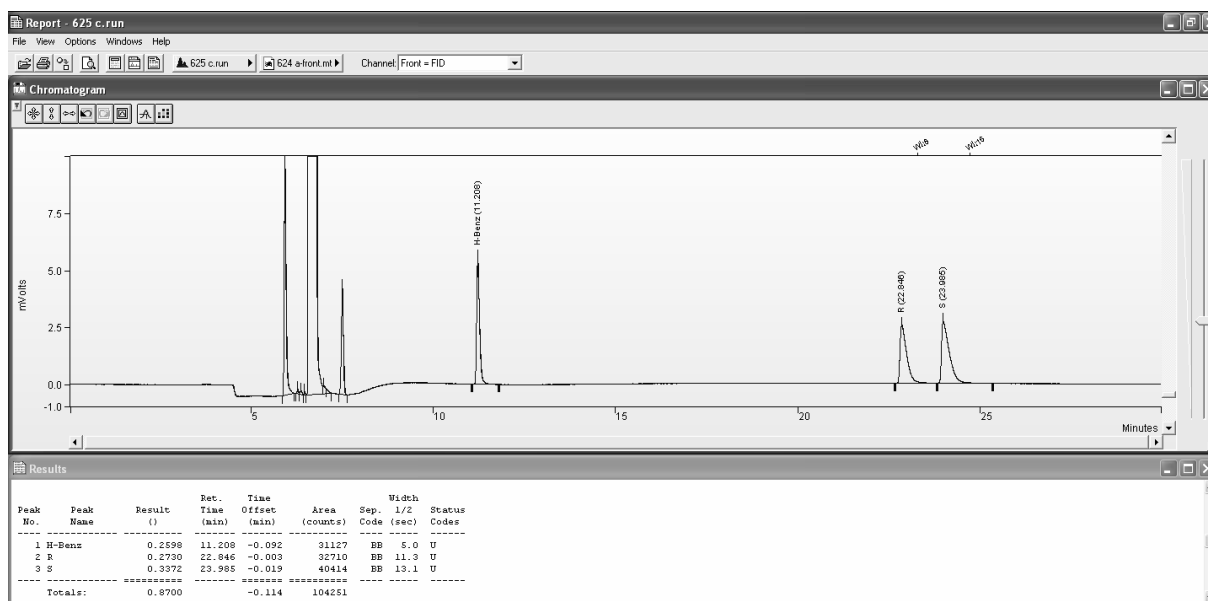
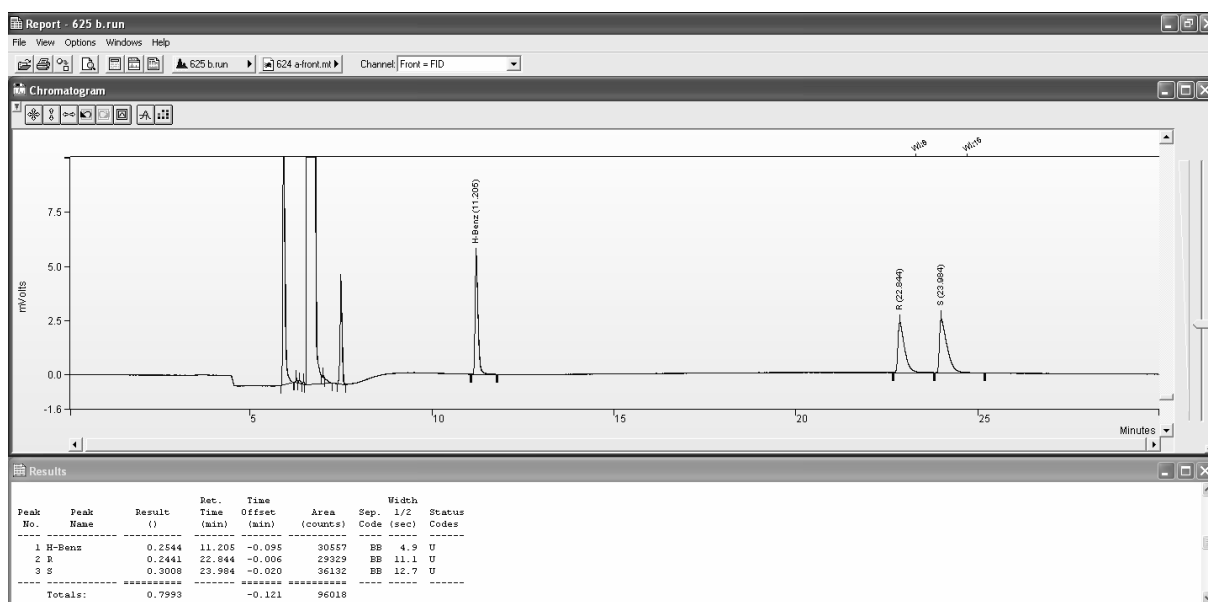
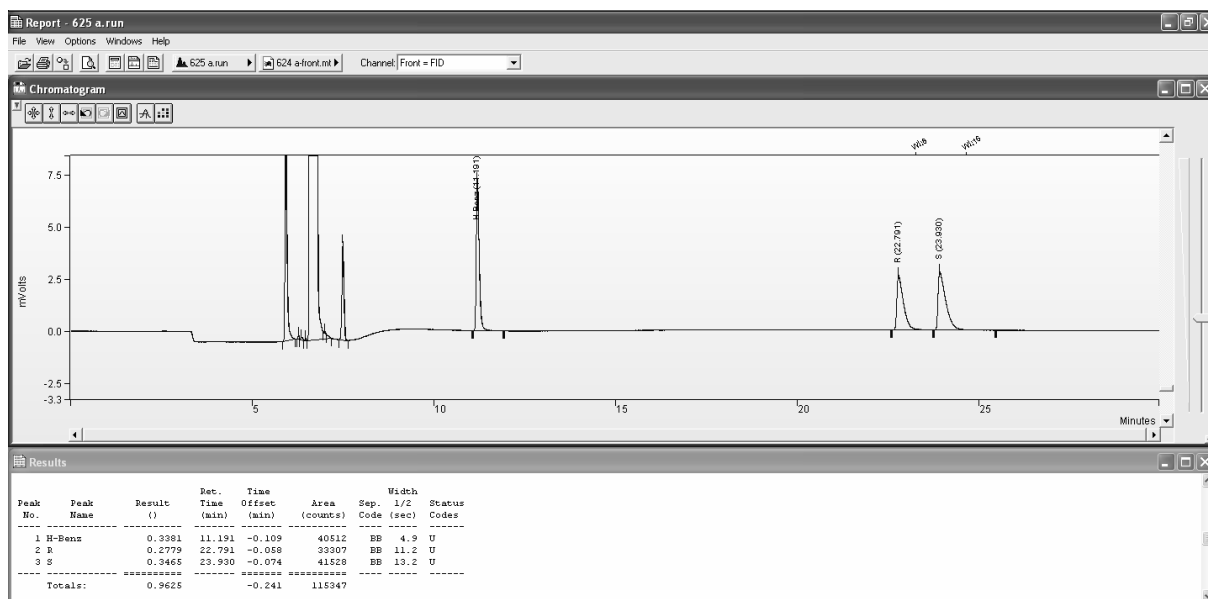
Supplementary Figure 5: Experimental $(\% \text{ Benzaldehyde})^{-1}$ vs time-plots of a) NBE (original data from ref. ²), b) NME-catalysed reactions. The ligands were used in their enantiopure form unless noted otherwise, at the indicated catalyst loading. The grey line in a) was obtained from 20 mol% racemic NBE which mostly precipitates. The mostly curved plots indicate a non-constant k_{obs} over time, which suggest a participation of the substrate/reactant and/or of the reaction product in the catalytic system.

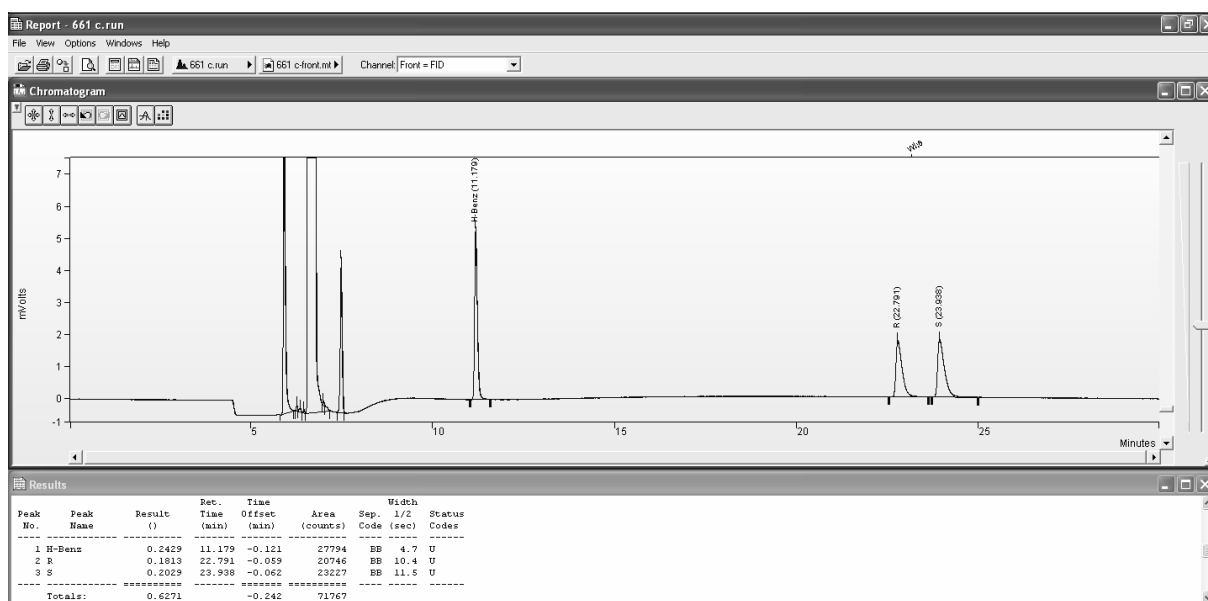
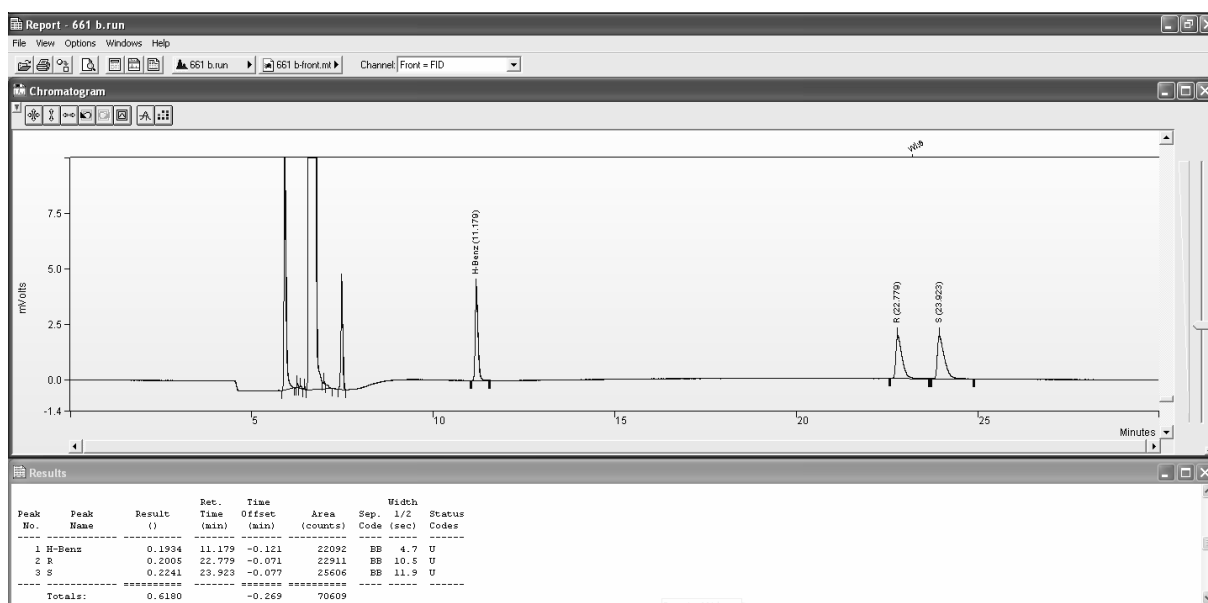
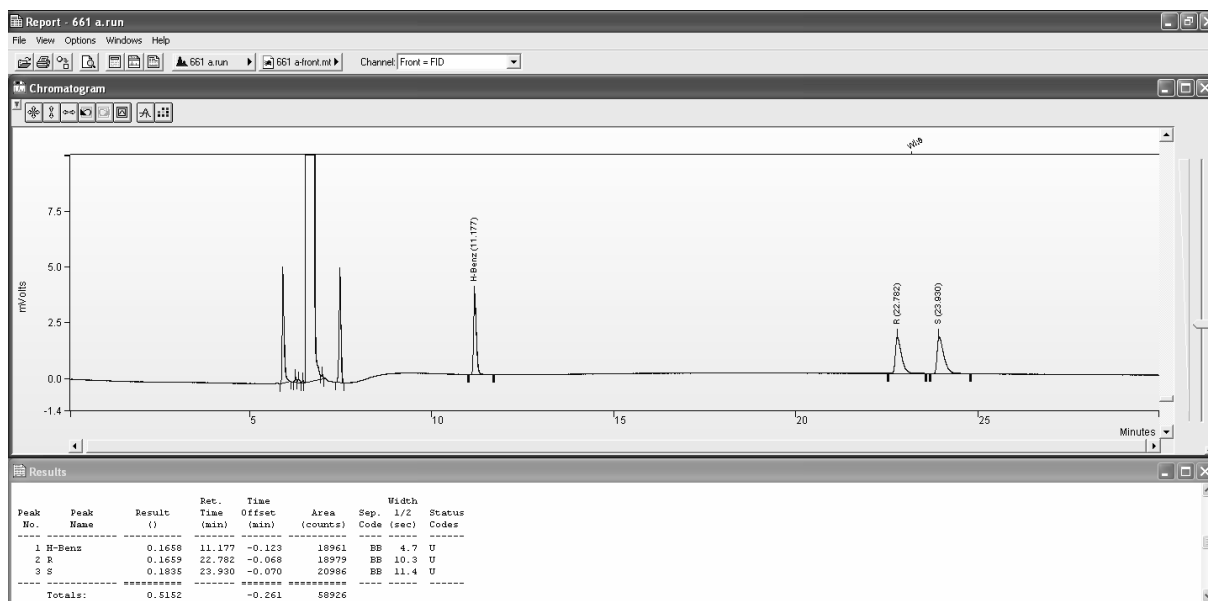


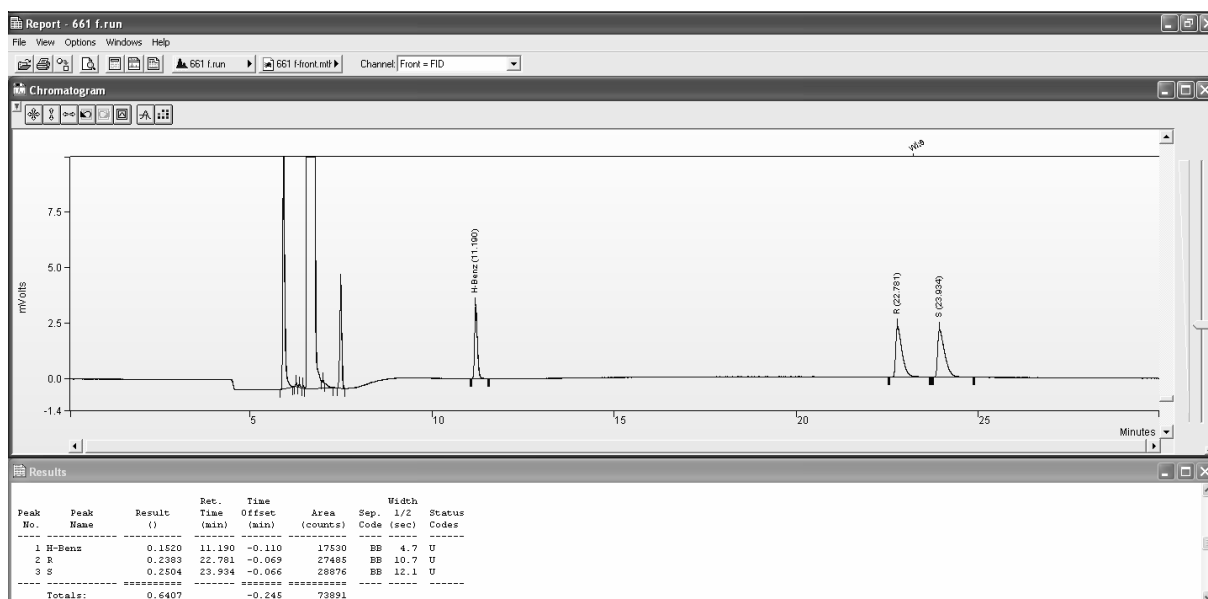
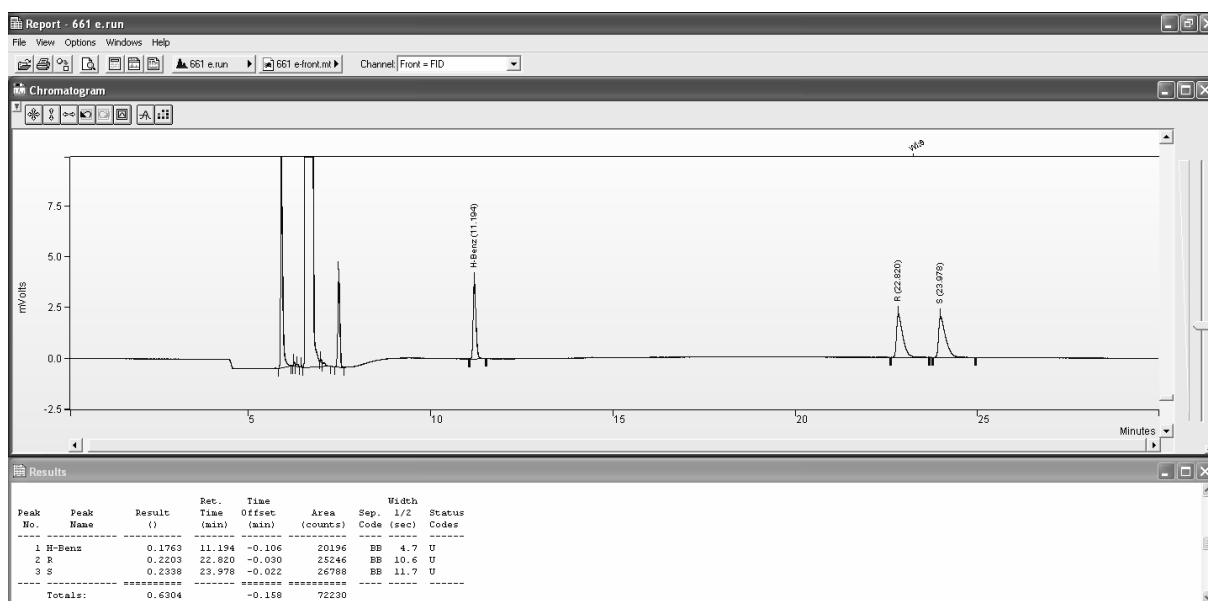
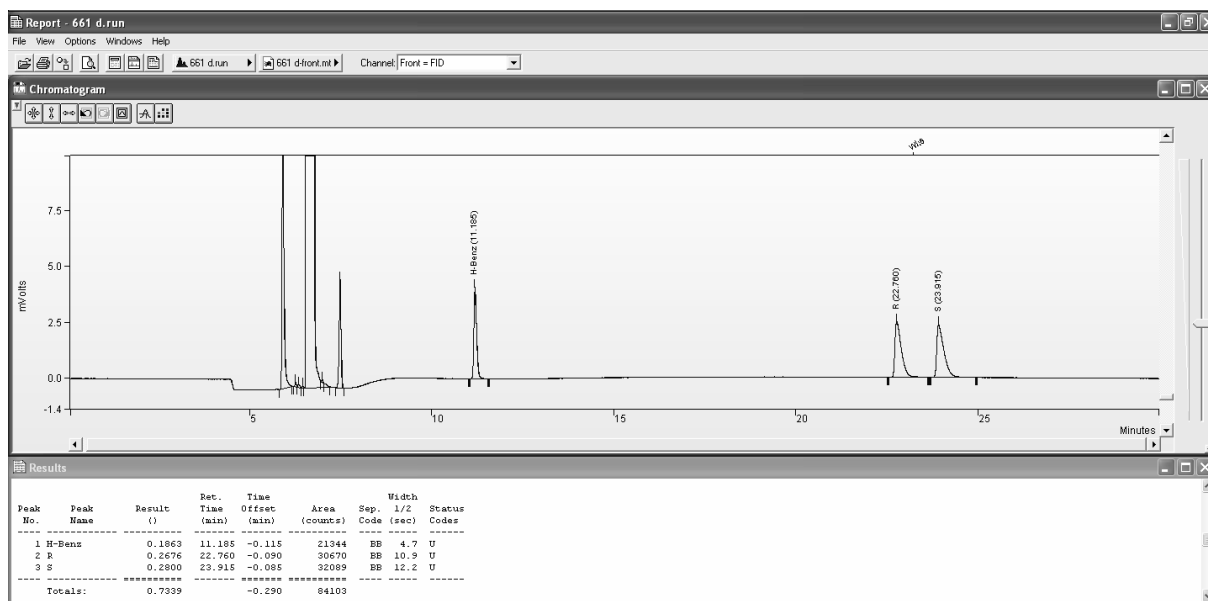
Supplementary Figure 6: Catalyst loading screening of the (-)-NME-catalysed addition of ZnMe_2 to 0.83 M benzaldehyde at 0 °C. Each point is the mean of three independent experiments; the vertical bars depict standard deviations. The product ee is defined as $(P_R - P_S)/(P_R + P_S)$. Upon addition of ZnMe_2 to 20 and 15 mol% (-)-NME (blue crosses), a white precipitate appeared which vanished over the course of the reaction; the runs with lower catalyst loading (blue dots) didn't exhibit any precipitate. This supports the hypothesis of a partly soluble homochiral aggregate which saturates the solution only when the catalyst concentration is sufficiently high. Therefore, the amount of soluble catalyst was limited by the aggregate's solubility in the runs at 15 and 20 mol%, which explains their similar ee_p-values. The vanishing of the precipitate over the course of the reaction can be explained by the continuous production of P_R and P_S , leading to catalyst-product-adducts which drive the solubilisation of the homochiral aggregate.

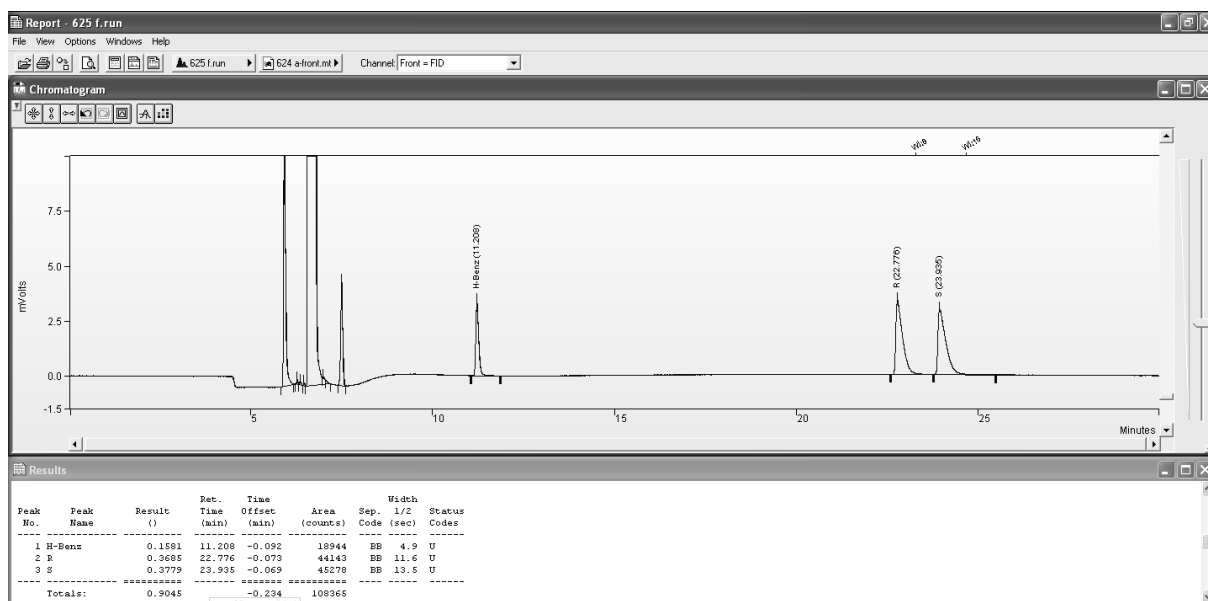
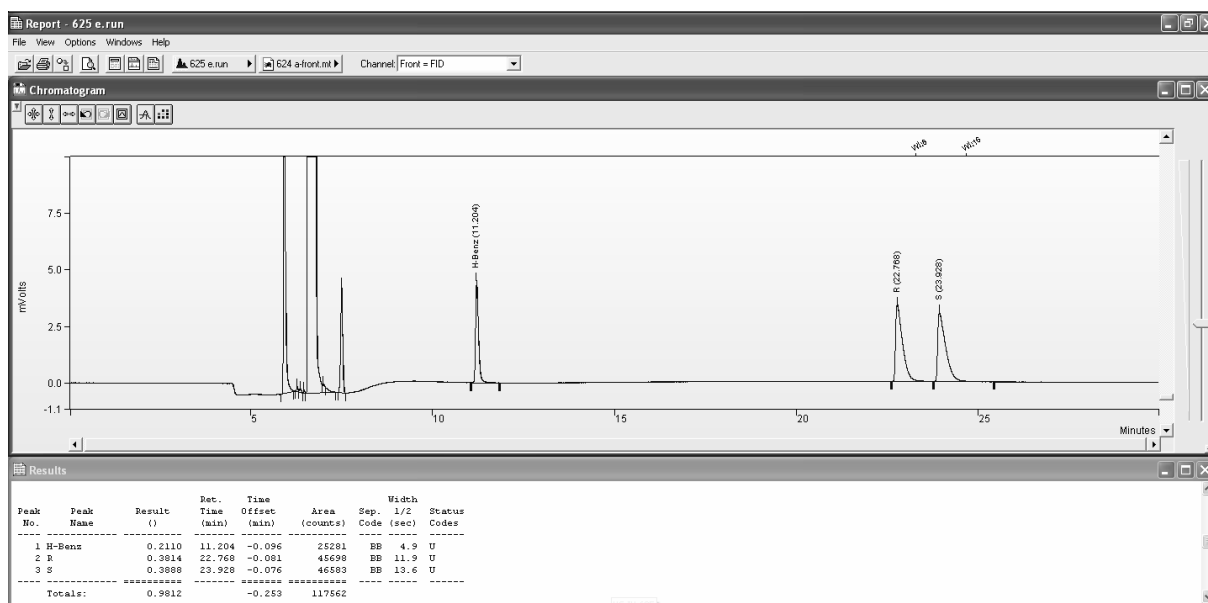
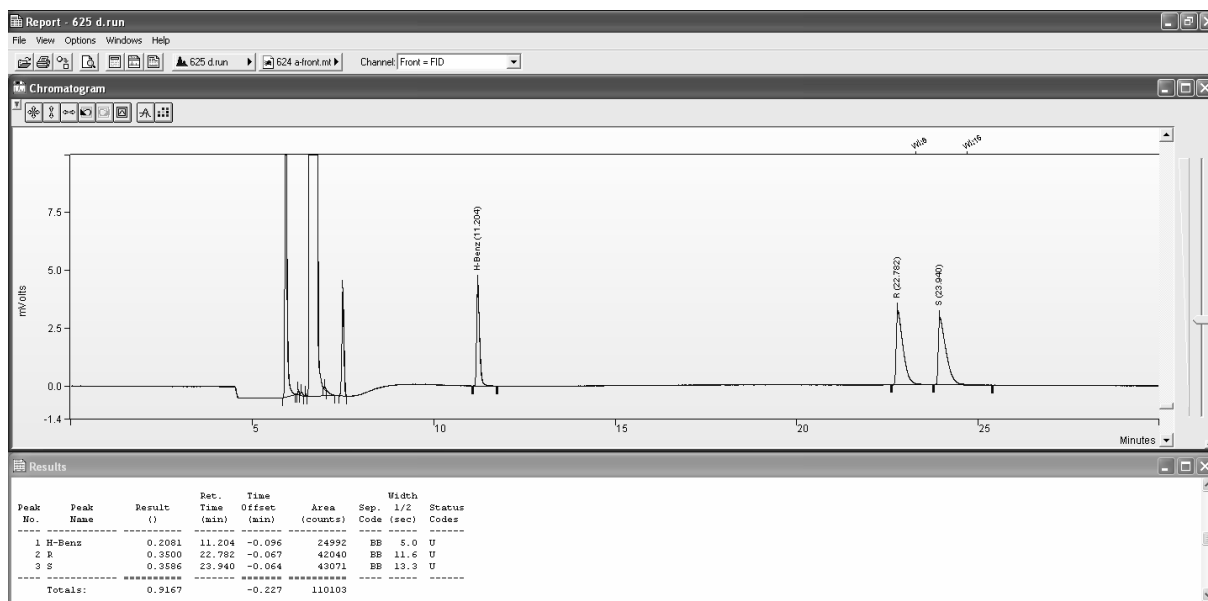
III: Supplementary Chromatograms

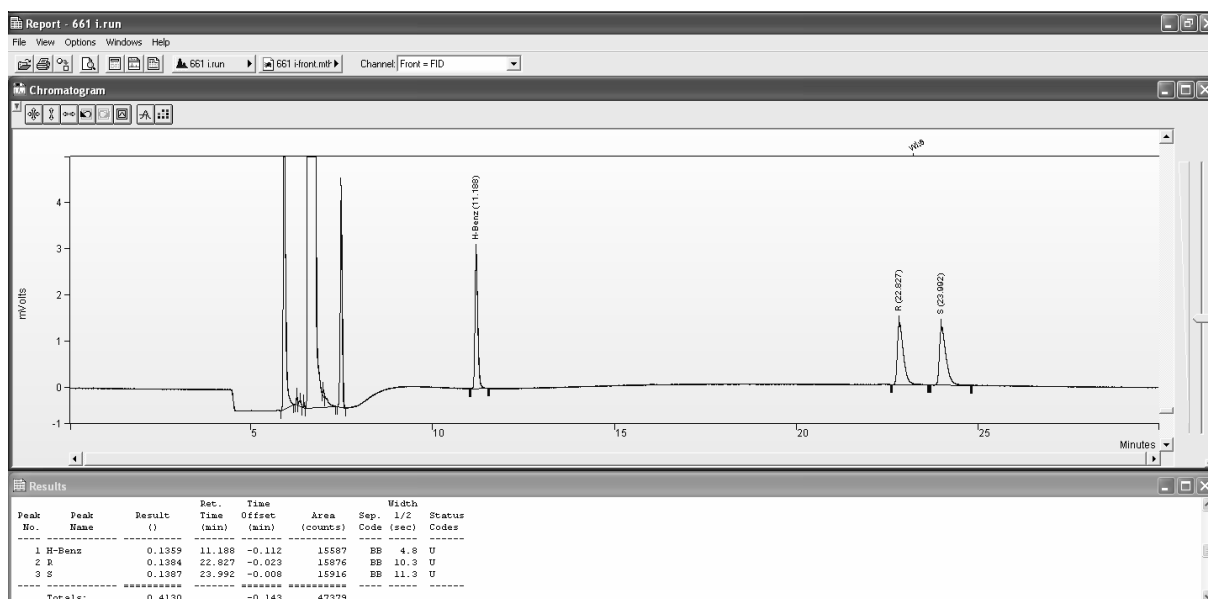
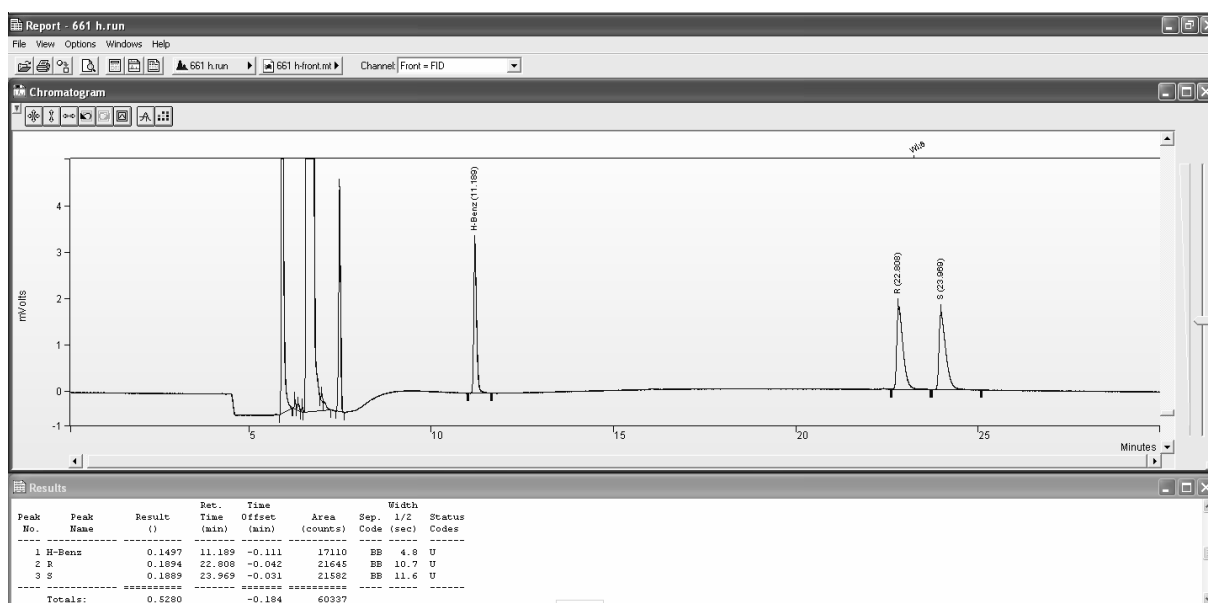
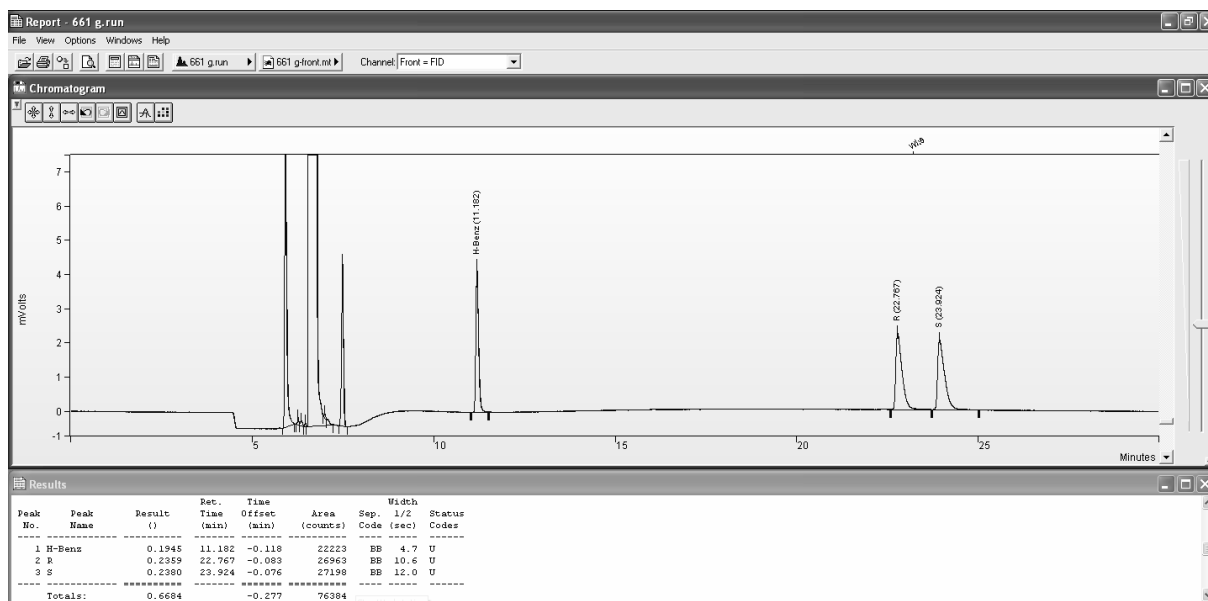
III.1 Figure 2a (NME)

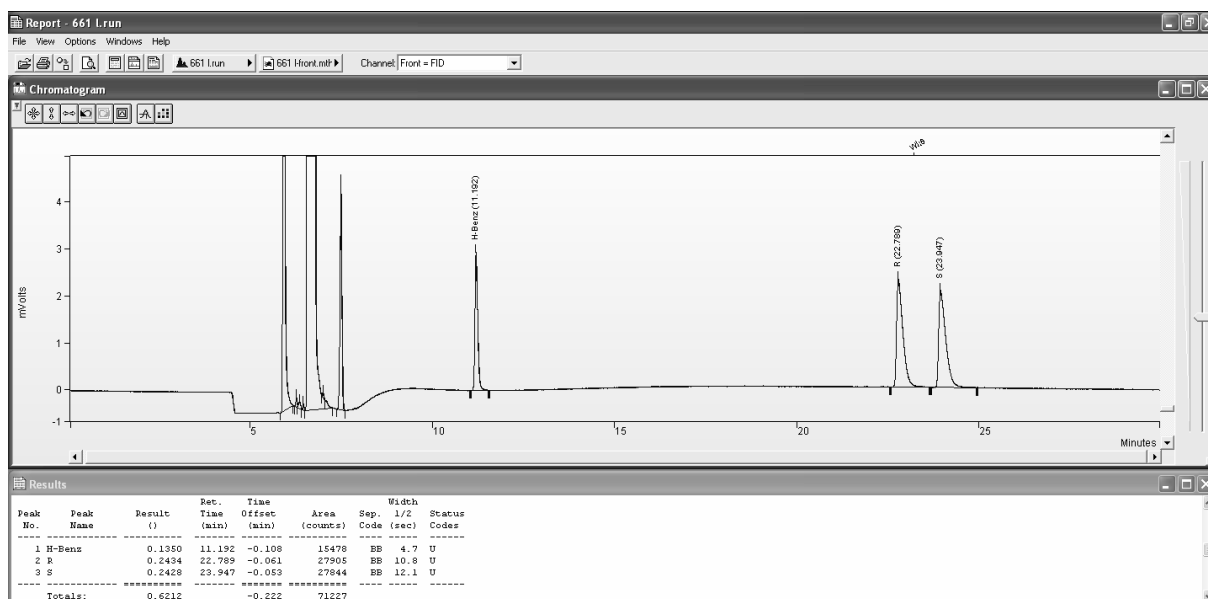
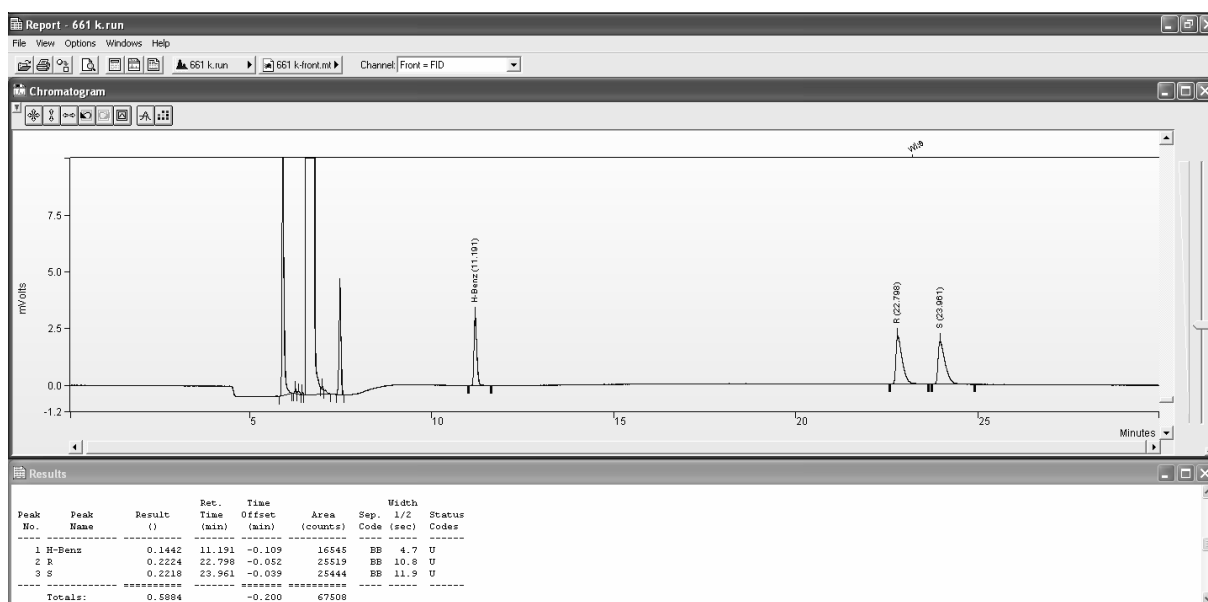
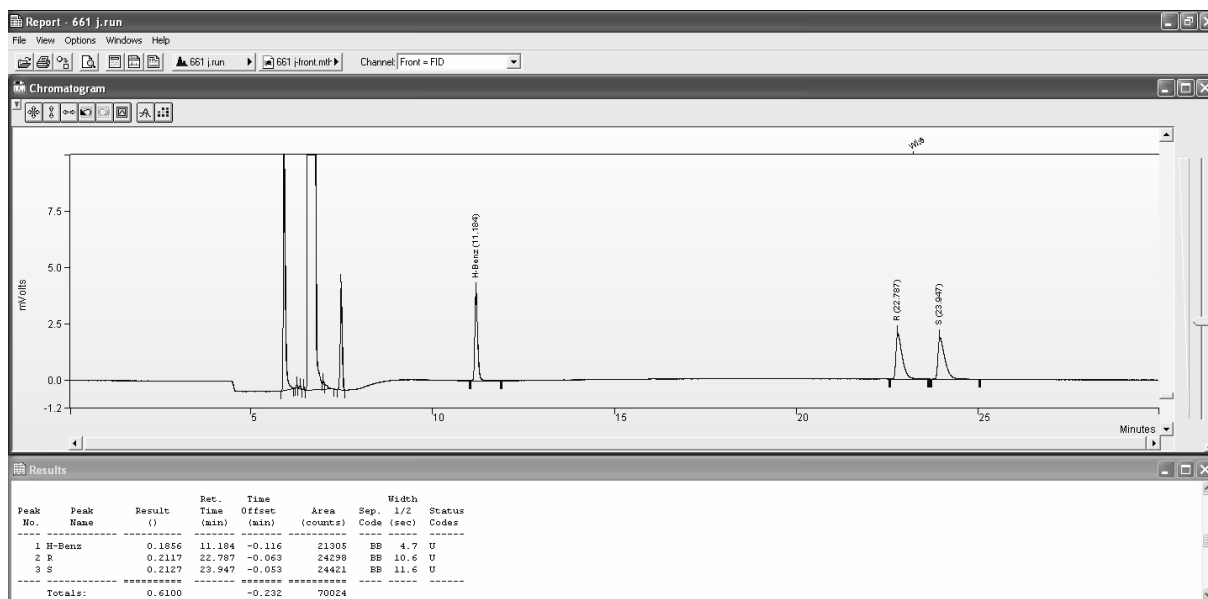




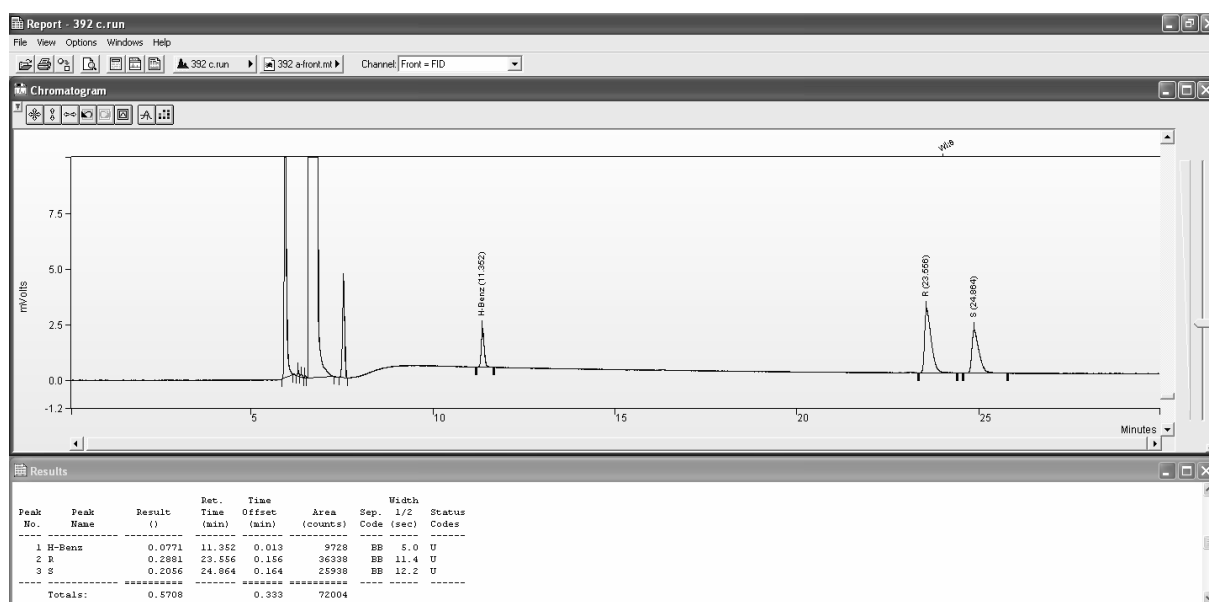
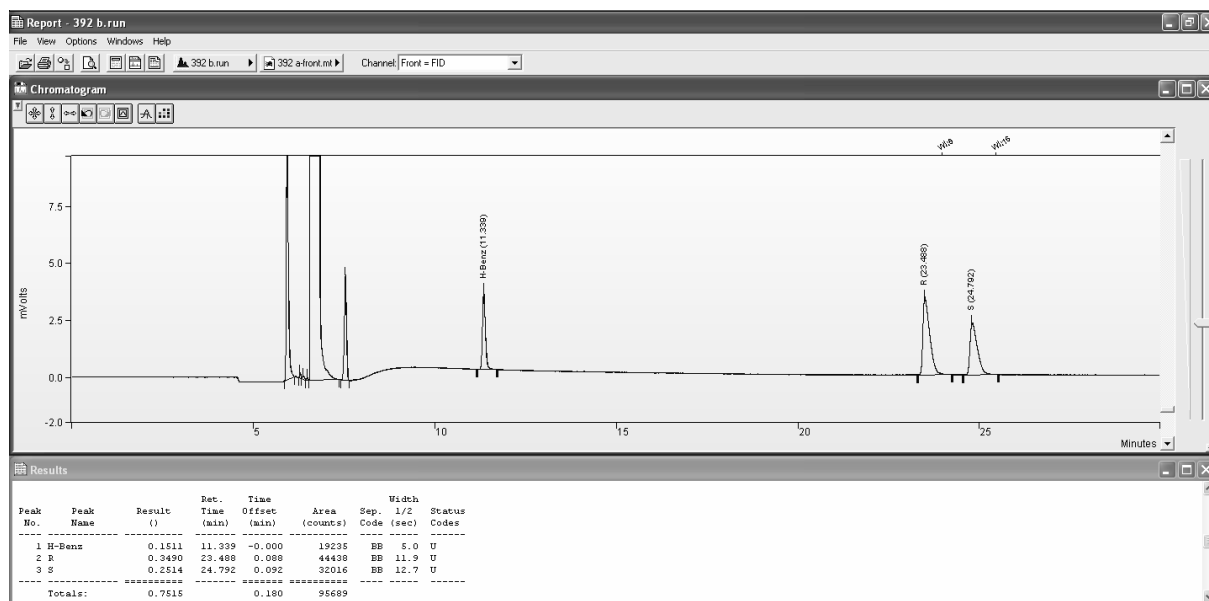


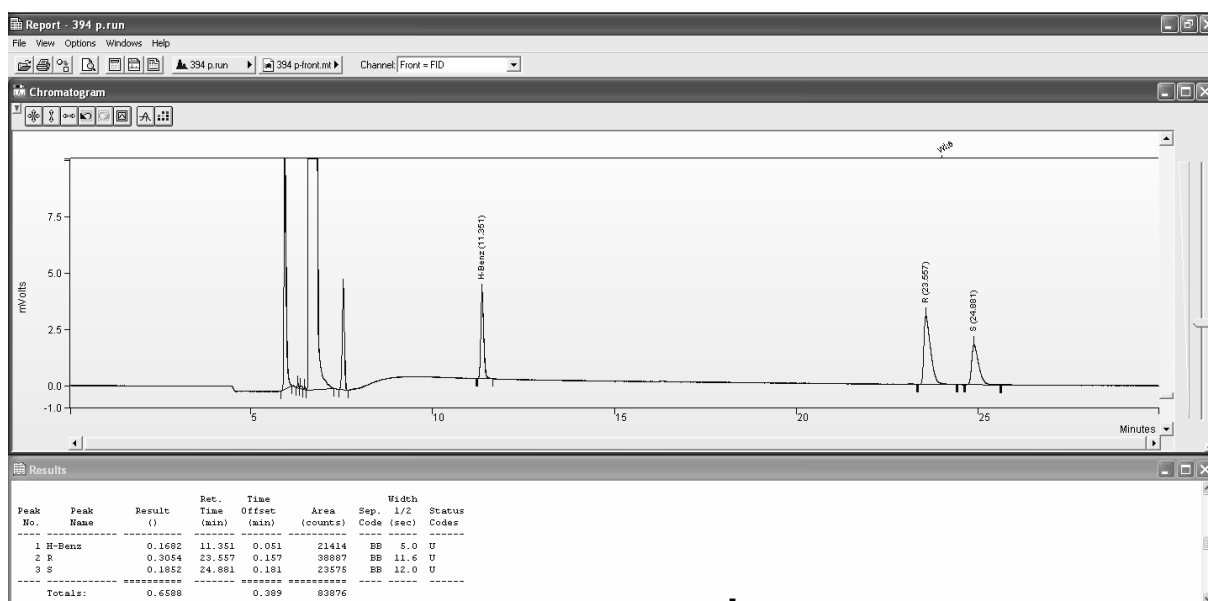
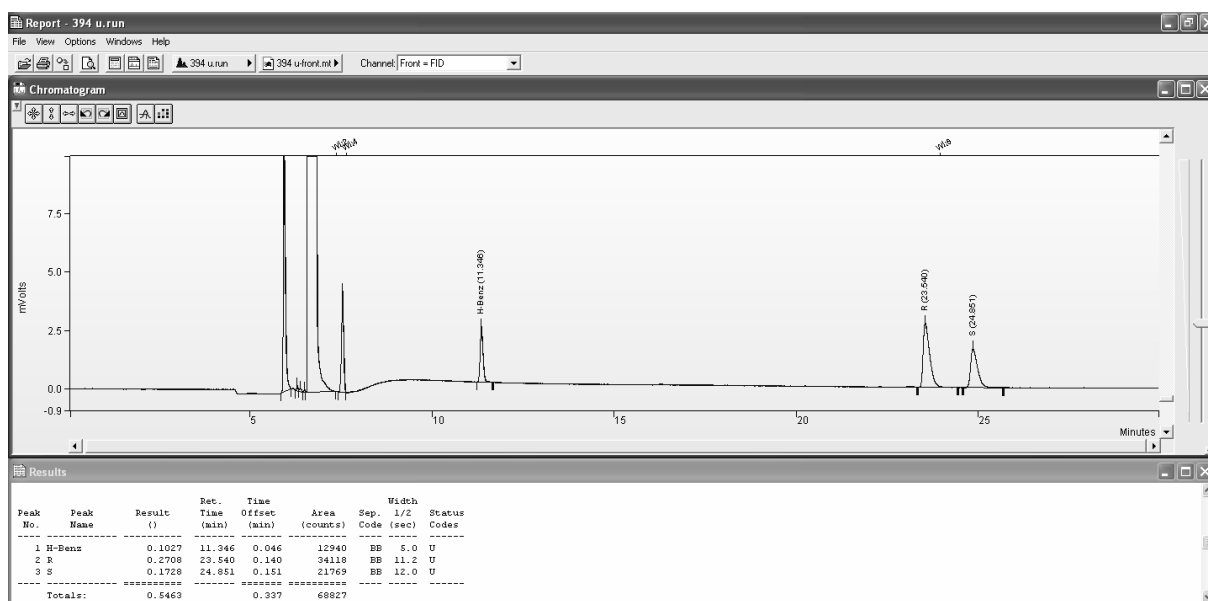
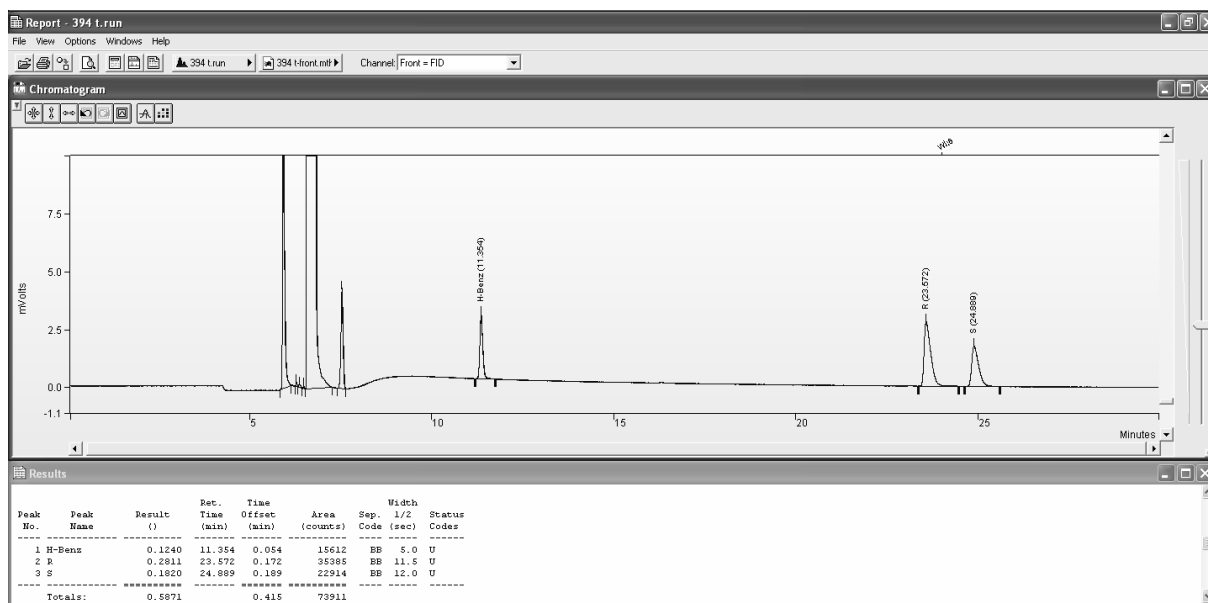


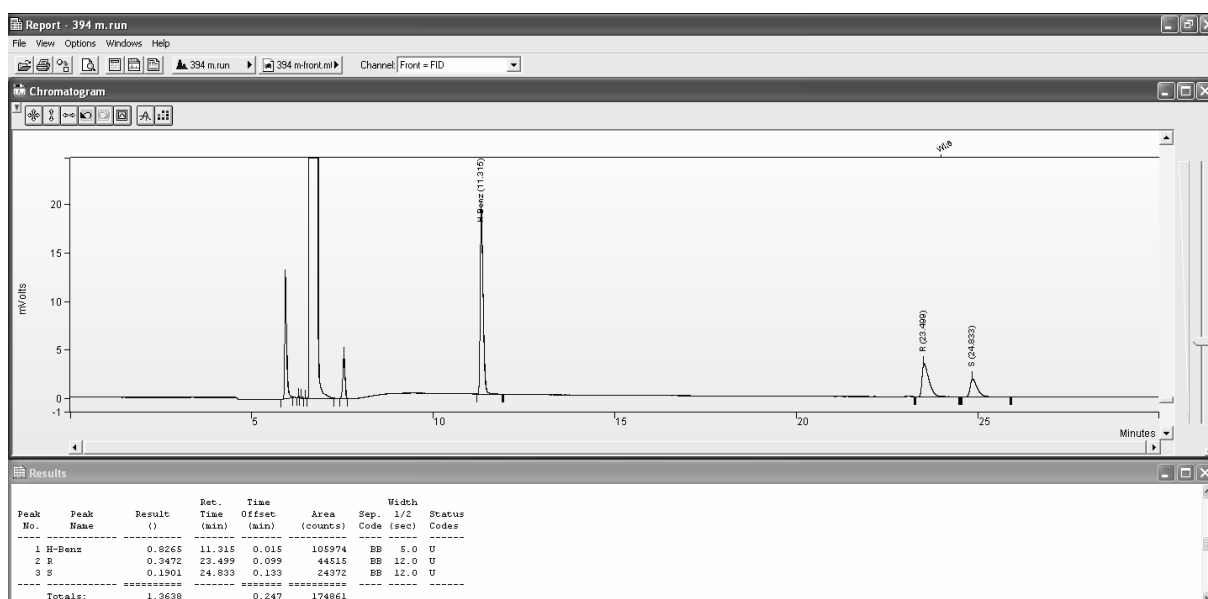
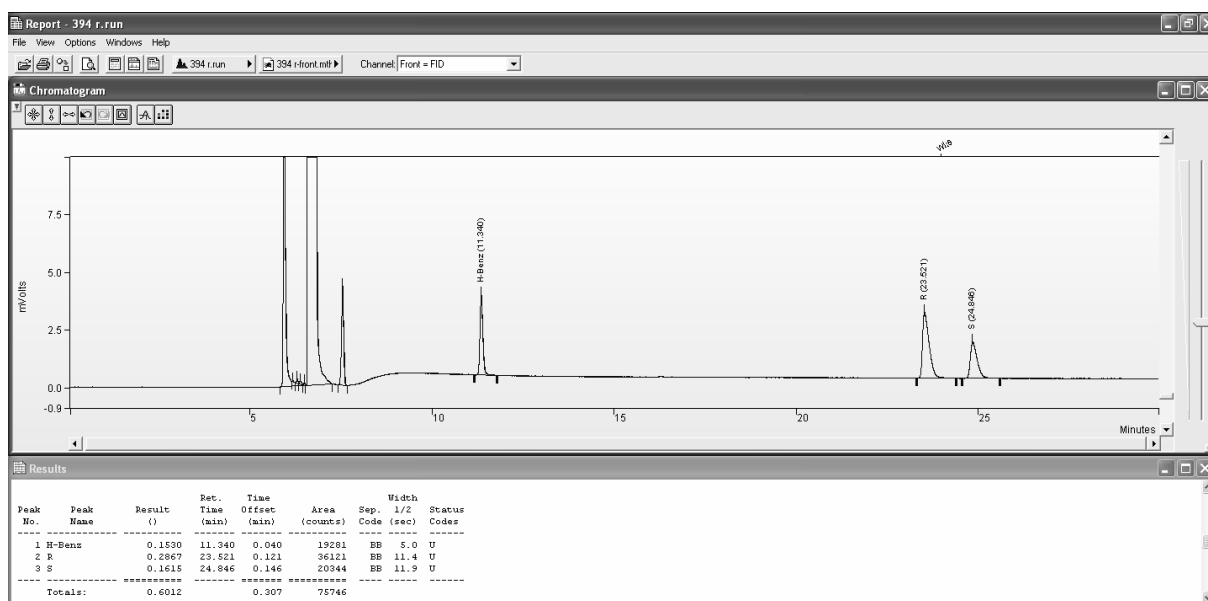
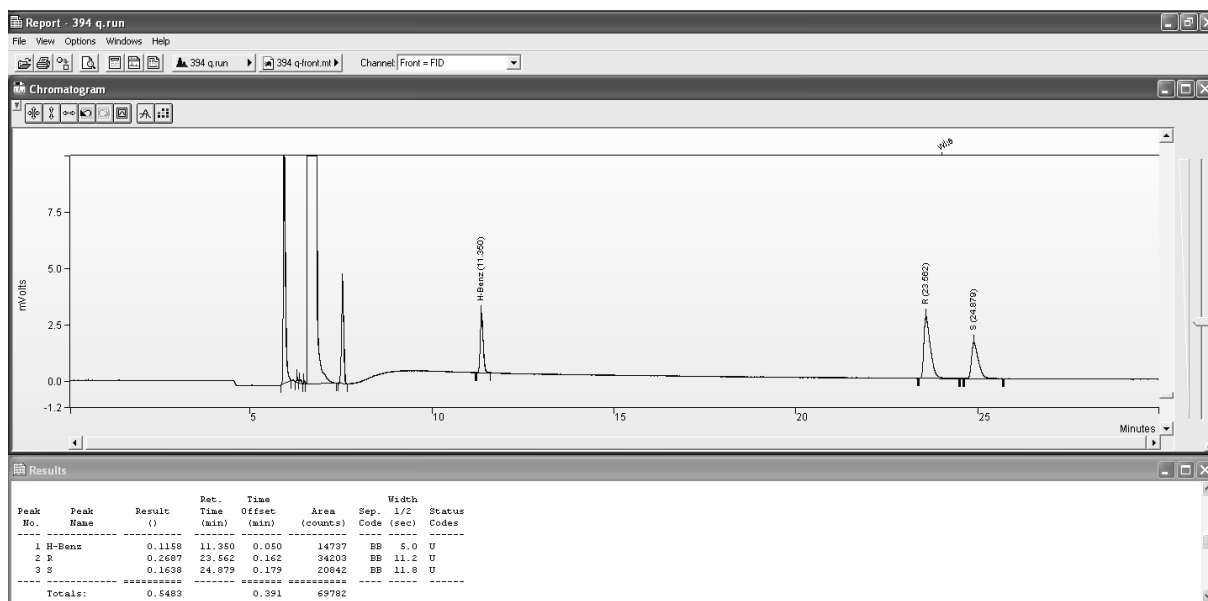


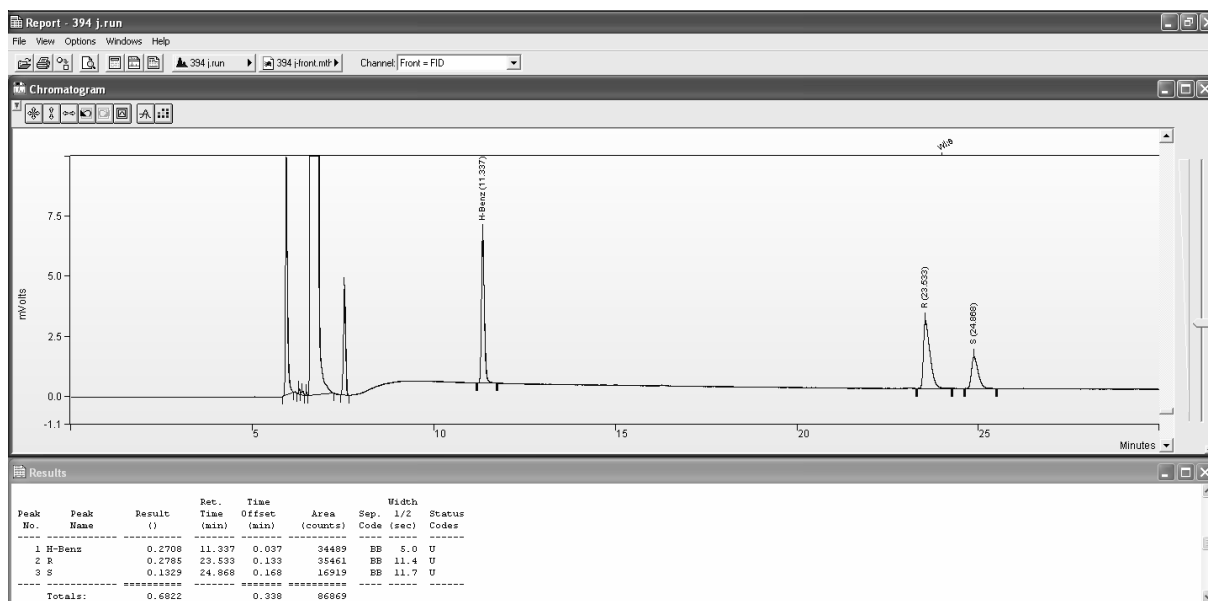
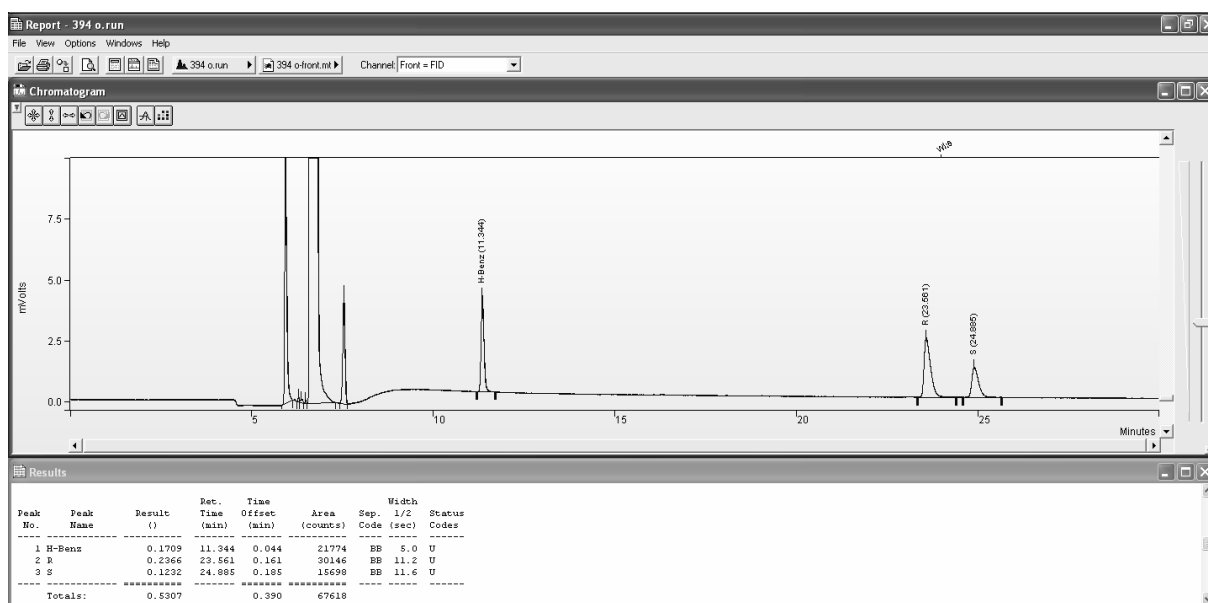
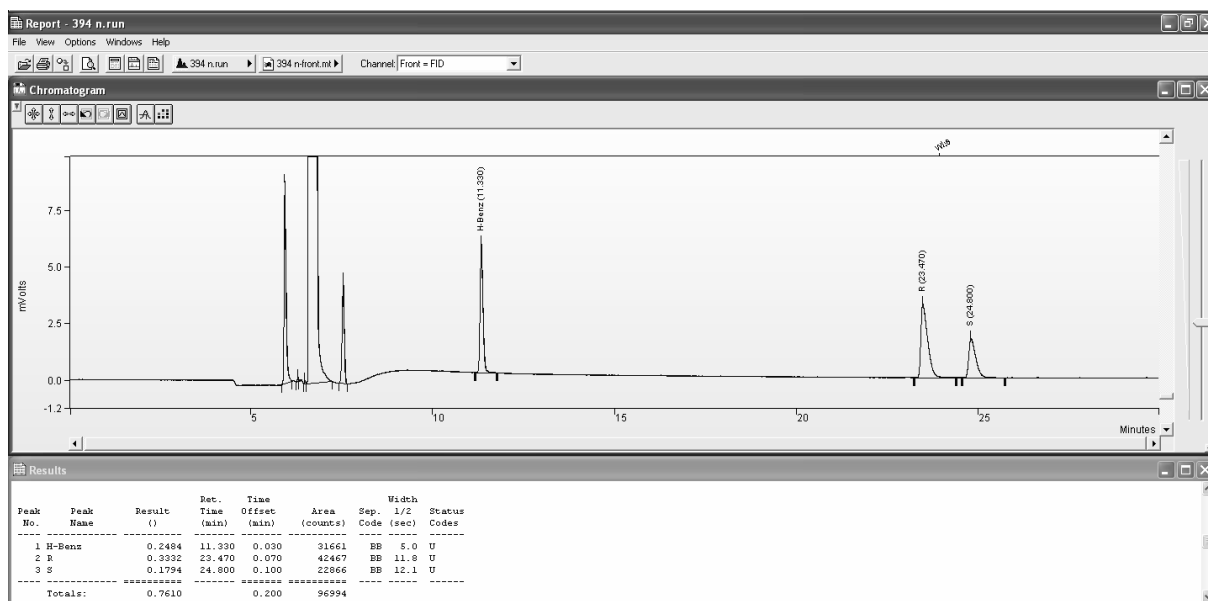


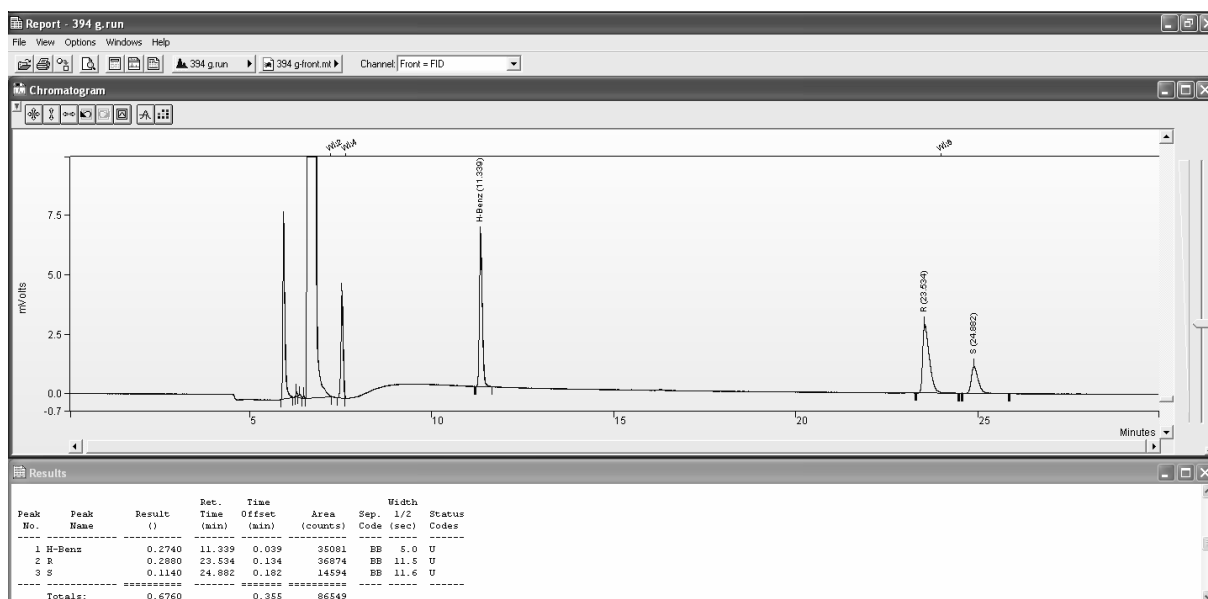
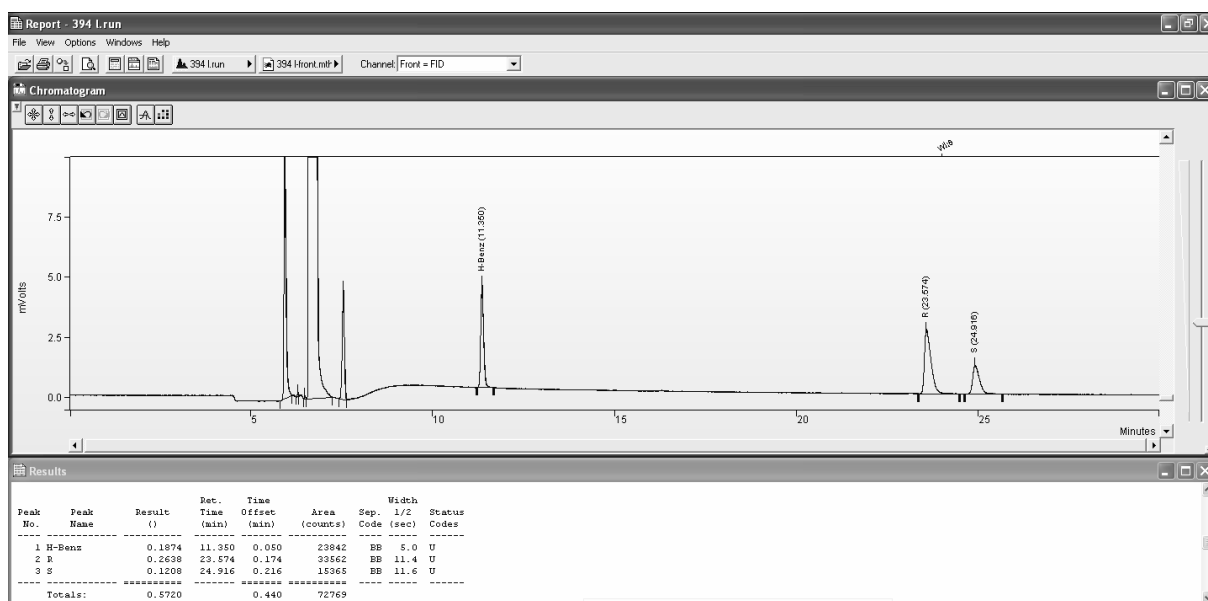
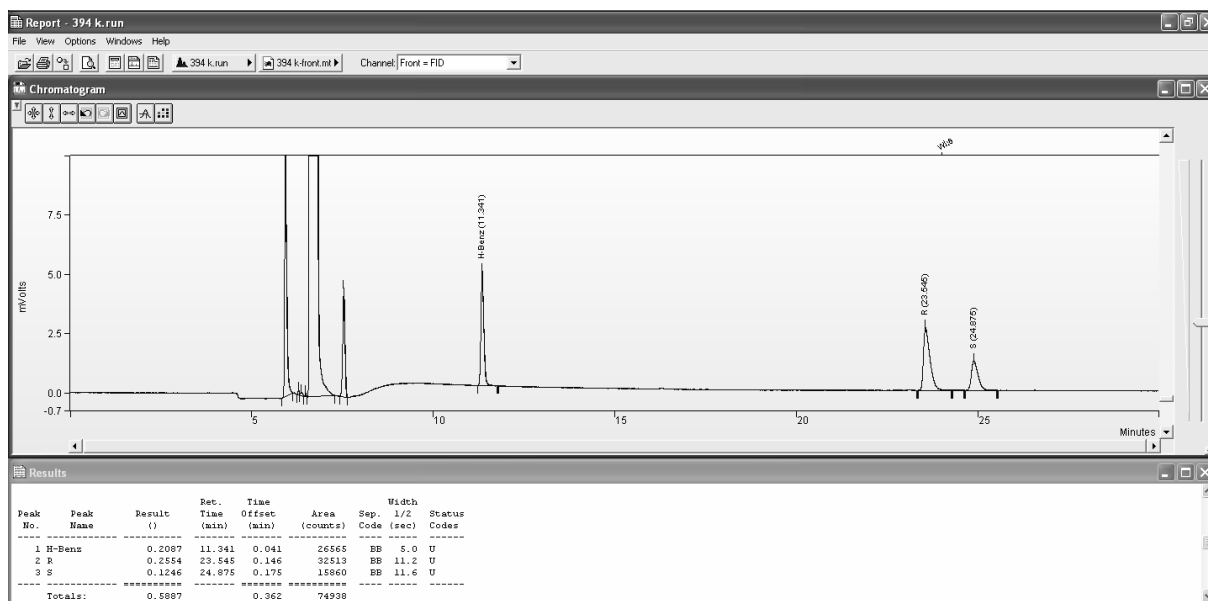
III.2 Figure 2a (NBE)

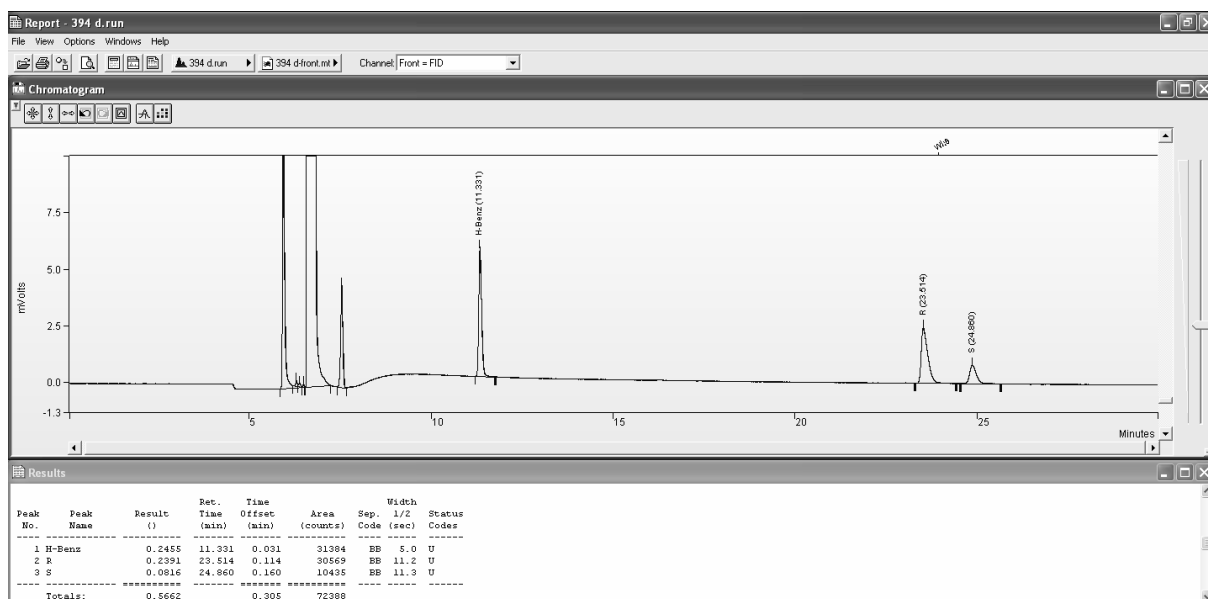
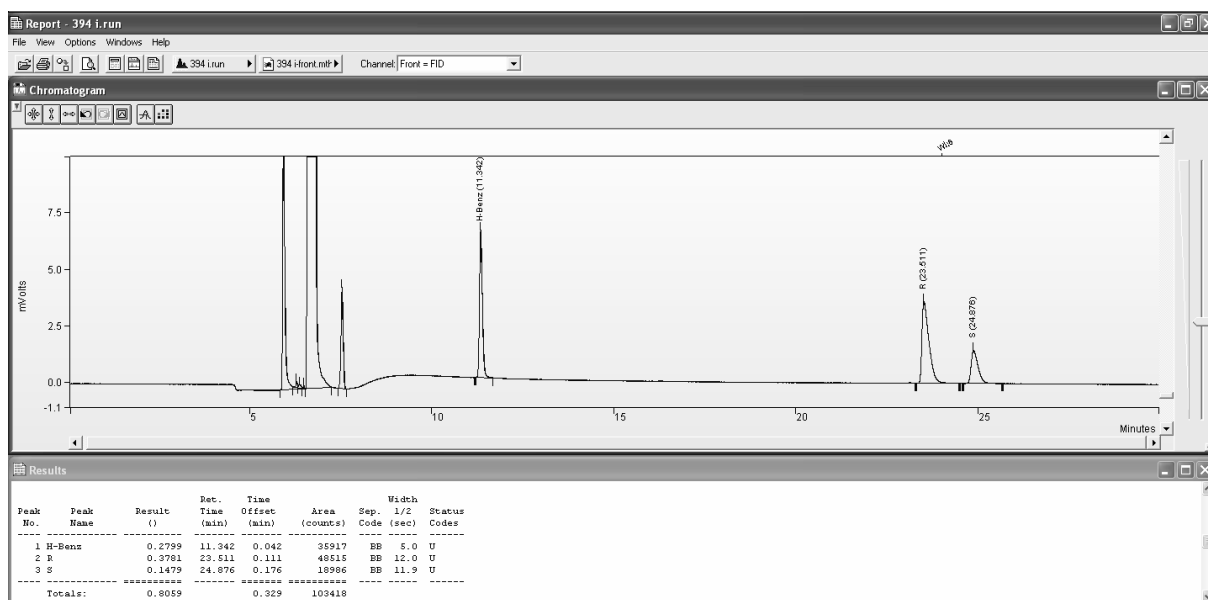
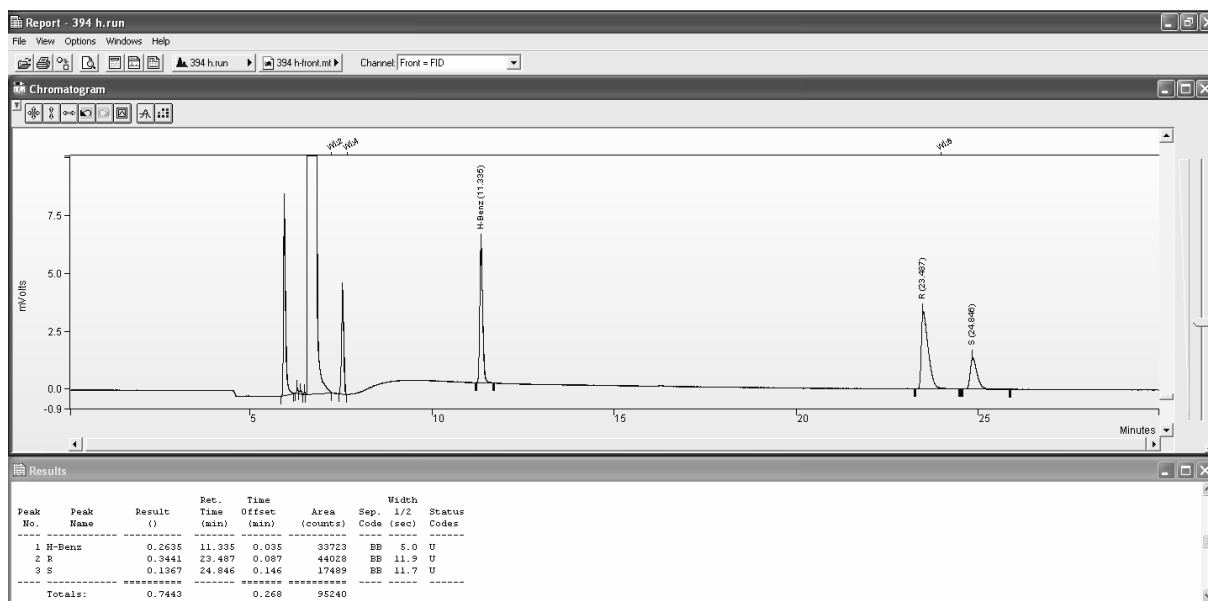


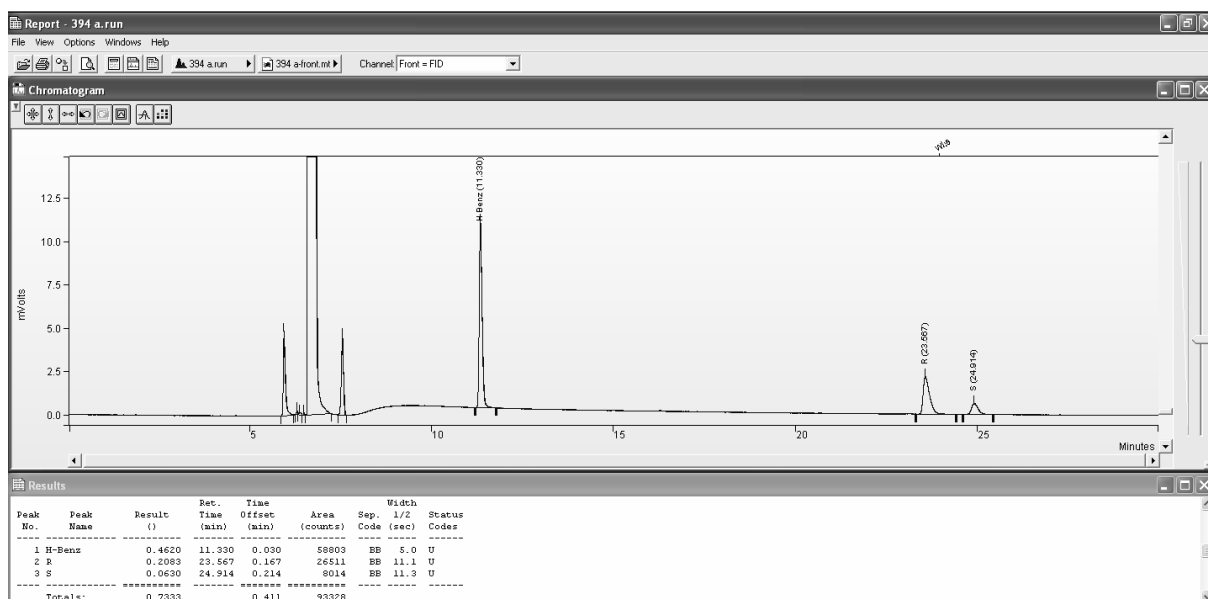
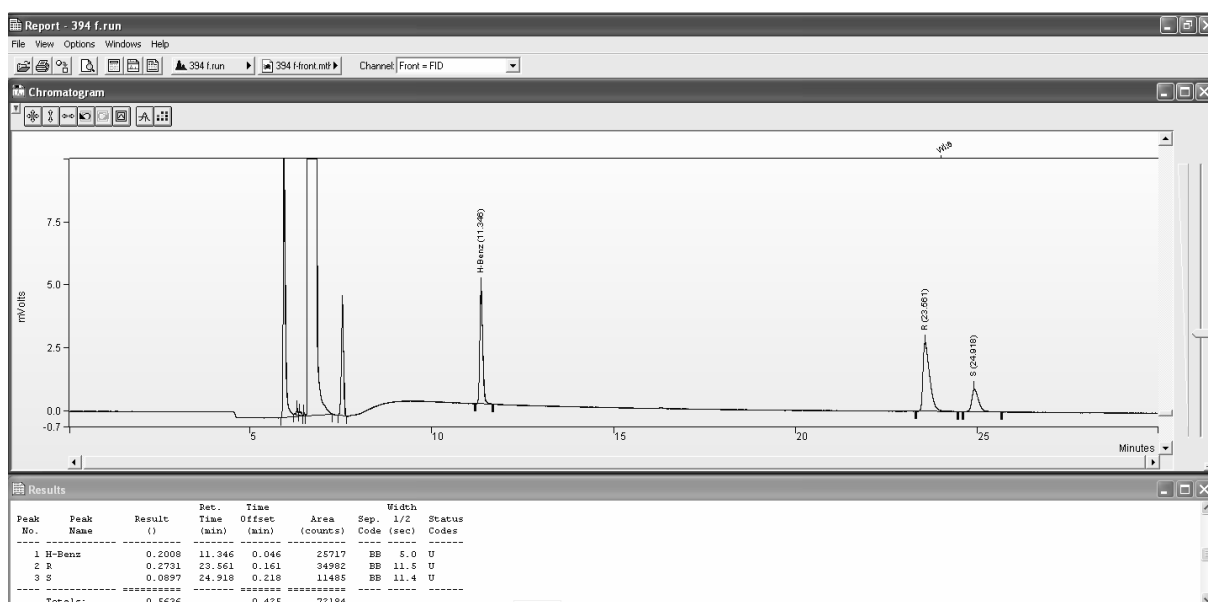
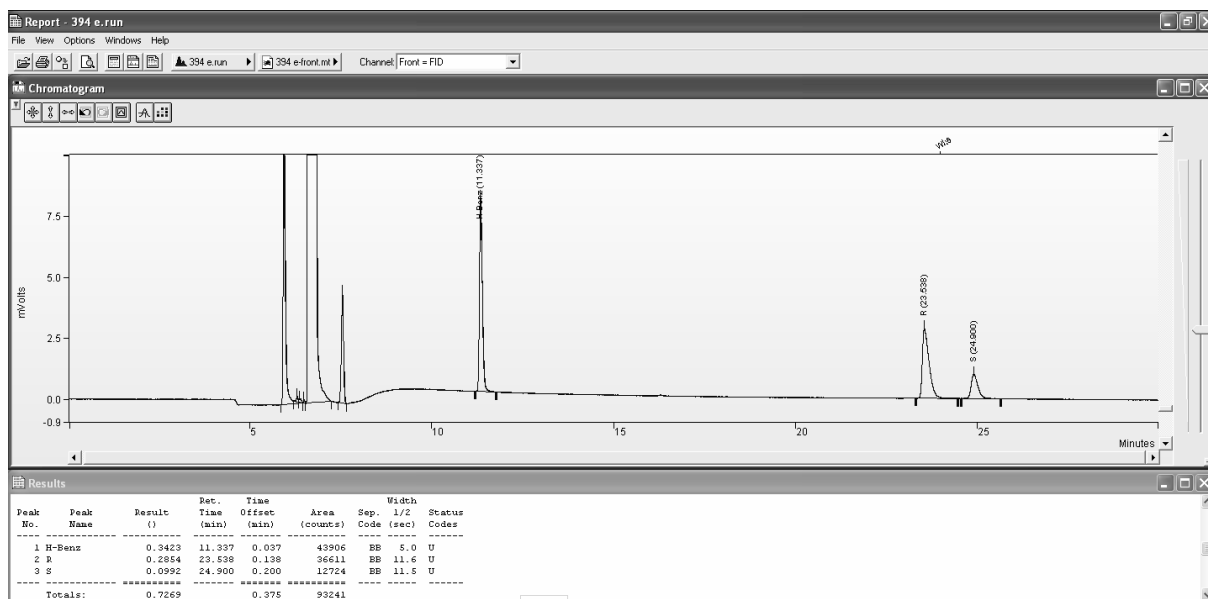


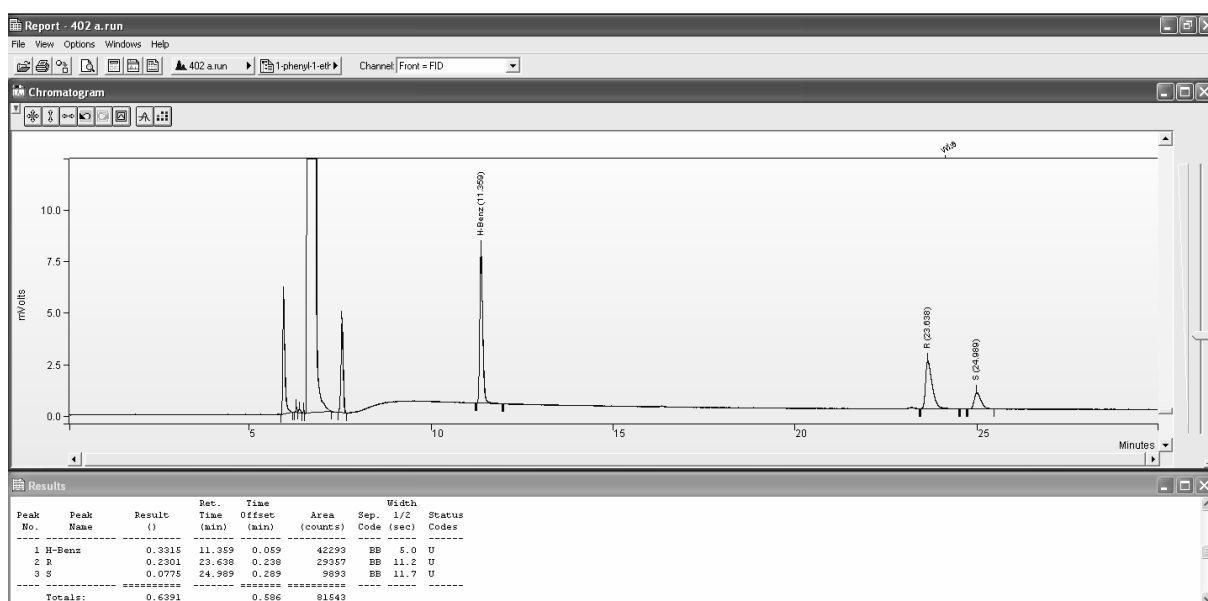
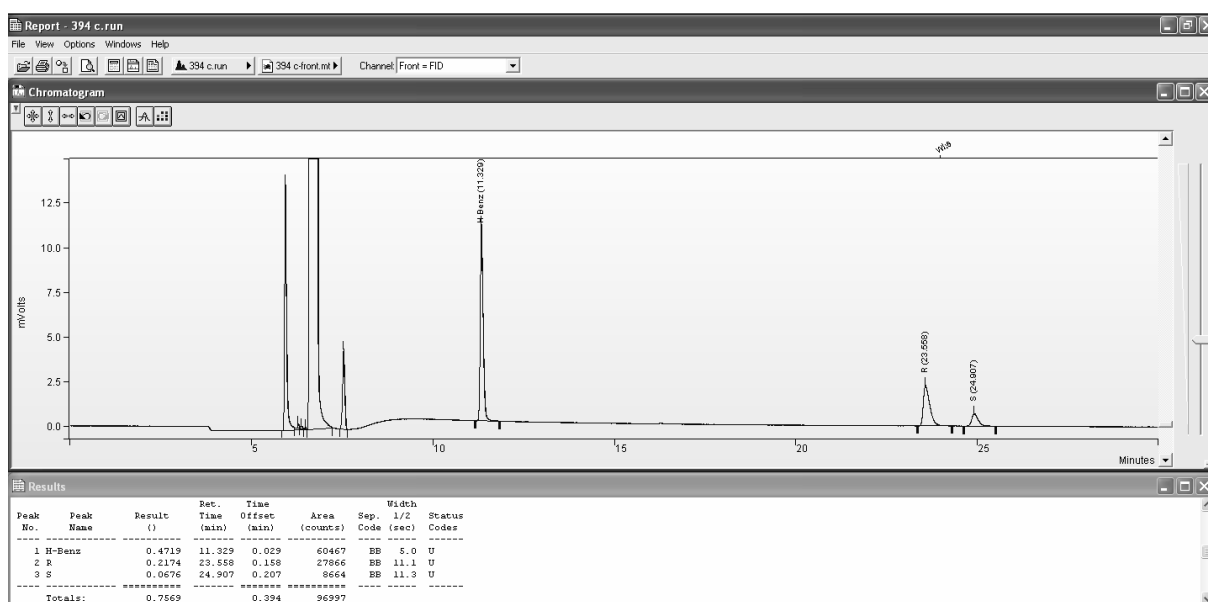
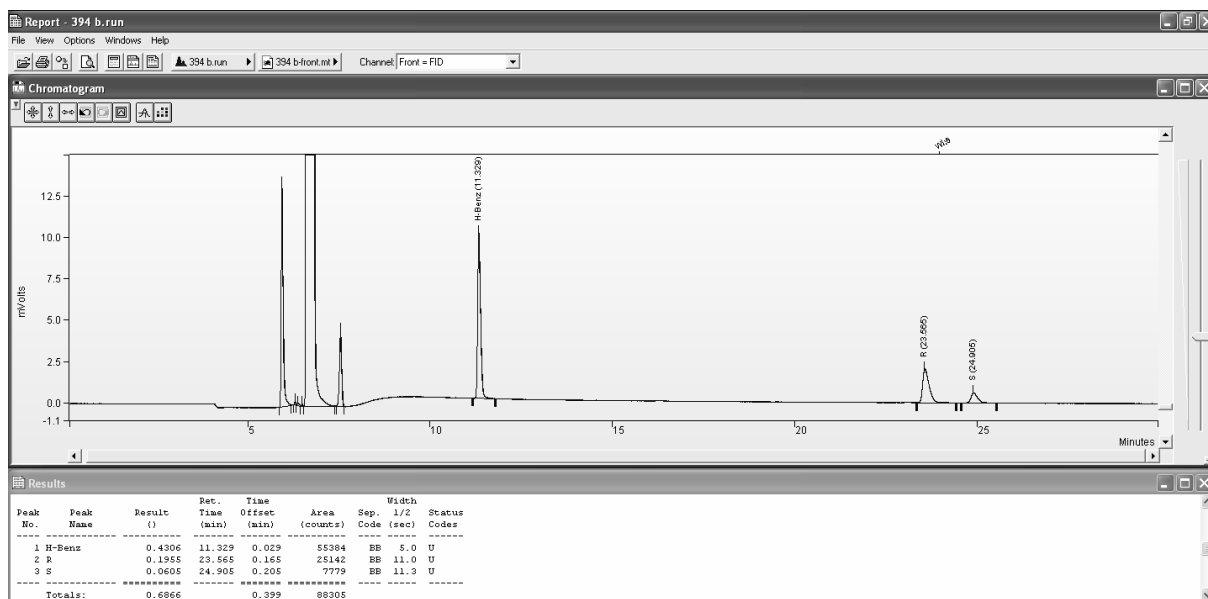


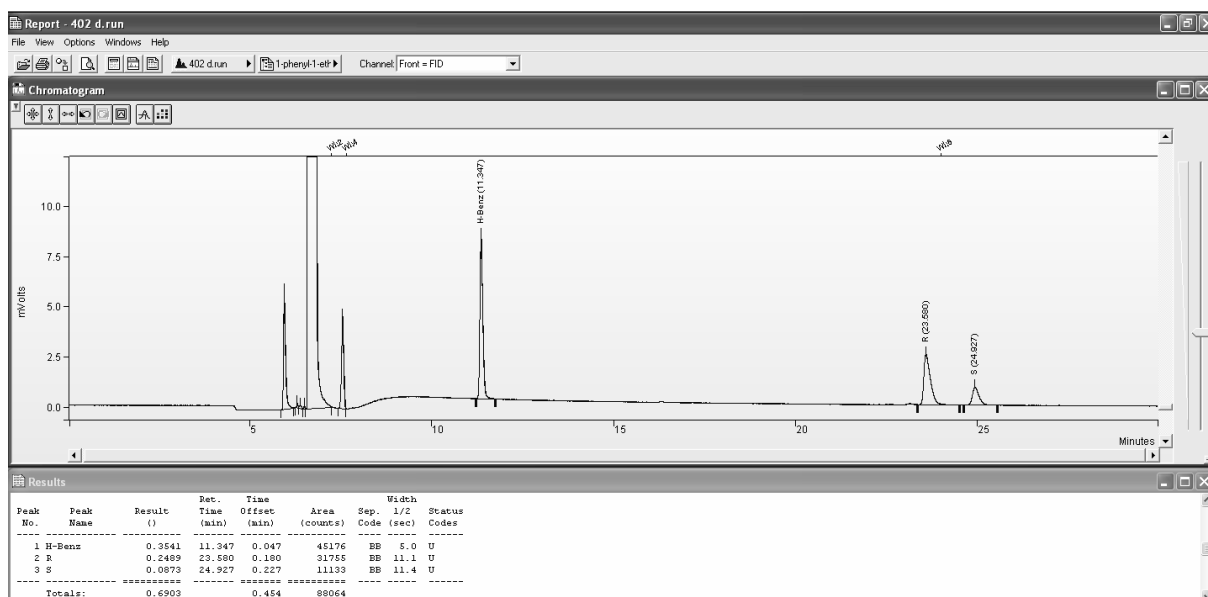
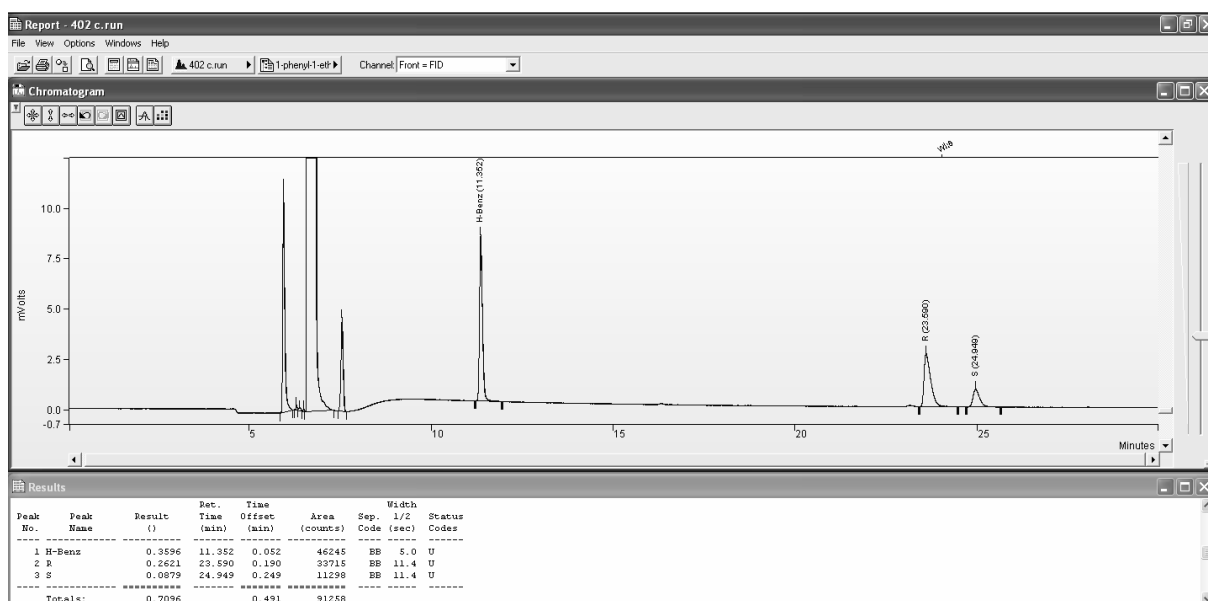
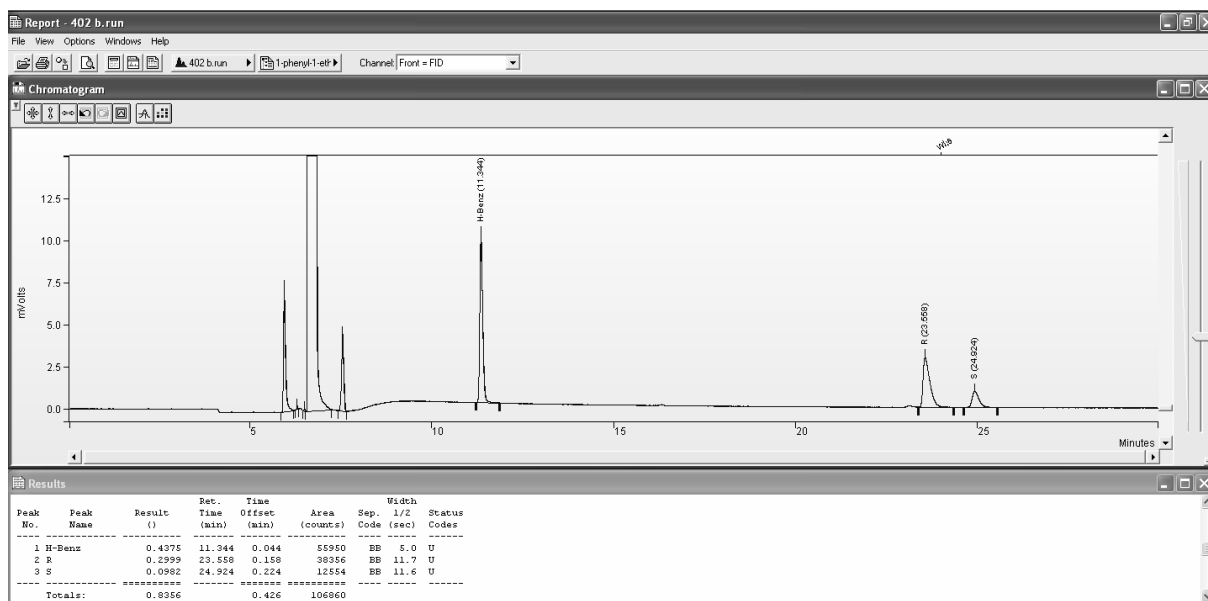


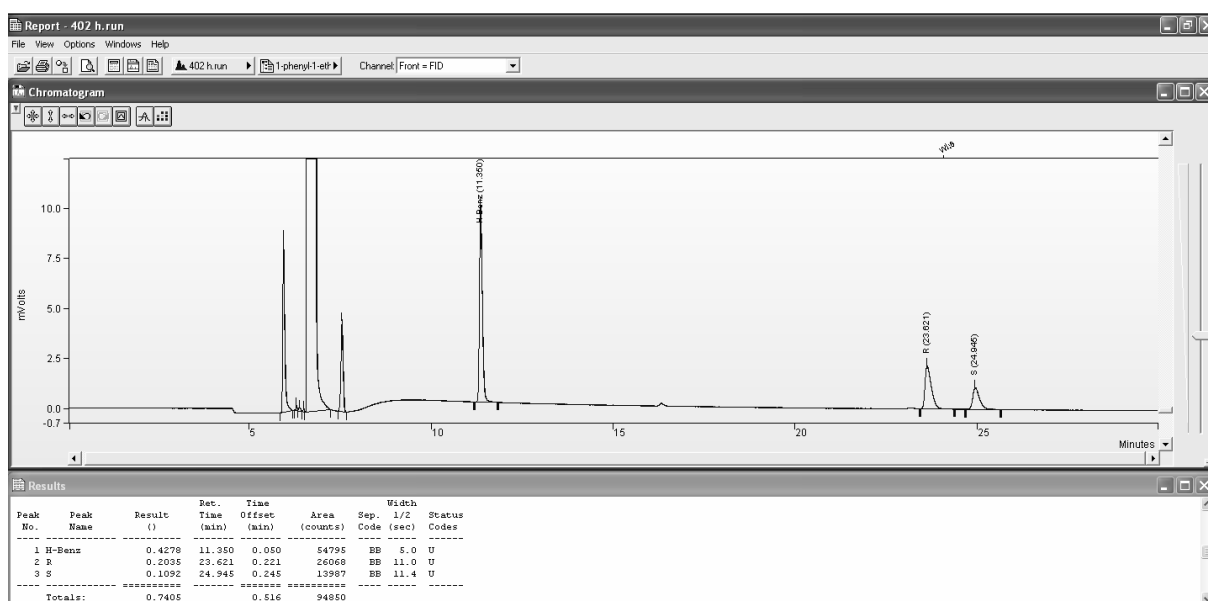
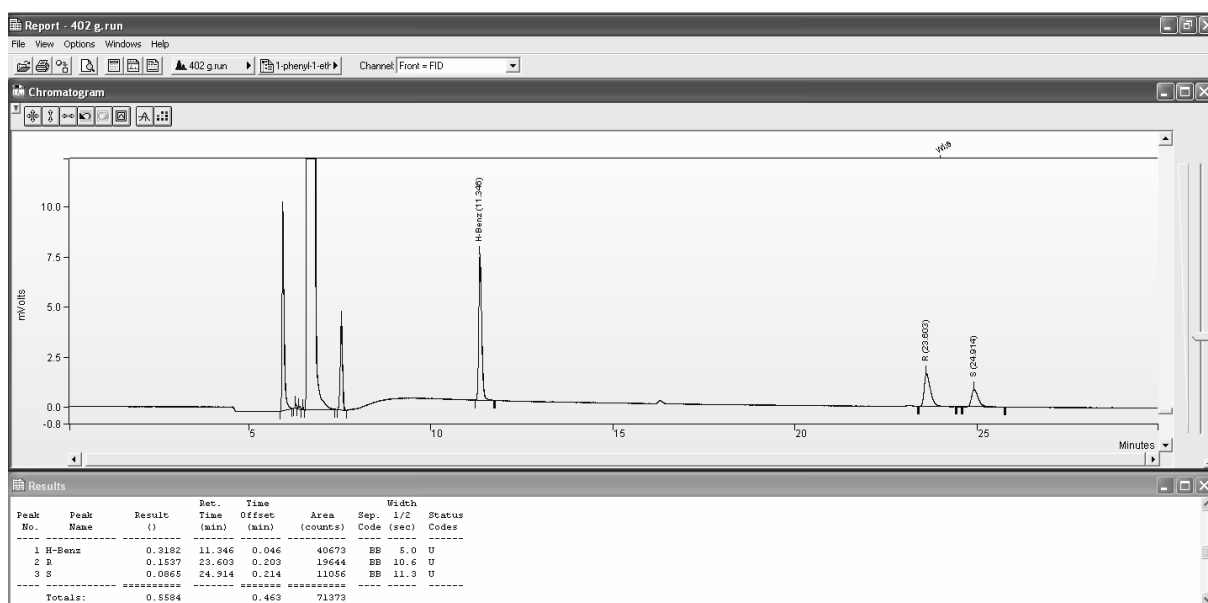
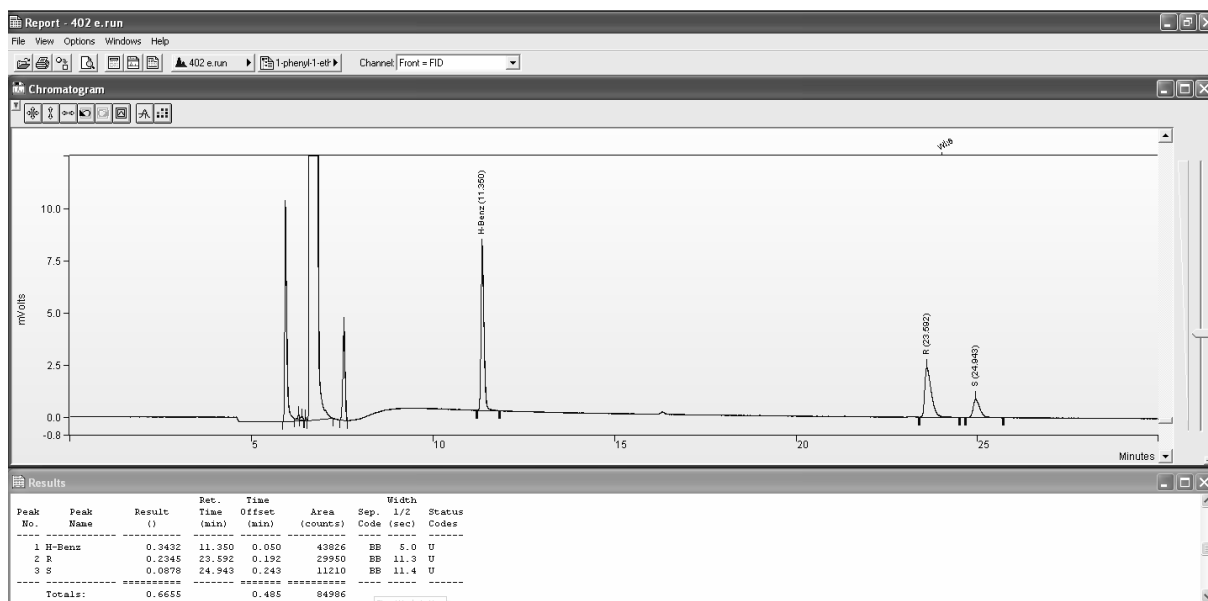


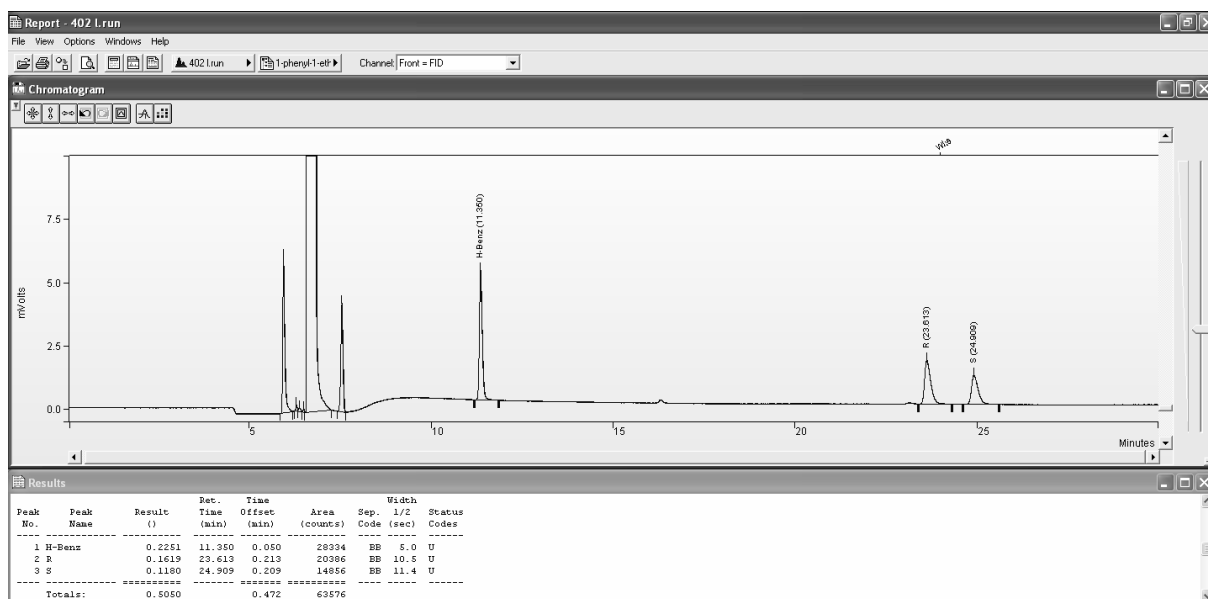
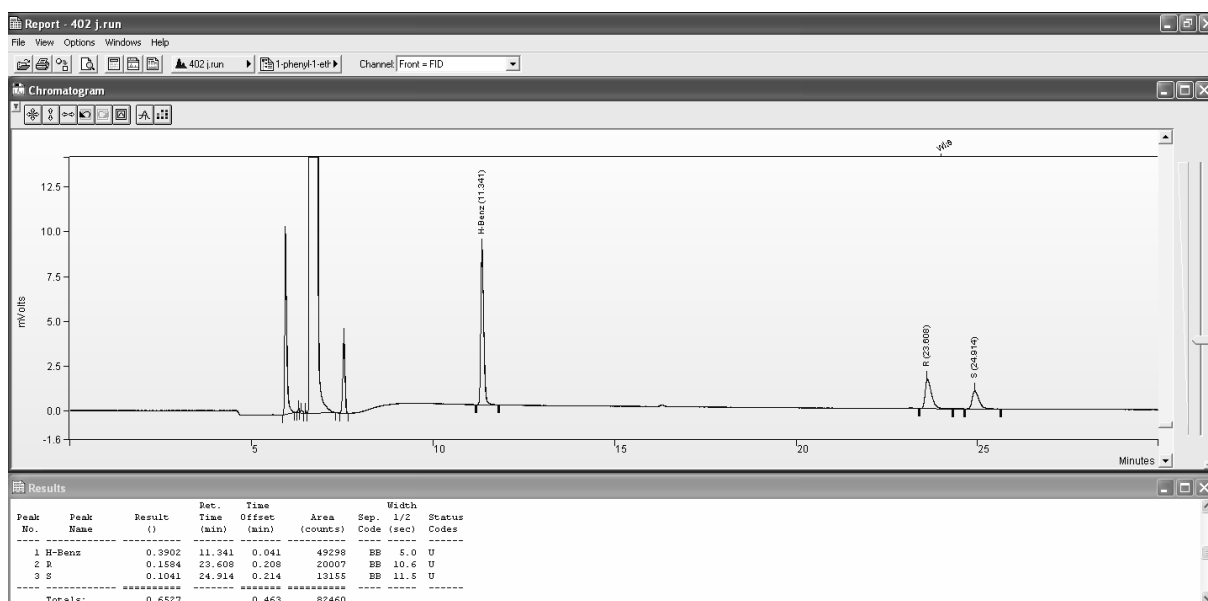
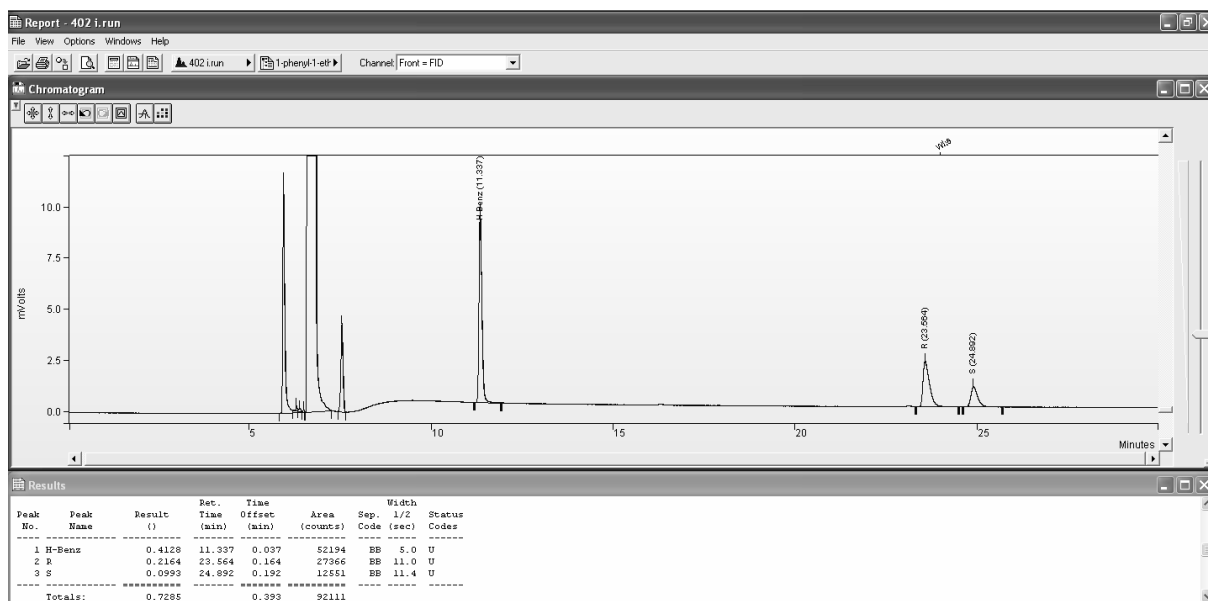




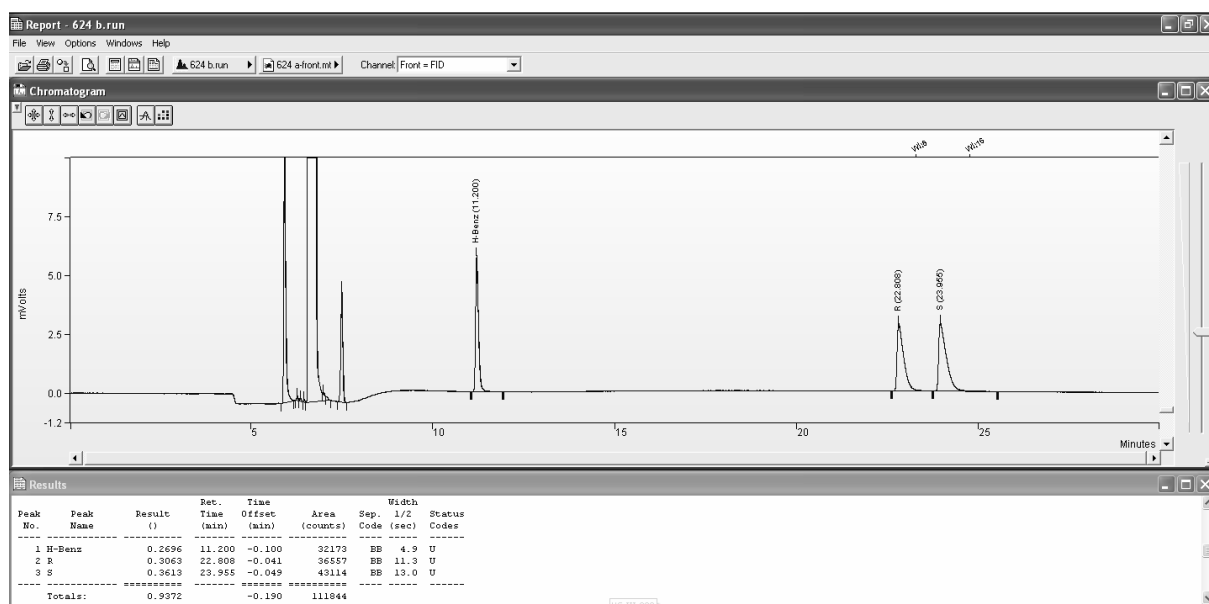
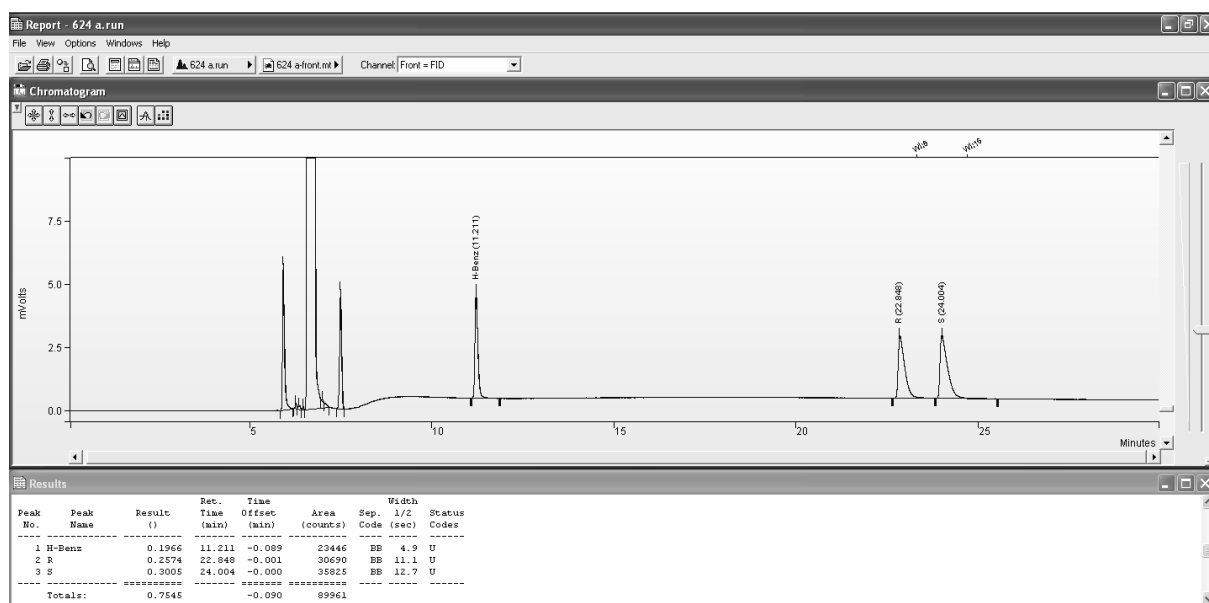


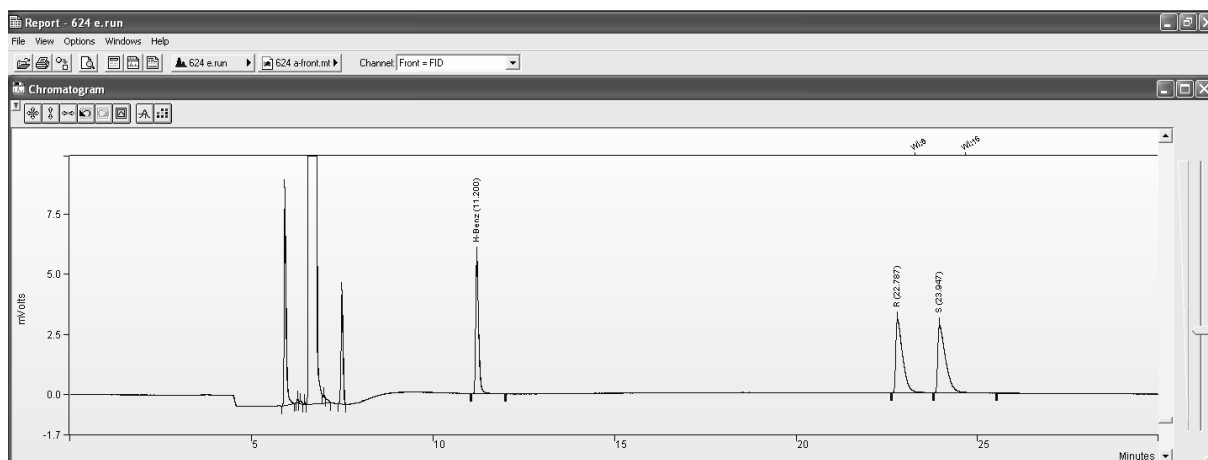
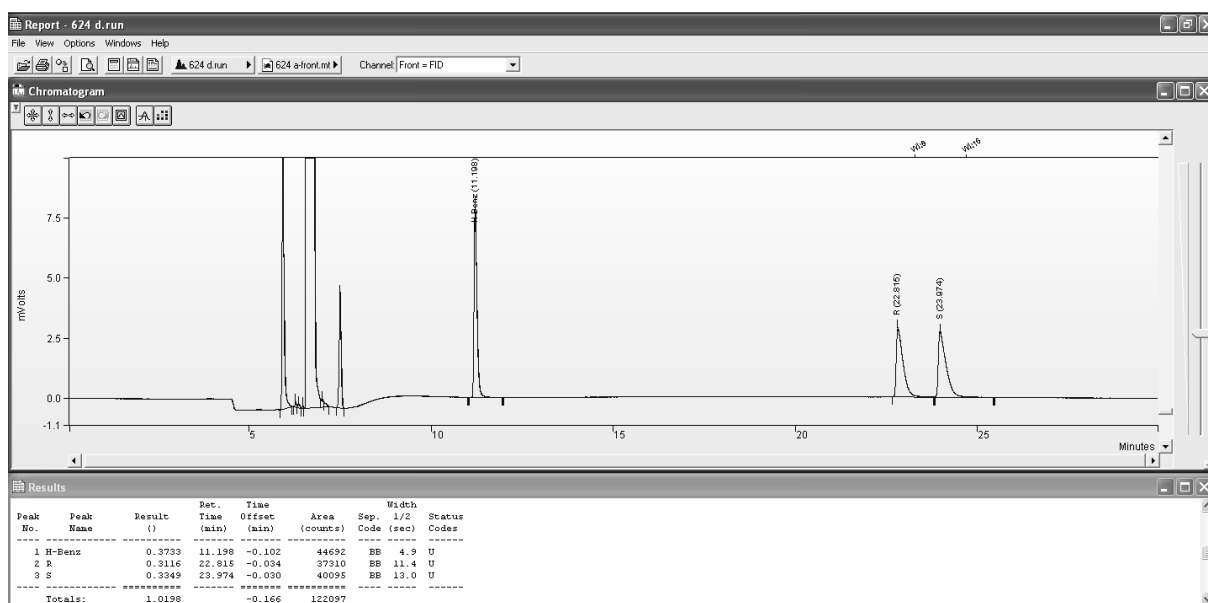
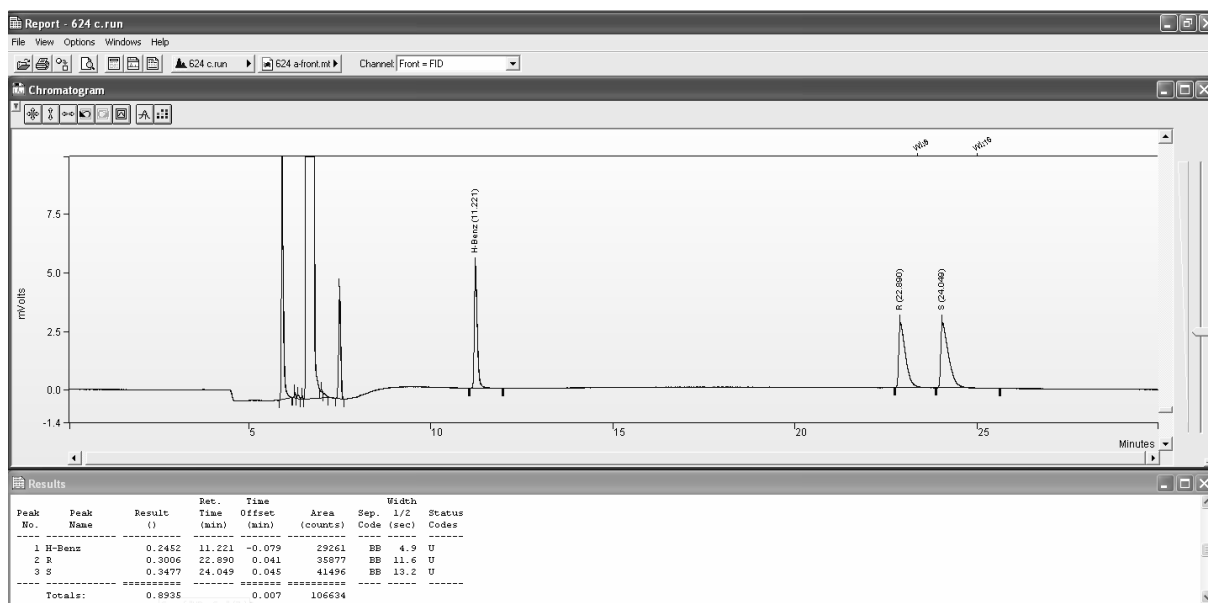


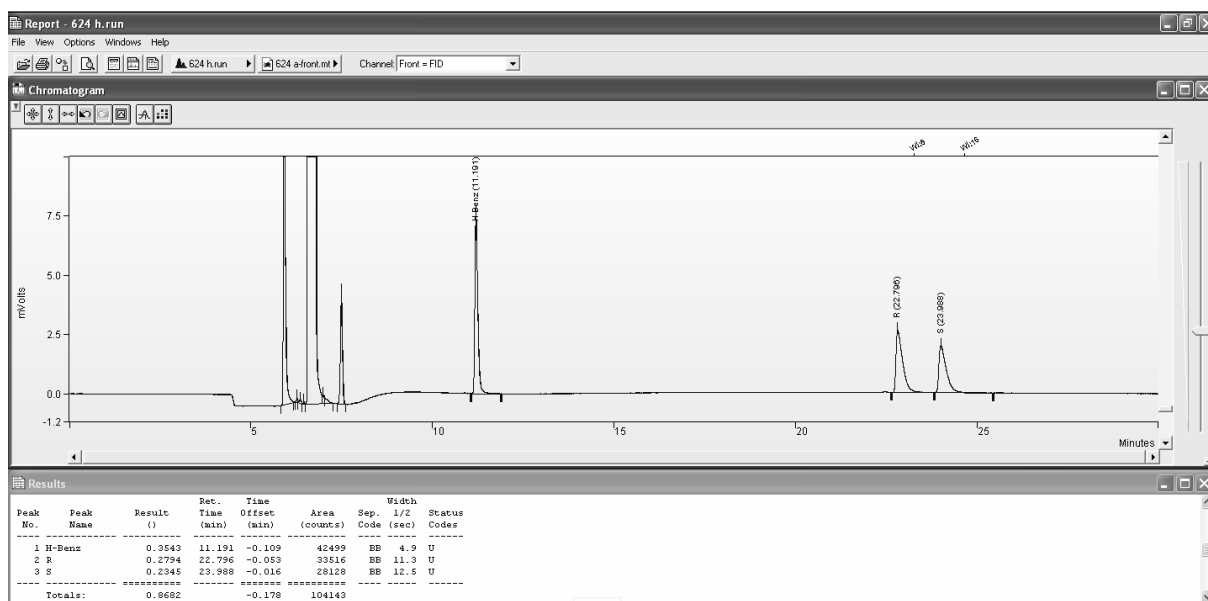
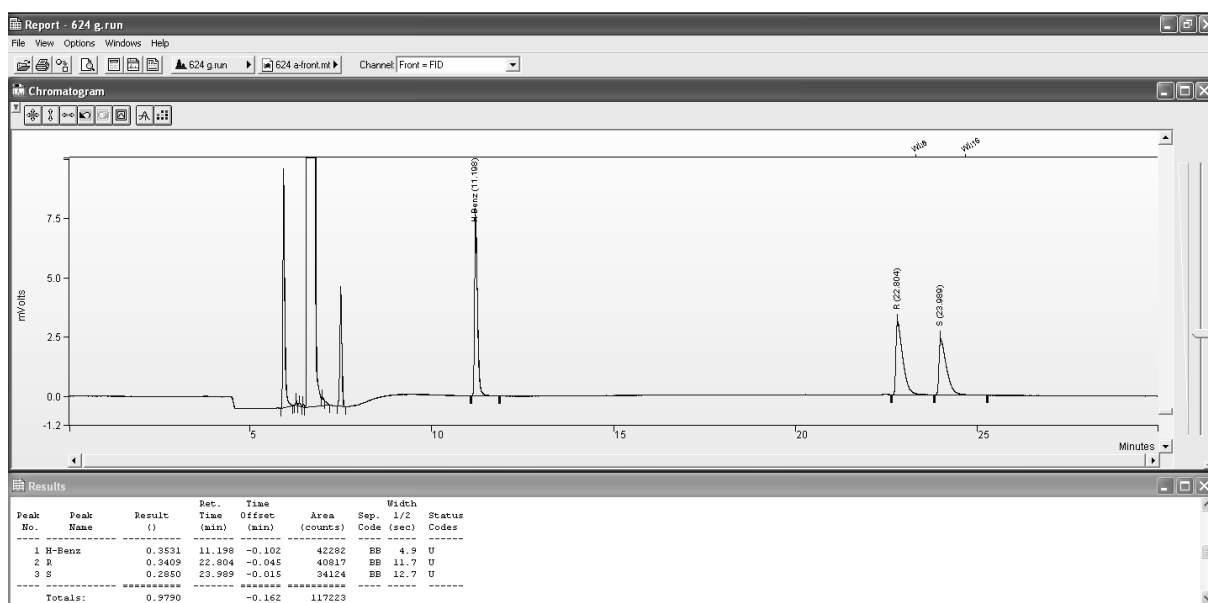
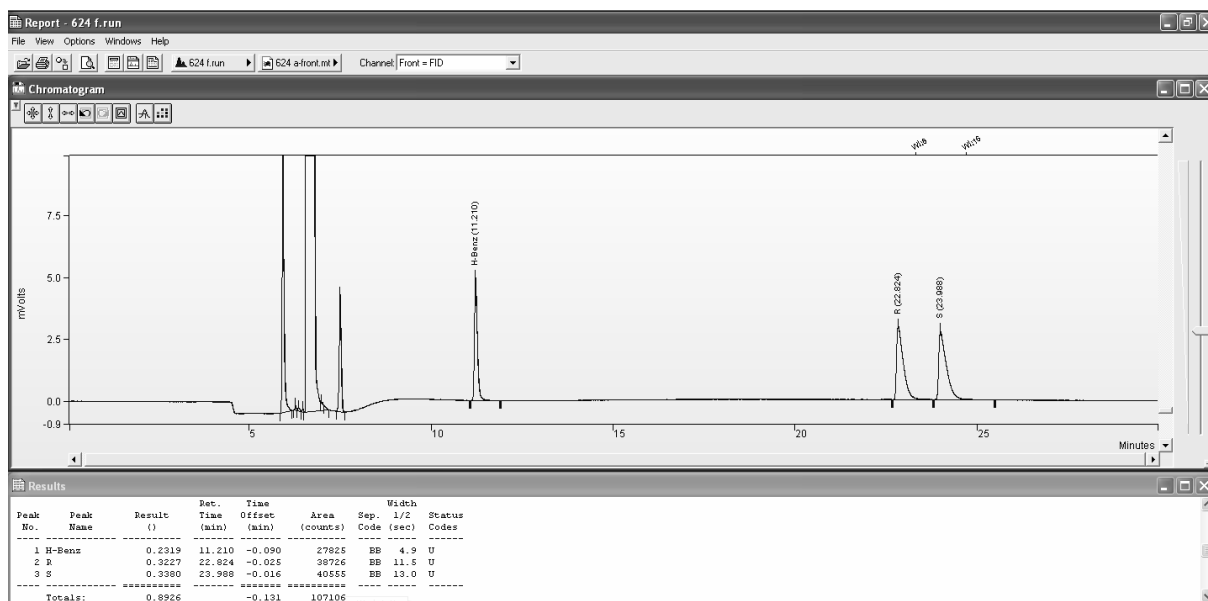


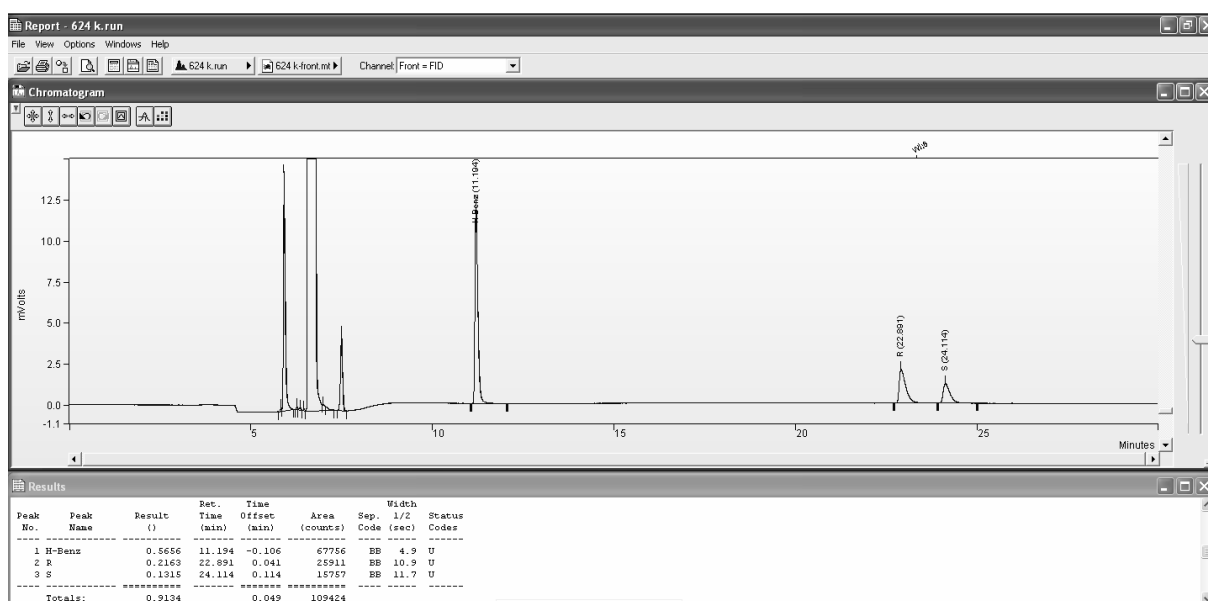
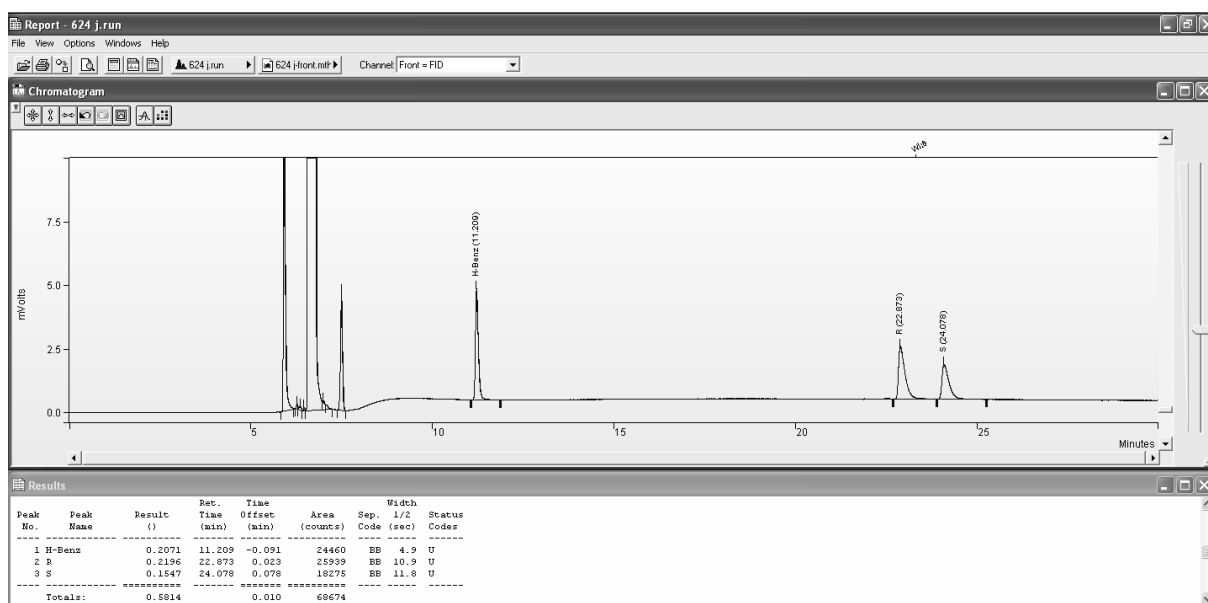
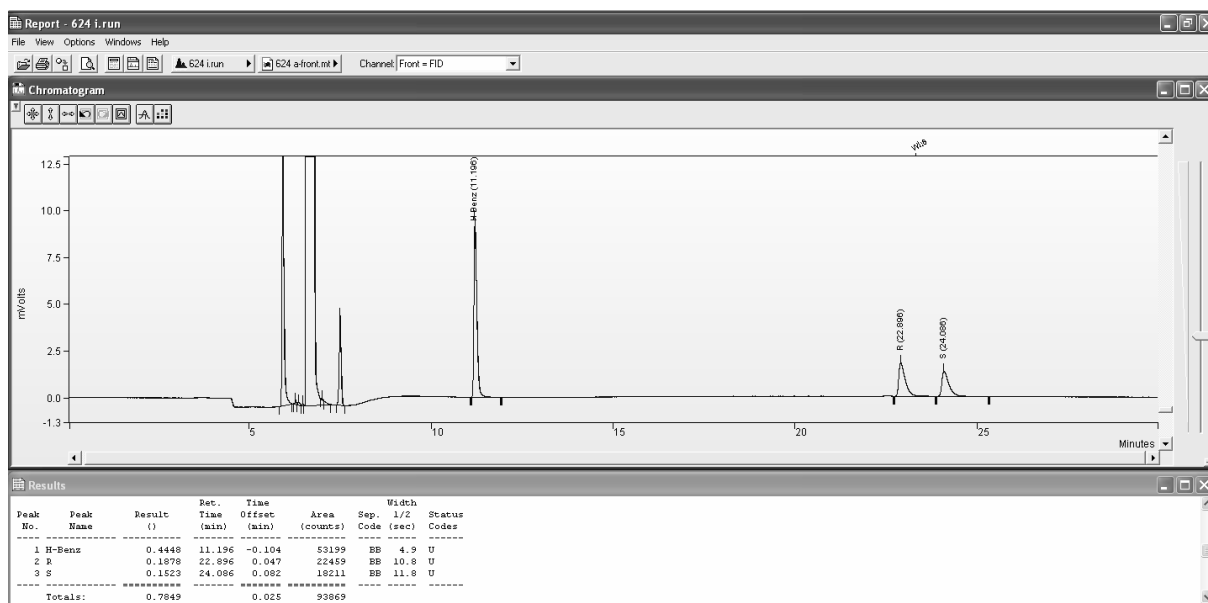


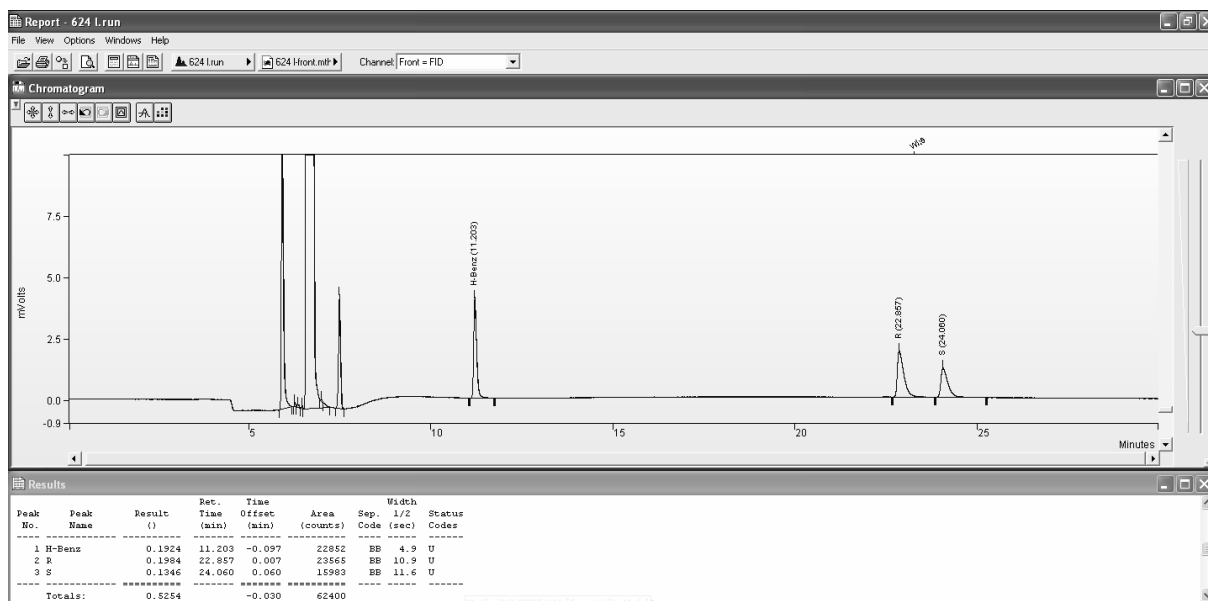
III.3 Figure 2b (NME)



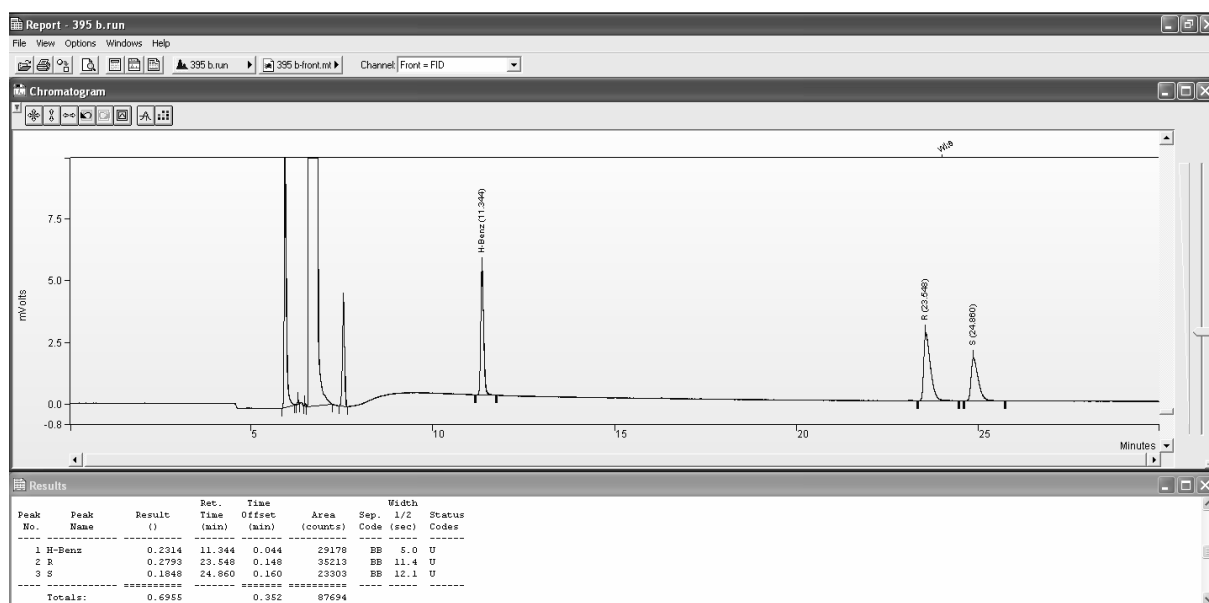
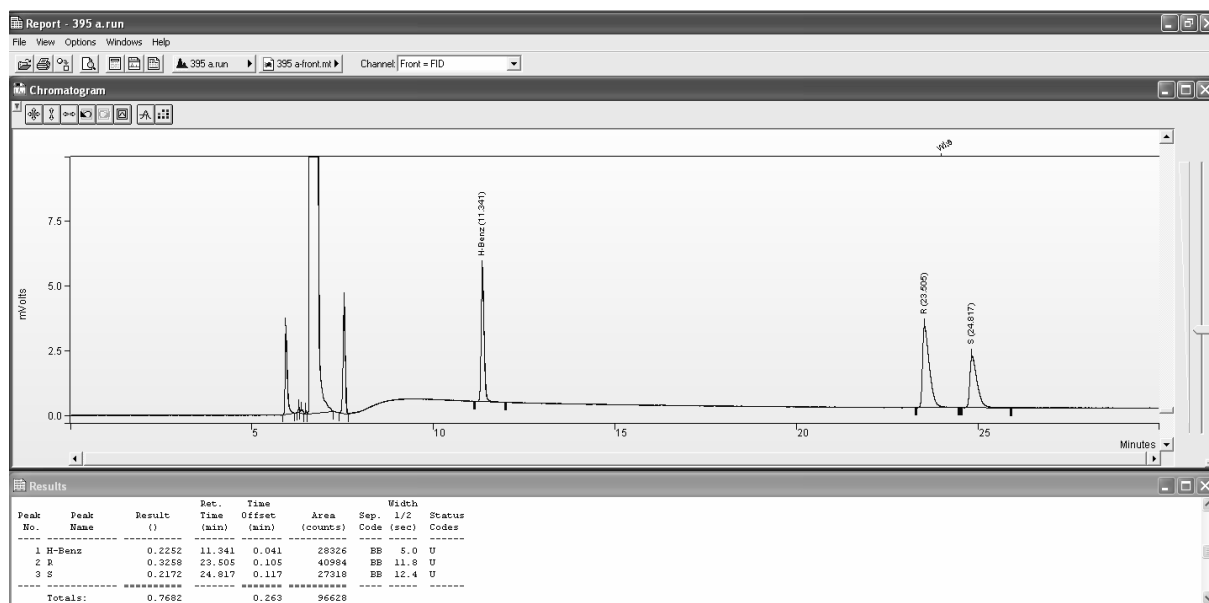


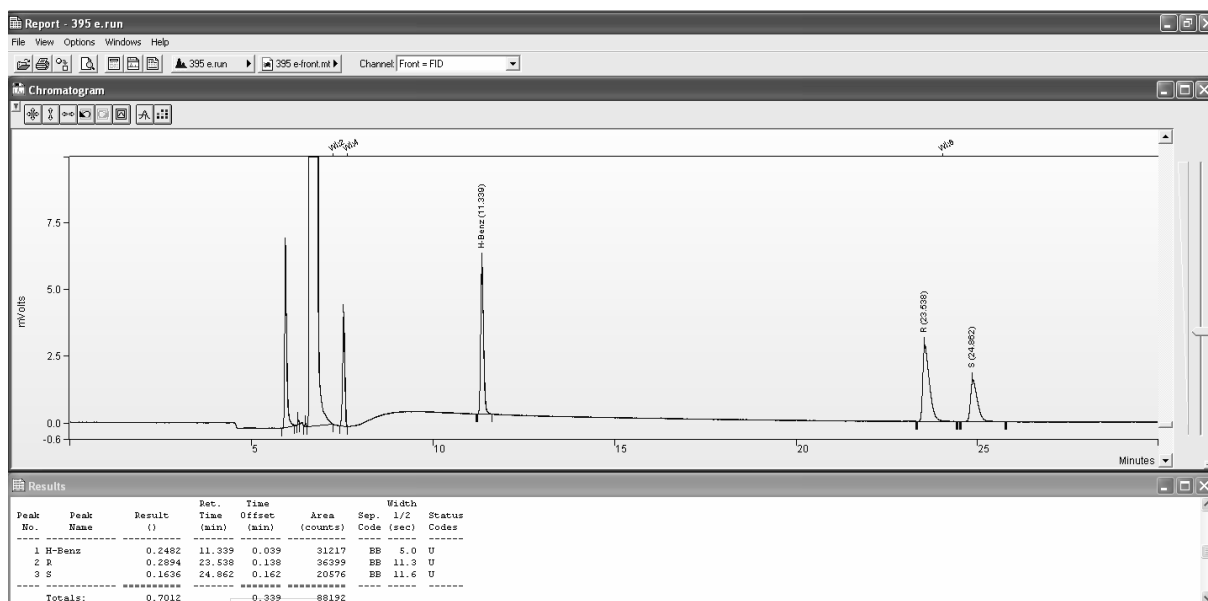
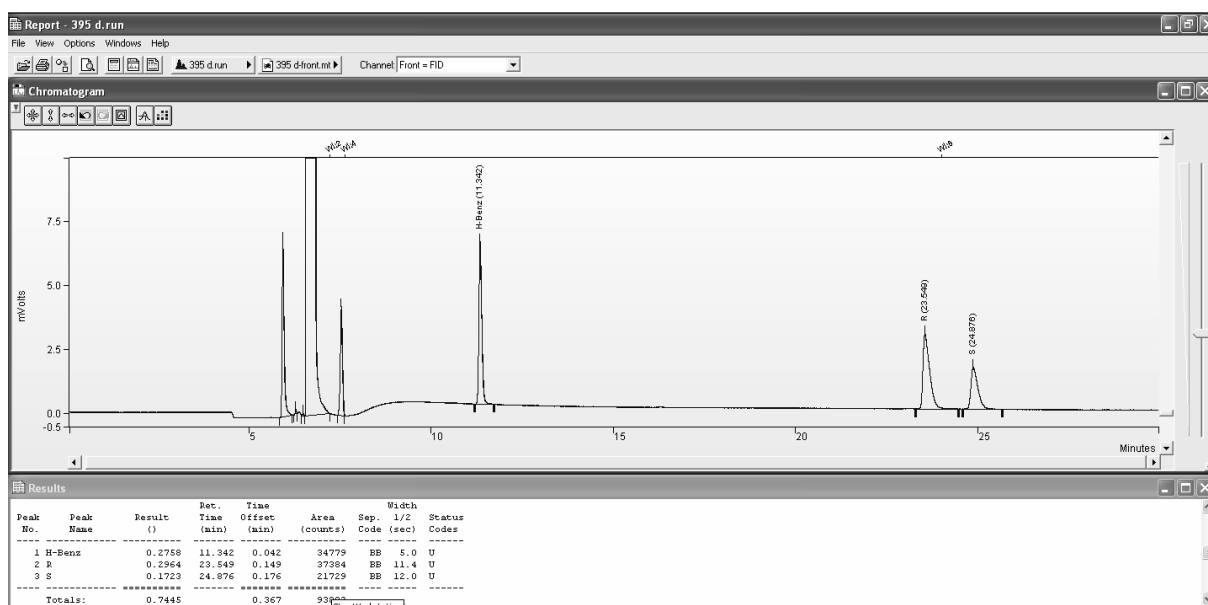
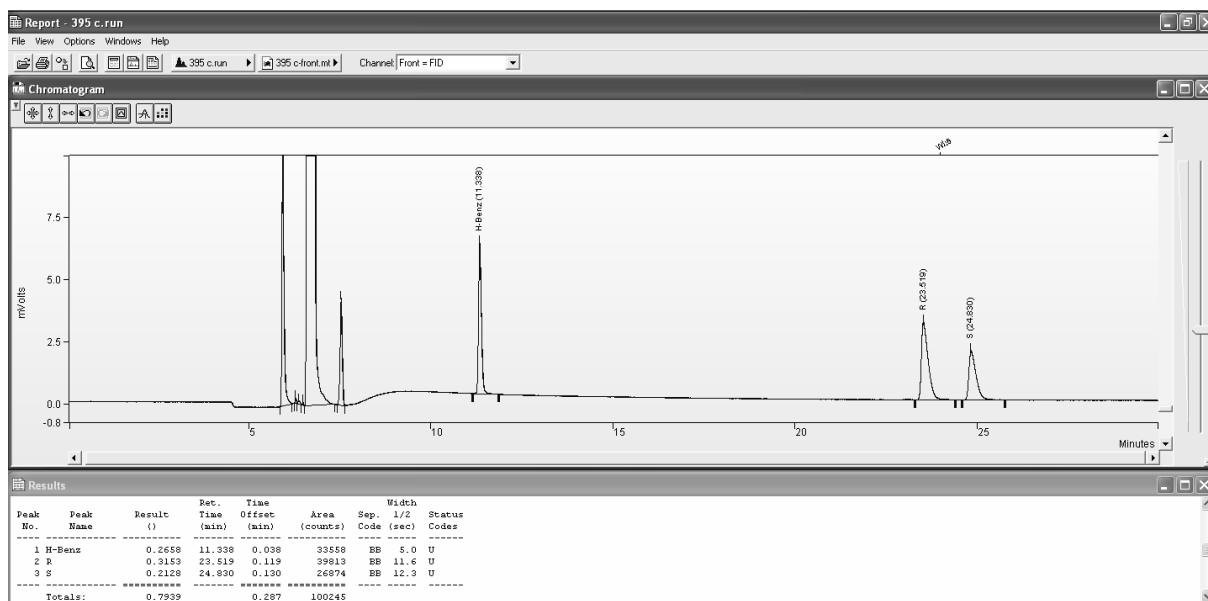


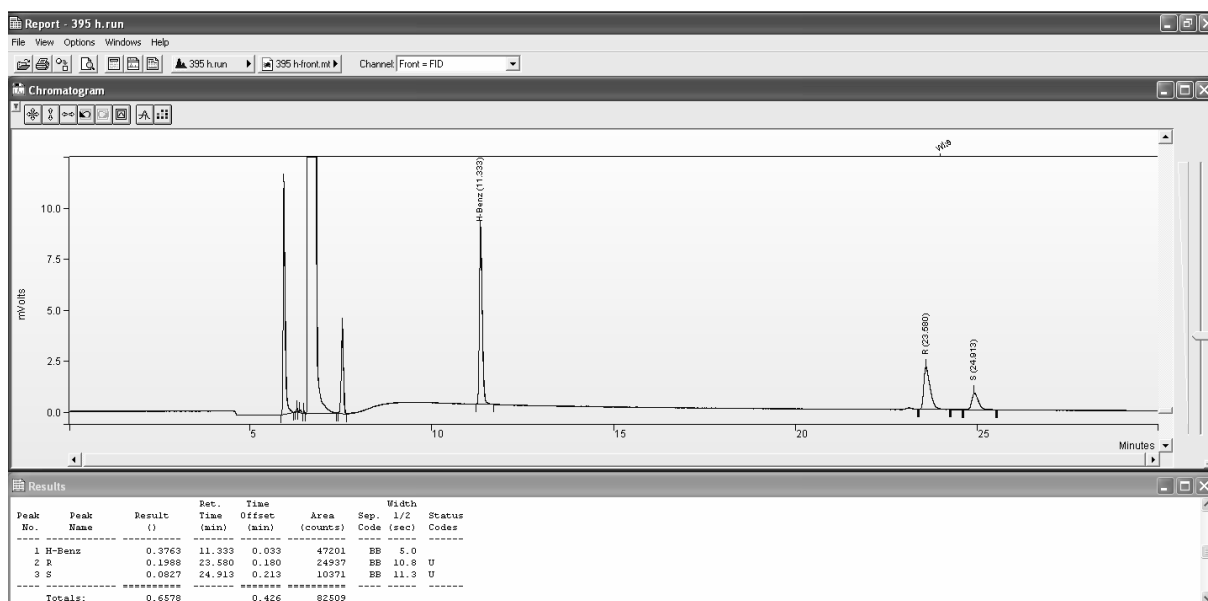
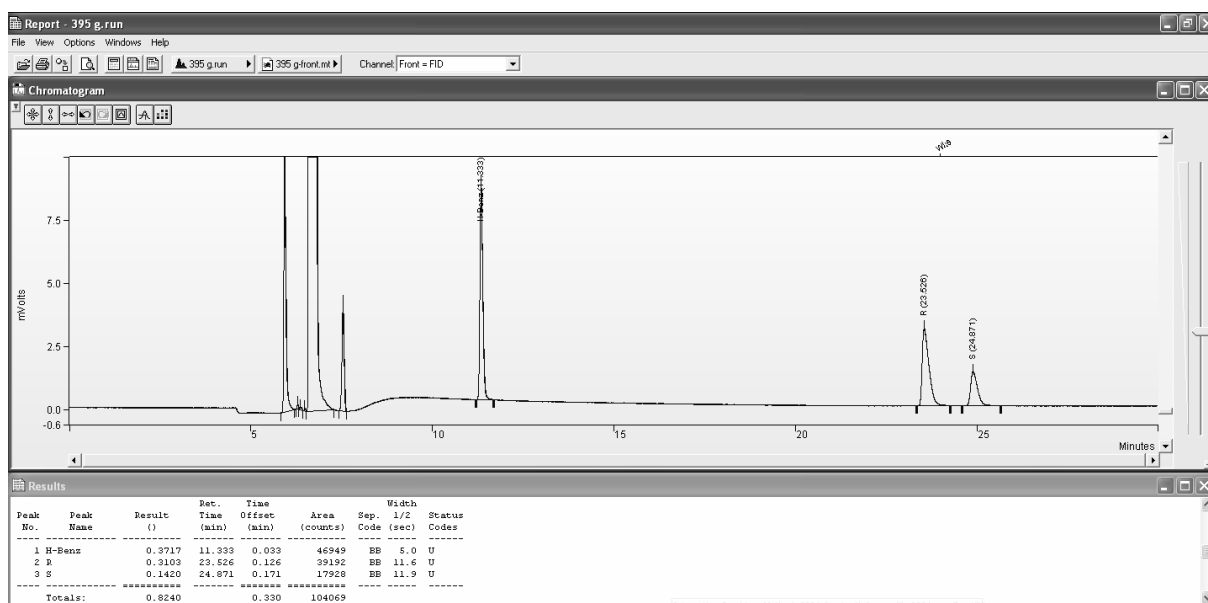
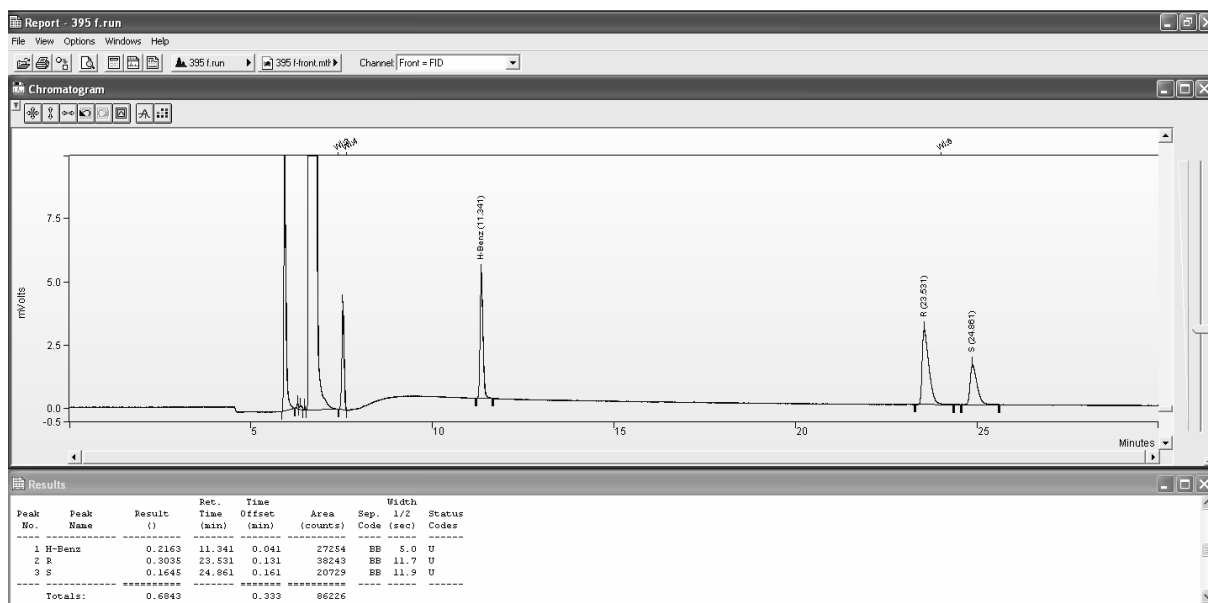


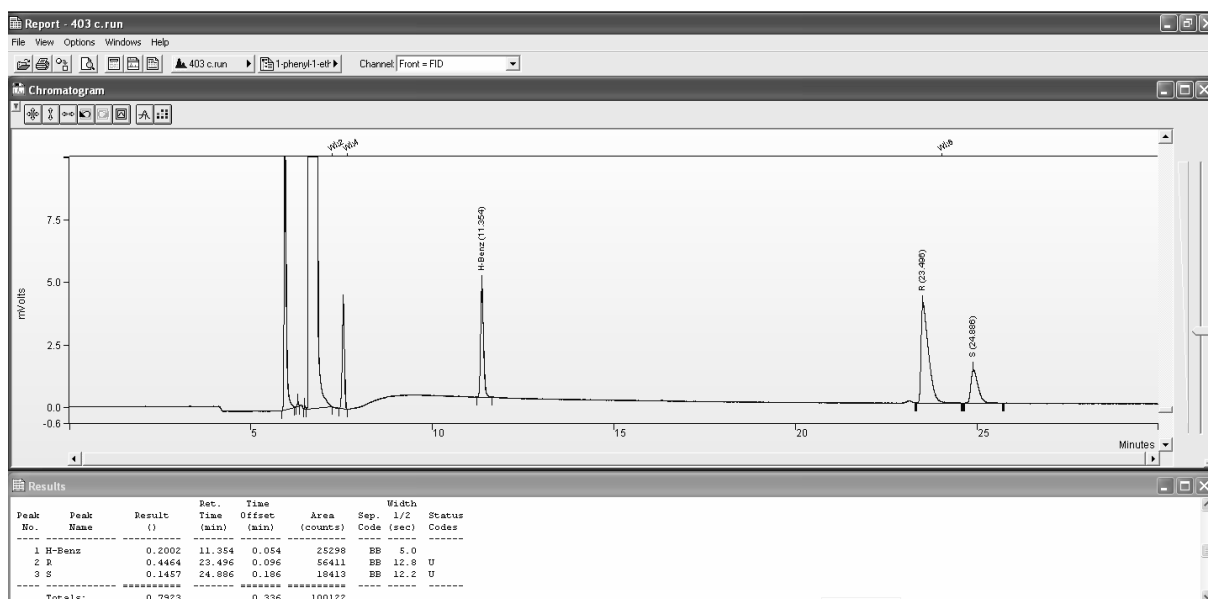
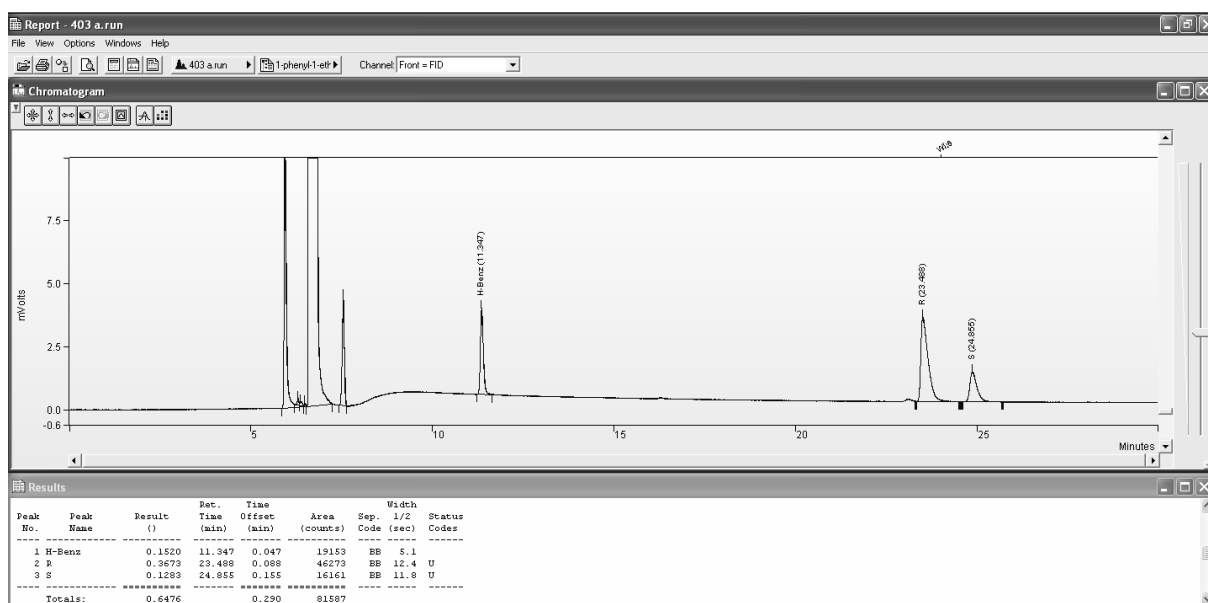
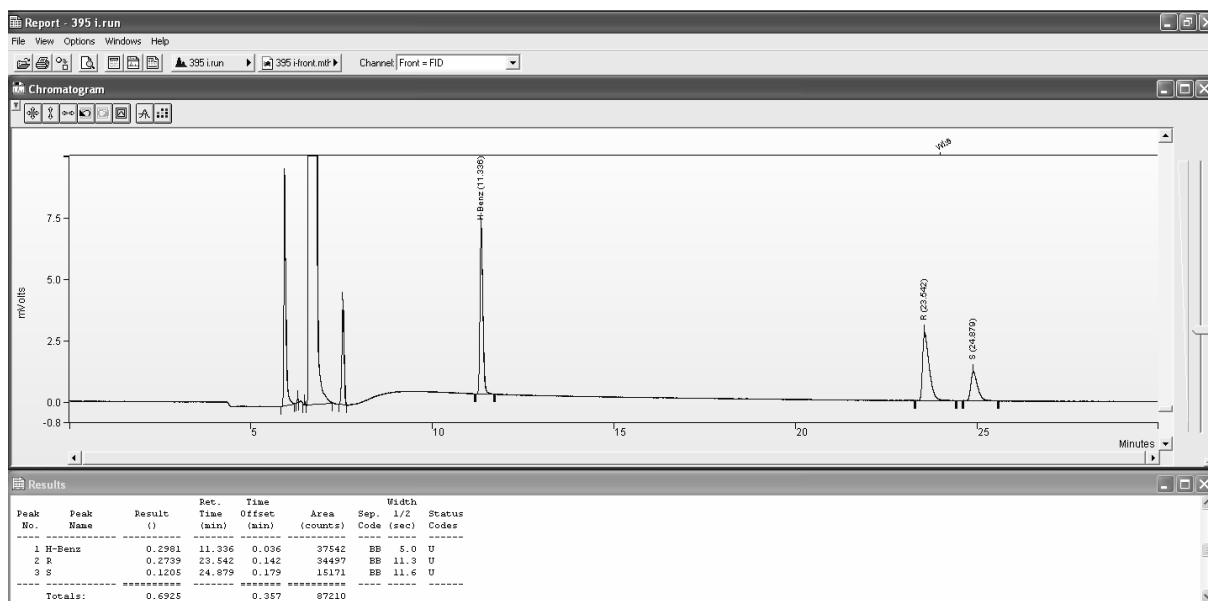


III.4 Figure 2b (NBE)

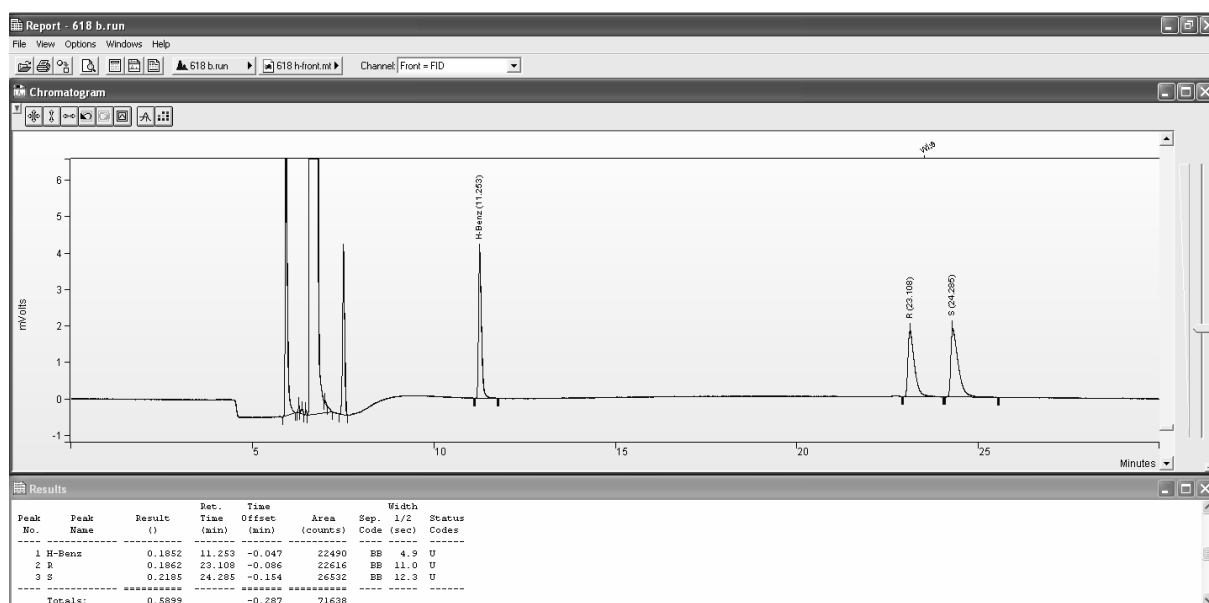
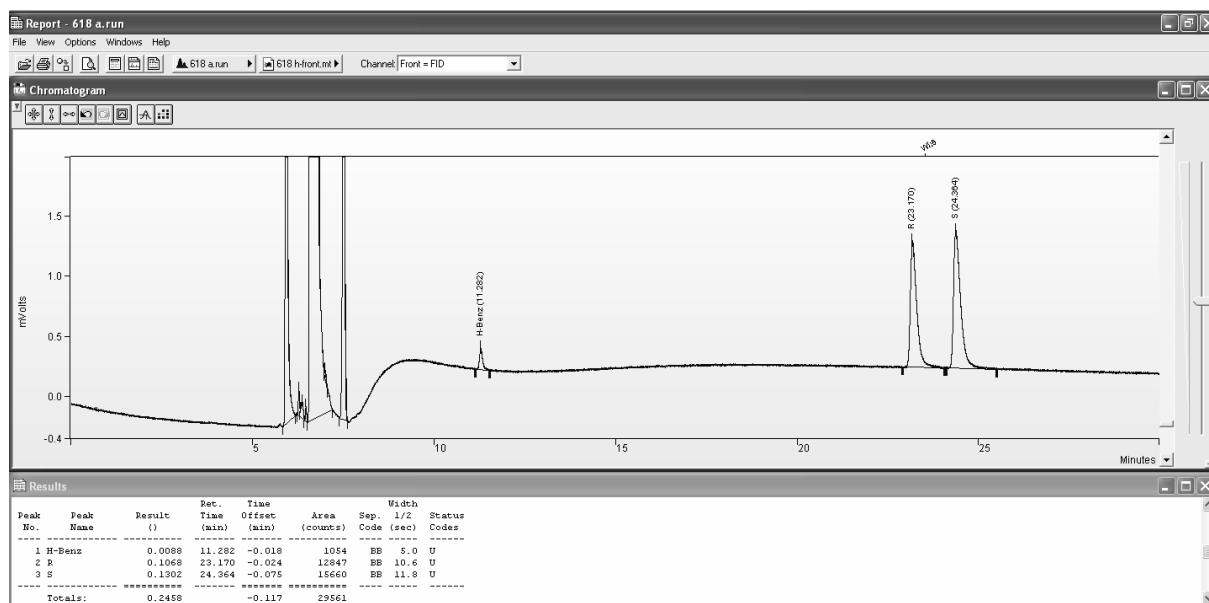


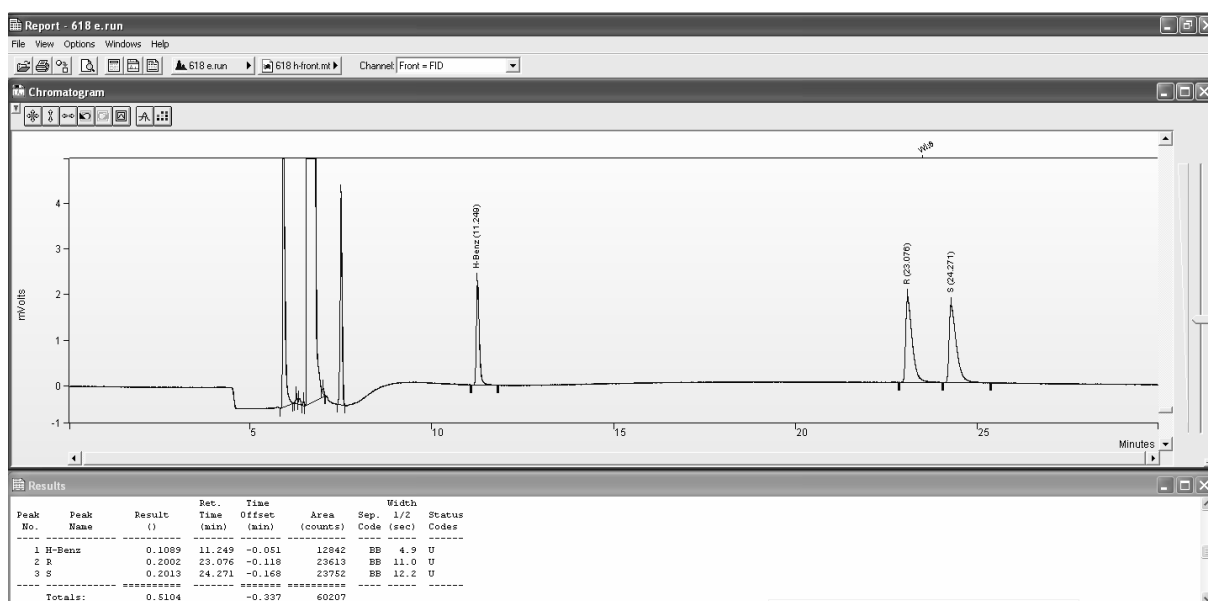
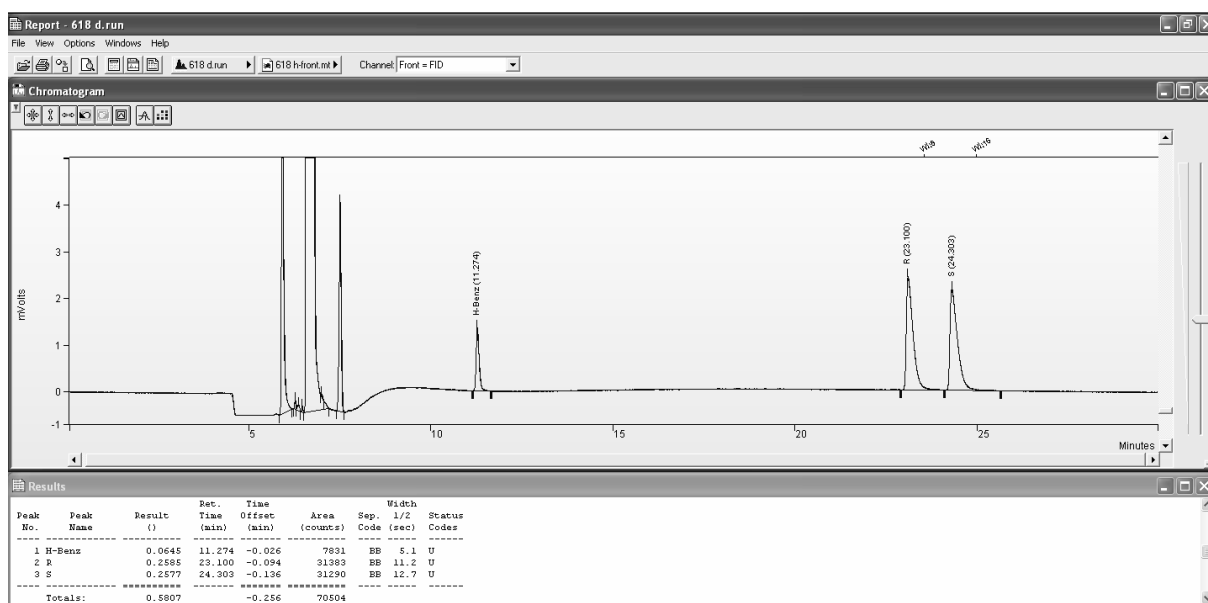
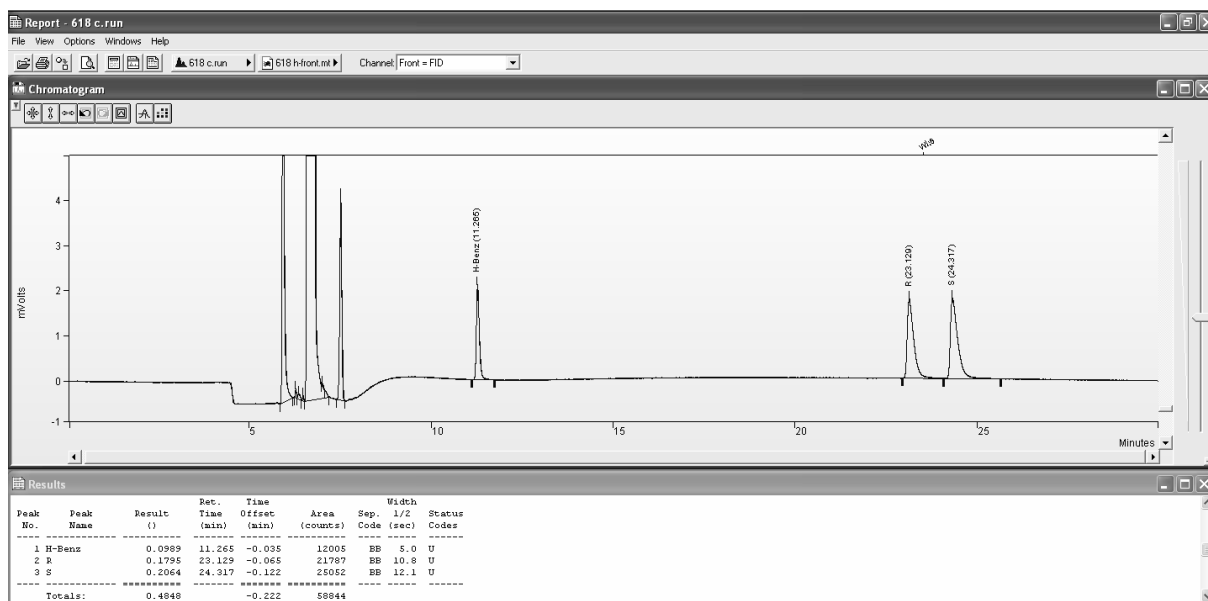


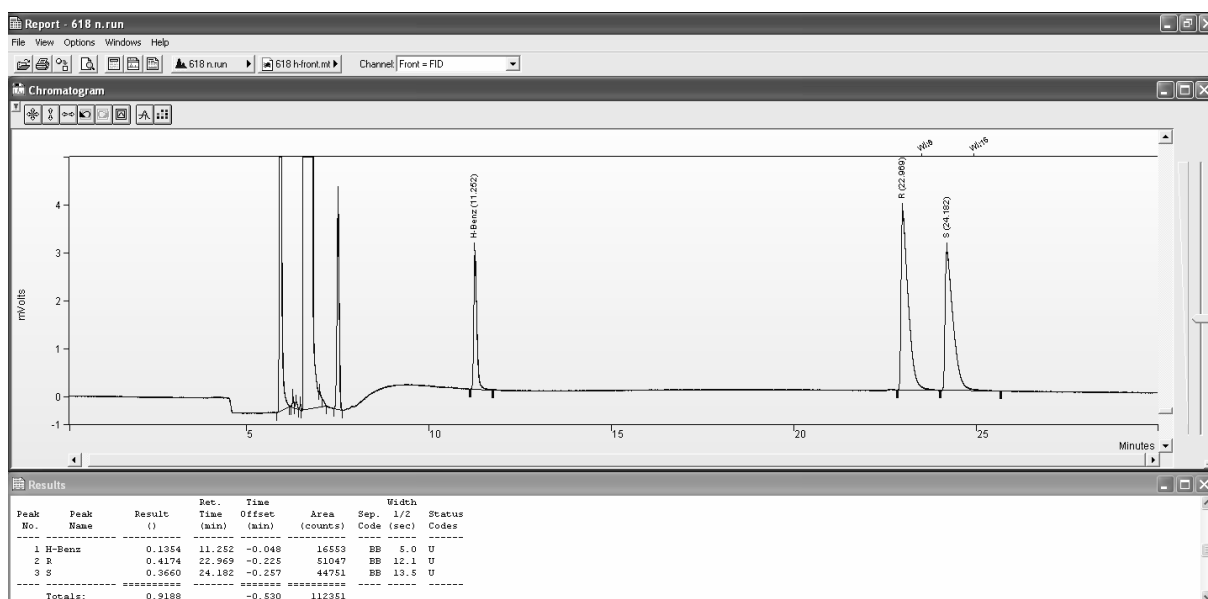
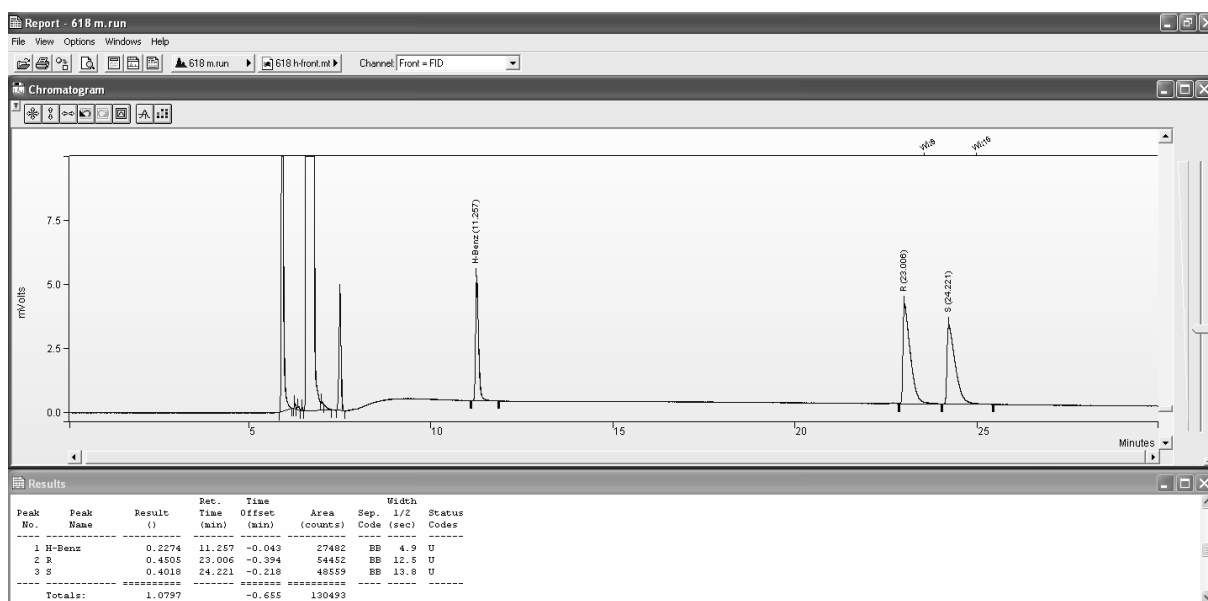
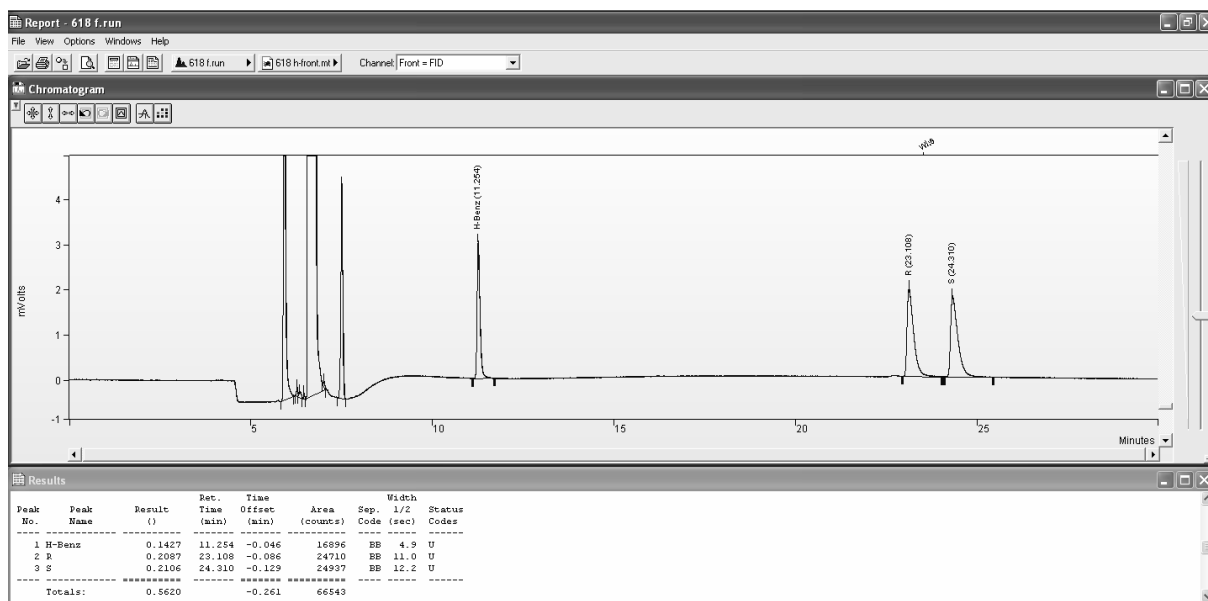


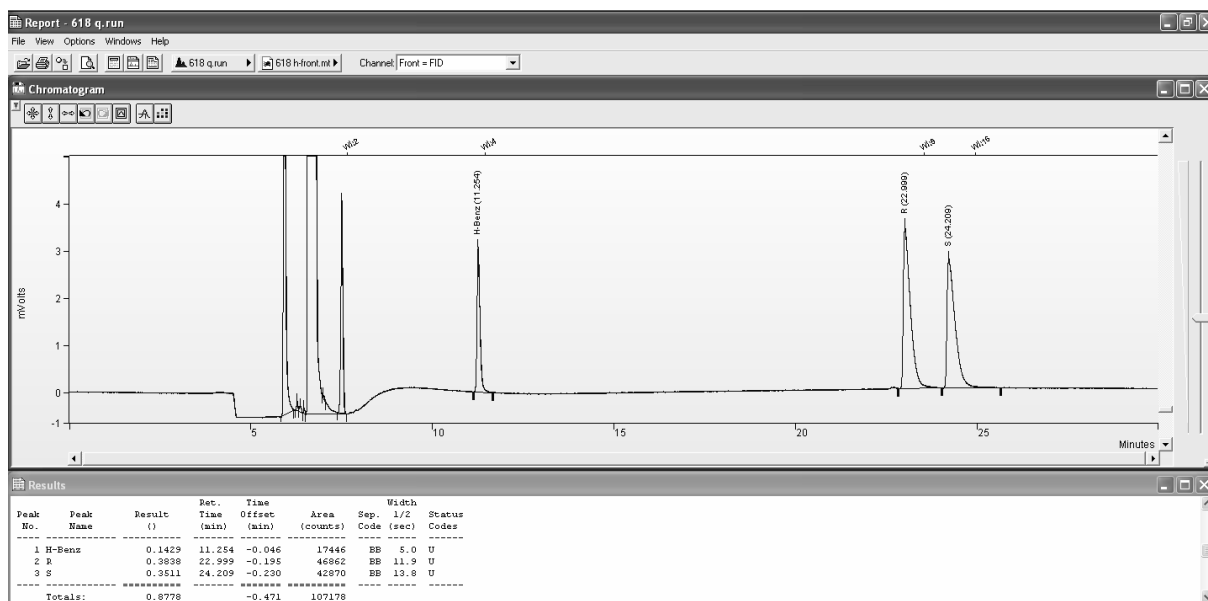
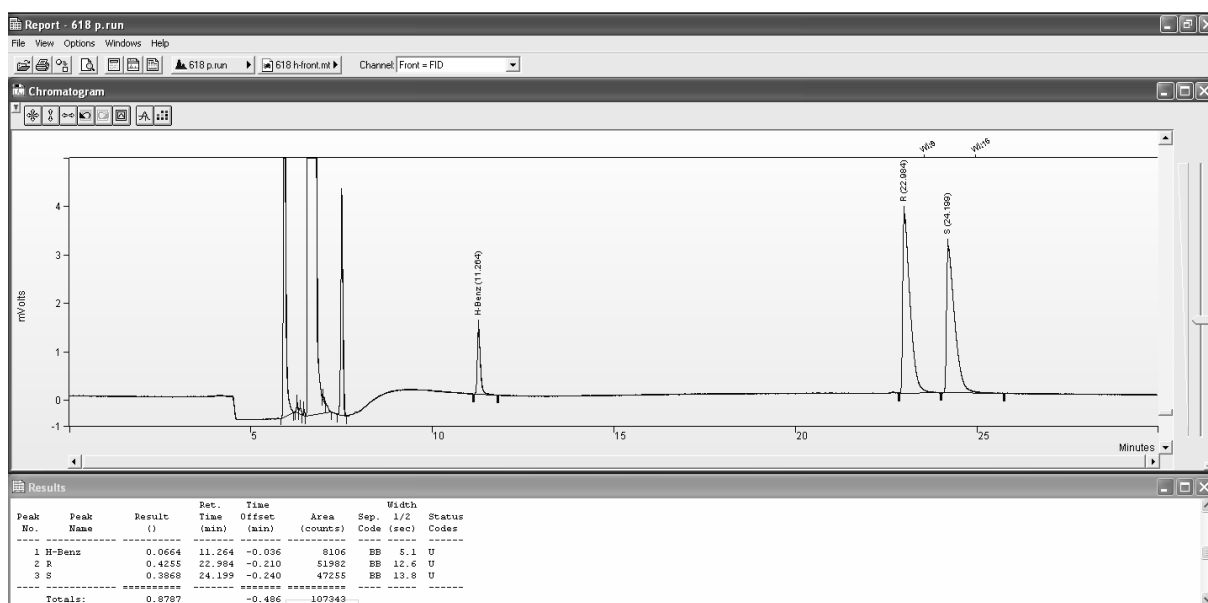
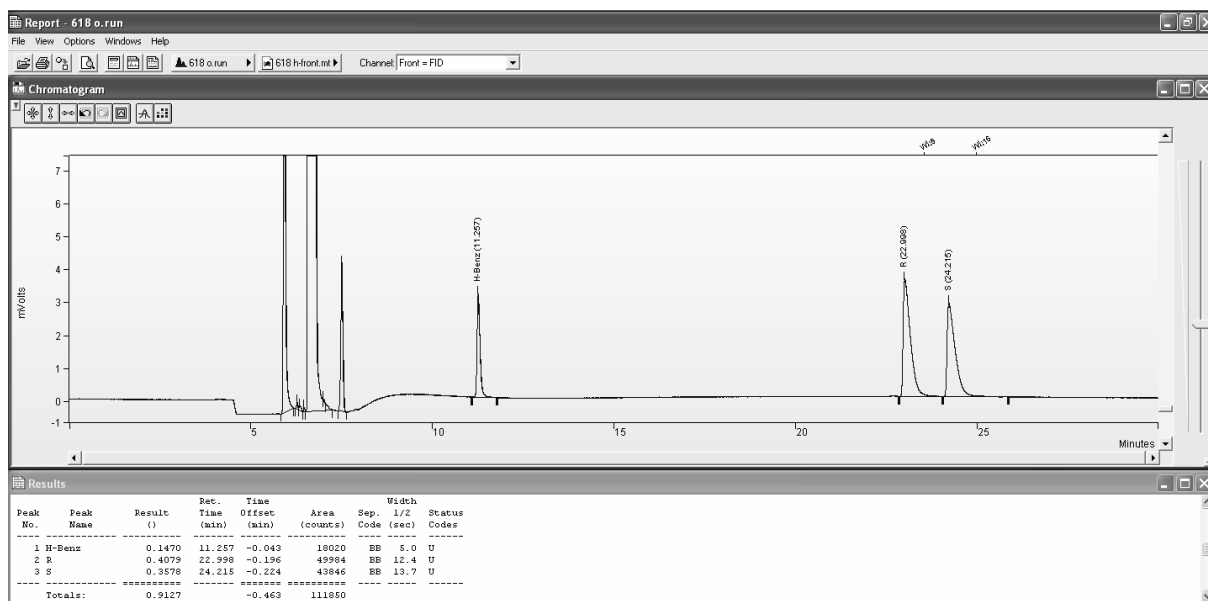


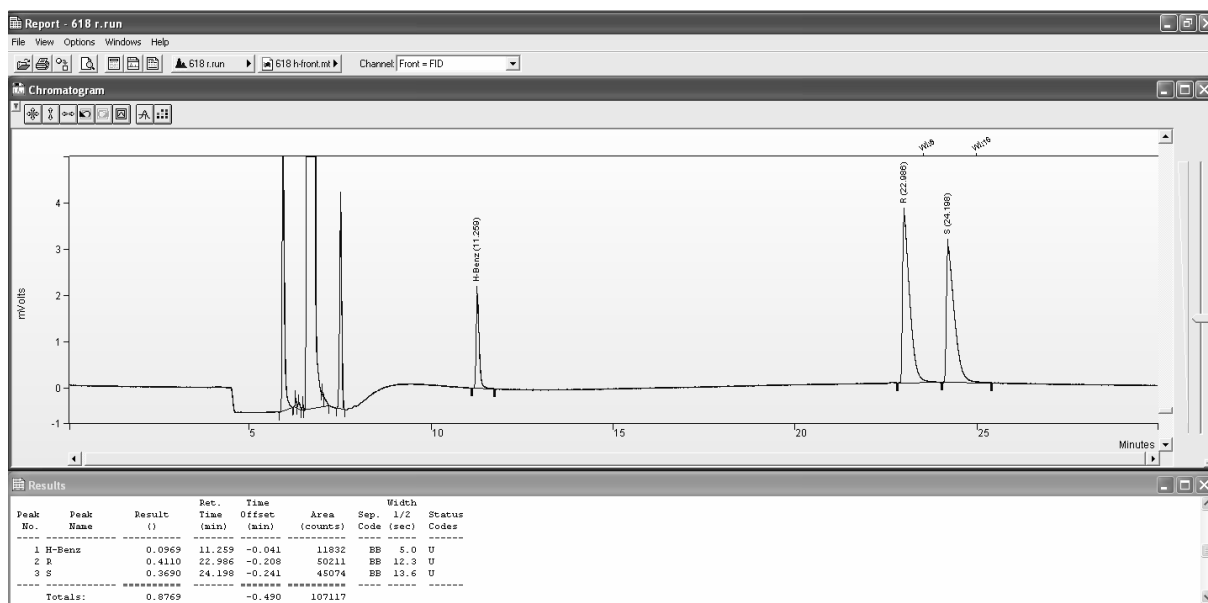
III.5 Figure 3a



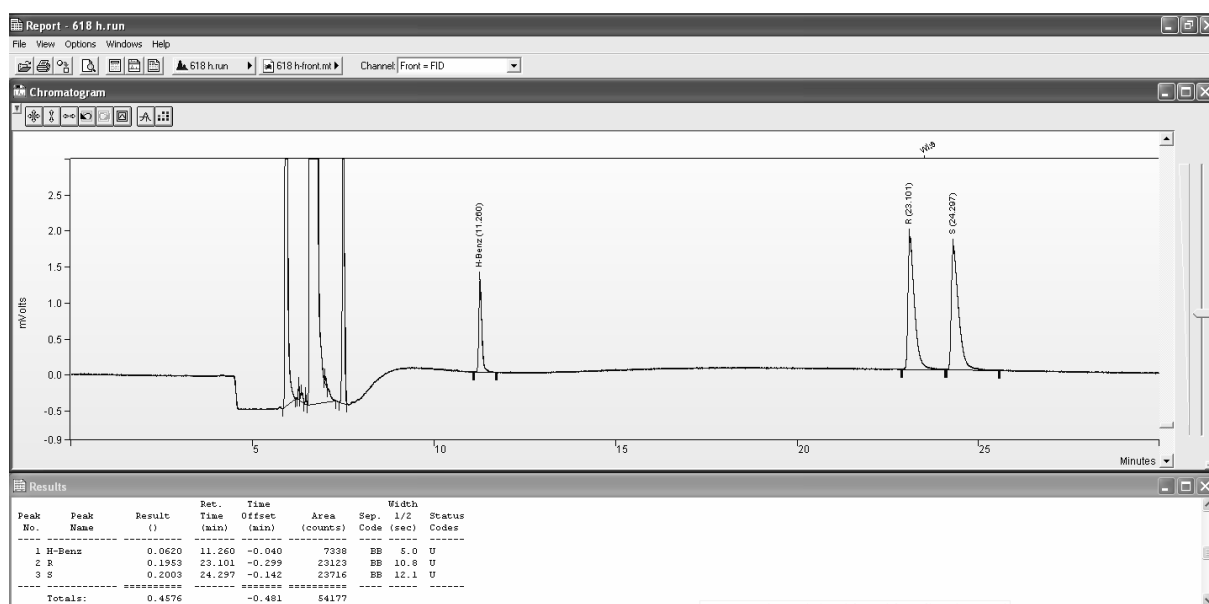
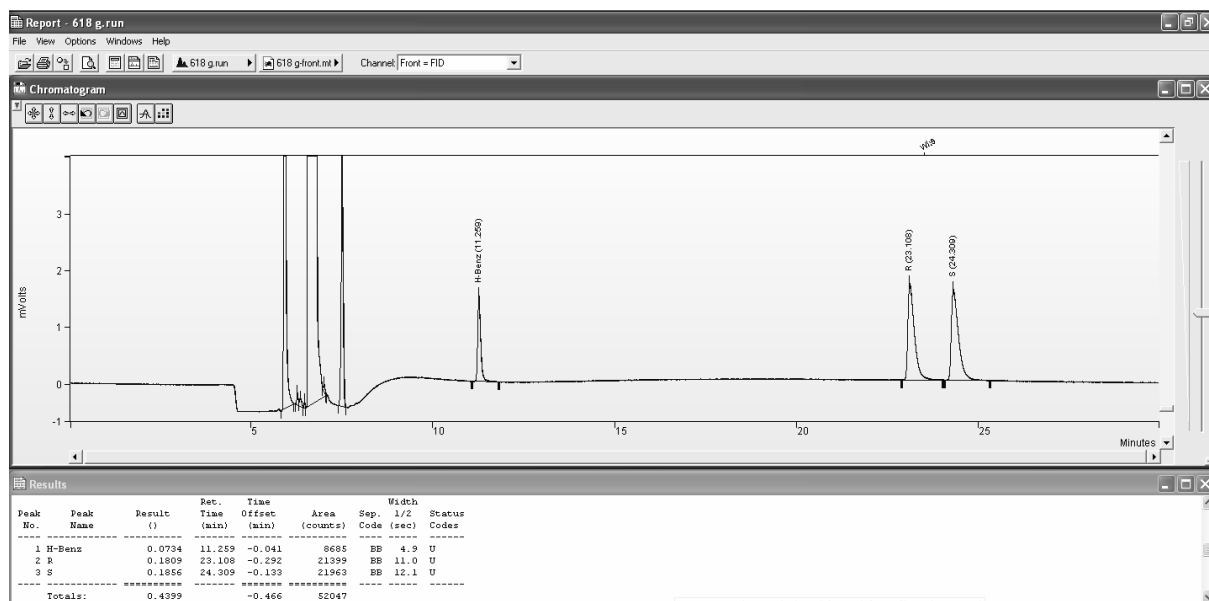


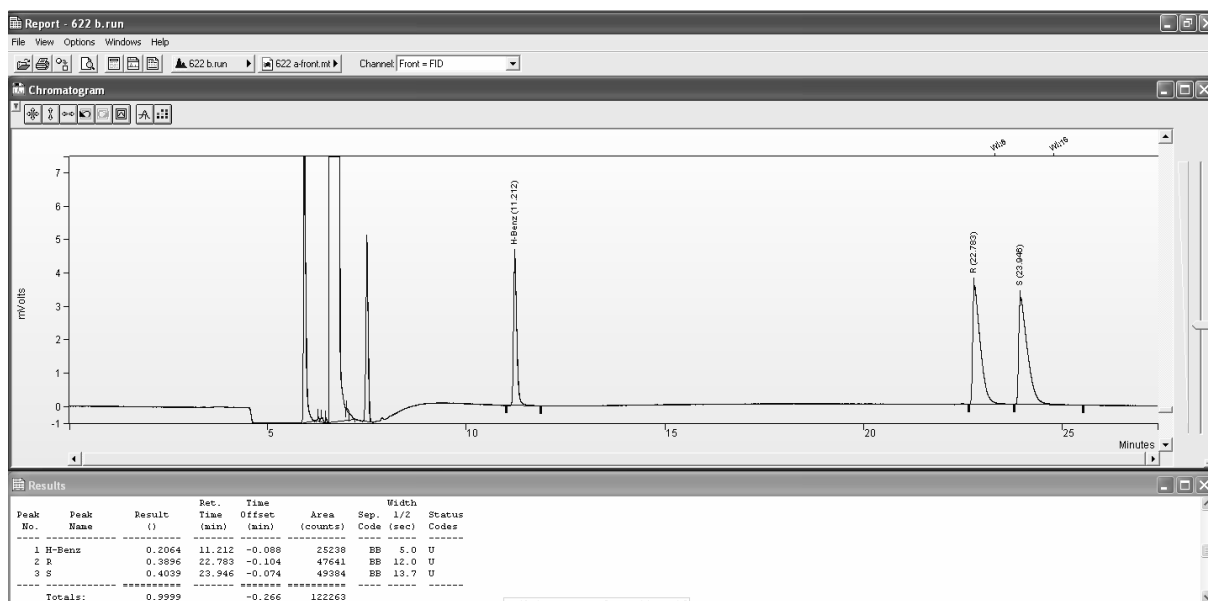
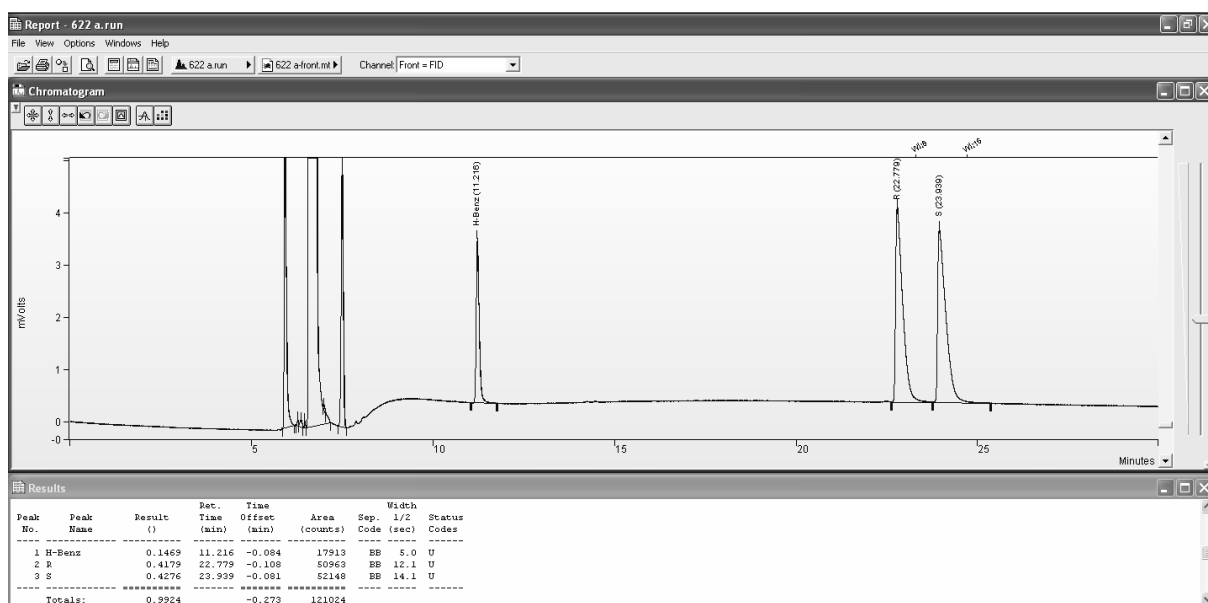
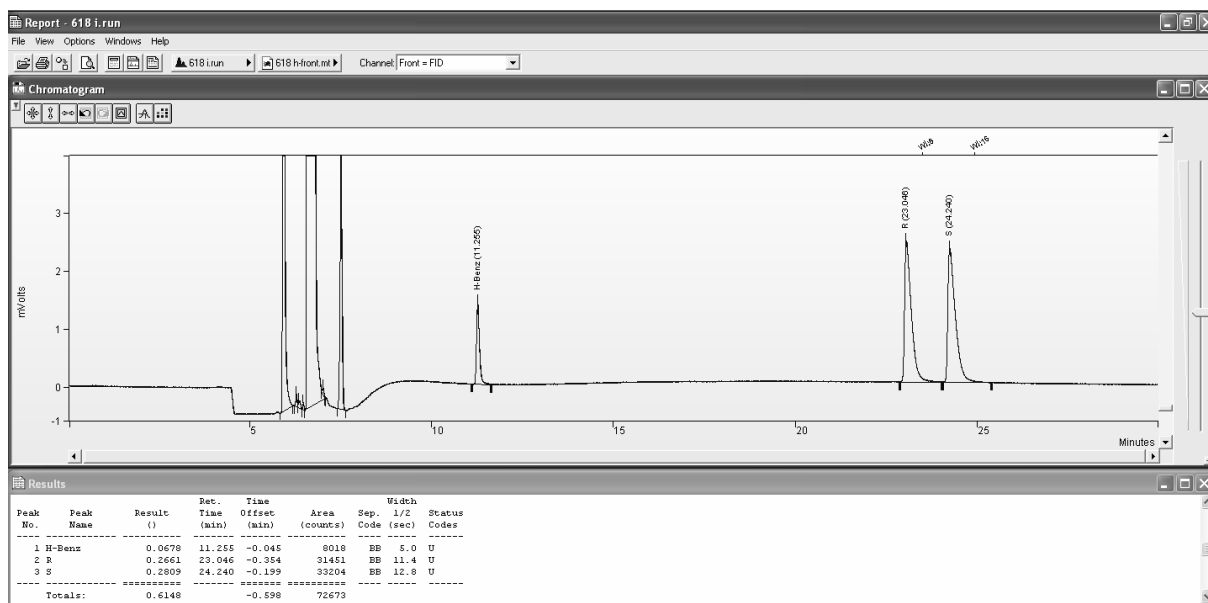


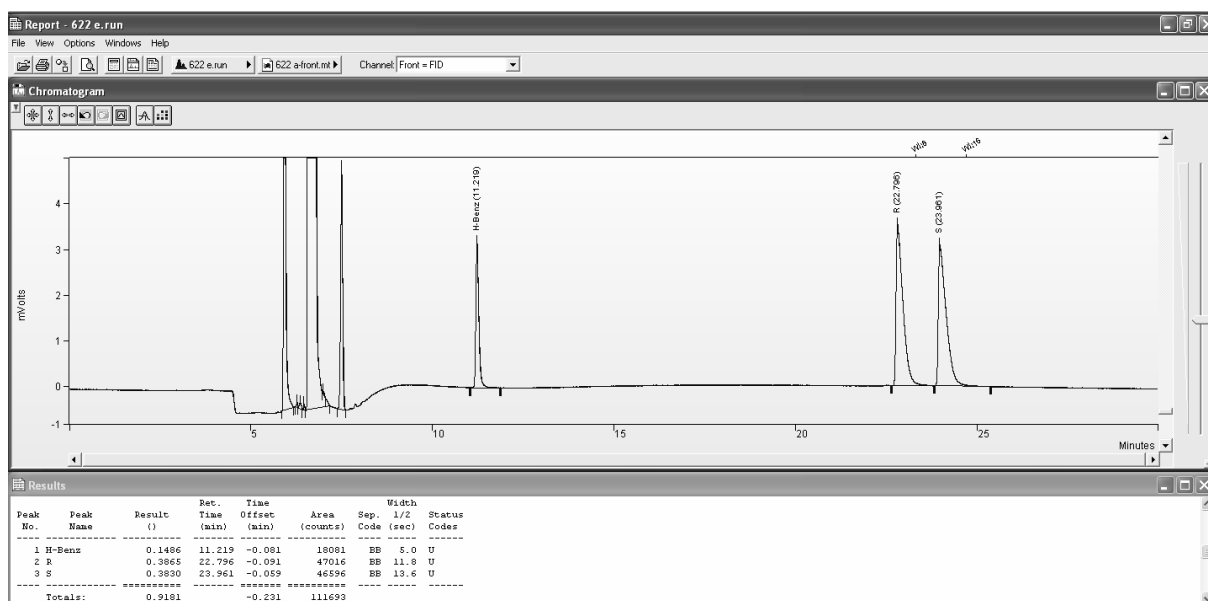
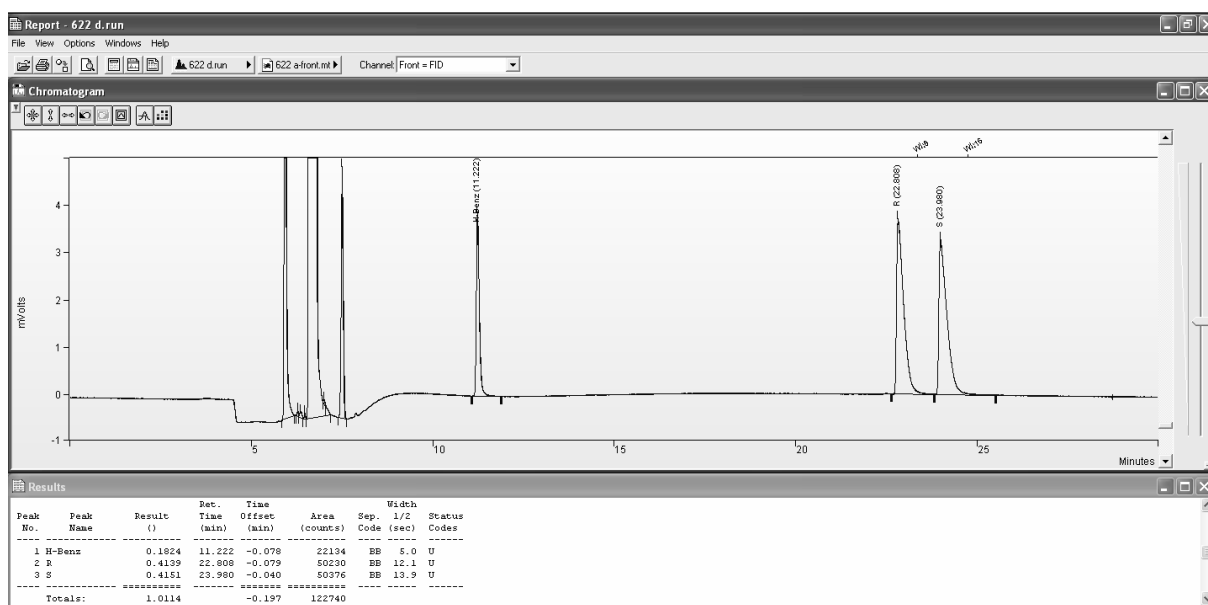
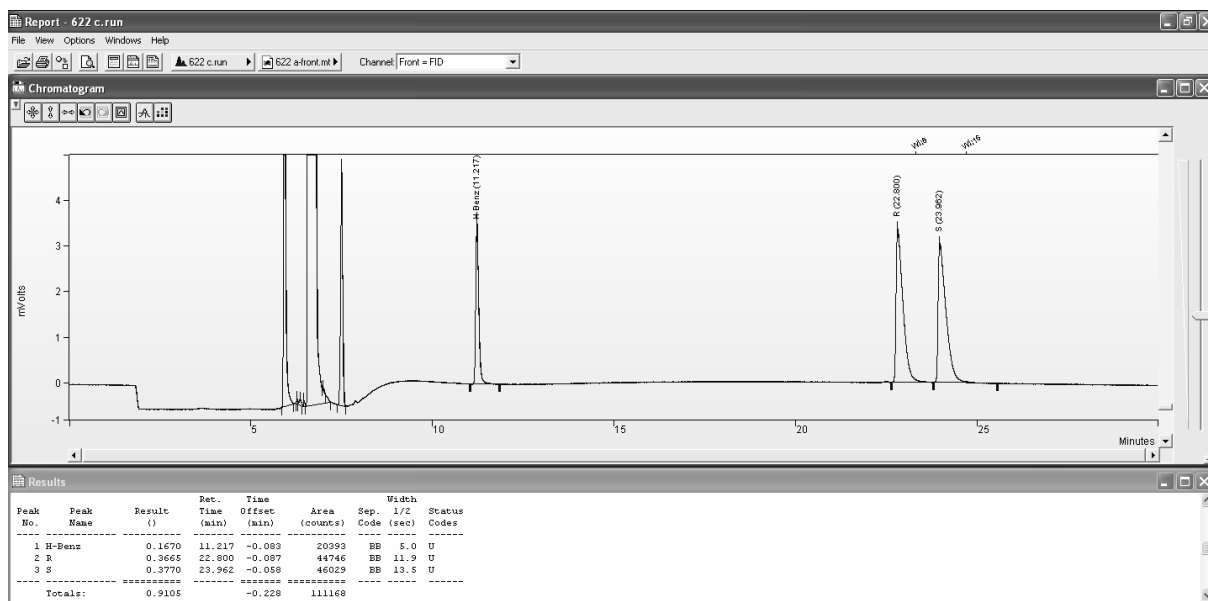


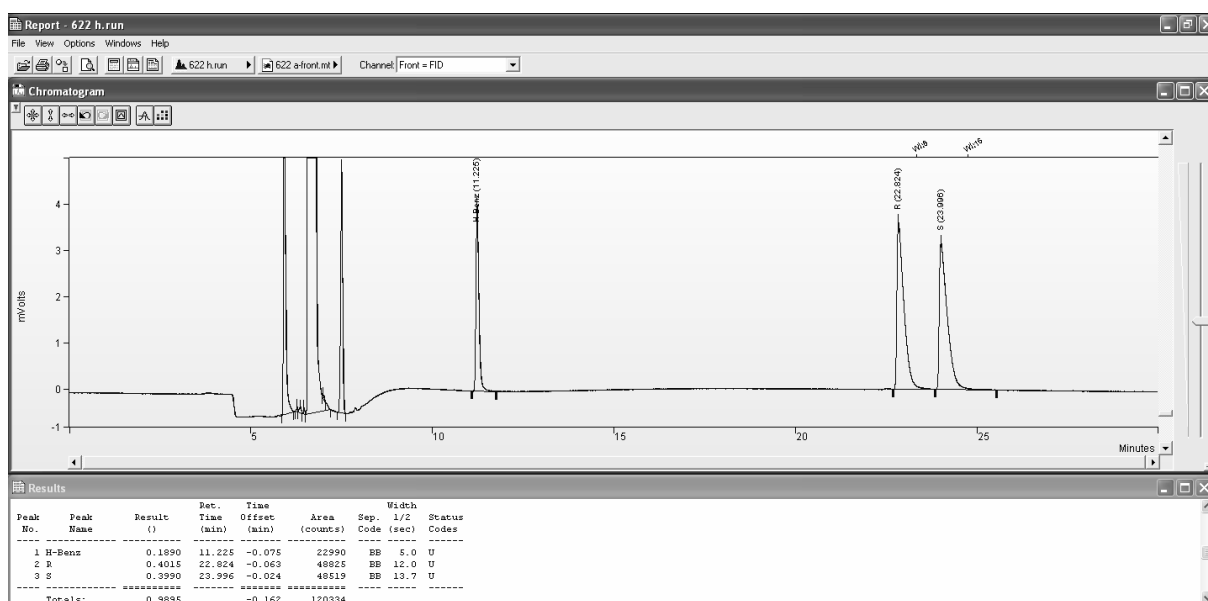
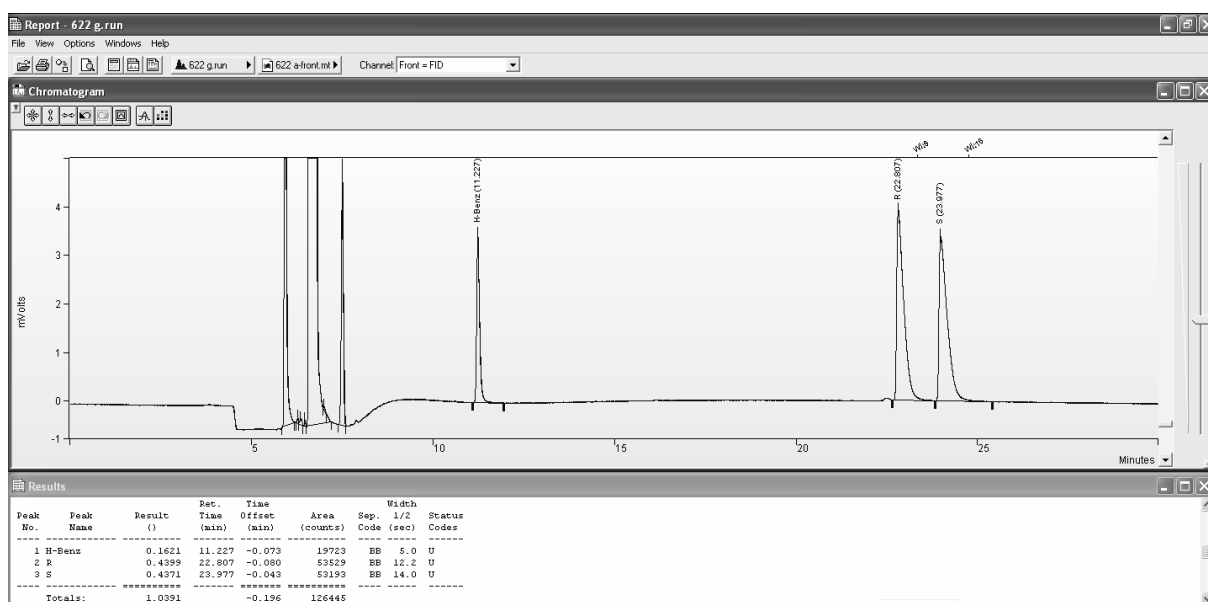
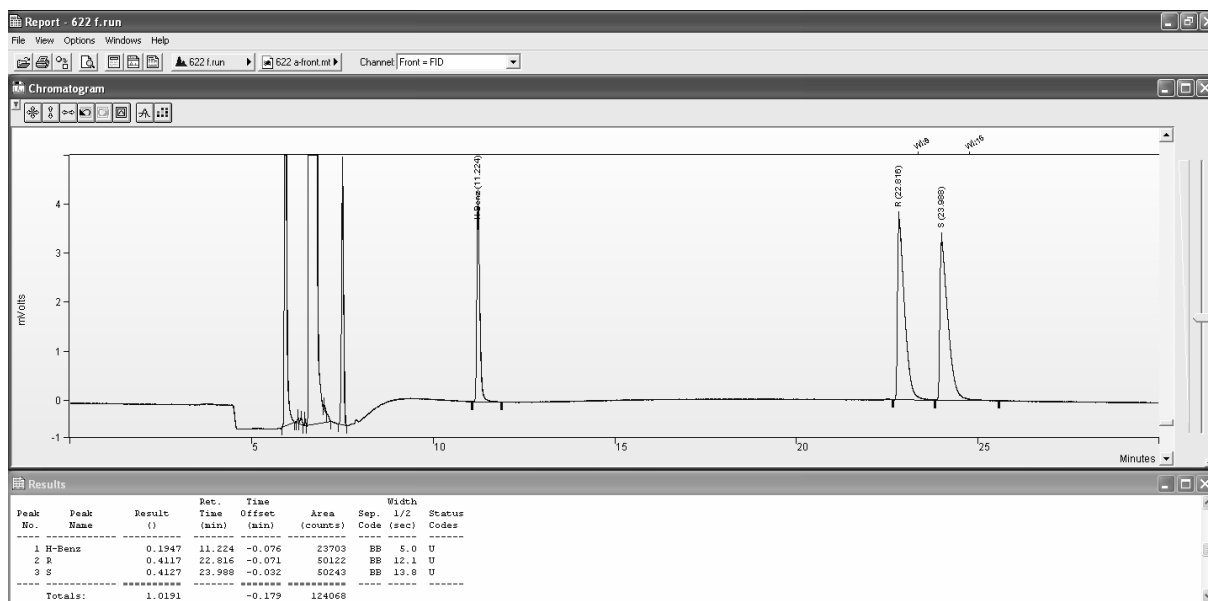


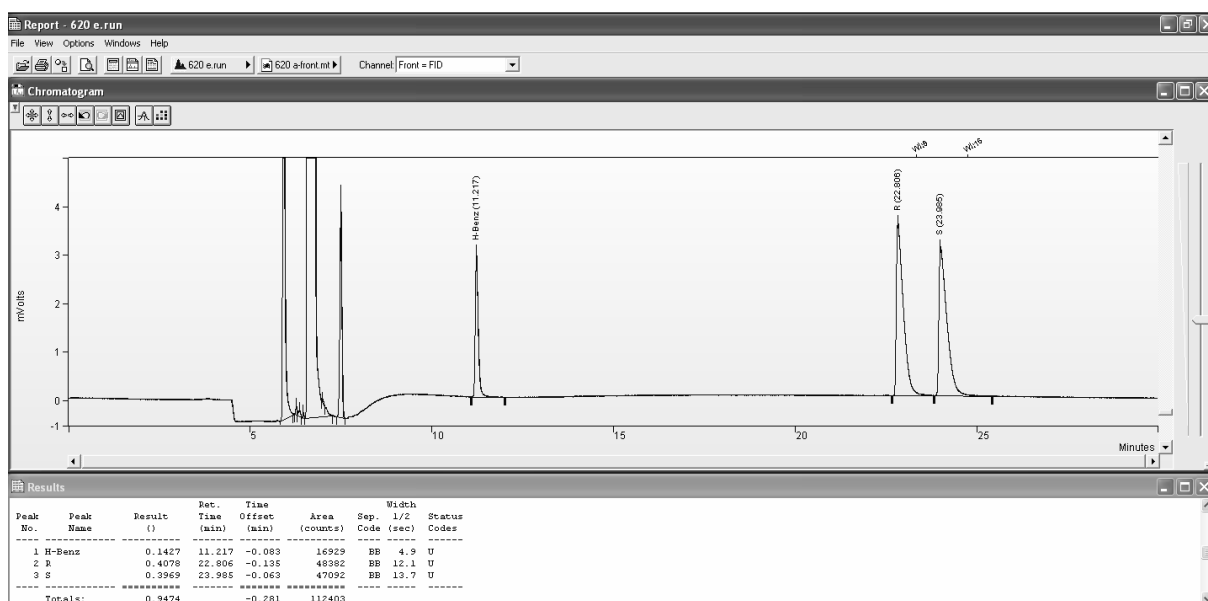
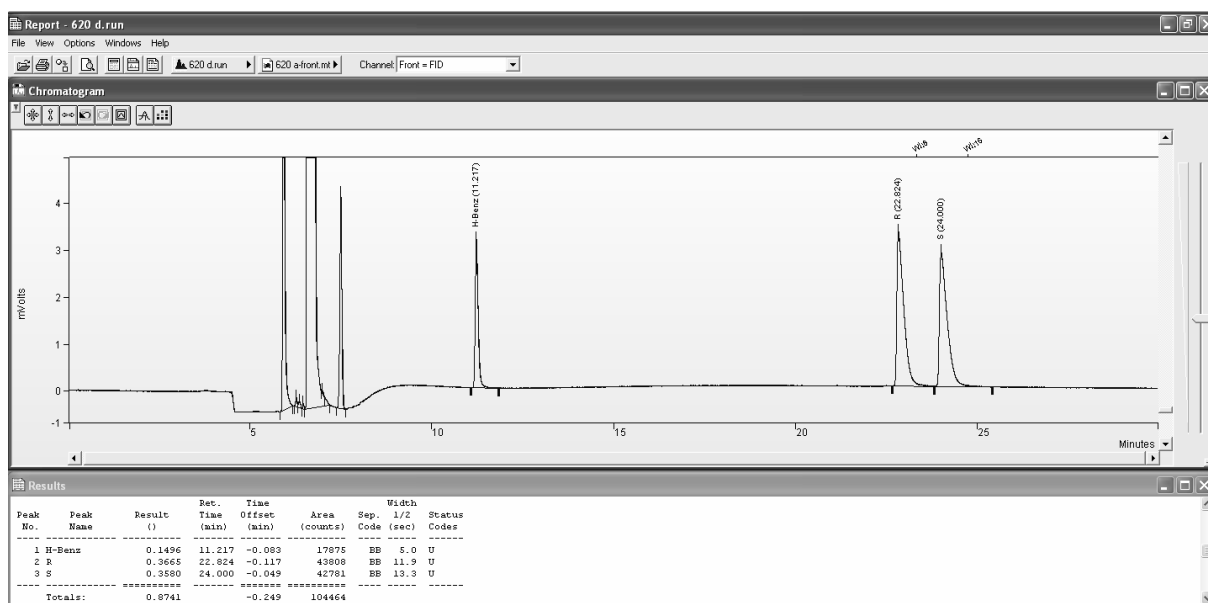
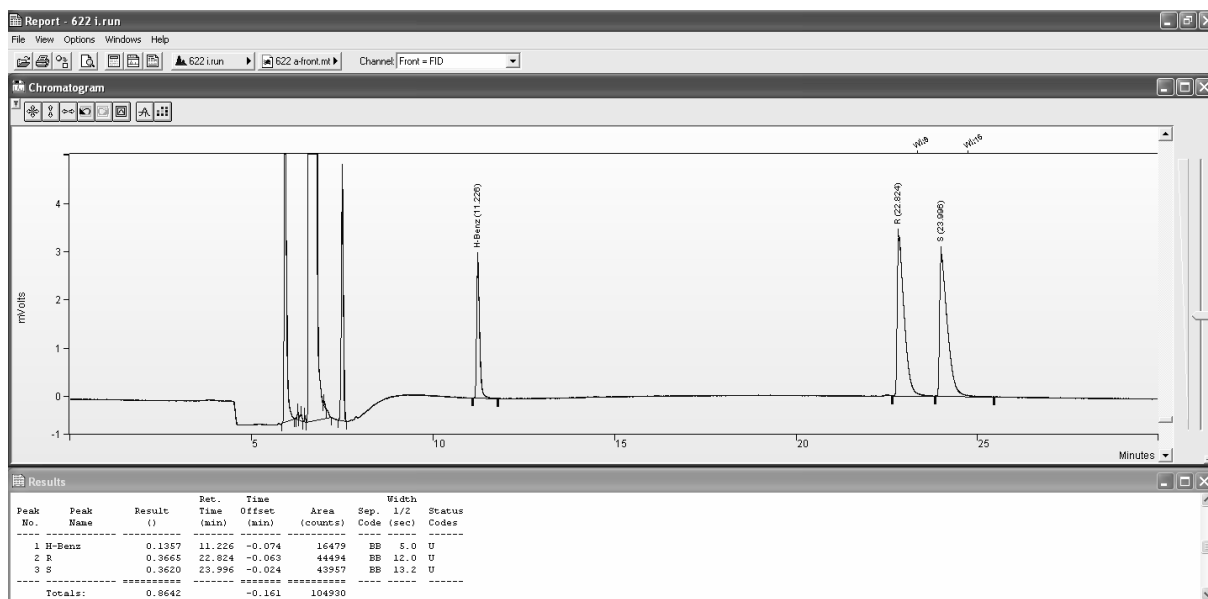
III.6 Figure 3b ((-)-NME)

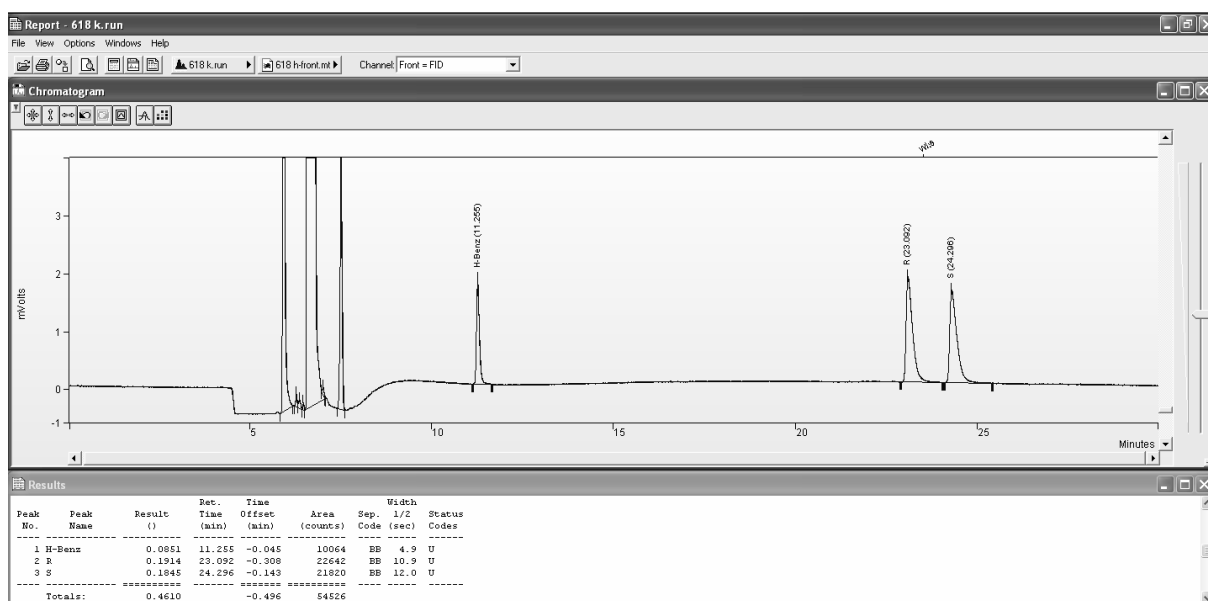
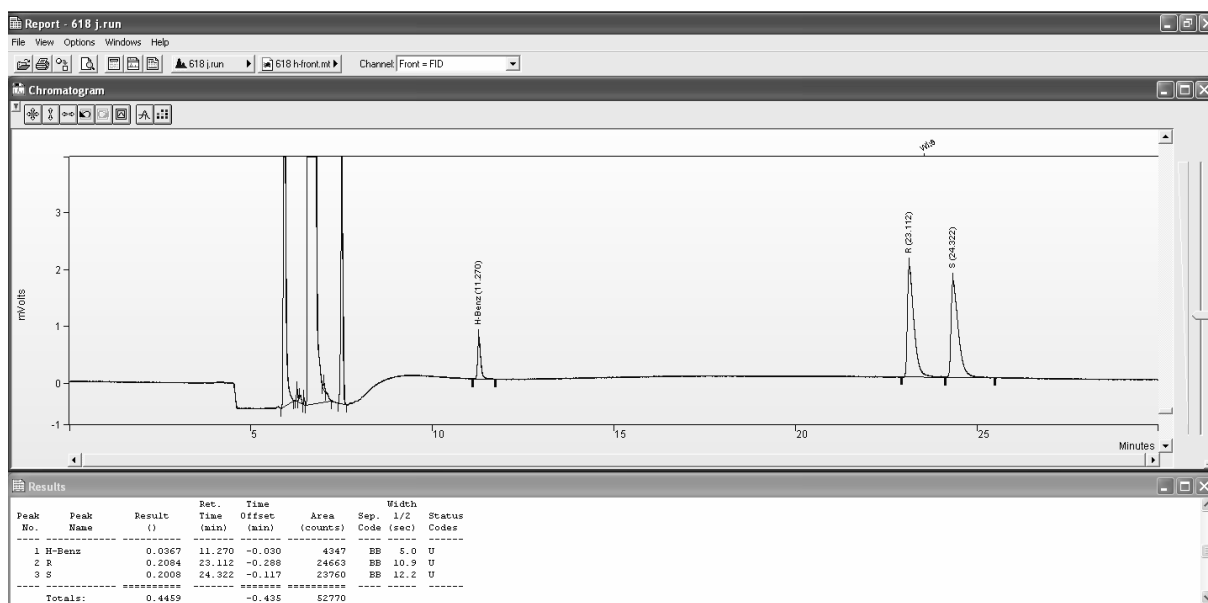
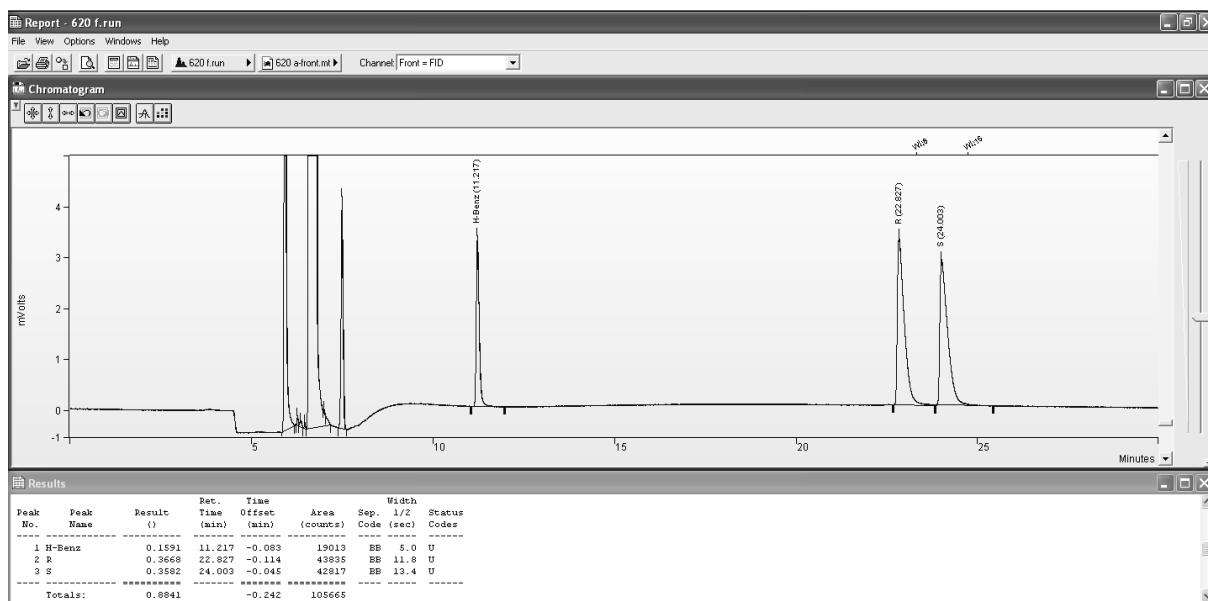


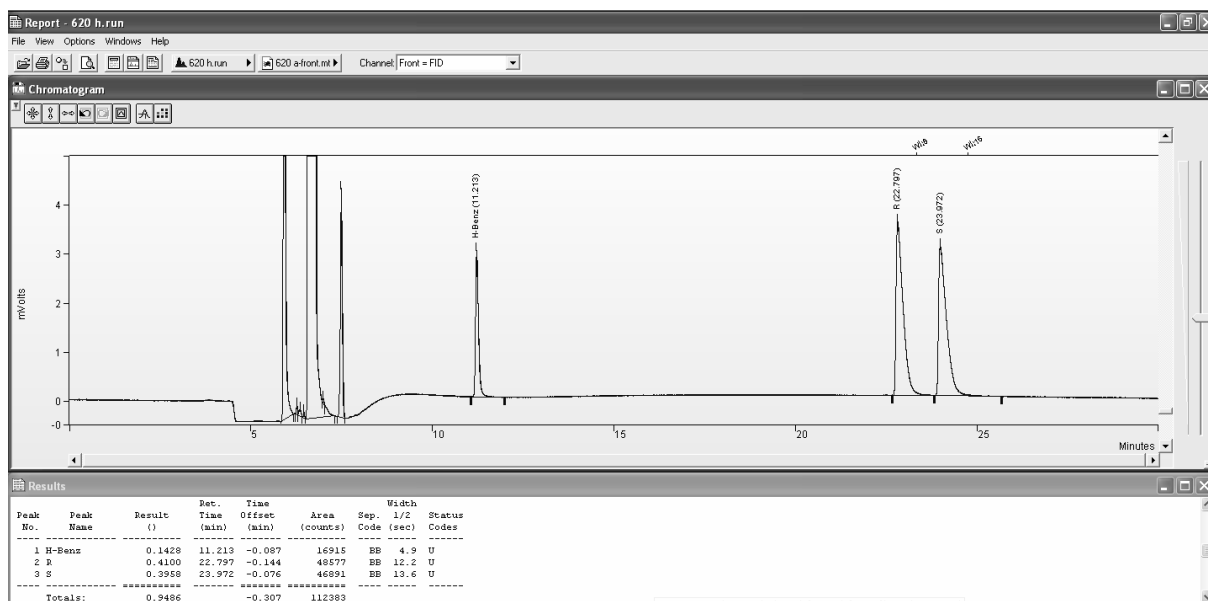
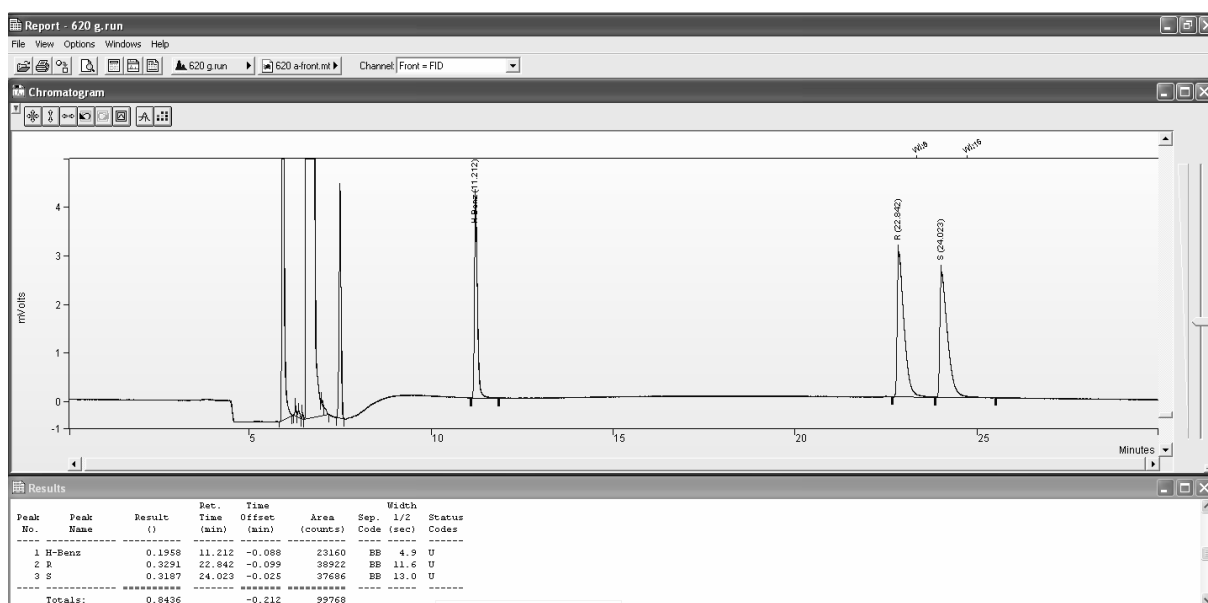
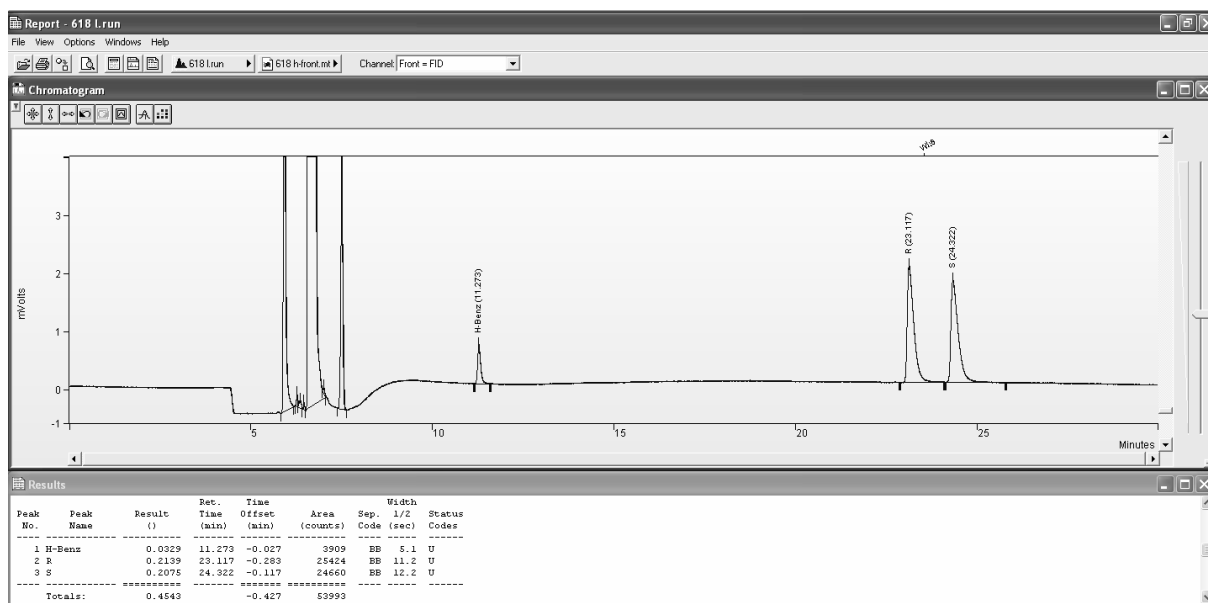


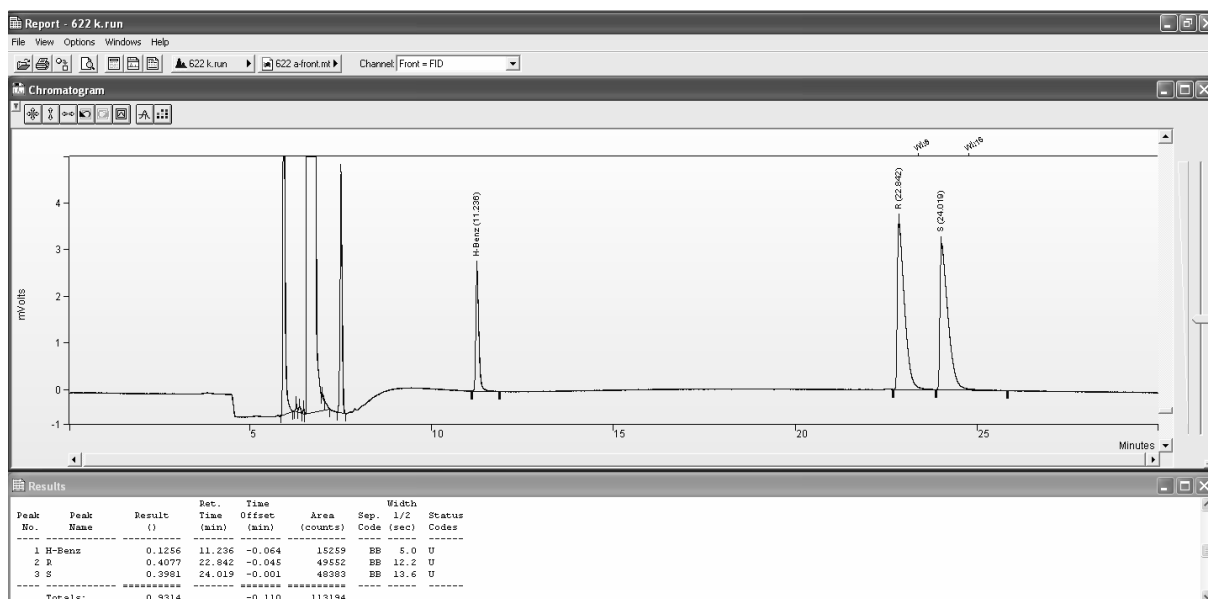
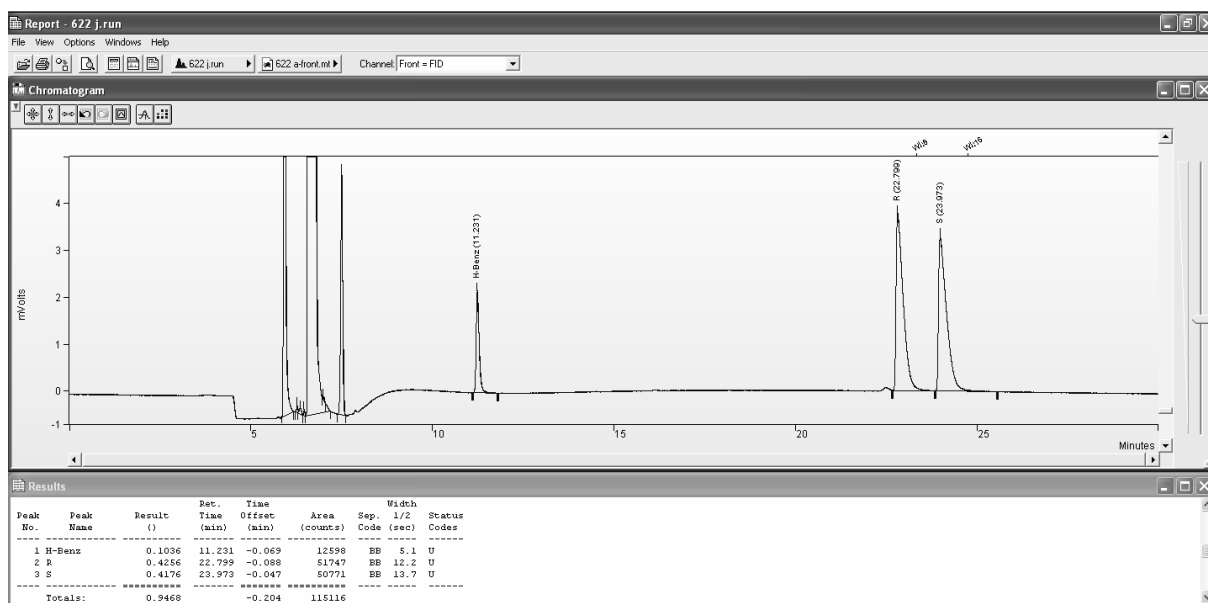
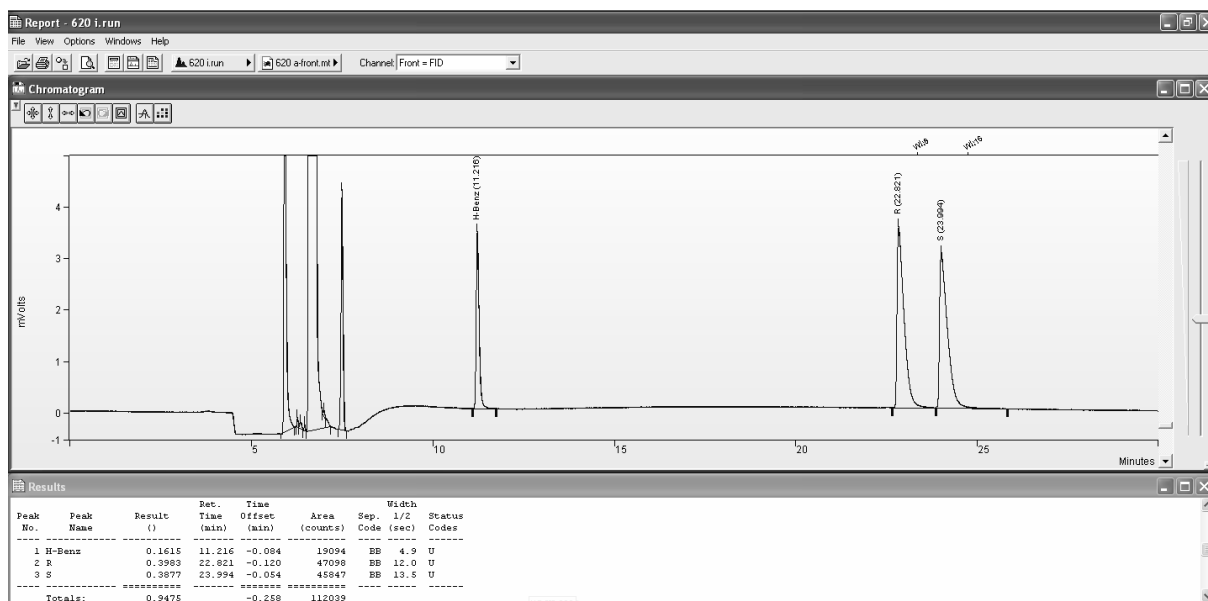


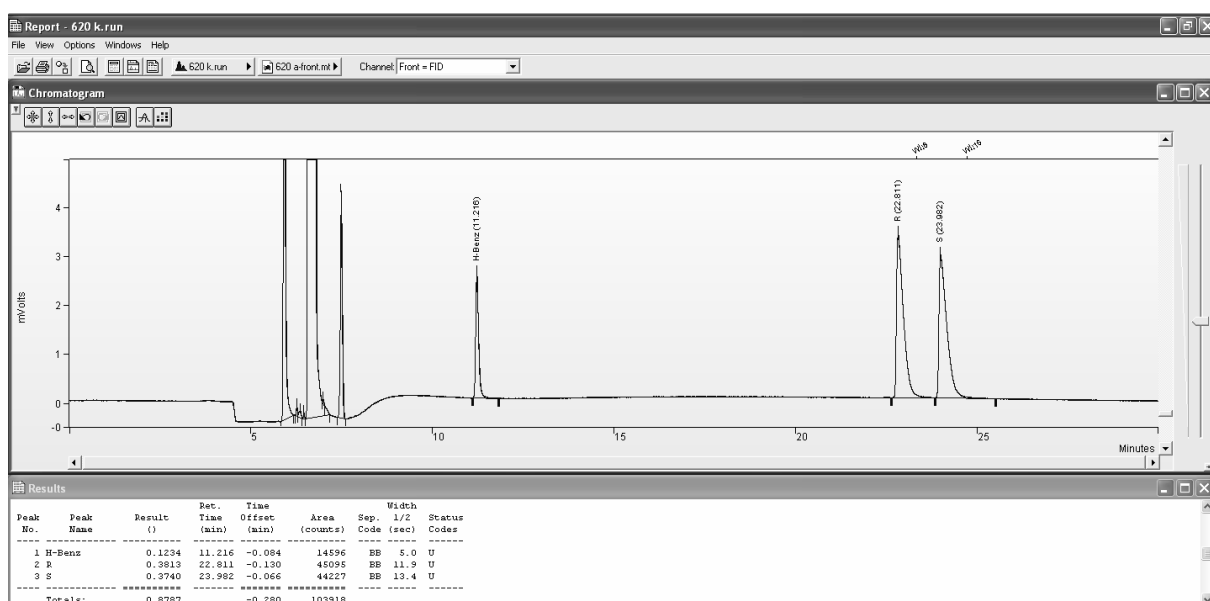
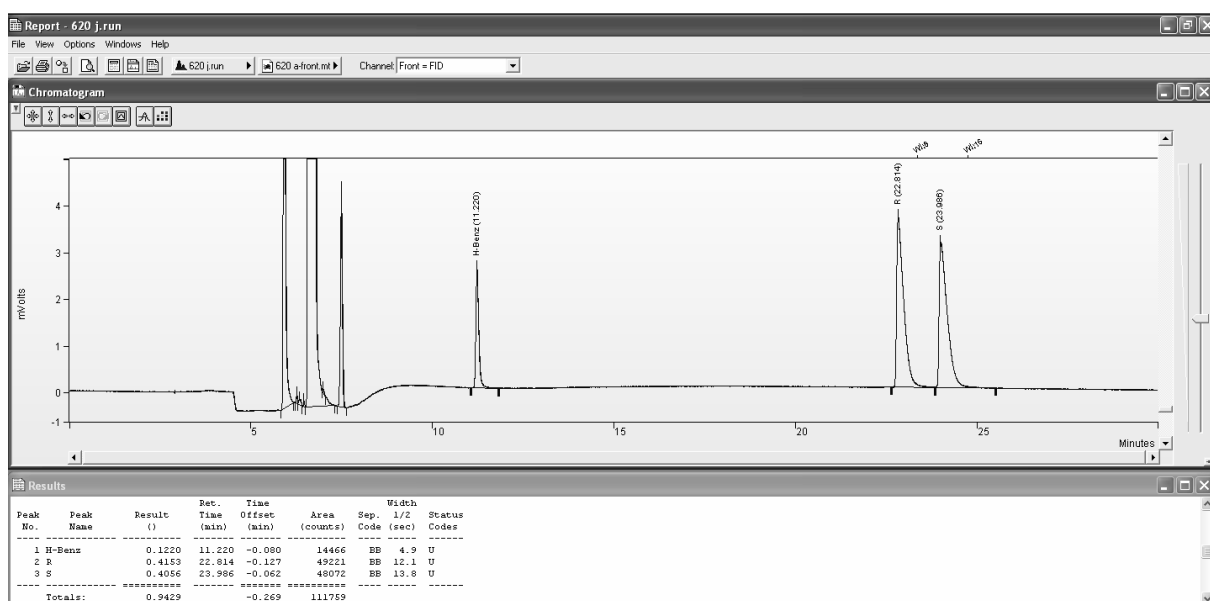
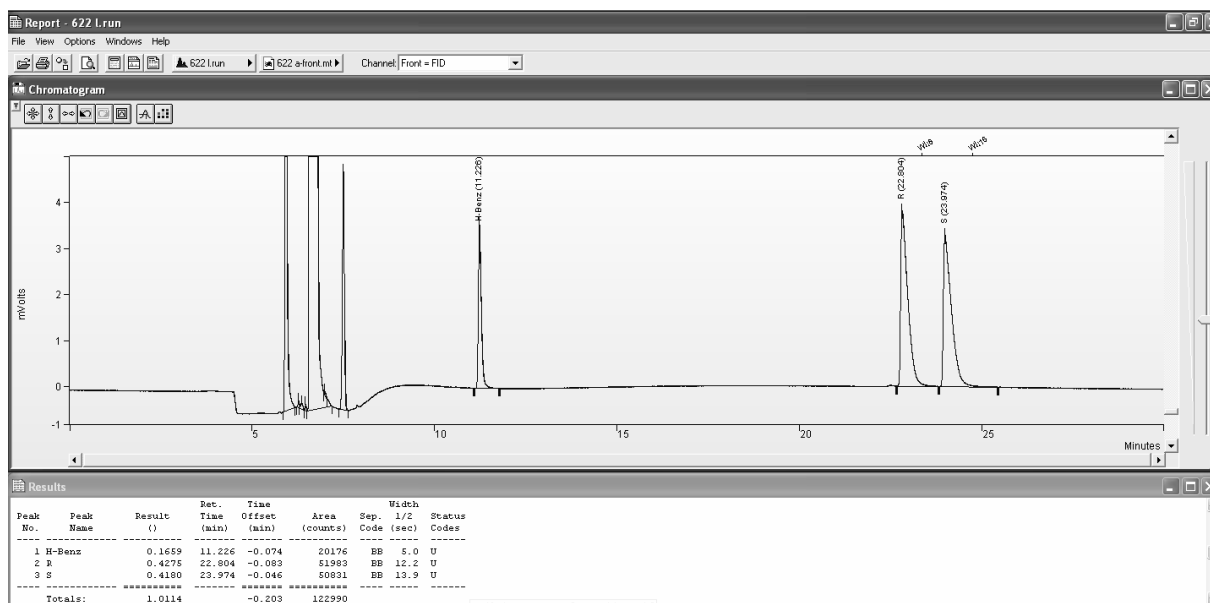


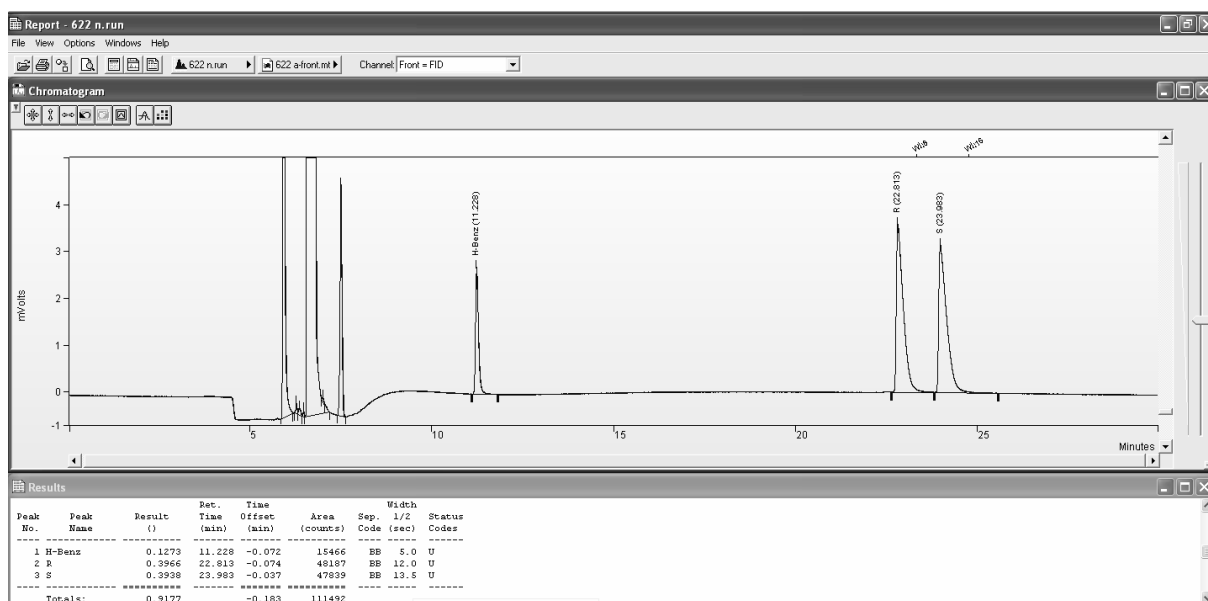
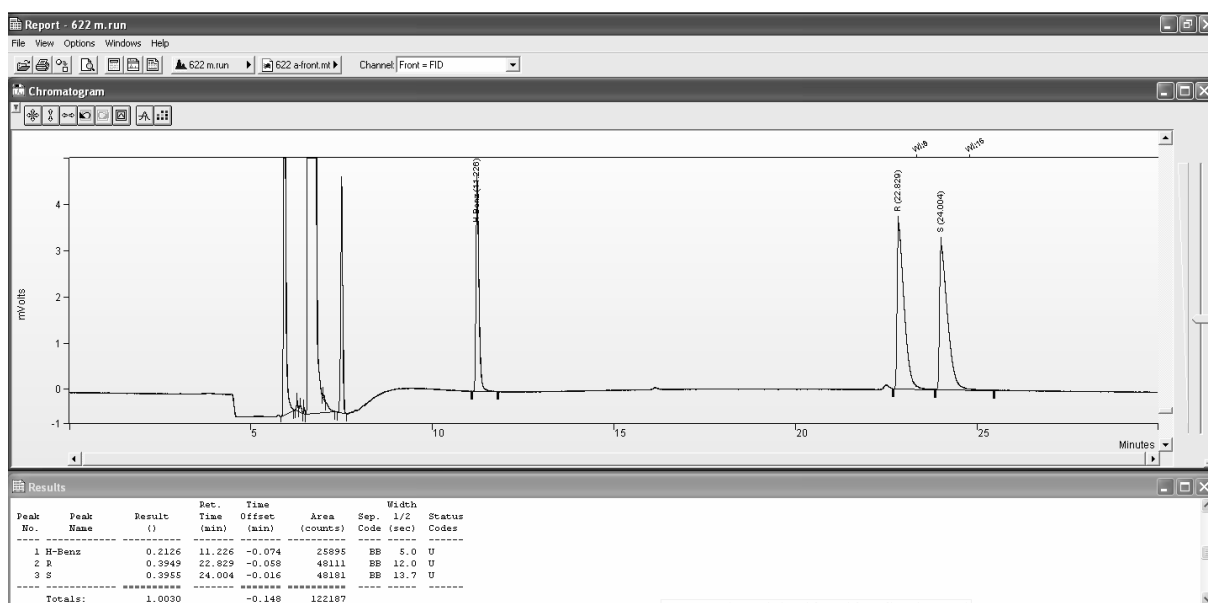
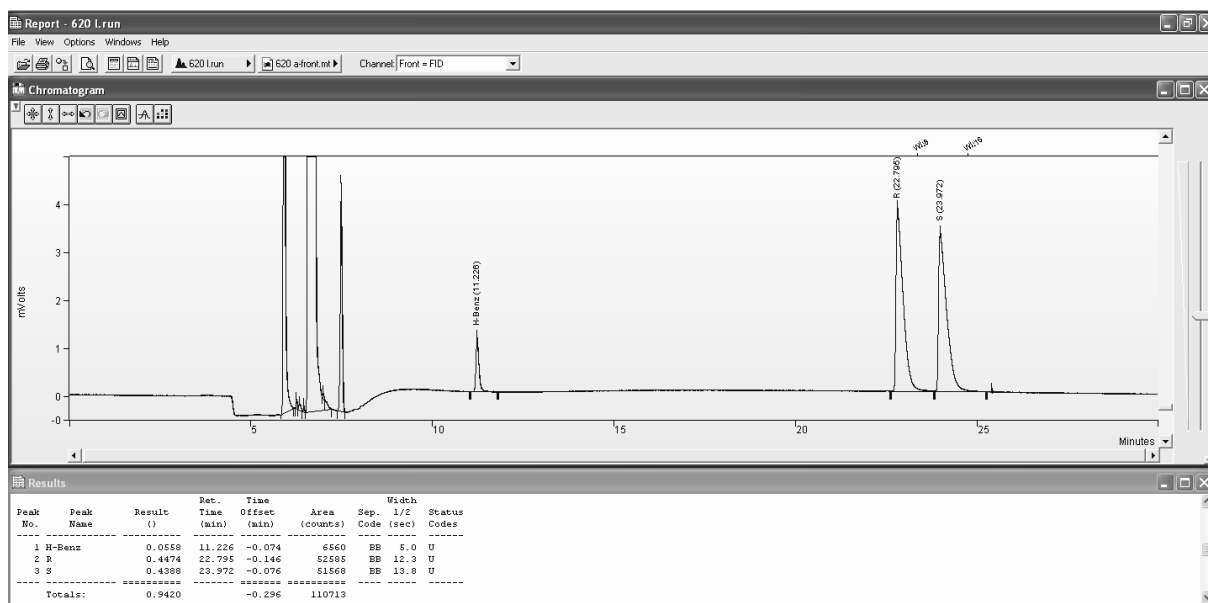


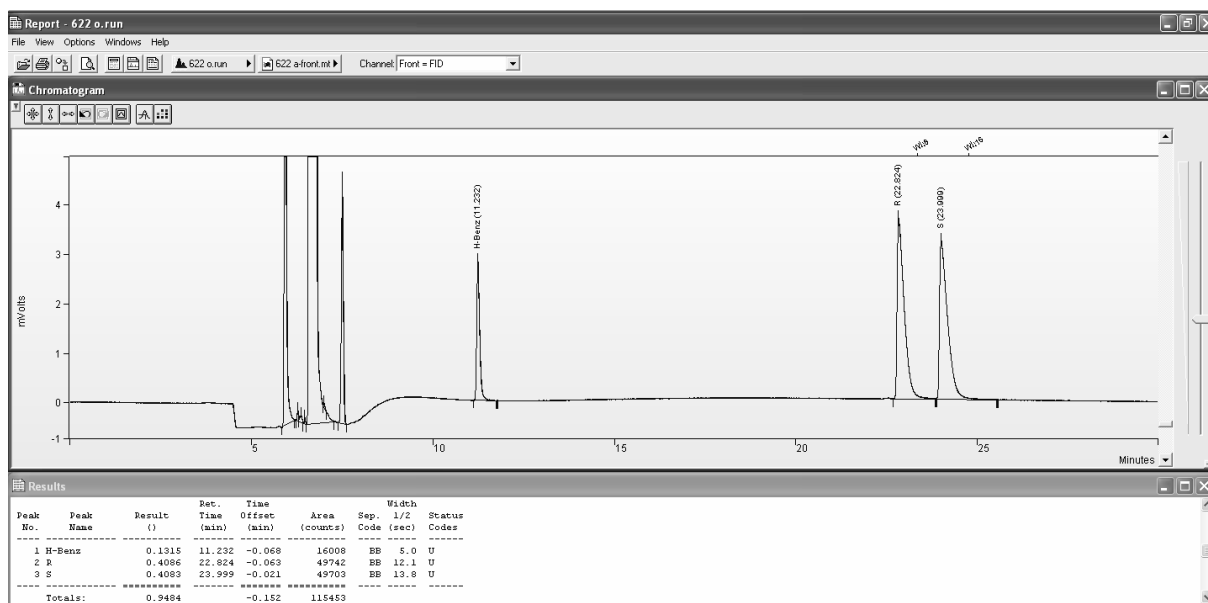




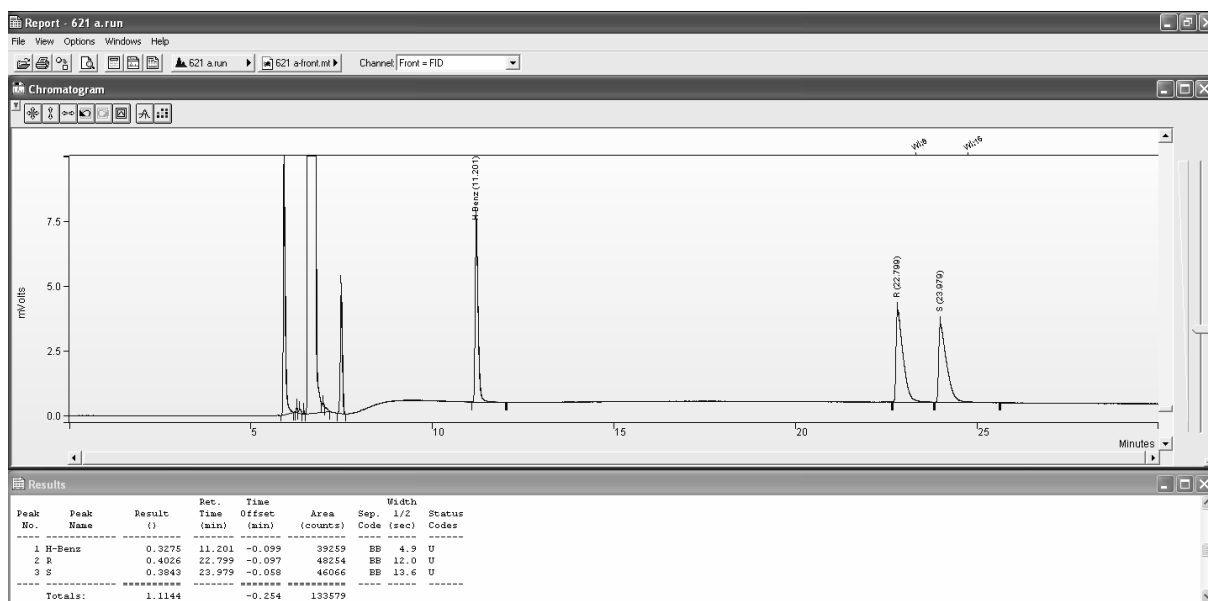


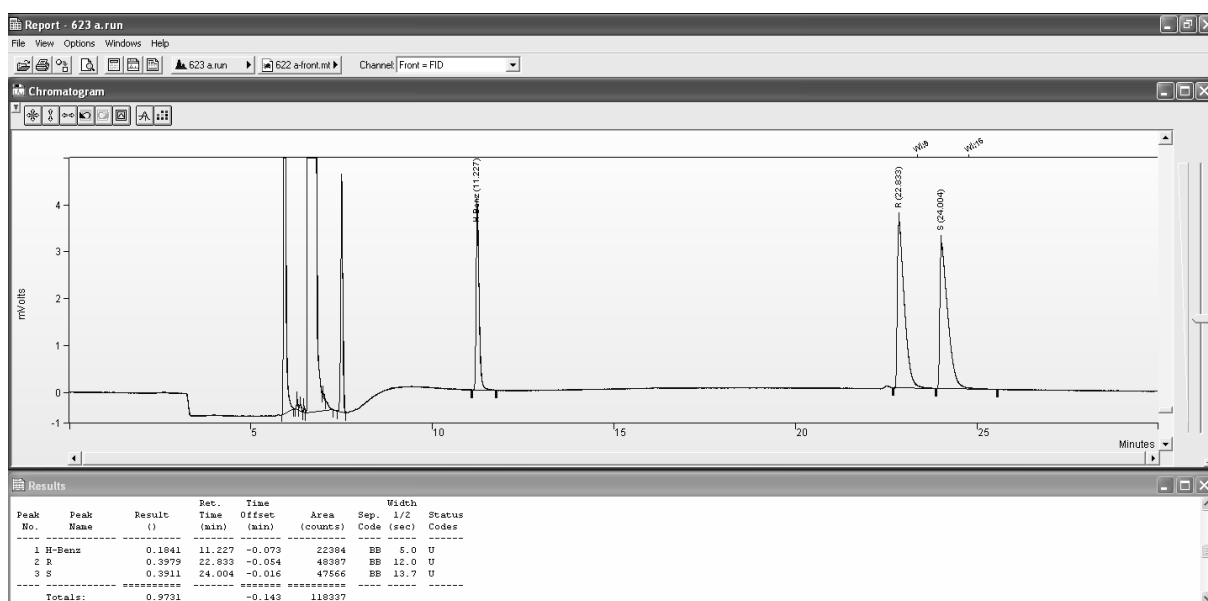
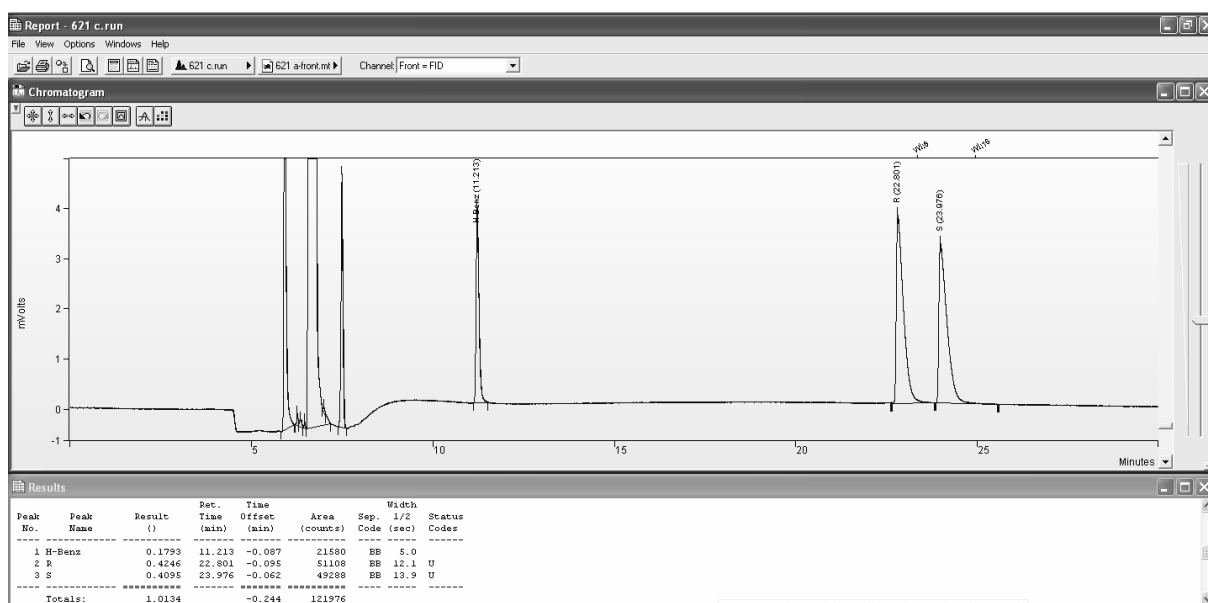
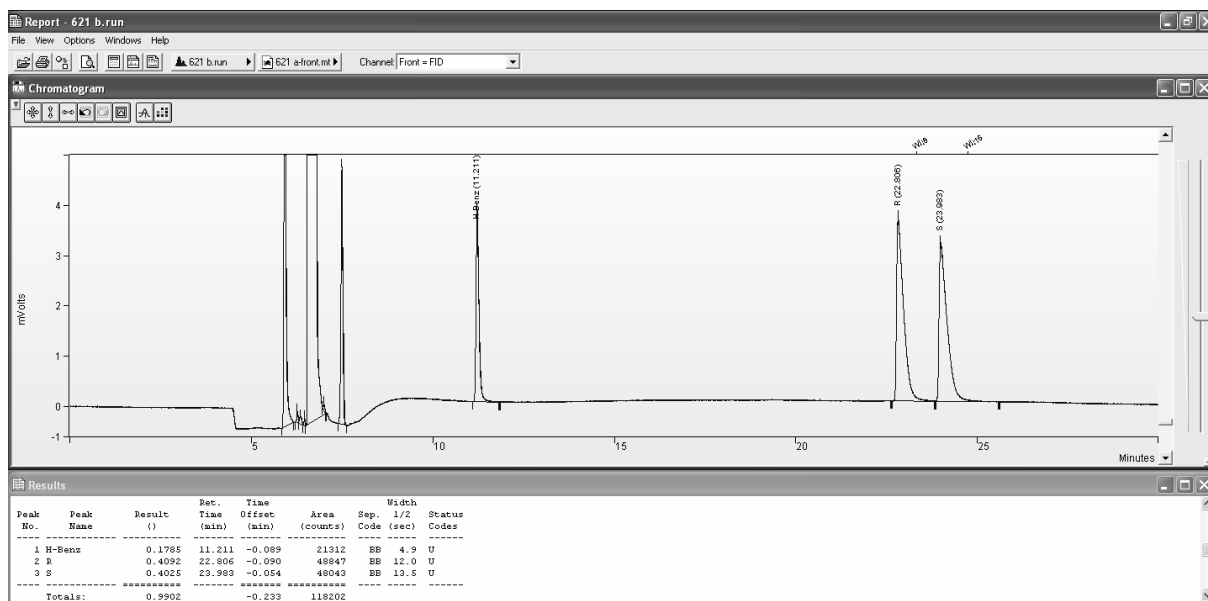


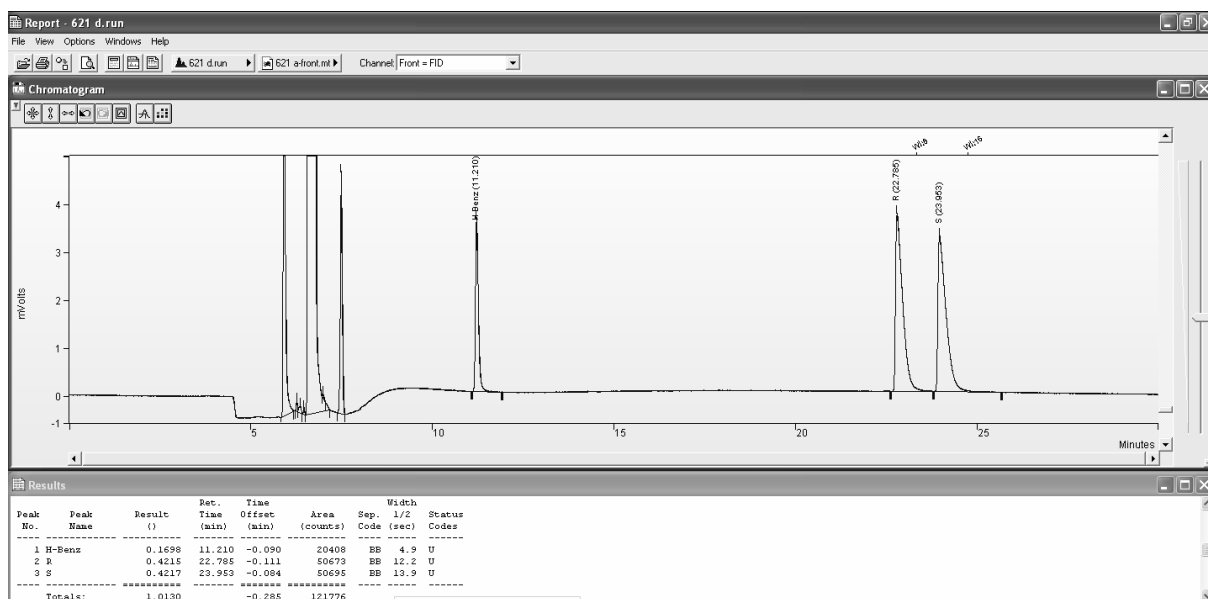
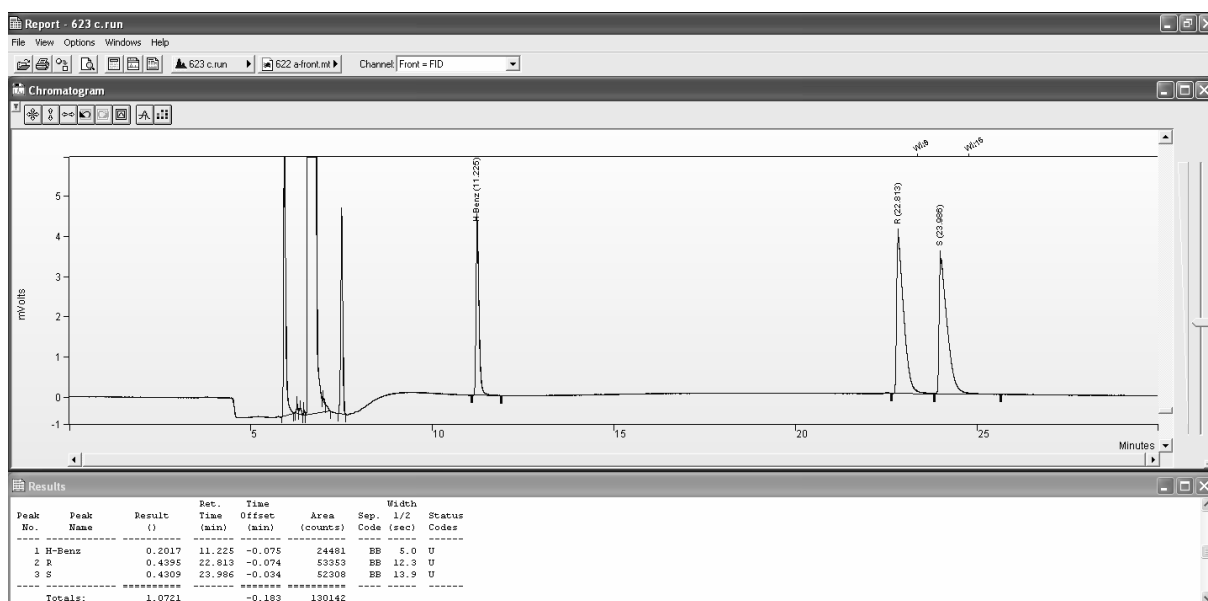
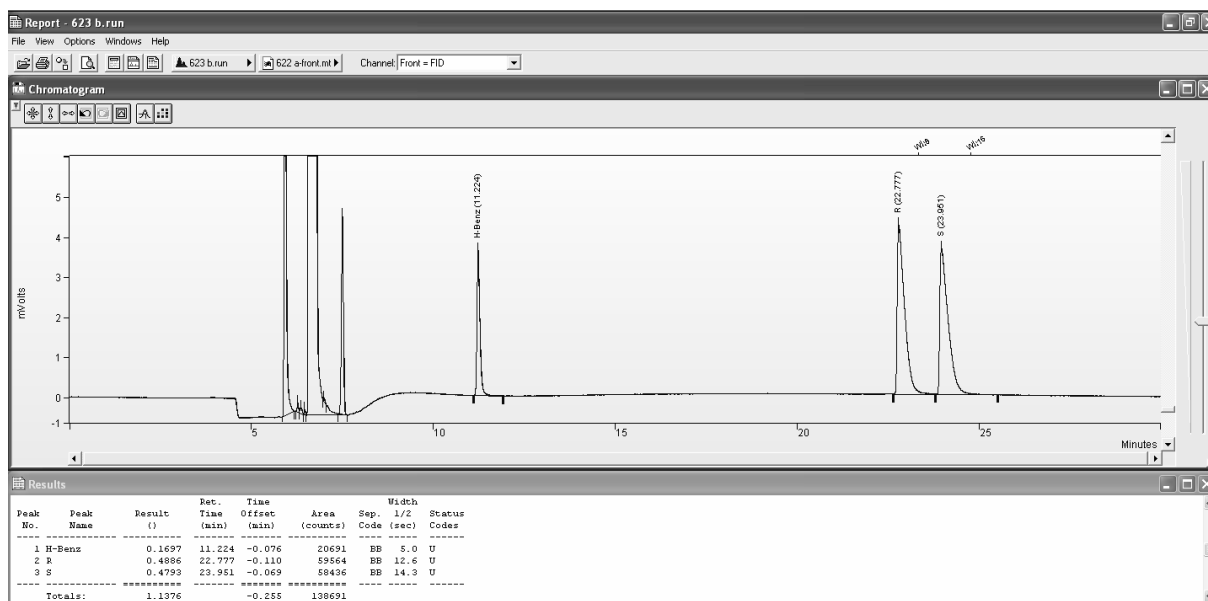


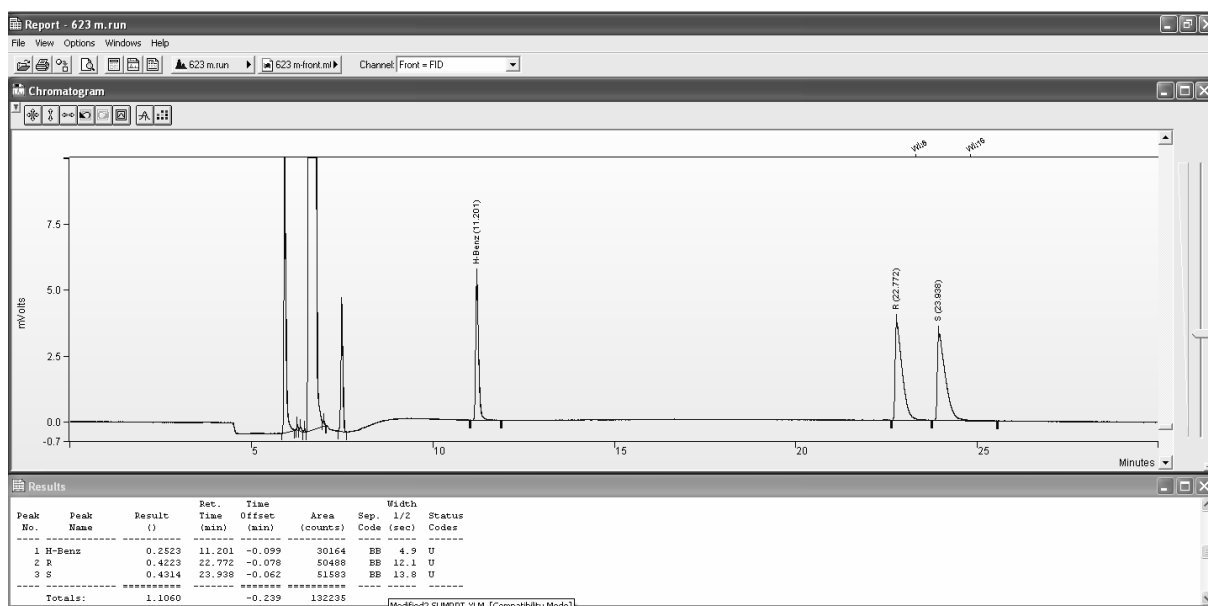
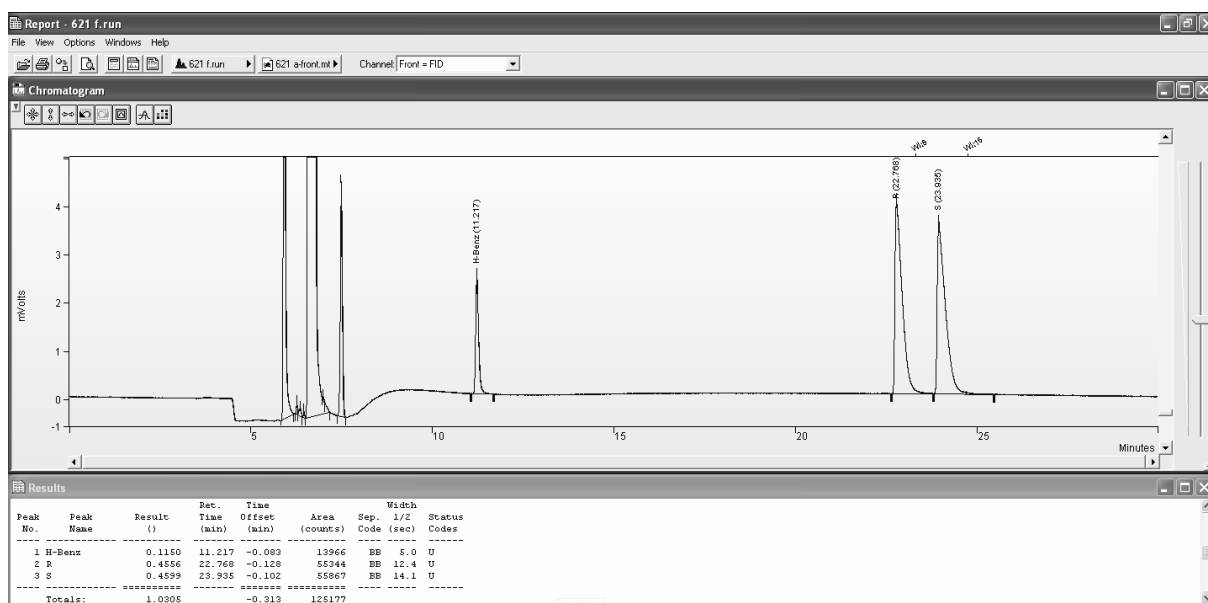
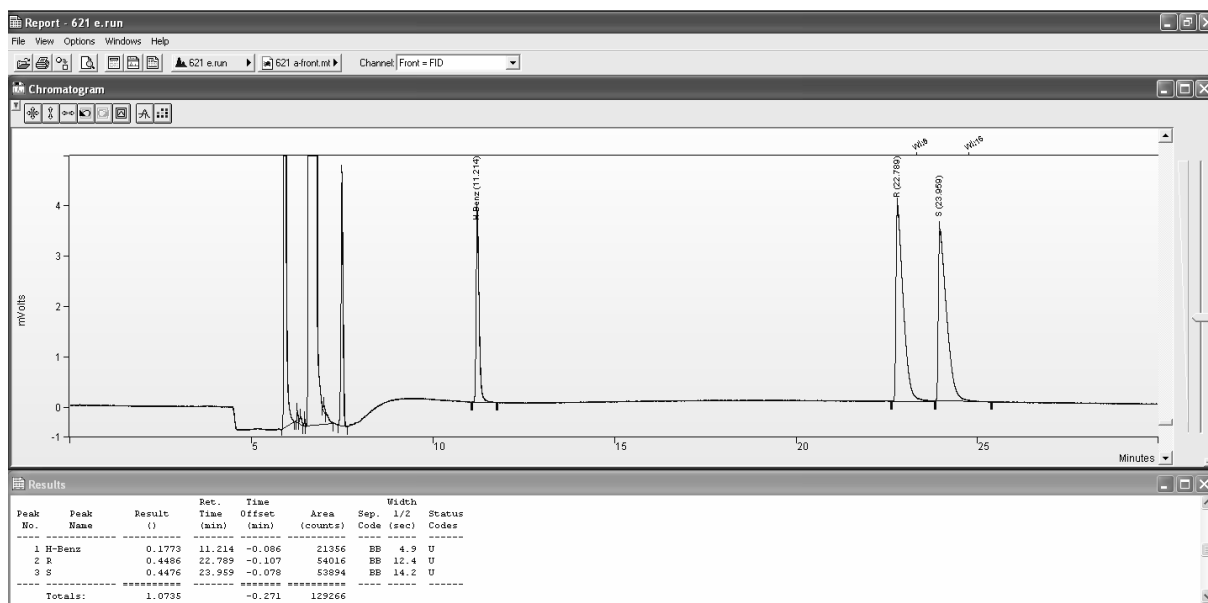


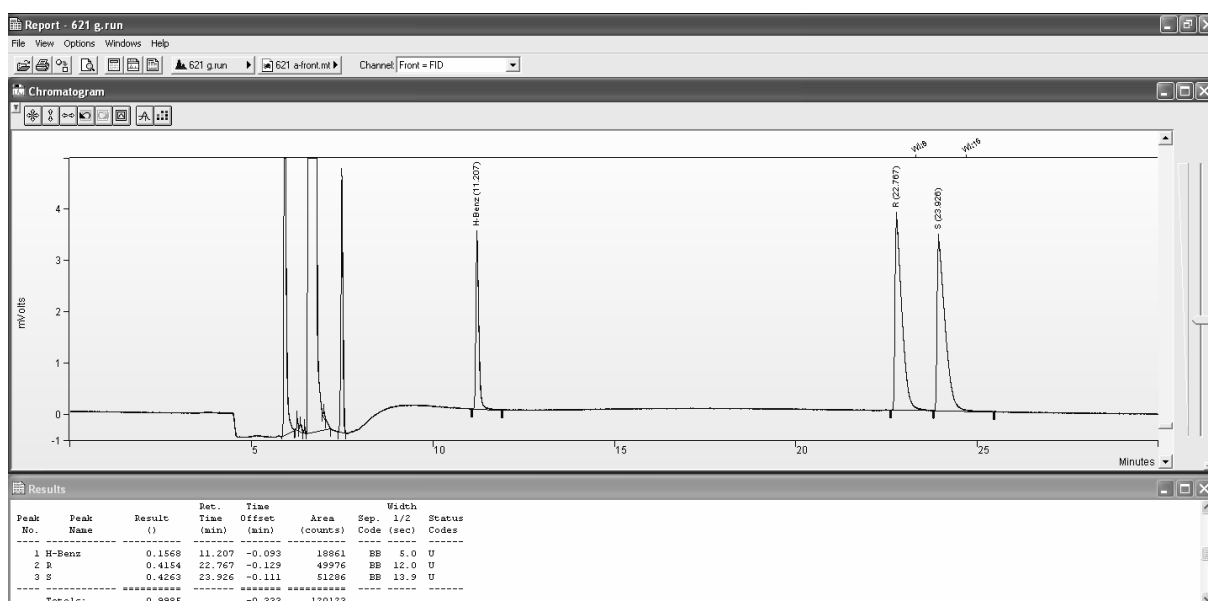
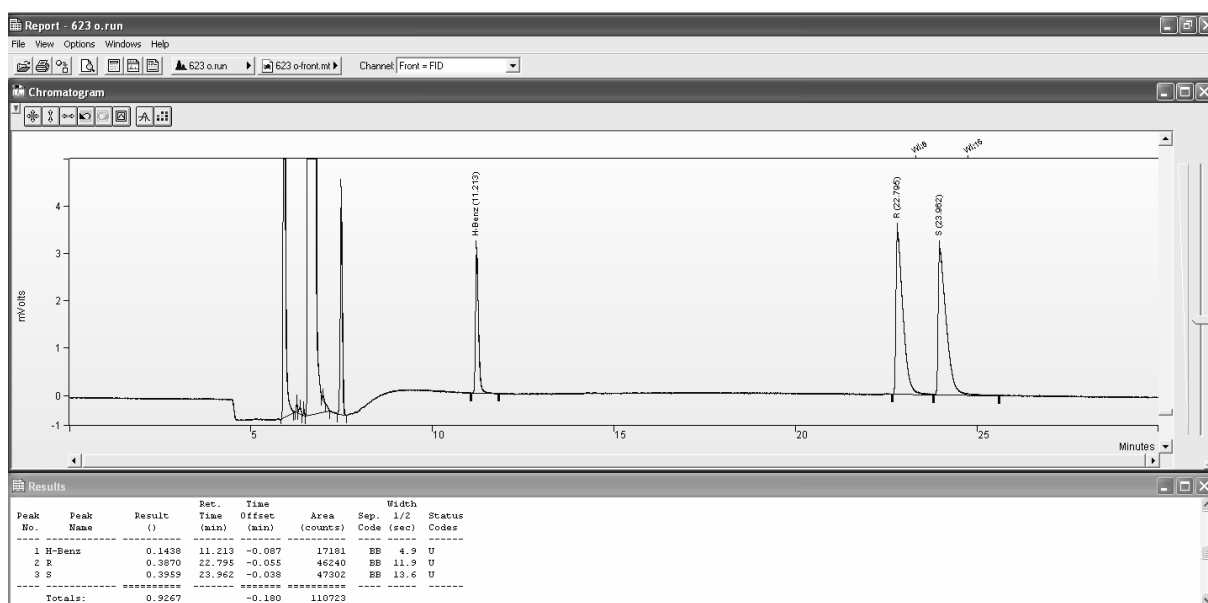
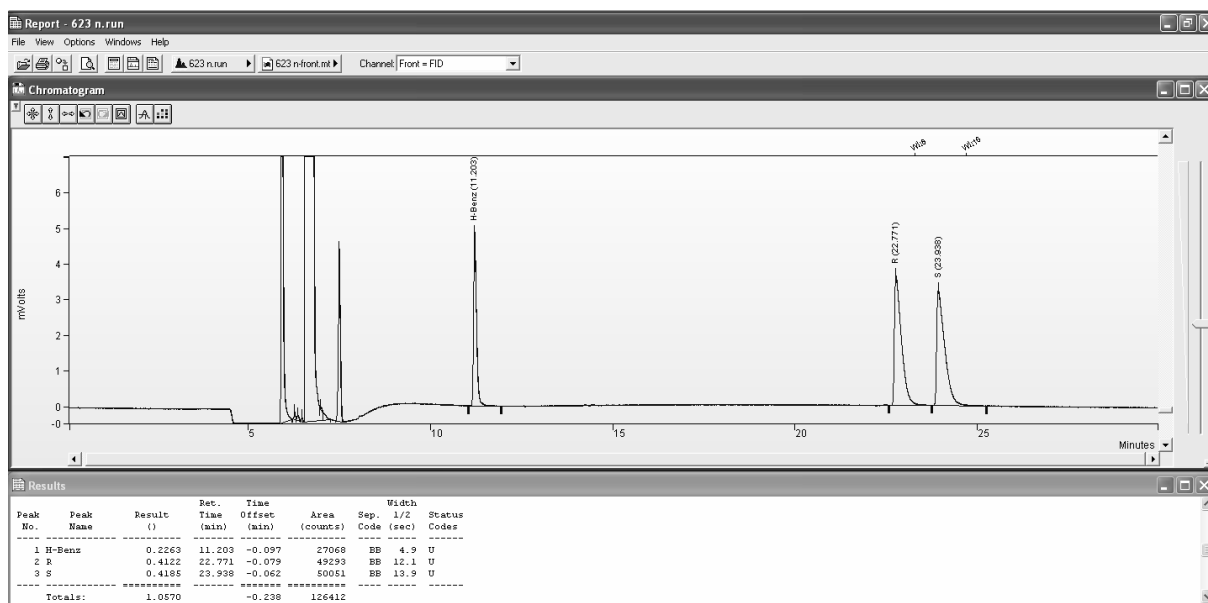
III.7 Figure 3b (+)-NME

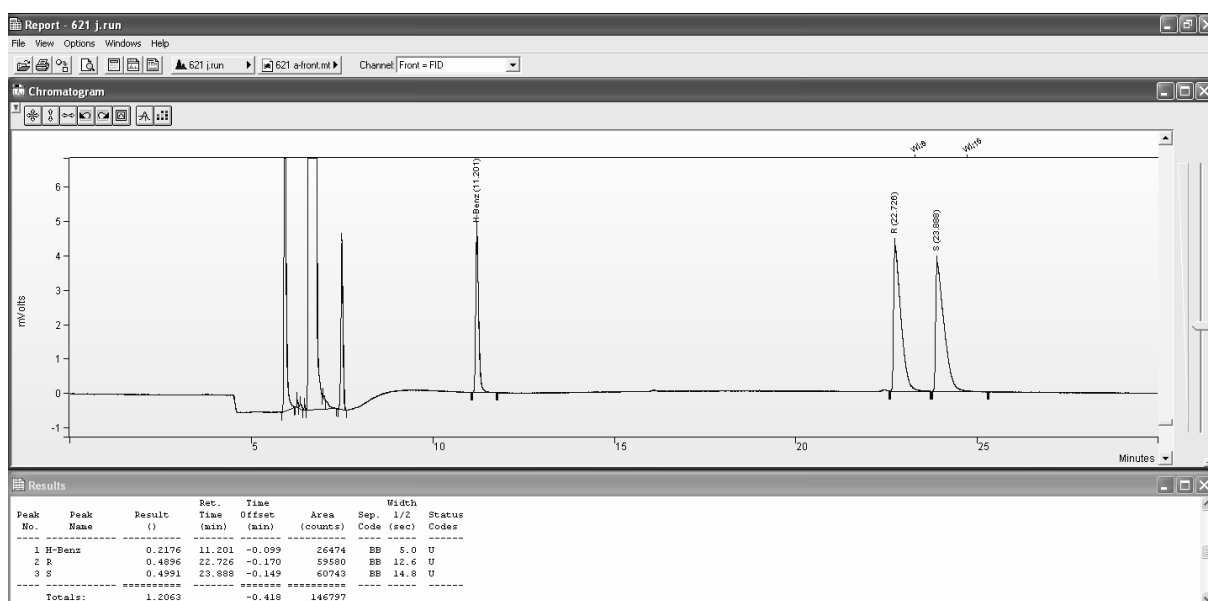
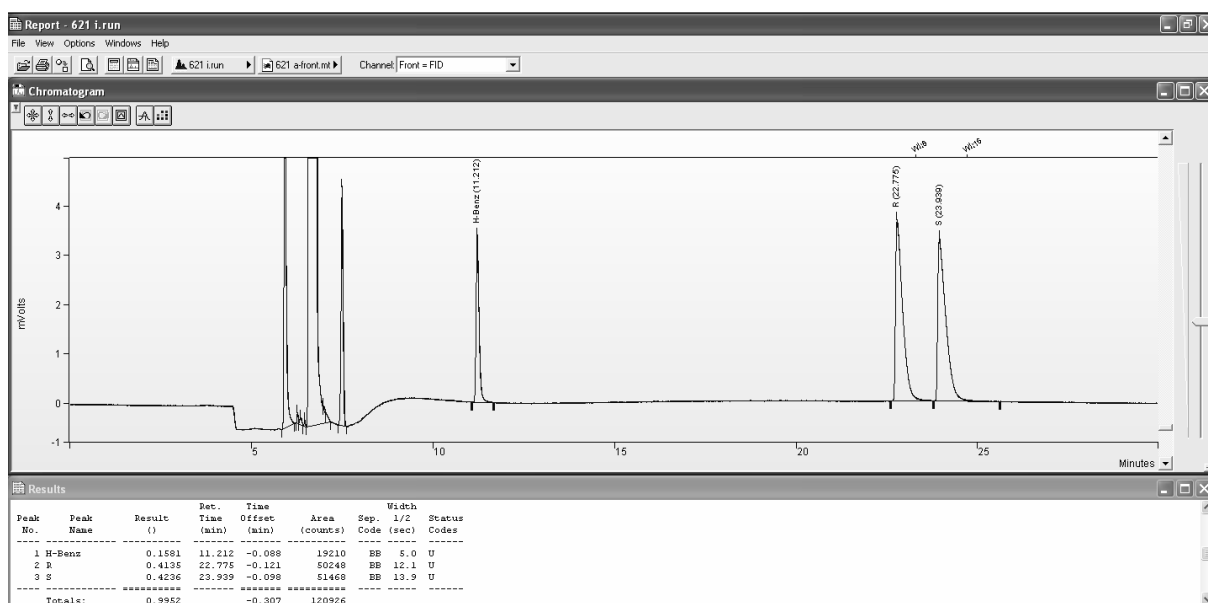
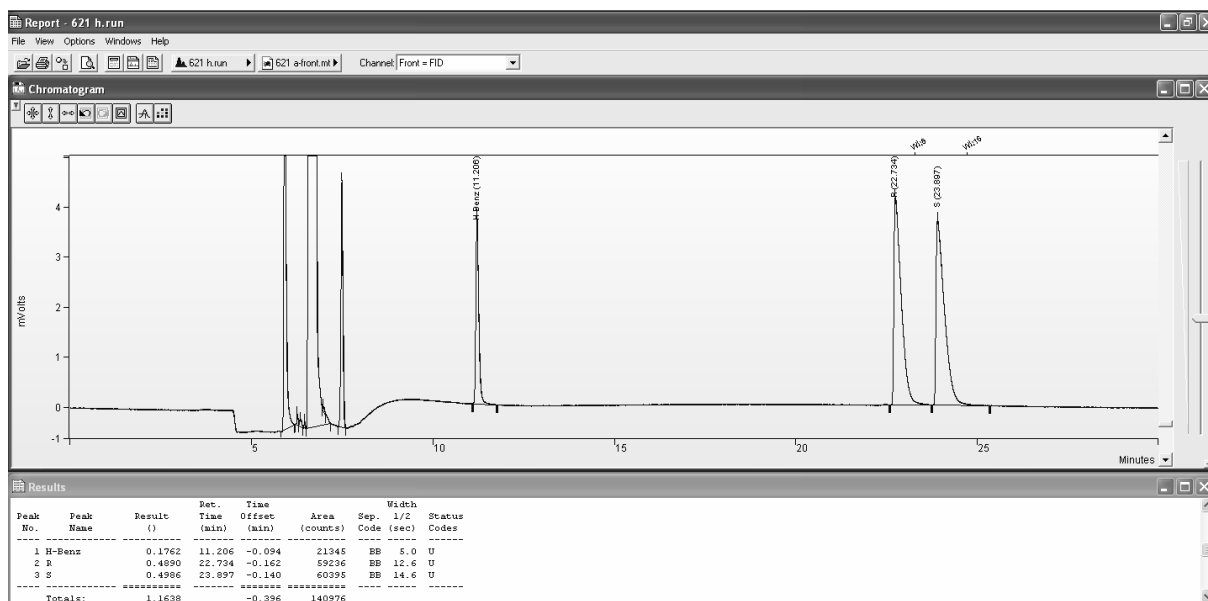


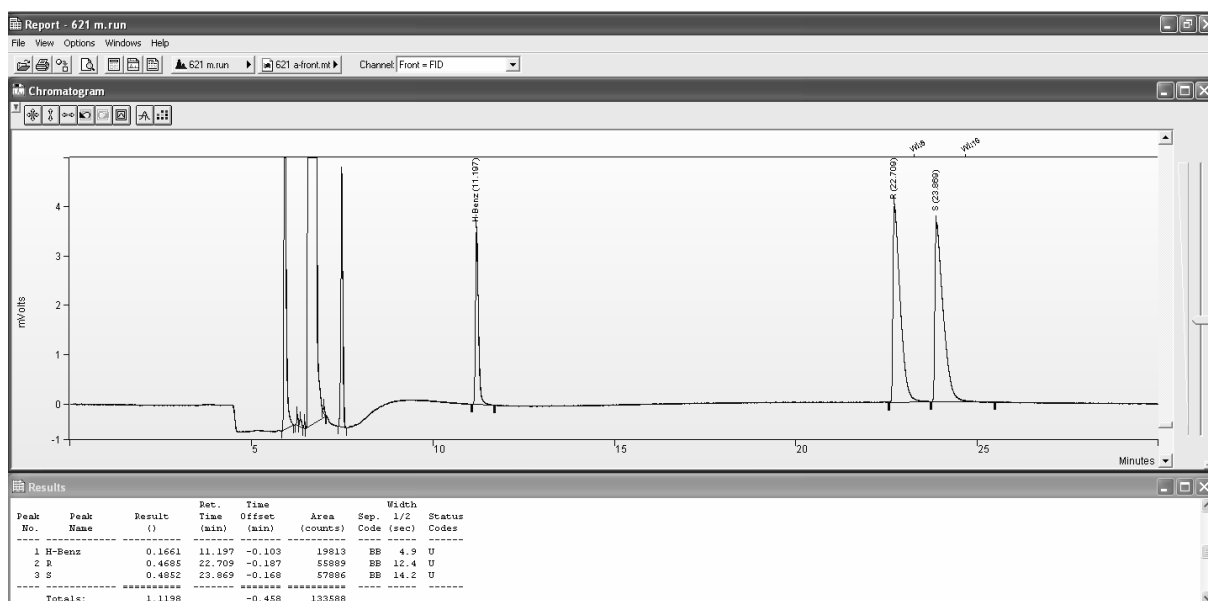
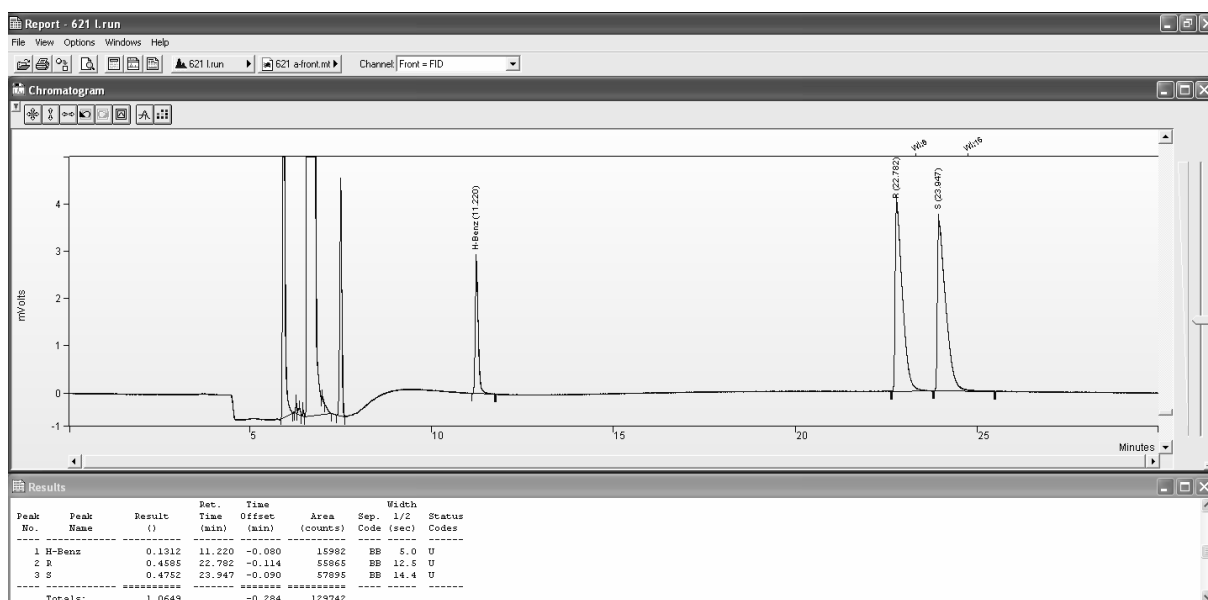
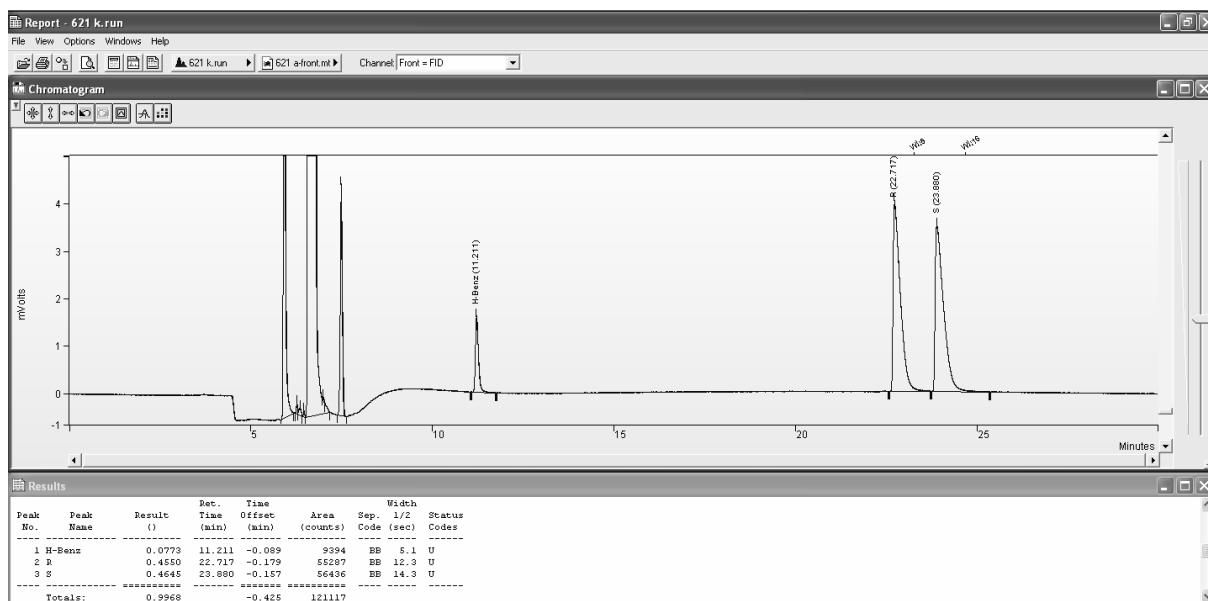


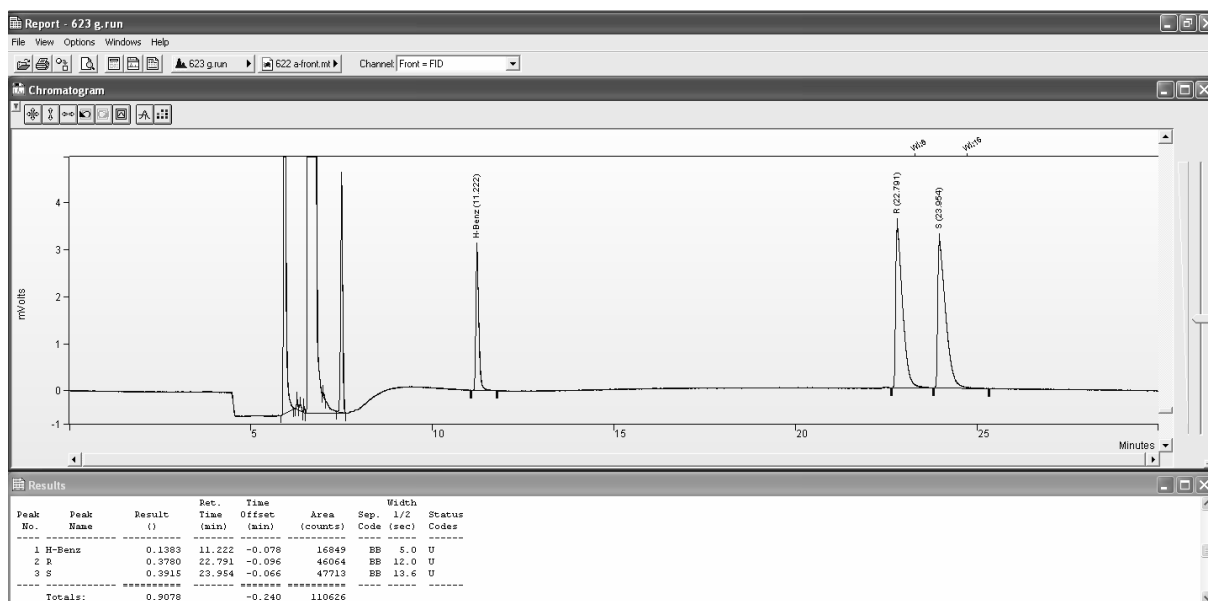
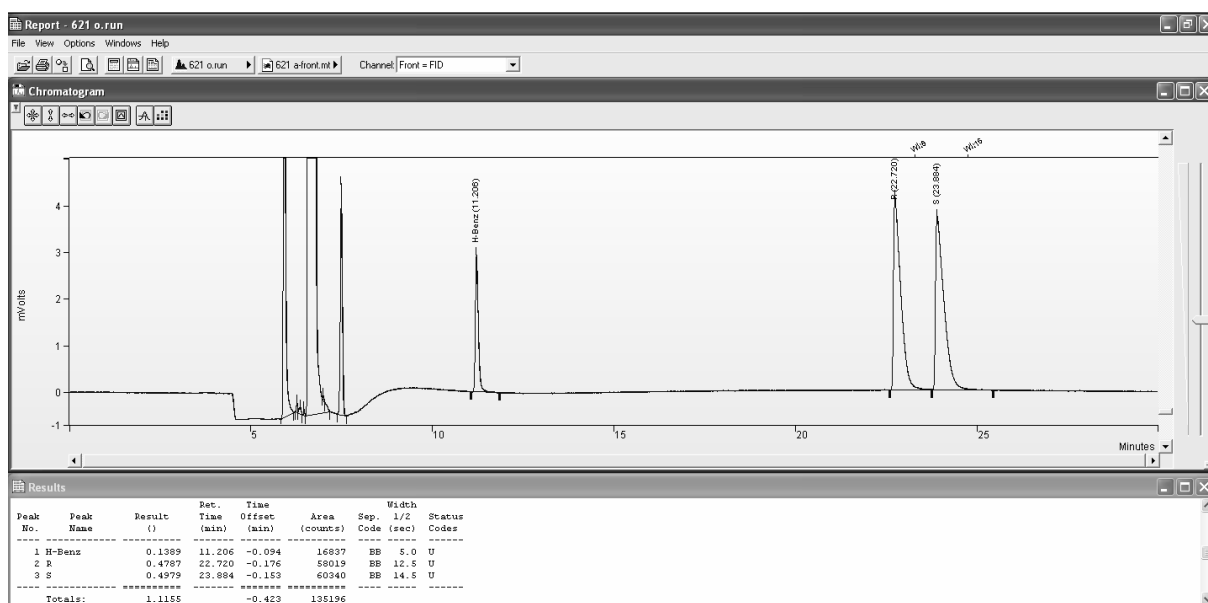
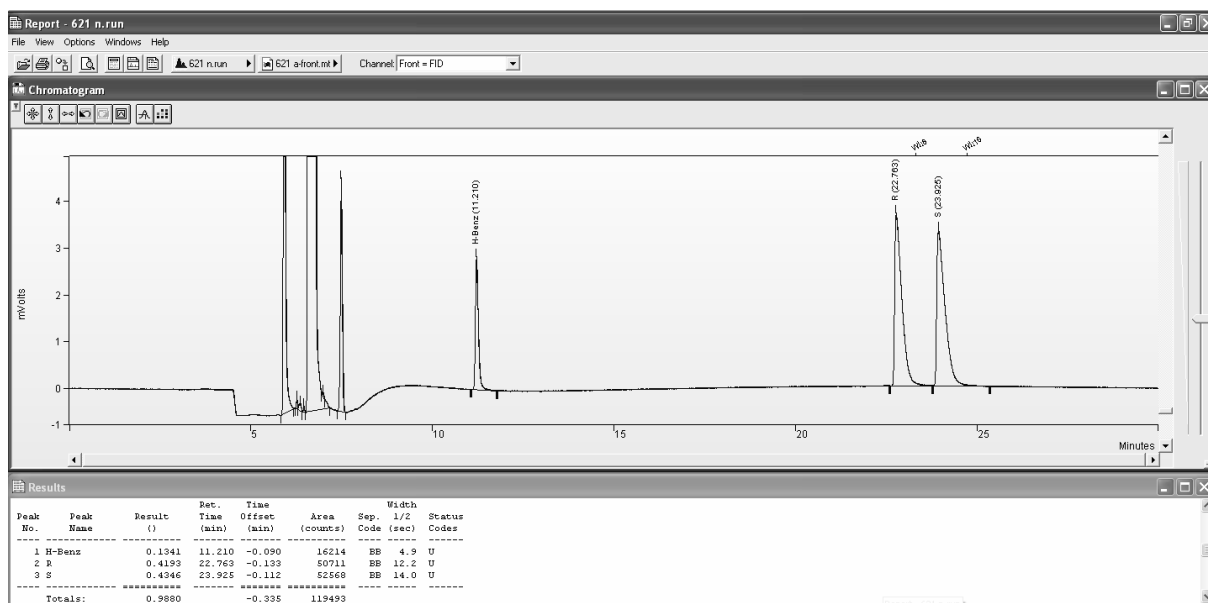


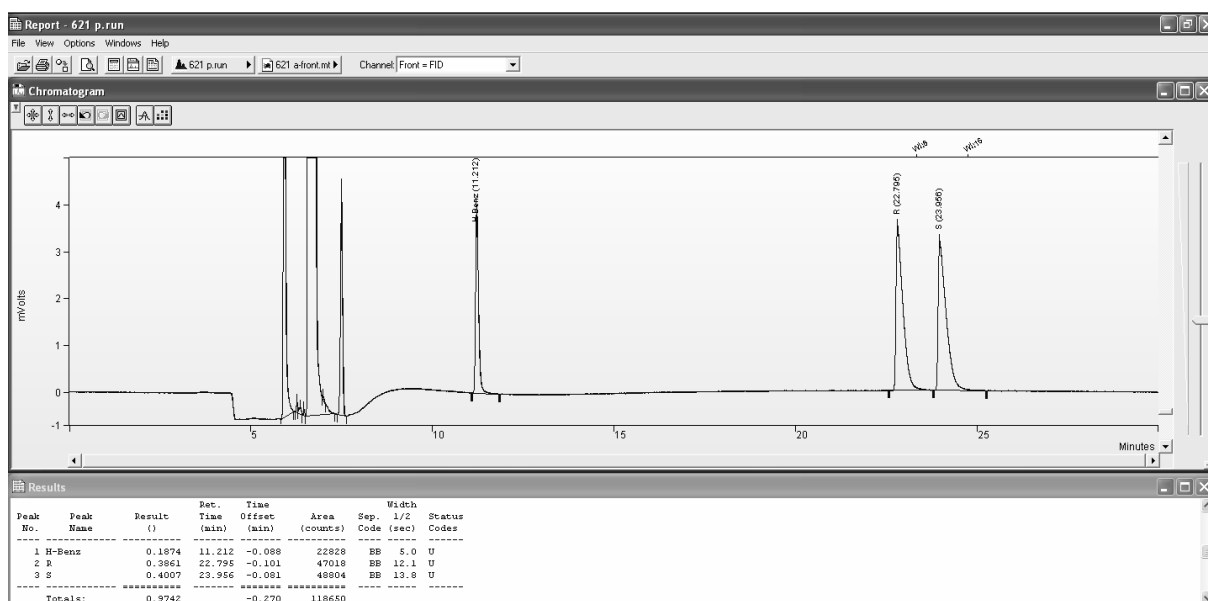
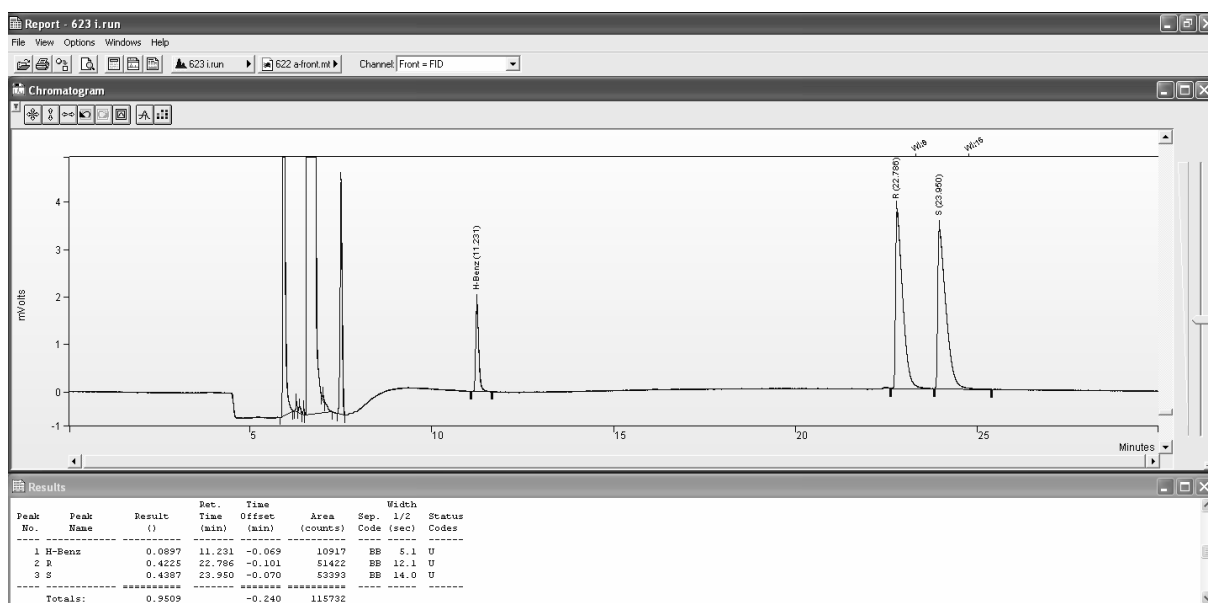
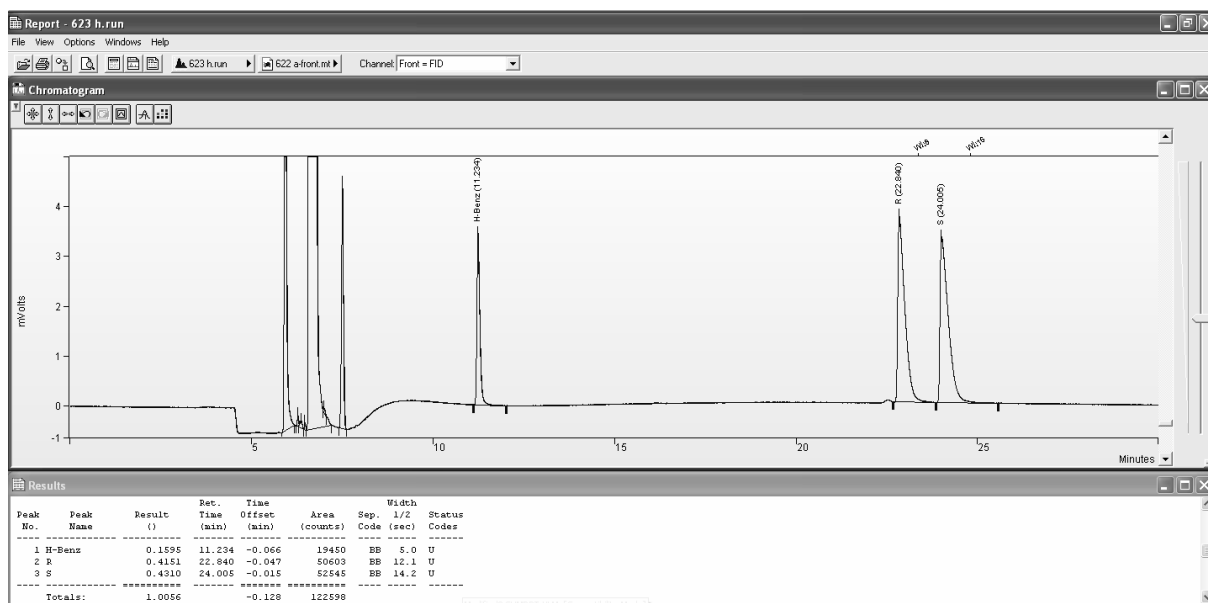


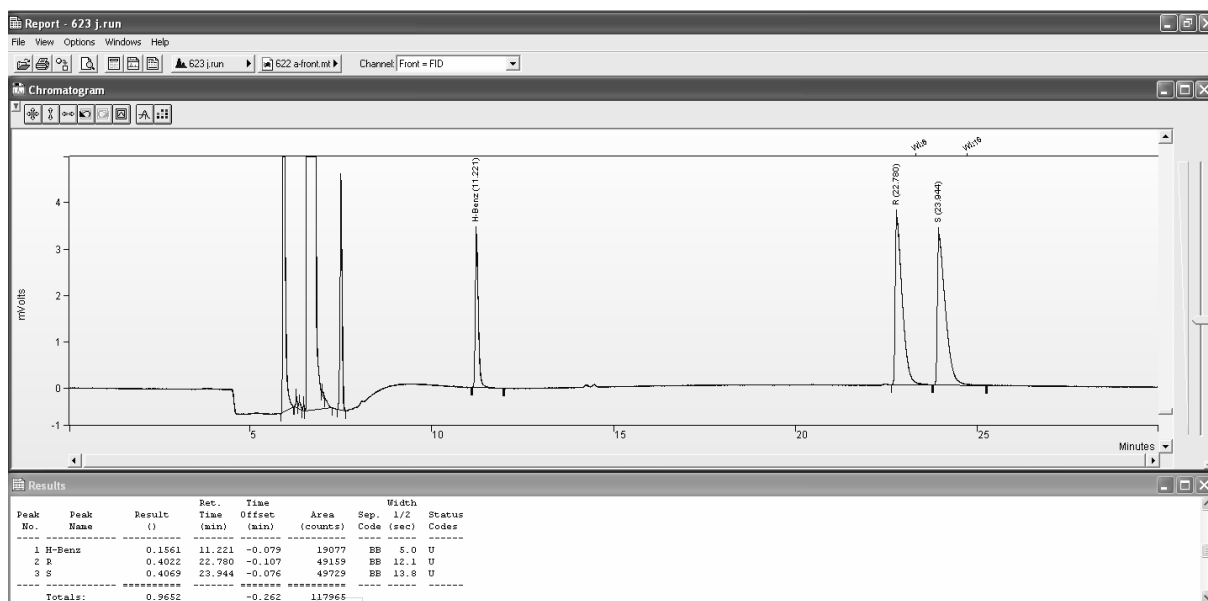
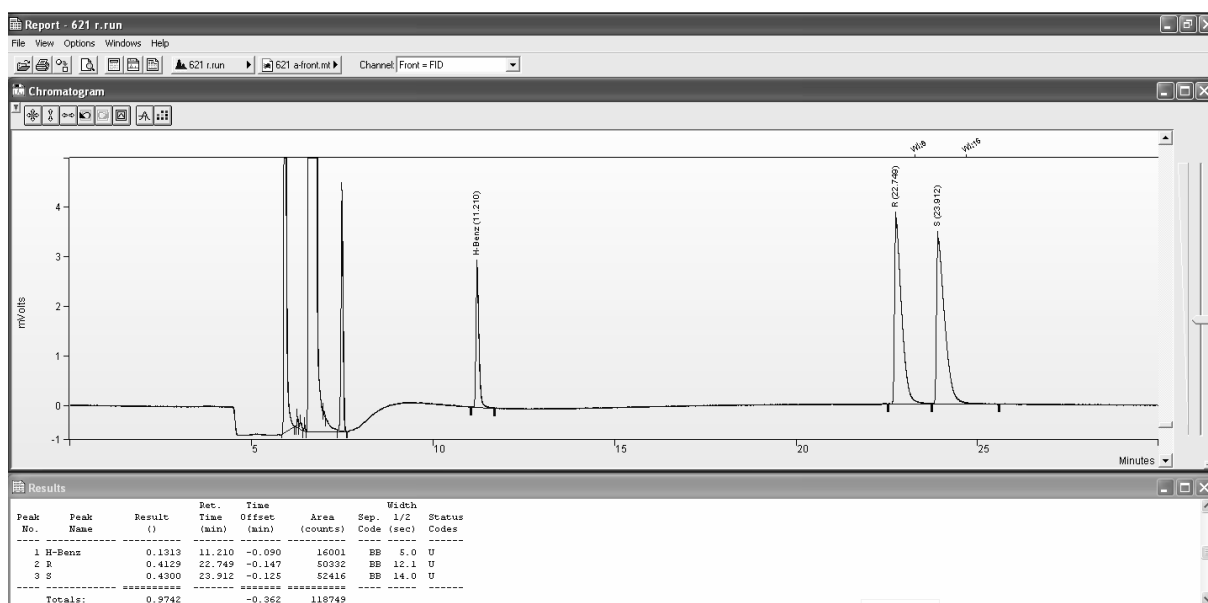
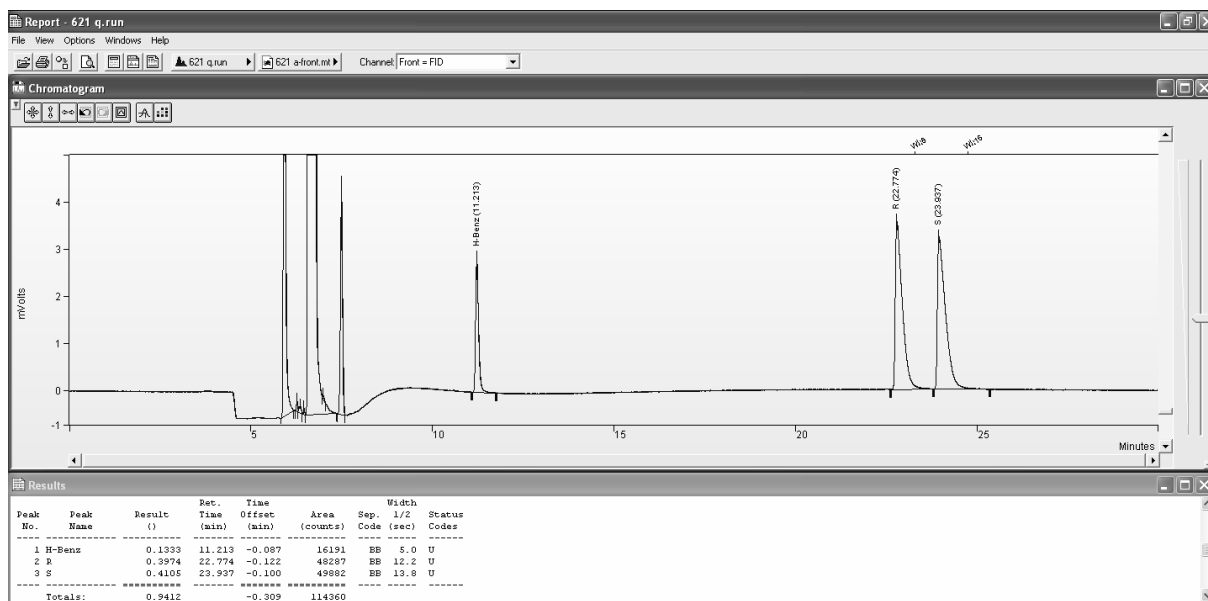


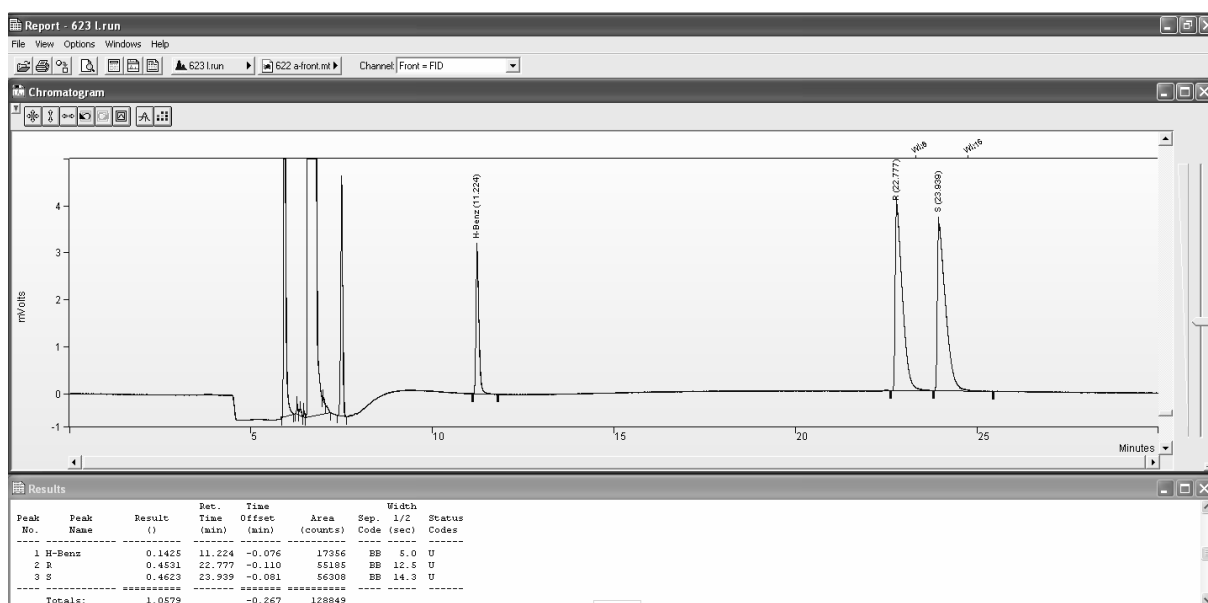
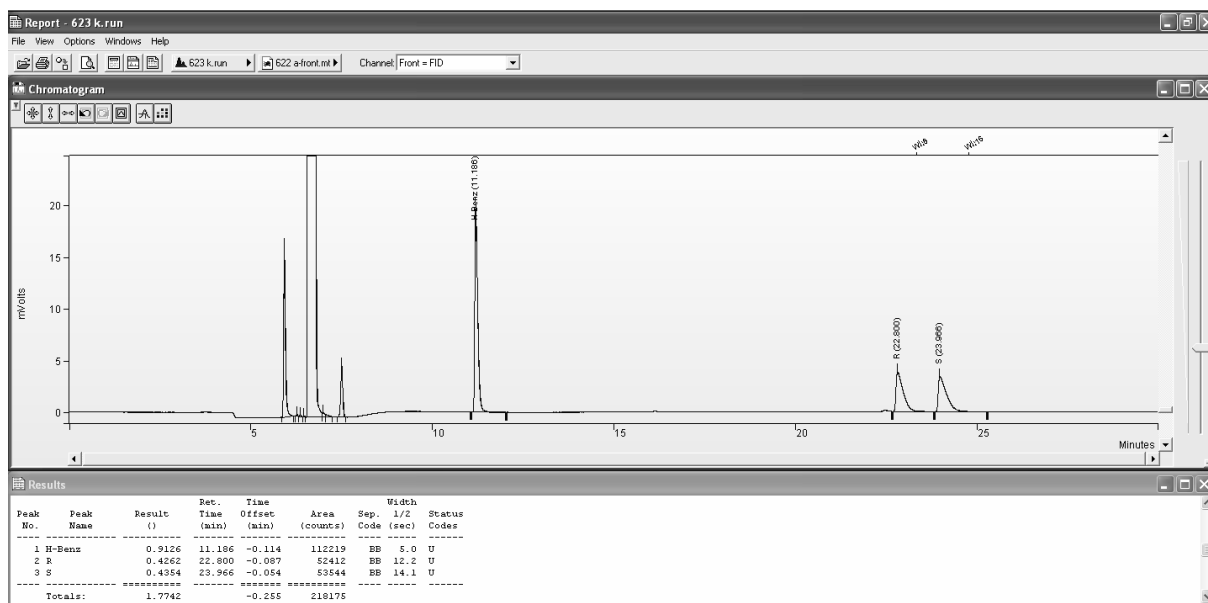




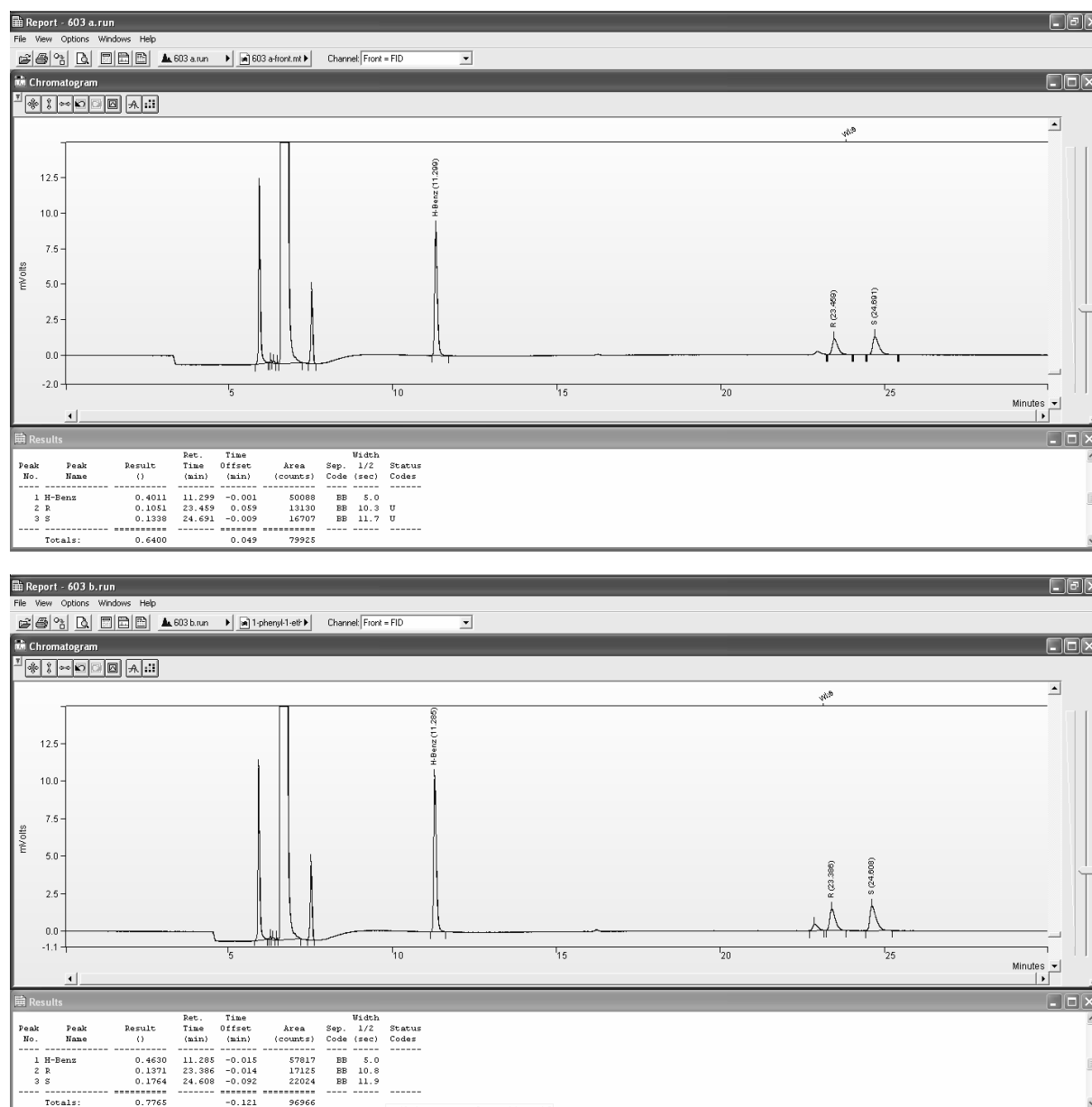


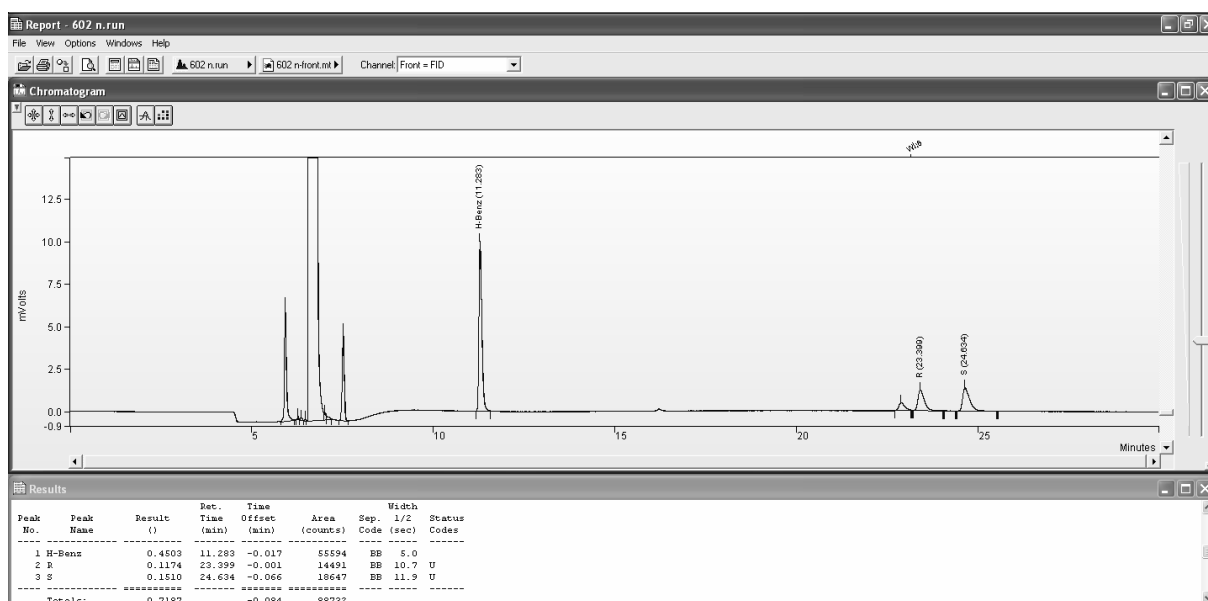
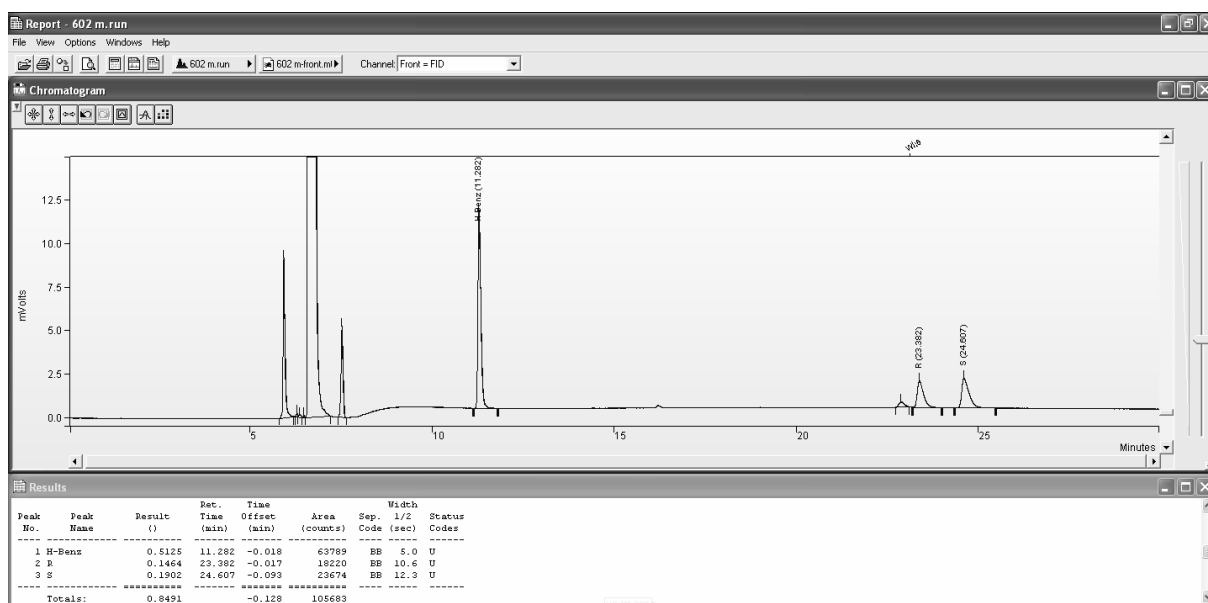
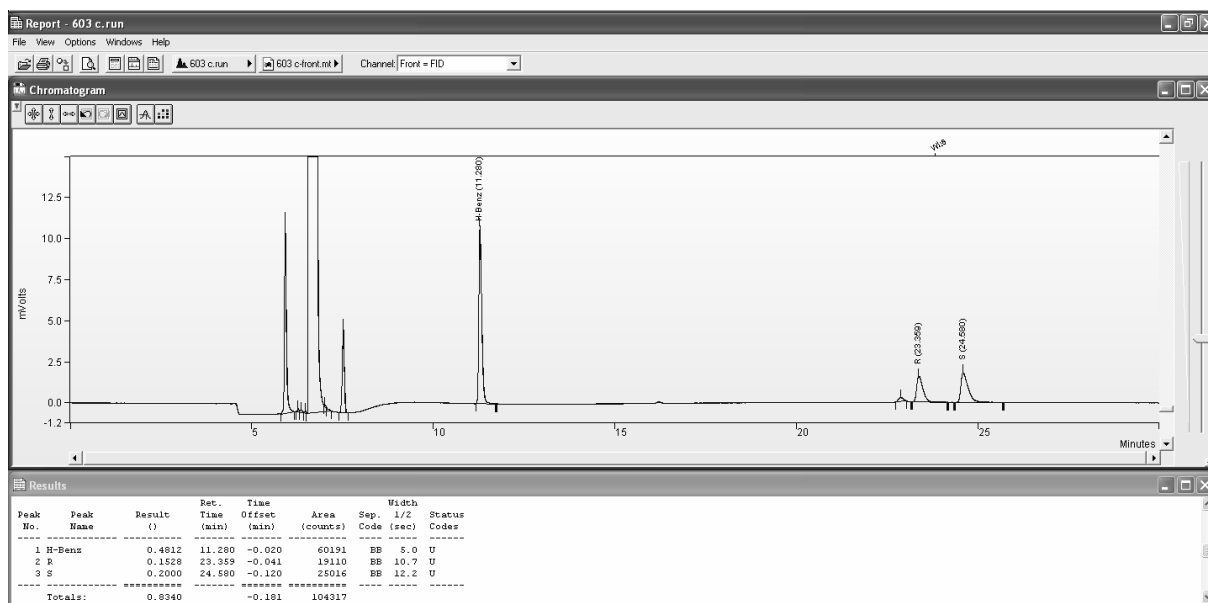


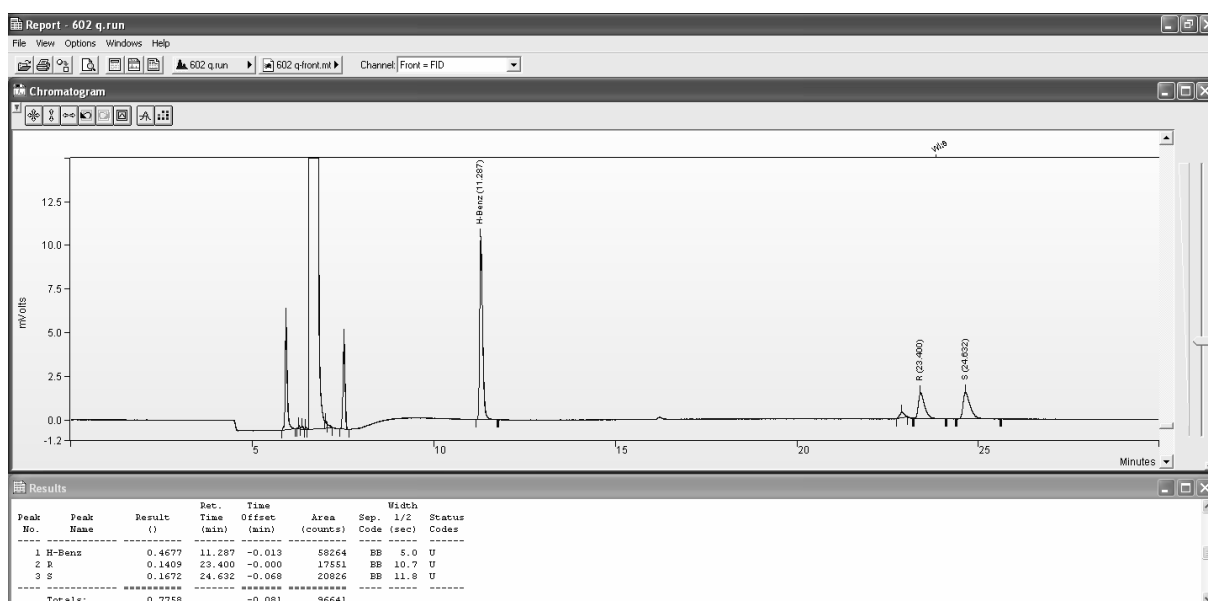
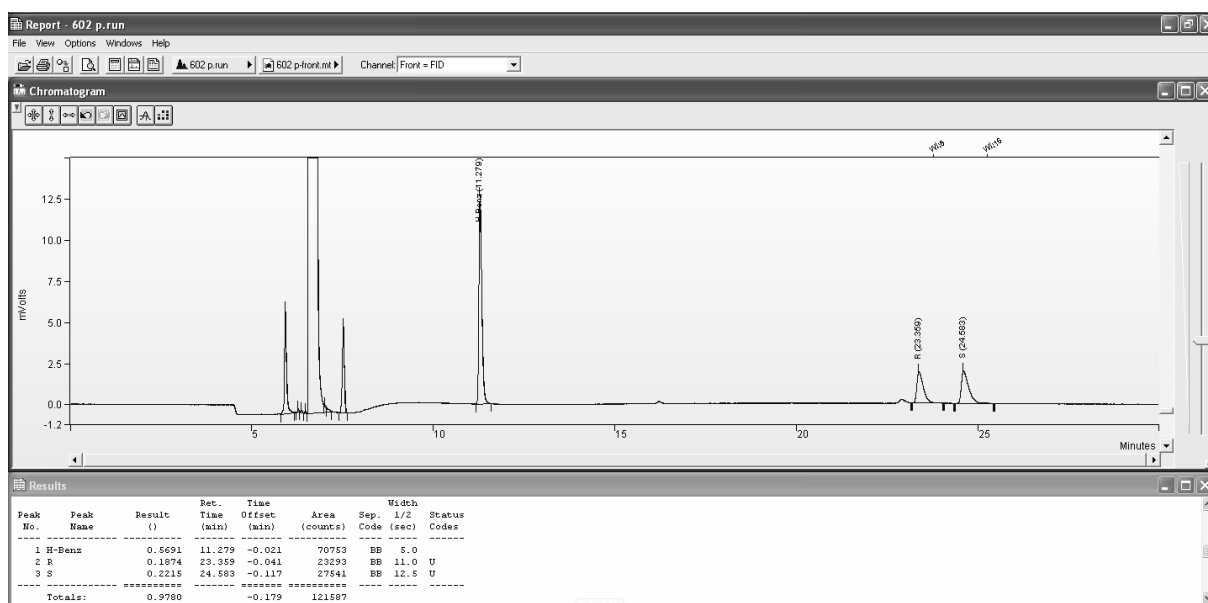
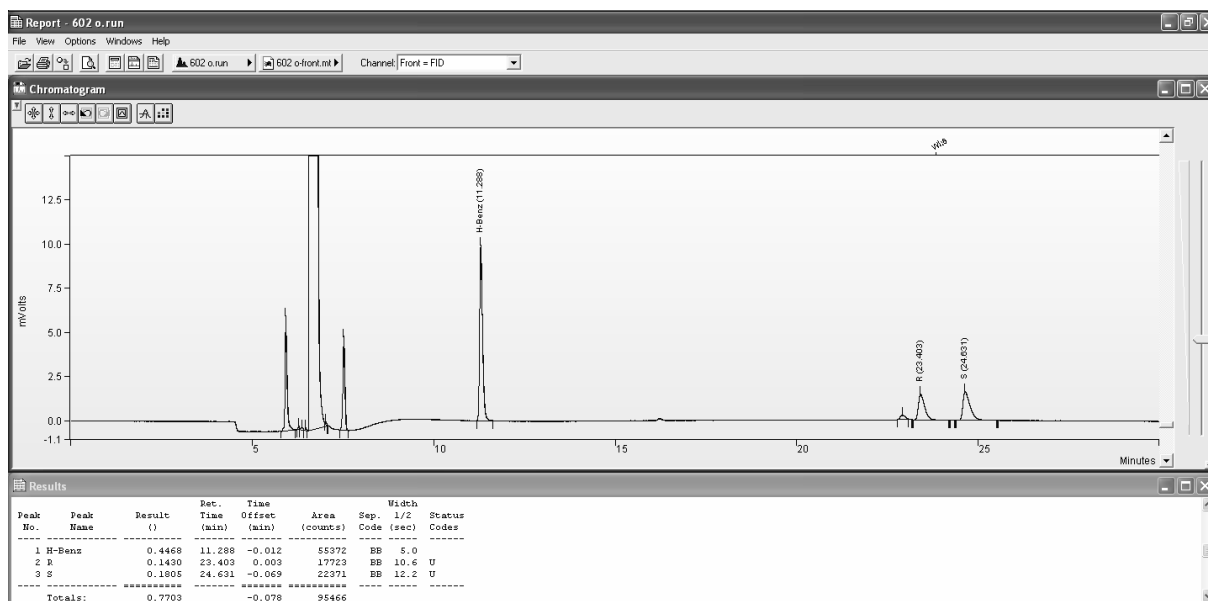


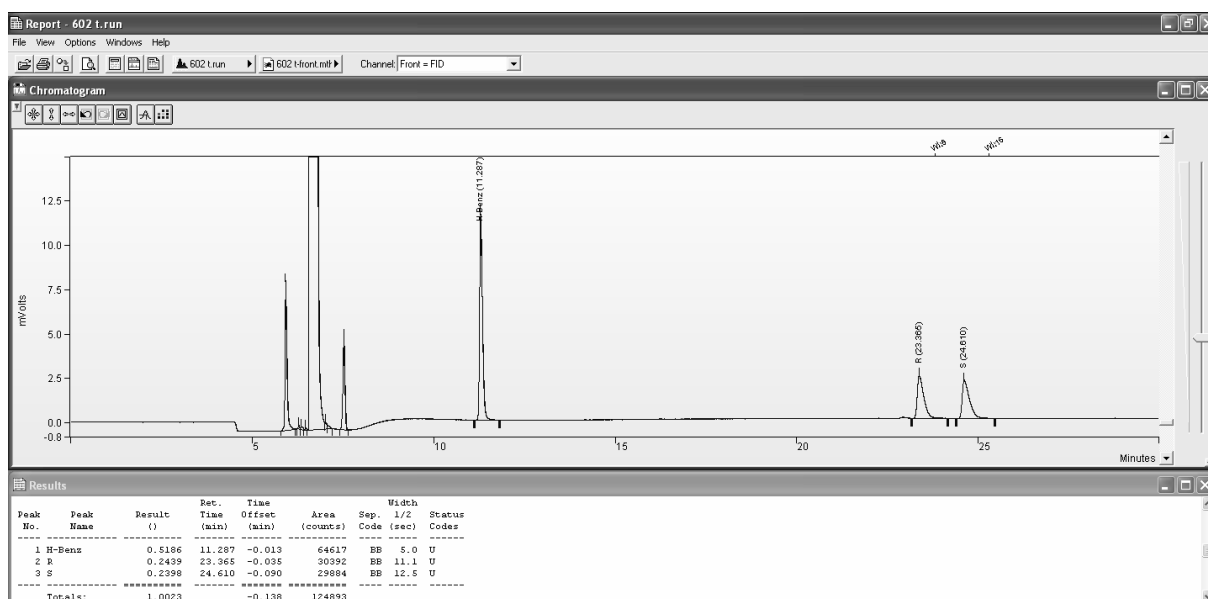
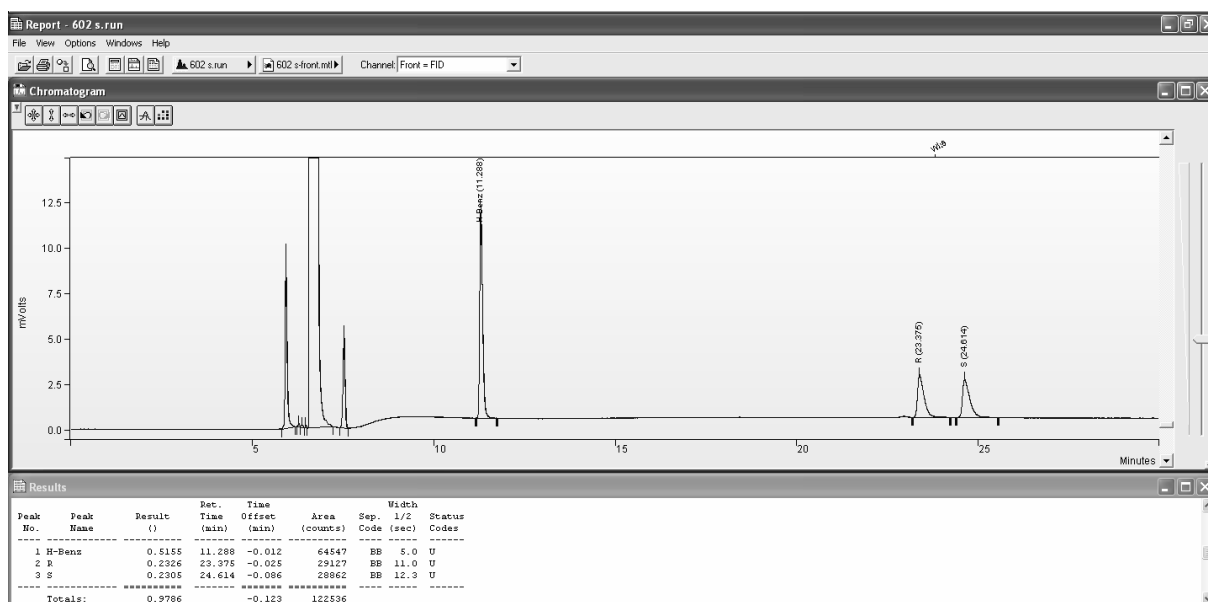
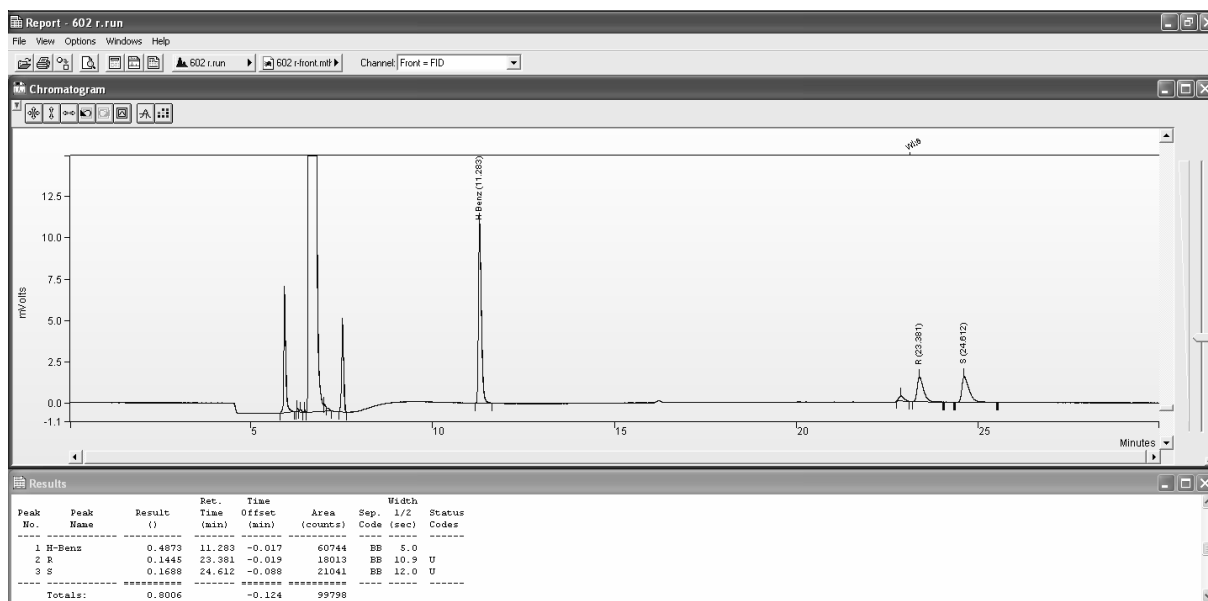


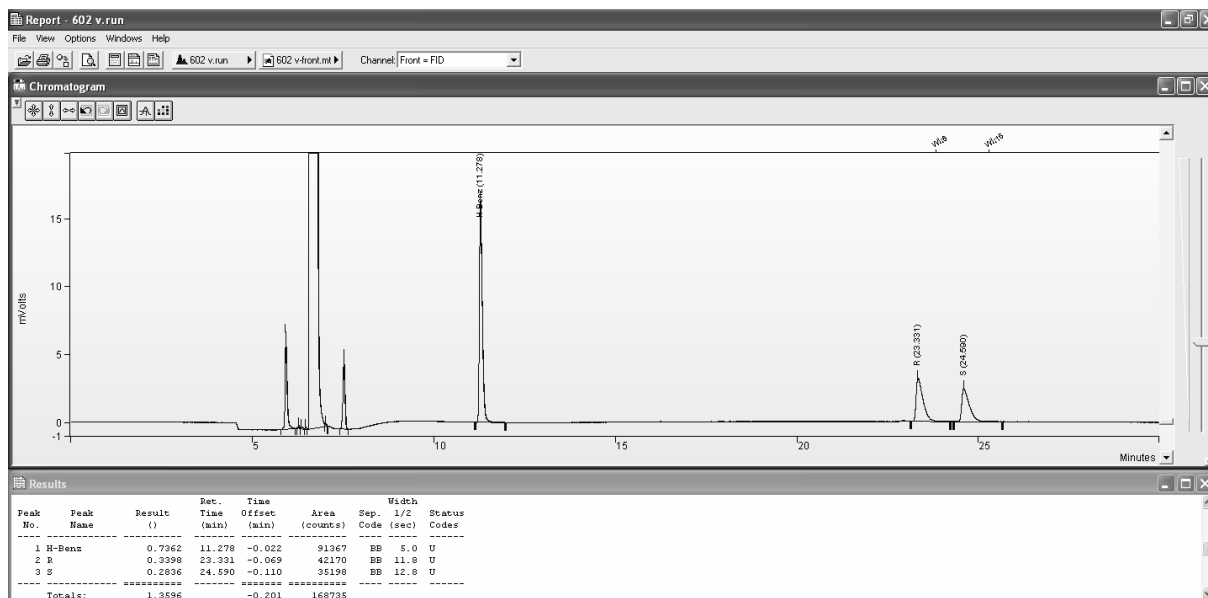
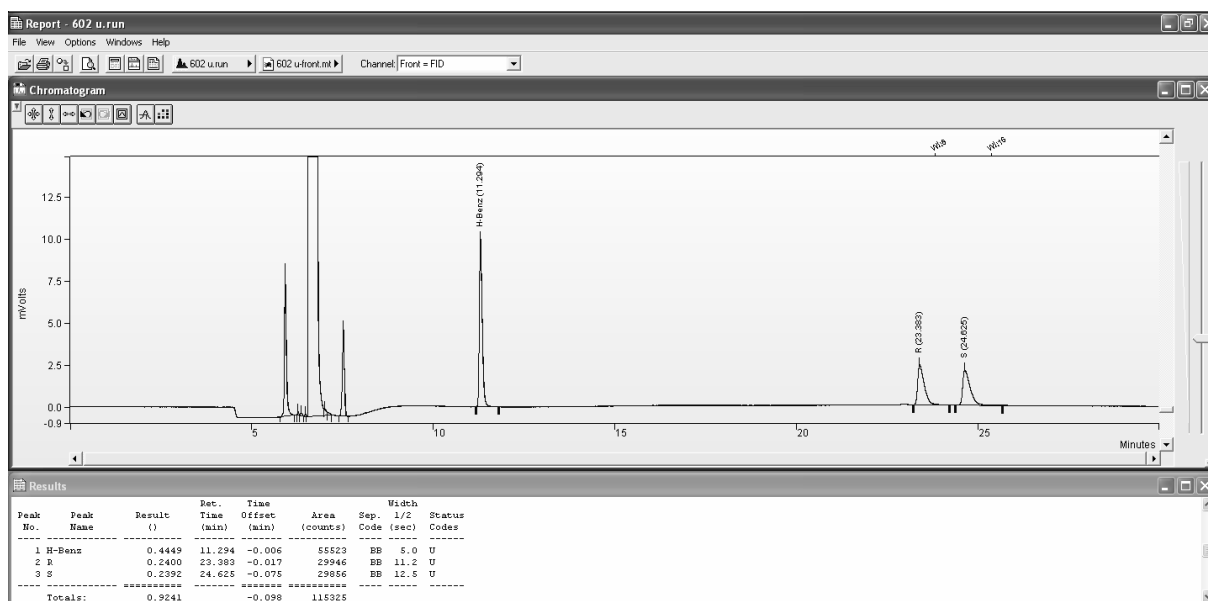
III.8 Sup. Figure 6

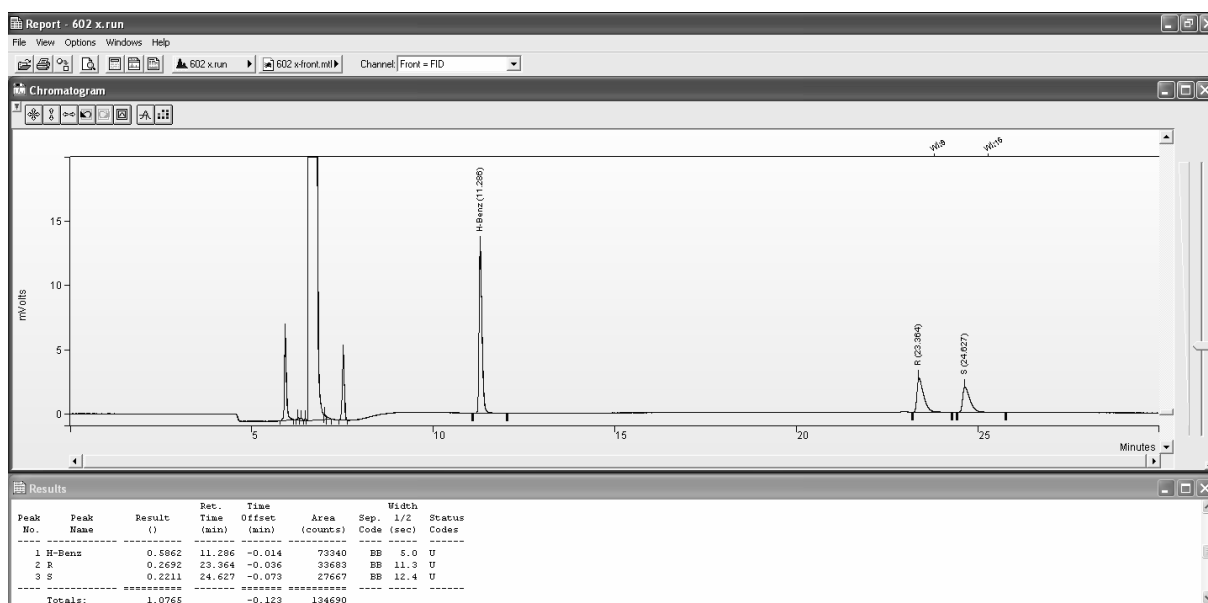
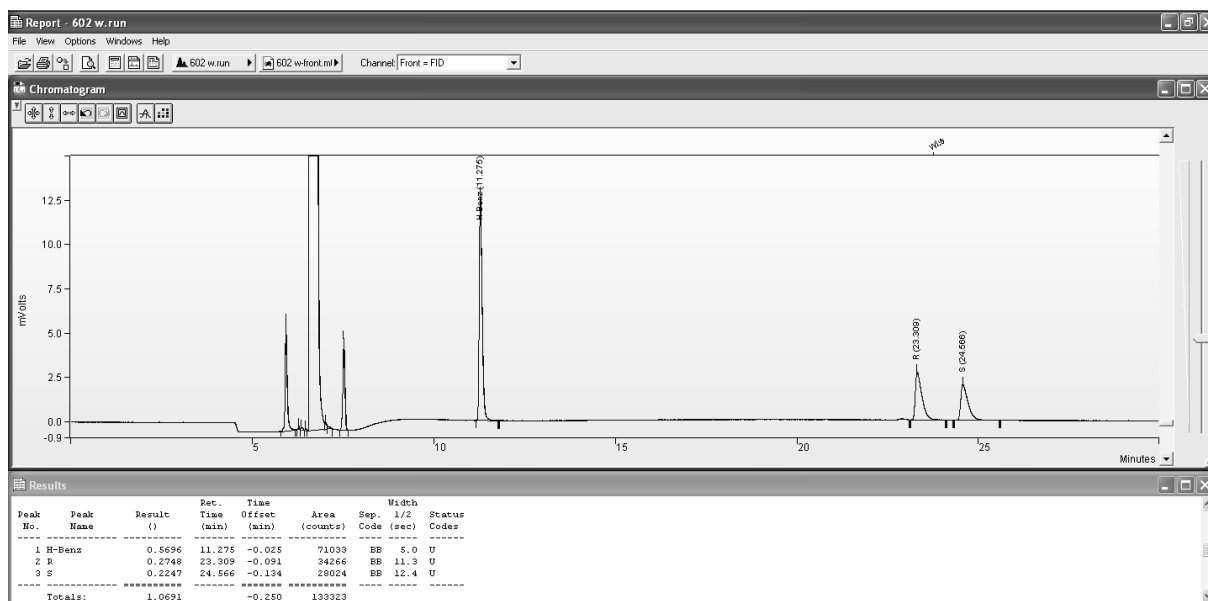




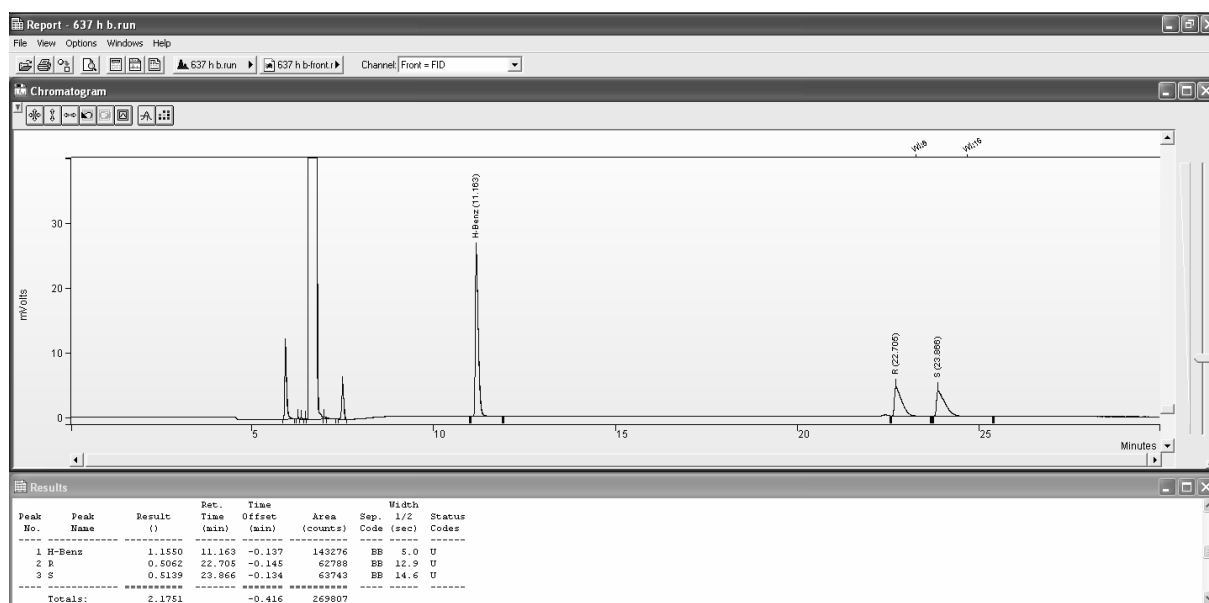
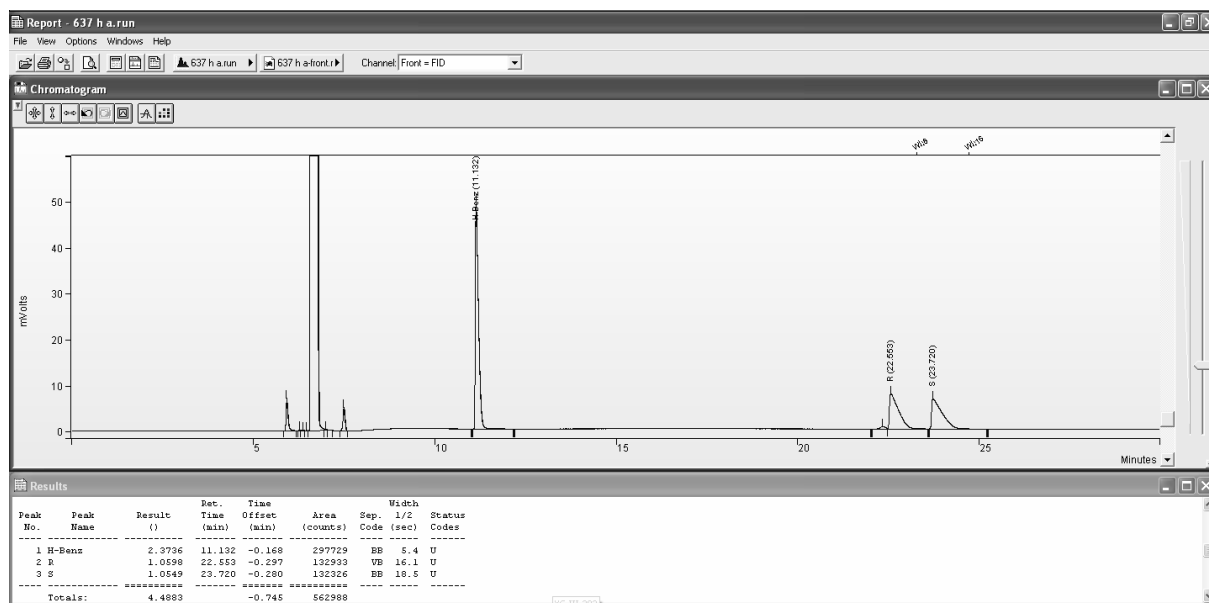


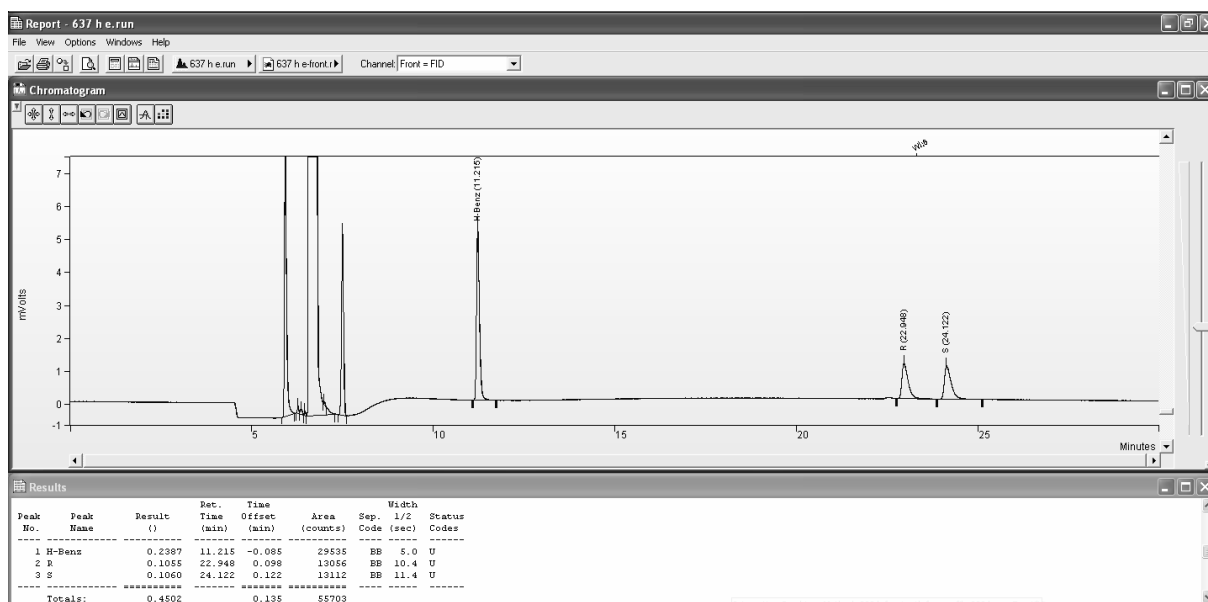
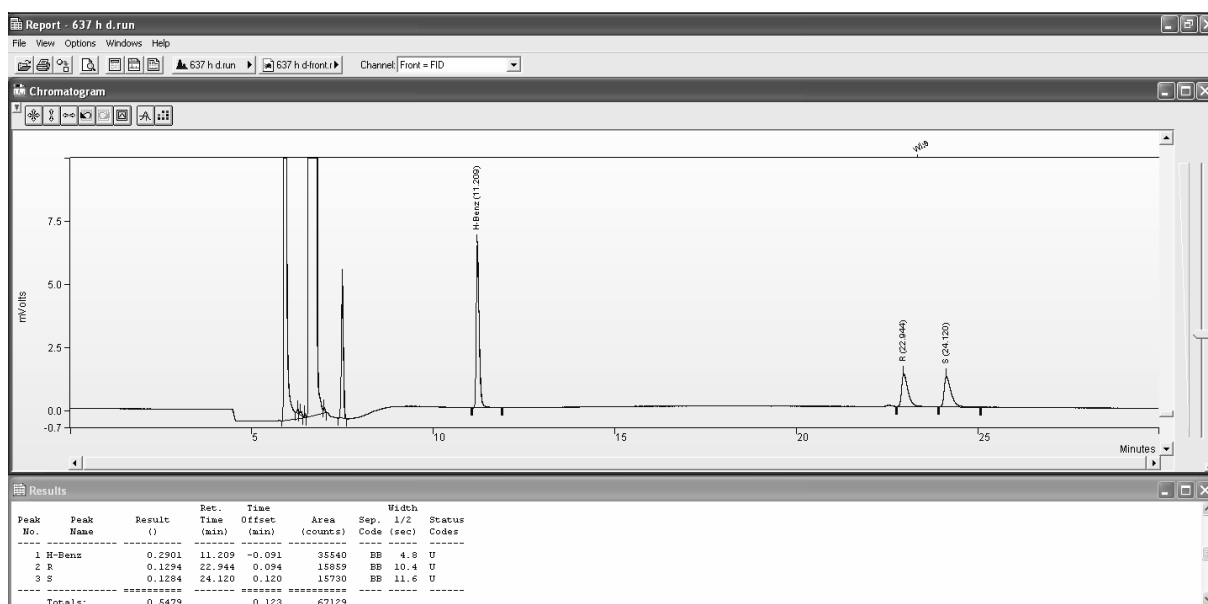
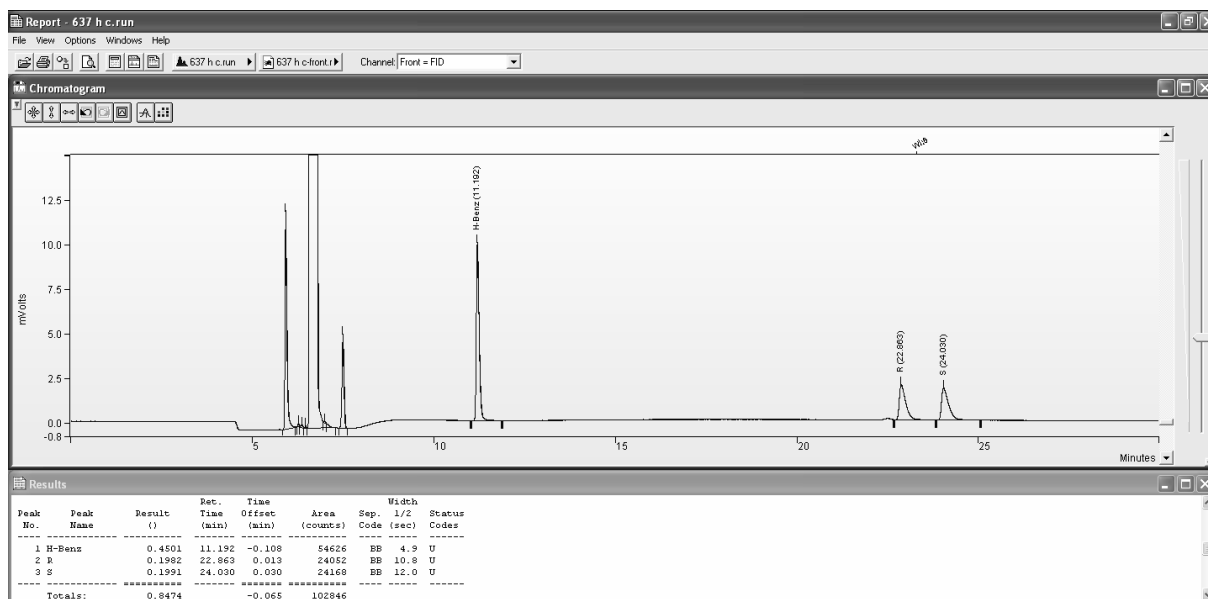






III.9 Benzaldehyde/1-phenyl-1-ethanol calibration curve





IV: References

- 1 G. D. Potter, M. C. Baird and S. P. C. Cole, A new series of titanocene dichloride derivatives bearing chiral alkylammonium groups; assessment of their cytotoxic properties, *Inorg. Chim. Acta*, 2010, **364**, 16–22.
- 2 Y. Geiger, T. Achard, A. Maise-François and S. Bellemin-Laponnaz, Hyperpositive nonlinear effects in asymmetric catalysis, *Nat. Catal.*, 2020, **3**, 422–426.
- 3 M. Watanabe and K. Soai, Enantioselective addition of diethylzinc to aldehydes using chiral polymer catalysts possessing a methylene spacer, *J. Chem. Soc., Perkin Trans. 1*, 1994, 837–842.
- 4 C. D.-T. Nielsen and J. Burés, Visual kinetic analysis, *Chem. Sci.*, 2019, **10**, 348–353.
- 5 M. Kitamura, S. Suga, H. Oka and R. Noyori, Quantitative Analysis of the Chiral Amplification in the Amino Alcohol-Promoted Asymmetric Alkylation of Aldehydes with Dialkylzincs, *J. Am. Chem. Soc.*, 1998, **120**, 9800–9809.